



Investigating the role the PI3K pathway plays in ependymoma pathogenesis

Jasper Estranero

BSc (Hons) Biological Sciences (Genetics)

Thesis submitted to the University of Nottingham for the degree of Doctor of Philosophy

“Our greatest weakness lies in giving up. The most certain way to succeed is always to try just one more time.”

Thomas A. Edison

Abstract ii

Acknowledgements iv

Table of Contents v

Table of Figures x

Table of Tables xii

List of Abbreviations xiii

ABSTRACT

Introduction: Ependymoma is the second most common malignancy of the central nervous system in paediatric cohorts, accounting for 6-12% of all cases of childhood brain tumours. Its clinical management remains a challenge at present, generally manifesting poor patient prognoses with a paucity of effective treatments. It was previously found that the PI3K signalling pathway, a cell survival cascade implicated in many cancers, was activated in 72% of primary ependymomas which suggests a significant role in disease pathogenesis. The PI3K pathway regulates a range of cellular processes that support tumourigenesis and its targeting has yielded therapeutic benefits in many malignancies. This study investigated the impact of signalling through the PI3K pathway in ependymoma survival and its prospect as an alternative target to treat these tumours.

Methods: The pan-PI3K inhibitor BKM120 was used to treat a panel of patient-derived ependymoma cell lines. Functional assays determined whether inhibition of the PI3K pathway conferred a cytostatic or cytotoxic response in ependymoma. Whole transcriptome analysis was used to elucidate the downstream effects of suppressing PI3K signalling on gene expression profiles. Based on this work, a proposed molecular mechanism for the instigation of the anti-tumourigenic effects of BKM120 treatment in ependymoma was functionally validated. Chemotherapeutic drugs which were predicted to work synergistically with PI3K pathway inhibition were subsequently investigated to evaluate their prospect as a treatment approach in ependymoma.

Results: Monotherapeutic treatment of ependymoma cells with BKM120 resulted in a significant decrease in cell viability at concentrations that have been shown to be achieved clinically. However, BKM120 treatment only resulted in a G_1/S phase cell cycle arrest, highlighting the induction of a cytostatic rather than a cytotoxic response. Gene expression analysis of BKM120-treated ependymoma cells identified a transcriptional profile consistent with a cell cycle arrest as well as a reduction in cellular responses that contribute towards tumourigenesis including regulation of DNA repair systems. A mechanism of G_1/S arrest induced FOXO1 control of Rb/E2F1 was proposed. Inhibition of the PI3K pathway resulted in a loss of FOXO1 and Rb phosphorylation. However, in experiments so far, no decrease in E2F-mediated luciferase reporter activity was found. Combining PI3K inhibition with gemcitabine, but not paclitaxel or cisplatin, resulted in a synergistic effect in ependymoma. Indications of potential resistance to BKM120-mediated PI3K inhibition in ependymoma have also been identified from the gene expression data through the positive regulation of the MAPK signalling pathway and reactivation of the PI3K pathway.

Conclusion: BKM120-mediated inhibition of the PI3K pathway in ependymoma impedes survival and viability, making it an attractive chemotherapeutic target to treat these tumours. However, it was only found to induce a cytostatic response as a single therapy thus highlighting its suitability for disease stabilisation instead of being used as a first-line of treatment. Clinical efficiency of PI3K pathway inhibitors in ependymoma might be more appreciated when administered as part of a combination treatment.

ACKNOWLEDGEMENTS

I would like to initially express my sincerest gratitude to my supervisors, Prof. Richard Grundy and Dr. Hazel Rogers, for giving me the opportunity to undertake such a challenging project. Thank you very much for putting your faith in my capabilities and skill set to accomplish such a big achievement. Your fantastic teaching, guidance and support over the last few years have made me the confident researcher that I am today. You have helped me ready for the next phase of my career and I will always be grateful for your wonderful insight. It has been such a pleasure to be under your supervision and I look forward to the chance that our paths would cross again in the field of science.

I would also like to give a big thank you to all of my colleagues at CBTRC. Your friendly faces and kind-hearted souls have helped me get through the tough times during my PhD. Thank you to Becky, Lisa and Maria for helping me bring out the best of my laboratory techniques. Thank you to Helen and Dawn for giving life and comic relief to my long days in the lab. Thank you to our knowledgeable post-docs and PI's for providing me with great life and career advices. To my fellow PhD students, Sophie, Hannah, Alice, Macha, Christine, Huda, Mohammed, Phoebe, Catherine, Louisa, Matt, Josh and Tim, you are a constant reminder of how there is always something positive despite the bad days. A special thank you is also extended to my lab buddy James who took the first stride with me in my feat with postgraduate life. I wish you all the very best in your own respective endeavours and keep the faith alive you guys!

To my Nottingham taekwondo family, thank you for reminding me that there is more to life than just work. Kicking, competing and training beside you have been one of the best experiences that I will certainly treasure during my time at the university. To my awesome pals, Vinny, Alvin, Binh, Sok, Fran, Paivs, Coleen and the honorary TKD member Val, you have no idea how much you have impacted my life in every possible way. You people are timeless!

This thesis was not made possible without the endless love and support from my family and friends. To my mum and dad, thank you very much for the patience and understanding especially in the last few months of my writing. Thank you for the encouragement, the words of wisdom and for being my rock. God bless you all and much love.

To God be the glory!

TABLE OF CONTENTS

CHAPTER 1. INTRODUCTION 1

1.1 Paediatric brain tumours 1

1.1.1 Classification 2

1.2 Paediatric ependymomas 3

1.2.1 Tumour classification 3

1.2.2 Treatment and management 5

1.2.3 Cell of origin 8

1.2.4 Genetics and molecular background 8

1.2.5 Ependymoma tumour subgrouping 12

1.2.6 Ependymoma prognostic markers 17

1.3 The PI3K pathway 18

1.3.1 PI3K enzyme isoforms 19

1.3.2 AKT isoforms 20

1.3.3 Downstream targets and PI3K signalling crosstalk 21

1.3.4 Aberrant activation of the PI3K pathway in cancers 29

1.4 Activation of PI3K signalling in paediatric brain tumours 33

1.4.1 PI3K signalling in paediatric ependymoma 34

1.5 The PI3K/AKT/mTOR pathway as a therapeutic target 35

1.5.1 Inhibiting the PI3K enzyme 35

1.5.2 Inhibiting AKT 38

1.5.3 Targeting mTOR 39

1.5.4 Resistance mechanisms to PI3K pathway inhibitors 40

1.6 Rationale, aims and hypothesis 44

CHAPTER 2. MATERIALS AND METHODS 46

2.1 Cell culture and cell based assays 46

2.1.1 Origin of cell lines and cell culture 46

2.1.2 Sub-culturing monolayer cells 49

2.1.3 Cell pelleting 49

2.1.4 Cell counting 49

2.1.5 Preparation of cell line stocks 49

2.1.6 Resuscitation of frozen cells from liquid nitrogen 50

2.2 Bacterial culture 50

2.2.1 Plasmid constructs 50

2.2.2 Culturing and plasmid preparation 50
2.2.3 Lipofectamine™-mediated transfection 51
2.2.4 Nucleofector™-mediated transfection 51
2.3 MTT viability assays 52
2.3.1 MTT assay standard protocol 52
2.3.2 Standard curve 53
2.3.3 Cell seeding 53
2.3.4 Drug treatment 54
2.3.5 IC_{50} estimation 57
2.3.6 Analysis of effects of BKM120 treatment combinations 57
2.4 Cell death assays 58
2.4.1 LDH assay 58
2.4.2 Cell cycle analysis using flow cytometry 60
2.5 Protein-based assays 62
2.5.1 Western blot 62
2.5.2 Luciferase assay 68
2.6 Microarray expression 69
2.6.1 Cell seeding and treatment 69
2.6.2 RNA extraction 69
2.6.3 Quality control and microarray run 70
2.6.4 Gene expression analysis 71

CHAPTER 3. FUNCTIONAL EFFECTS OF CANONICAL PI3K/AKT/mTOR SIGNALLING IN EPENDYMOMA 73

3.1 Introduction 73
3.2 Results 74
3.2.1 Treatment of ependymoma cells with BKM120 resulted in a decrease in PI3K/mTOR signalling pathway 74
3.2.2 Treatment with BKM120 decreased viability of ependymoma cells 75
3.2.3 PI3K pathway inhibition and cell death in ependymoma 77
3.2.4 Investigating autophagy as a cell death mechanism in ependymoma 81
3.2.5 Inhibition of mTOR signalling activates autophagy in ependymoma 85
3.2.6 Investigating whether BKM120 inhibition in ependymoma was mediated through the canonical PI3K/AKT signalling node 86
3.3 Discussion 90
3.3.1 The canonical PI3K pathway and its subsequent effects in ependymoma 90

3.3.2 Functional investigation of cellular responses in ependymoma post-BKM120 treatment 95
3.3.3 Conclusion 98
3.4 Summary of chapter findings 98

CHAPTER 4. GLOBAL ELUCIDATION OF DOWNSTREAM TARGETS OF THE PI3K PATHWAY IN EPENDYMOMA 100

4.1 Introduction 100
4.2 Results 101
4.2.1 Sample preparation for transcriptomic analysis 101
4.2.2 Quality control (QC) 103
4.2.3 Functional enrichment of differentially expressed genes (DEGs) in BKM120 treated ependymoma cells 107
4.2.4 Transcription factors involved in the regulation of DEGs in BKM120 treated ependymoma cells 129
4.3 Discussion 135
4.3.1 Inhibition of BXD-1425EPN and EPN1 cells resulted in a downregulation of cell cycle processes 135
4.3.2 Downstream mechanism of cell cycle arrest in ependymoma post-PI3K pathway inhibition 137
4.3.3 BKM120 treatment induced a reduction of expression in G_2/M-related genes in ependymoma 138
4.3.4 BKM120 treatment induced a reduction of expression in DNA repair genes in ependymoma 140
4.3.5 The upregulated genes induced by BKM120 treatment in ependymoma 141
4.3.6 Future work: analysis of trancriptomic profile at various timepoints 142
4.3.7 Conclusion 143
4.4 Summary of chapter findings 144

CHAPTER 5. POST-TRANSCRIPTOMIC FUNCTIONAL ANALYSIS OF DOWNSTREAM PI3K PATHWAY TARGETS 145

5.1 Introduction 145
5.2 Results 147
5.2.1 Inhibition of the PI3K pathway led to loss of phosphorylation of FOXO1 but not FOXO3 in ependymoma 147
5.2.2 Co-inhibition of FOXO1 did not increase cell viability in BKM120-treated ependymoma cells 148
5.2.3 Inhibition of the PI3K pathway led to loss of phosphorylation of Rb protein in ependymoma 149

5.2.4 Investigation of E2F1 transcription as a downstream effector of PI3K signalling 150
5.2.5 Identifying the potential value of combining PI3K inhibition with conventional chemotherapeutic drugs 156
5.3 Discussion 162
5.3.1 The role of FOXOs in ependymoma cell cycle arrest 163
5.3.2 The involvement of the Rb/E2F1 pathway in ependymoma cell cycle arrest 165
5.3.3 PI3K pathway inhibition as part of a combination therapy in ependymoma 167
5.3.4 Conclusion 171
5.4 Summary of chapter findings 172

CHAPTER 6. FINAL DISCUSSION AND FUTURE WORK 174

6.1 PI3K pathway inhibition – a therapeutic prospect 175
6.1.1 The role of canonical PI3K/AKT signalling in ependymoma 177
6.1.2 Inhibiting the PI3K pathway in ependymoma: tipping the balance towards cell death 179
6.2 The PI3K signalling network and identification of other suitable co-targets in treating ependymoma 181
6.2.1 The synergy behind gemcitabine and PI3K pathway inhibition in ependymoma 181
6.2.2 Potential targeting of gene functions in ependymoma that were upregulated following PI3K pathway inhibition 182
6.2.3 *C11orf95/RELA* fusion gene and the NFκB pathway 184
6.3 Establishing the molecular mechanisms that promote the responses to PI3K pathway inhibition in ependymoma 185
6.4 Proposed general future work 187
6.4.1 The PI3K pathway as a regulator of migration 187
6.5.1 Data collection at various endpoints 187
6.5.2 Proteomics 187
6.5.3 Advancement from using 2D ependymoma models 188
6.5.4 Final conclusion 189

BIBLIOGRAPHY 191

APPENDIX 239

Appendix 1: RCAS GFP plasmid details (Chen, C.M., Smith et al. 1999) 239
Appendix 2: LB agar 239
Appendix 3: LB media 239

Appendix 4: Protease cocktail buffer 239
Appendix 5: Gel buffers and recipes 240
Appendix 6: Western blot buffers 241
Appendix 7: Significant DEGs identified in the transcriptomic work for the BXD-1425EPN dataset 242
Appendix 8: Significant DEGs identified in the transcriptomic work for the EPN1 dataset 255
Appendix 9: Overlapping ependymoma DEGs identified in the transcriptomic work 285
Appendix 10: Genes associated with GO enrichment identified with DAVID analysis 292
Appendix 11: Publications 294

LIST OF FIGURES

Figure 1-1: Various CNS tumours that arise in children.....1
Figure 1-2: The supratentorial and posterior fossa regions of the brain.....2
Figure 1-3: Activation of the PI3K pathway.....19
Figure 1-4: Activation of the mTOR pathway.....23
Figure 1-5: Regulation of Wnt pathway.....24
Figure 1-6: Regualation of NF-κB pathway.....25
Figure 1-7: Regulation of the MAPK pathway.....26
Figure 1-8: Regulation of cell cycle.....27
Figure 1-9: Regulation of cell survival.....28
Figure 1-10: Involvement of GPCRs in PI3K pathway activation.....32
Figure 1-11: Increase in RTK expression and activity post-PI3K pathway inhibition.....41
Figure 1-12: Involvement of the JAK2/STAT5 pathway in inducing resistance to PI3K pathway inhibition.....42
Figure 2-1: Ependymoma cell density optimisation set up for LDH cell death assays.....59
Figure 3-1: Investigation of the status of the PI3K/AKT/mTOR signalling following BKM120 treatment.....75
Figure 3-2: MTT viability assays in response to BKM120 treatment.....76
Figure 3-3: LDH cytotoxicity assays in response to BKM120 treatment.....78
Figure 3-4: Investigation of apoptosis in response to BKM120 treatment.....79
Figure 3-5: 24 hour cell cycle analysis in response to BKM120 treatment.....80
Figure 3-6: 72 hour cell cycle analysis in response to BKM120 treatment.....81
Figure 3-7: Investigation of autophagy activation in response to BKM120 treatment.....82
Figure 3-8: Dose-limiting toxicity of CQ.....83
Figure 3-9: Immunoblot analysis of BKM120/CQ co-treatment.....83
Figure 3-10: MTT viability assay of BKM120/CQ co-treatment.....84
Figure 3-11: Investigation of the mTOR signalling pathway as a negative regulator of autophagy.....85
Figure 3-12: Perifosine treatments in ependymoma.....87
Figure 3-13: GDC-0068 treatments in ependymoma.....89
Figure 4-1: Western blot analysis for optimisation of sample preparation for transcriptomics experiments.....102
Figure 4-2: MTT viability assay of 24 hour BKM120 treatment.....102
Figure 4-3: Electrophoretic profile of transcriptomics samples.....104
Figure 4-4: Electropherogram traces of transcriptomics samples.....105
Figure 4-5: Sources of variation plot.....106
Figure 4-6: Principal Component Analysis plot.....107
Figure 4-7: Volcano plot for the different microarray gene probes.....109

Figure 4-8: Initial Partek®-mediated gene enrichment analysis of BXD1425-EPN cells 110
Figure 4-9: Detailed gene enrichment analysis of the cell proliferation processes in BXD1425-EPN cells 111
Figure 4-10: Additional cell proliferation sub-functions in BXD1425-EPN cells 114
Figure 4-11: Enrichment of processes for CNS maintenance and preservation of neurological activities in BXD-1425EPN cells 115
Figure 4-12: Overrepresentation of cell-cycle related functions in EPN1 cells 116
Figure 4-13: Enrichment for CNS stem cell activity and osteoblast-related proliferations in EPN1 cells. 120
Figure 4-14: Cellular reponses to an abiotic stimulus in BXD1425-EPN and EPN1 cells 121
Figure 4-15: Enrichment for response to radiation in EPN1 cells 122
Figure 4-16: Venn diagram showing 202 significantly overlapping gene probes in BXD1425-EPN and EPN1 cells 124
Figure 4-17: Interaction map of the 202 elucidated ependymoma DEGs 132
Figure 4-18: Querying of the genetic interaction map for E2F4 and its targets 133
Figure 4-19: Querying of the genetic interaction map for E2F6 and its targets 134
Figure 5-1: Proposed downstream mechanism for the induction of ependymoma cell cycle arrest 145
Figure 5-2: Western blot analyses of phosphorylated FOXO1 and FOXO3 147
Figure 5-3: MTT viability assay of BKM120/AS1842856 co-treatment 148
Figure 5-4: Western blot analysis of phosphorylated Rb 149
Figure 5-5: Transfection efficiency of 500 ng DNA incubated for 24 hours in BXD-1425EPN cells 151
Figure 5-6: Transfection efficiency of 500 ng DNA incubated for 48 hours in BXD-1425EPN cells 151
Figure 5-7: Transfection efficiency of 1 µg DNA incubated for 24 hours in BXD-1425EPN cells 152
Figure 5-8: Fluorescence imaging of BXD1425-EPN cells transfected with pmaxGFP constructs using Nucleofection™ 153
Figure 5-9: Flow cytometry analysis of propidium iodide stained BXD-1425EPN cells transfected with pmaxGFP constructs using Nucleofection™: 154
Figure 5-10: E2F-mediated luciferase reporter gene activity 156
Figure 5-11: BKM120 treatment in combination with paclitaxel 158
Figure 5-12: BKM120 treatment in combination with cisplatin 160
Figure 5-13: BKM120 treatment in combination with gemcitabine 162

LIST OF TABLES

Table 1-1: Histological grading of ependymoma tumours according to the WHO classification system. 4
Table 1-2: CGH studies to determine chromosomal aberrations in ependymoma..... 9
Table 1-3: aCGH studies for fine mapping of common gains and losses in epedymoma. 9
Table 1-4: Novel ependymoma oncogenes. 11
Table 1-5: Novel ependymoma TSGs 12
Table 1-6: Summary of the various compartment-specific ependymoma subgroups 15
Table 1-7: Summary of the recently established PFA ependymoma subgroups and subtypes..... 16
Table 1-8: Retrospectively identified prognostic markers in paediatric ependymoma. .. 17
Table 2-1: Clinical and in vitro characteristics of the different ependymoma cell lines... 47
Table 2-2: Drug details for various experimental set-ups 54
Table 2-3: Single drug treatment for IC50 determination..... 55
Table 2-4: Details of drug combination treatments 56
Table 2-5: Combination index (CI) to determine effects of drug interaction 58
Table 2-6: Details of antibodies used in Western blot analysis 67
Table 3-1: Analysis of significant differences in ependymoma cell viability inhibition 77
Table 4-1: RIN Scores of transcriptomic samples..... 104
Table 4-2: Significantly identified genes per biological enrichment in BKM120-treated BXD1425-EPN cells..... 112
Table 4-3: Significantly identified genes per biological enrichment in BKM120-treated EPN1 cells 117
Table 4-4: Top biological processes regulated by the 202 overlapping genes..... 125
Table 4-5: List of upregulated genes following inhibition of the PI3K pathway..... 127
Table 4-6: GO analysis of positively regulated genes..... 129
Table 4-7: Identification of significantly associated transcription factors involved in the regulation of the 202 overlapping genes 131
Table 5-1: Summary of transfection efficiencies of LipofectamineTM-mediated transfection of GFP plasmid constructs in BXD-1425EPN cells 152
Table 5-2: Summary of the flow cytometry analysis of propidium iodide-stained BXD-1425EPN cells transfected with pmaxGFP constructs using NucleofectionTM..... 155
Table 5-3: Chou-Talalay analysis of BKM120/gemcitabine combination treatment in EPN12A cells 162

LIST OF ABBREVIATIONS

5-FU	5-fluorouracil
aCGH	Array comparative genome hybridisation
AIEOP	Italian association for paediatric haematology and oncology
ALL	Acute lymphoblastic leukaemia
AMPK	AMP kinase
APC	Adenomatous polyposis coli
ATRT	Atypical teratoid/rhabdoid tumours
BBB	Blood brain barrier
BLBP	Brain lipid binding protein
BSA	Bovine serum albumin
BTK	Bruton's tyrosine kinase
cAMP	Cyclic AMP
CCND1	Cyclin-D1
CDK	Cyclin-dependent kinase
CGH	Comparative genome hybridisation
CI	Combination index
CIMP	CpG Island Methylator Phenotype
CKI	Cyclin-dependent kinase inhibitor
CLL	Chronic lymphocytic leukaemia
CNA	Copy number alterations
CNS	Central nervous system
COG	Children's Oncology Group
CQ	Chloroquine
CRT	Confocal radiotherapy
CSC	Cancer stem cells
CSF	Cerebrospinal fluid
CXCR1	Chemokine (CXC motif) receptor 1
DAC	5-aza-2'-deoxycytidine
DEG	Differentially expressed gene
dFdC	2'-2'-difluorodeoxycytidine (gemcitabine)
dFdCTP	2'-2'-difluorodeoxycytidine triphosphate
DIPG	Diffuse intrinsic pontine glioma
DMEM	Dulbecco's modified eagle medium
DMSO	Dimethyl sulfoxide
Dsh	Dishevelled

ECL	Enhanced chemiluminescence
EGF	Epidermal growth factor
EGFR	Epidermal growth factor receptor
eIF4E	Eukaryotic translation initiation factor 4E
eIF4EBP1	Eukaryotic translation initiation factor 4E-binding protein 1
ENCODE	Encyclopaedia of DNA elements
ERK	Extracellular-signal related kinases
ESC	Embryonic stem cell
FACS	Fluorescence activated cell sorting
FBS	Foetal bovine serum
FDA	United States Food and Drug Administration
FDR	False discovery rate
FGFR	Fibroblast growth factor receptor
FKB12	FK506-binding protein-12
FOXO	Forkhead box O-subfamily
Fz	Frizzled
GAP	GTPase-activating protein
GBM	Glioblastoma multiforme
GEF	Guanine nucleotide exchange factor
GFP	Green fluorescent protein
GLAST	Astrocyte-specific glutamate transporter
GO	Gene ontology
GOrilla	Gene ontology enrichment analysis and visualization Tool
GPCR	G-protein coupled receptor
GSEA	Gene set enrichment analysis
GSK3β	Glycogen synthase kinase 3β
GTR	Gross tumoural resection
HBSS	Hank’s balanced salt solution
HDAC	Histone deacetylase
HDACi	Histone deacetylase inhibitor
HGG	High grade glioma
HRP	Horse radish peroxidase
IDH	Isocitrate dehydrogenase
IGFR	Insulin-like growth factor receptor
IL	Interleukin
IMRT	Intensity modulated radiotherapy

IRS	Insulin receptor substrate
JAK	Janus kinases
KO	Knockout
LDH	Lactate dehydrogenase
LB	Luria broth
LRP	Lipoprotein receptor-related protein
MAML2	Mastermind like transcriptional coactivator 2
MAPK	Mitogen activated protein kinase
MCM complex	Mini-chromosome maintenance complex
MPE	Myxopapillary ependymoma
mTOR	Mammalian target of rapamycin
mTORC1	Mammalian target of rapamycin complex 1
mTORC2	Mammalian target of rapamycin complex 2
NASC	Nottingham Arabidopsis Stock Centre
NFI/II	Neurofibromatosis type I/II
NGS	Normal goat serum
NSC	Neural stem cell
NTRK	Neurotrophin receptor kinase
OS	Overall survival
PBRT	Proton beam radiotherapy
PBS	Phosphate saline buffer
PCA	Principal component analysis
PDGFR	Platelet-derived growth factor receptor
PDK1	Phosphoinositide-dependent kinase 1
PF	Posterior fossa
PFA	Paraformaldehyde
PFA	Posterior fossa group A
PFB	Posterior fossa group B
PFS	Progression free survival
PH	Pleckstrin homology
pHGG	Paediatric high grade glioma
PHTS	PTEN Hamartoma Tumour Syndrome
PI3K	Phosphoinositide 3-kinase
PI	Propidium iodide
PIKK	PI3K-related kinase
PIP_2	Phosphotidylinositol (4,5)-bisphosphate
PIP_3	Phosphotidylinositol (3,4,5)-trisphosphate
PKA	Protein kinase A

PKB	Protein kinase B
PKC	Protein kinase C
PLB	Passive lysis buffer
pLGG	Paediatric low grade glioma
PP2A	Protein phosphatase 2A
PPARγ	Peroxisome proliferator-activated receptor-γ
PRC2	Polycomb repressive complex 2
PtdIns	Phosphatidylinositol
PTEN	Phosphatase and tensin homologue
qRT-PCR	Quantitative real-time polymerase chain reaction
Rb	Retinoblastoma
RBD	Ras binding domain
RCC	Renal cell carcinoma
RegINS	Regulatory interaction networks
RGC	Radial glial cell
RIN	RNA integrity number
RMA	Robust multi-array average
RPMI	Rosewell Park Memorial Institute
RTK	Receptor tyrosine kinase
SE	Subependymoma
SEGA	Subependymal giant cell astrocytoma
SFM	Serum free media
SFOP	French Society for Paediatric Oncology
SIOP	Internation Society for Paediatric Oncology
SHH	Sonic hedgehog
SNP	Single nucleotide polymorphism
SP	Spinal
SREBP1	Sterol regulatory element binding protein 1
ST	Supratentorial
STAT	Signal transducer and activator of transcription proteins
SNV	Single nucleotide variation
TBS	Tris-buffered saline
TBS-T	Tris-buffered saline-tween
TCGA	The cancer genome atlas
TE	Trypsin-EDTA
TERT	Telomerase reverse transcriptase
TFT	Transcription factor target
TMS	Temsirolimus

TMZ	Temozolomide
TNF	Tumour necrosis factor
TNM	Tumour, lymph node, metastasis
TRAIL	Tumour necrosis factor-related apoptosis-inducing ligands
TSC1/2	Tuberous sclerosis 1/2
TSG	Tumour suppressor gene
UPP	Ubiquitin proteosome pathway
VEGF	Vascular endothelial growth factor
WGS	Whole genome sequencing
WNT	Wingless/Integrated
WHO	World Health Organisation
XIAP	X-linked inhibitor of apoptosis protein
YAP1	Yes-associated protein 1

CHAPTER 1. INTRODUCTION

1.1 Paediatric brain tumours

Brain tumours are the most common paediatric solid tumours, which account for 20% of all childhood malignancies (Parkin, Pisani et al. 1999). Brain tumours have a higher mortality rate than any other paediatric cancers, representing at least a third of all childhood cancer-related deaths (Children with Cancer UK, 2018). There are various types of Central Nervous System (CNS) tumours with distinct morphological, biological and clinical features. Their classification is usually determined by their cell of origin, the CNS region from which they develop and the histological grade. Tumours are subsequently categorised into further subgroups based on their established molecular signatures, also taking into consideration the revised World Health Organization (WHO) classification system. These include, for instance, the WNT- and SHH- subgroups in medulloblastoma, IDH-related status in glioblastoma multiforme (GBM) and the *C11orf195/RELA* fusion gene in ependymomas (Louis, Perry et al. 2016). An overview of the various CNS tumours that arise in paediatric cohorts is shown in Figure 1-1.

Currently, no common aetiology has been identified for the development of childhood brain tumours due to its multifactorial nature. Evidence of genetic predispositions has been highlighted in a few familial syndromes particularly, Neurofibromatosis types I (NFI) and II (NFII) (Guillamo, Creange et al. 2003, Johansson, Andersson et al. 2016), which have been associated with the onset of astrocytomas, ependymomas and even meningiomas despite its prevalence in adults.

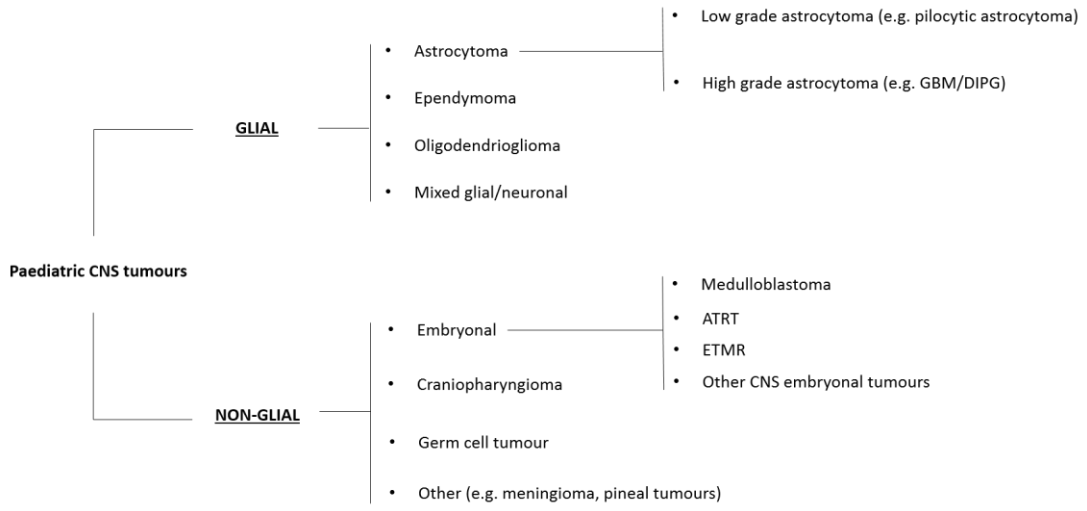


Figure 1-1 Various CNS tumours that arise in children, their sub-classifications and their cell of origin. Image derived from Hutter, Bolin et al. (2017).

1.1.1 Classification

Most paediatric CNS tumours are of intracranial origin, which could be divided into the supratentorial and posterior fossa regions. These regions are delineated by the tentorium cerebelli, an extension of the dura mater which is one of the layers that make up the meninges. The supratentorial region relates to the cranial structures above the tentorium cerebelli which mainly constitute the cerebrum. The posterior fossa region lies below the tentorium cerebelli which encompasses the cerebellum and brainstem (Figure 1-2). Like many paediatric malignancies, development of childhood brain tumours is not necessarily restricted to a particular region of the CNS. These tumours usually develop from precursor cells that give rise to the different CNS structures, hence defining these neoplastic growths by morphology rather than location (Birch, Marsden 1987). In children, low-grade astrocytomas, medulloblastomas and ependymomas are the three most common brain tumours (Nejat, El Khashab et al. 2008).

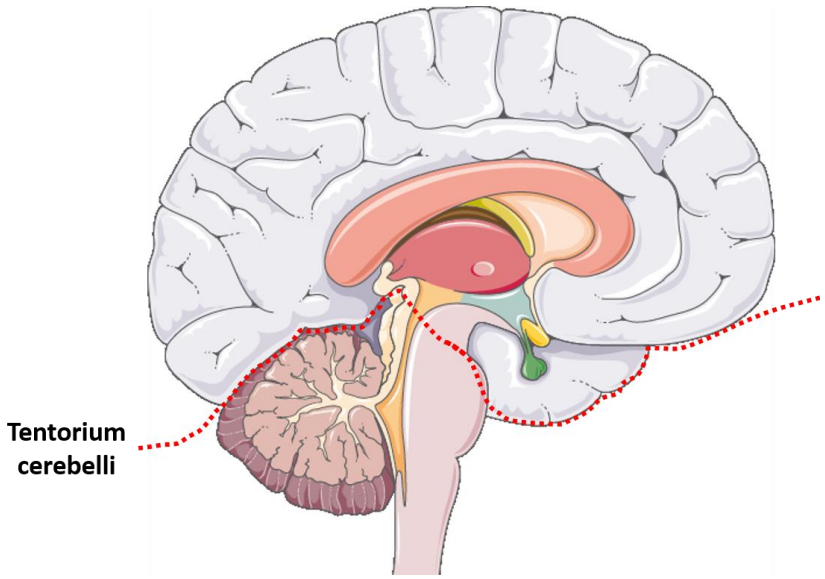


Figure 1-2 The supratentorial and posterior fossa regions of the brain are delineated by the tentorium cerebelli, which is indicated by the dashed red line on the schematic. Image was taken from Smart Servier Medical Art and modified using Microsoft PowerPoint.

Tumour grades are determined to discern the degree of malignancy according to the World Health Organisation criteria (Louis, Perry et al. 2016). Yet, anticipating disease outcomes based on histopathological factors remain ambiguous. Tumours are graded between I and IV. Grades I and II tumours generally have a low proliferative index with a high feasibility of achieving gross tumoural resection. Grades III and IV tumours consist of poorly differentiated cells with a high proliferative profile and are usually characterised with a necrotic core. Patients with high-grade tumours also tend to perform worse despite undergoing aggressive treatment regimes (Louis, Perry et al. 2016).

1.2 Paediatric ependymomas

Ependymomas are the second most common malignancy of the CNS in paediatric cohorts, accounting for 6-12% of cases and 2% of all childhood malignancies (Ostrom, Gittleman et al. 2015). Morphologically, they resemble the ependymal lining of the brain's ventricular system and central canal of the spinal cord, which secrete the cerebrospinal fluid (CSF) (Lehman 2008). Ependymomas can occur anywhere along the neurospinal axis but intracranial neoplasms are more common in children with 70% of tumours occurring in the posterior fossa and 30% in the supratentorial region (Kilday, Rahman et al. 2009). Patients diagnosed with ependymoma show a relatively poor prognosis with a 5-year survival rate of 39 – 64% and a 5-year progression free survival (PFS) rate of 23 – 45% (Shim, Kim et al. 2009). The intrinsic resistance to therapy, coupled with local tumour recurrence following surgical excision in about 50% of cases (Haresh, Gandhi et al. 2017) partly contributes to the high mortality rates manifested by the disease. Due to its unpredictable clinical behavior, current research into ependymal tumours has adopted a more molecular rather than a clinicopathological and histological approach to improve understanding of its pathogenesis, leading to identification of disease biomarkers and putative therapeutic targets.

1.2.1 Tumour classification

The World Health Organisation (WHO) has classified ependymal tumours into three grades: myxopapillary ependymoma and subependymoma (Grade I), classic ependymoma (Grade II) and anaplastic ependymoma (Grade III) (Louis, Perry et al. 2016), as described in Table 1-1. The grading system was updated following the discovery of the *C11orf95/RELA* fusion gene (Parker, Mohankumar et al. 2014). It is currently an accepted molecular signature by WHO, which defines a subgroup of Grade II and III supratentorial tumours.

Historically, histopathological factors have been central towards determining disease outcomes in brain tumours including ependymoma, yet its validity as a prognostic marker has remained controversial due to confounding factors (Armstrong, T. S., Vera-Bolanos et al. 2011, Mack, Witt et al. 2014, Wu, J., Armstrong et al. 2016). The histopathological variability of ependymal tumours also adds complexity to its reliability as a prognostic marker, particularly with regards to the issue of reproducibility among histopathologists. For instance, there is difficulty in differentiating grade II and III tumours as classic (grade II) ependymomas can sometimes contain pockets of anaplastic regions that are characteristic in aggressive grade III tumours (Bouffet, Perilongo et al. 1998). In a study by Ellison, Kocak et al. (2011), little consensus was achieved between

pathologists who independently graded tumours from three trial cohorts (SFOP, CNS9204, CNS9904). It was only after an agreement on a new WHO-derived classification system did they achieve an increase in grading concordance with the re-evaluation of the CNS9904 cohort and a separate trial (AIEOP). Despite the increase in grading consensus amongst pathologists, prognostic significance was only observed in the AIEOP trial but not in the others, suggesting that histopathological markers on its own are insufficient to predict patient outcome.

Table 1-1 Histological grading of ependymoma tumours according to the WHO classification system.

Grade	Subtype	Description
I	Myxopapillary ependymoma	These are more prevalent in adults where they predominantly occur along the spinal cord, particularly towards the caudal region. The cells appear to be cuboidal or elongated with a papillary-like arrangement around the vasculature and the stroma.
	Subependymoma	They are particularly associated with the brain's ventricular system. These tumours present with a dense fibrillary matrix of glial cell aggregates containing small uniform nuclei, often accompanied by cysts. Pleiomorphic nuclei are more common in multicystic tumours.
II (Classic)	• Cellular • Papillary • Clear cell • Tanycytic	Their monomorphic nuclei are usually round to oval shaped. Tumours display perivascular pseudorosettes which are radial arrangements of ependymal cells projecting towards the blood vessels. Rare ependymal rosettes can also be observed where the cells are arranged in a way that mimics normal ependymal cavity.
III (Anaplastic)		They have a relatively high mitotic index leading to increased cellularity within the tissue. Microvascular proliferation, relating to multi-layered vasculature consisting of large activated endothelial cells, is also observed alongside palisading necrosis.

1.2.2 Treatment and management

1.2.2.1 Surgery

Ependymomas are considered a surgical disease due to their tendency to remain local to the site of origin with minimal invasion of adjacent structures or metastasis through leptomeningeal dissemination (Yuh, Barkovich et al. 2009). However, even after complete surgical resection, adjuvant therapy is necessary; even then recurrence is observed in 50% of cases. Extent of resection remains the most consistent prognostic factor for paediatric ependymomas (Cage, Clark et al. 2013, Marinoff, Ma et al. 2017). Gross tumoural resection (GTR) precedes focal irradiation and adjuvant chemotherapy as part of a standard treatment regime for ependymoma. It has also been reported that treatment of intracranial ependymomas can be performed through surgery alone without further therapeutic interventions (Chamberlain 2003), as demonstrated in supratentorial tumours (Robertson, Zeltzer et al. 1998, Bouffet, Perilongo et al. 1998). In a separate cohort of patients with supratentorial ependymomas, long-term disease-free outcomes were observed with only one recurrence after 10 years (Palma, Celli et al. 2000). However, achieving GTR is a challenging task due to concerns of disease sequela arising from aggressive surgical procedures (Wu, J., Armstrong et al. 2016). This is particularly valid in highly invasive anaplastic tumours as well as those occurring in inaccessible brain regions with which cases of mutism and pseudobulbar palsy have been documented (Pollack, Polinko et al. 1995, Gadgil, Hansen et al. 2016). This has warranted the need for second-look surgeries should incomplete resection was only achieved in the first attempt rather than performing a “one-off” resection as demonstrated by the success rates in one prospective trial (Godfraind, Kaczmarska et al. 2012).

1.2.2.2 Radiotherapy

Irradiation of the tumour bed serves as a preventative measure as it aims to eradicate residual disease post-maximal tumour resection. At present, no trials have been conducted to determine whether radiotherapy following surgery is superior over surgery alone as a treatment approach for paediatric ependymoma. Therapeutic interventions usually involve irradiation of locally affected areas with 54 – 59.4 Gy in which recipients have generally shown better disease outcomes (Merchant, Li et al. 2009, Swanson, Amdur et al. 2011). In about 30% of ependymoma cases, tumour metastasis takes place through leptomeningeal dissemination, prompting the administration of radiotherapy along the cerebrospinal axis (Pollack, Gerszten et al. 1995). The notion of re-irradiation is also strongly being considered in current disease management due to its prospective survival benefits in patients especially those who undergo relapse. However, concerns regarding radiotherapy-induced neurocognitive adverse effects have resulted in many institutions refraining from irradiating young patients aged <3 years (Mulhern, Hancock et

al. 1992, Grill, Renaux et al. 1999). Modifications in radiotherapeutic regimes have been introduced to minimise adverse effects in recipients such as 3D Conformal Radiotherapy (3D CRT) and Intensity-Modulated Radiotherapy (IMRT) (Merchant, Mulhern et al. 2004, Schroeder, Chintagumpala et al. 2008). On the other hand, the superiority of Proton Beam Radiotherapy (PBRT) in treating paediatric ependymomas has been highlighted due to little damage induced in neighbouring tissues by decreasing entrance dose and subsequently minimising exit dose (Kirsch, Tarbell 2004). Several studies have reported that PBRT recipients displayed an overall favourable outcome with reduced disease sequelae and no evident impact on cognitive faculties (Macdonald, S. M., Sethi et al. 2013, Greenberger, Pulsifer et al. 2014, Eaton, Yock 2014). Nevertheless, opting in radiotherapy as a post-operative measure to effectively ensure local control and reduce recurrence rates remains controversial. Several clinical trials have already started to investigate the therapeutic value of post-operative radiotherapy in ependymoma patients especially that conducted by the Children's Oncology Group (COG) (NCT01096368). In this study, radiotherapeutic outcomes were analysed in all patients who underwent GTR except those with non-anaplastic supratentorial tumours. Delivery of same total radiation doses in shorter time intervals (hyperfractionated radiotherapy) has also been put forward but any conclusive survival advantages are yet to be reported (Conter, Carrie et al., 2009).

1.2.2.3 Chemotherapy

Chemotherapy is used as a substitute for delaying post-operative radiotherapy in young patients and infants as an adjuvant therapeutic approach. It is also administered to patients with residual disease, aiming to either gain a chemotherapeutic response or to facilitate second look surgery. However, its advantage over radiotherapy is ambiguous as indicated by several contradicting study findings. A follow up on recipients of chemotherapy only indicated a 3-year overall survival (OS) rate of 79.3% with no metastasis followed by 63.4% at 5 years (Grundy, Wilne et al. 2007), validating post-operative chemotherapy as a viable treatment approach. These results were refuted by an earlier study in which less than 50% of participants manifested significant responses to chemotherapy (Grill, Le Deley et al. 2001). They found that only 40% of patients in this series survived during a two-year follow up after starting chemotherapy, which further declined to 23%, two years later. Increasing dosage also conferred no significant improvements in outcome (2 year OS= 54%), and was associated with more incidences of toxicity-related mortalities. The Head Start III clinical trial concluded that adjuvant chemotherapy was consistently effective against supratentorial tumours while posterior fossa tumours would benefit more from irradiation (Venkatramani, Ji et al. 2013).

The paucity of effective ependymoma targets prompted research to explore any underlying biological mechanisms that are deemed pathologically vital. Some of these have already been investigated in clinical studies including the upregulated *ERBB2* receptor in which lapatinib-mediated inhibition was well tolerated by patients yet yielding modest therapeutic outcomes when administered as a monotherapy (Fouladi, Stewart et al. 2013). Unfortunately, the general progress of patient-based studies based on molecular targets is lagging due to the need for extensive pre-clinical evaluation. In particular, Atkinson, Shelat et al. (2011) identified several biological processes in their high-throughput drug screen that showed therapeutic potential in ependymoma when targeted pharmacologically. These include inhibiting the insulin signalling pathway and centrosome cycle as well as the anti-metabolite 5-fluorouracil (5-FU), which was well tolerated by patients and showed promising efficacies in a Phase I trial (Wright, Daryani et al. 2015). The search for other therapeutic targets is in progress with the integration of genomic, epigenetic and molecular data clarifying the heterogeneous nature of these enigmatic tumours (Pajtler, Witt et al. 2015, Mack, Pajtler et al. 2018).

1.2.2.4 Administration of both chemotherapy and radiation

For many brain malignancies, the extent of the infiltration into surrounding brain parenchyma that is usually evaluated following surgery could influence subsequent treatment modalities. With neither an apparent existing effective chemotherapy against ependymal tumours nor an absolute clinical advantage with radiotherapy, it is thought that concurrent or sequential receipt of chemotherapy and radiation (chemoradiotherapy) would encourage better patient outcomes. The presumed synergy for their co-treatment is on the basis that residual tumour cells that were not successfully eradicated by radiotherapy at the surgical margin could be targeted through pharmaceutical agents. Efficacies of chemoradiation in CNS tumours have not been consistent, with results yielding from poor outcomes in gliomas (Stupp, Hegi et al., 2009, Lai, Tran et al., 2011) to increased disease-free survival rates in medulloblastoma (Packer, Sutton et al., 1994, Packer, Goldwein et al., 1999). Patient outcomes following chemoradiation have also been investigated in ependymoma. In an early study by Timmermann, Kortmann et al. (2000), participants were administered chemotherapy with a subset having received prior radiotherapy. Nevertheless, chemotherapy showed no significant prognostic impact. The COG ACNS0121 trial also investigated the use of chemotherapy prior to radiotherapy especially in patients with suboptimal tumour debulking. 5 year-event free survival rates for this patient series was found to be less than those with GTR followed by irradiation. This study may have highlighted that radiotherapy may not be as detrimental as originally presumed in young patients yet despite the therapeutic prospect of combining chemotherapy and radiation, its clinical benefit remains speculative in ependymoma.

Complete tumour resection is still put forward as an essential factor for predicting favourable prognoses.

1.2.3 Cell of origin

In an *in vivo* study by Taylor, Poppleton et al. (2005), it was found that radial glial cells (RGCs) are the cells of origin of ependymomas. They showed that the tumours derived from the different CNS regions displayed unique gene expression patterns that resemble those of the progenitor cells that give rise to the structures of their respective compartments. For instance, supratentorial tumours were enriched for components that drive Ephrin and Notch signalling which is essential for neural stem cell maintenance in the cerebral subventricular zone (Conover, Doetsch et al. 2000). On the other hand, spinal tumours displayed an upregulation of HOX gene family members which control anterior-posterior body planning during embryogenesis (Dasen, Liu et al. 2003). Expression of these genes was positively detected *in situ* in the corresponding CNS compartment. Incidentally, the spatiotemporal expression of these signature genes coincided with the time when RGCs differentiate into ependymal cells.

Johnson, R. A., Wright et al. (2010) has substantiated the finding that ependymomas in different CNS regions develop from distinct populations of progenitor cells in the corresponding region. In their study, they demonstrated that challenging cerebral neural stem cells (NSCs) isolated from *Ink4a*$^{-}$*/Arf*$^{-}$ transgenic mice with *Ephb2* developed into tumours that recapitulated the histology of human cerebral ependymomas. This was not observed when the same test was performed using hindbrain-derived NSCs. Comprehensive analysis of transcriptomic profiles also showed indistinguishable expression signatures between *Ephb2*-driven *Ink4a*$^{-}$*/Arf*$^{-}$ cerebral mouse tumours and its human cerebral counterpart. Enrichment of these NSCs for stem cell characteristics resulted in tumour spheres with surface expression of CD133, Nestin, RC2, BLBP (brain lipid binding protein) and GLAST (astrocyte-specific glutamate transporter), which positively identifies RGCs as the cell of origin of ependymomas. These studies highlighted that ependymal tumours of comparable histology develop from anatomically distinct subsets of susceptible RGCs, which obtained mutational combinations that consequently define the various tumour subgroups.

1.2.4 Genetics and molecular background

1.2.4.1 Genomic alterations in ependymoma

Early studies into investigating the genomic changes in ependymoma involved approaches such as karyotypic analysis and Comparative Genome Hybridisation (CGH).

These identified cytogenetic anomalies that are characteristic in paediatric and adult cohorts, suggesting that these tumours are biologically distinct (Kilday, Rahman et al. 2009) (Table 1-2). One common alteration in ependymal tumours is the gain in chromosome 1q which was observed in 50% of paediatric cases but only apparent in 8% of its adult counterparts. Gain of 1q has also been found to correlate with an aggressive tumour phenotype and poor survival outcome especially for tumours of the posterior fossa (Carter, Nicholson et al. 2002, Kilday, Rahman et al. 2009). Fine-mapping of these genomic alterations has established several candidate oncogenes and tumour suppressor genes (TSGs) including *EGFR, TWIST1* and *HDAC9* (chromosome 7), *CDKN2A* (chromosome 9p) as well as *NF2* (chromosome 22) (Yao, Y., Mack et al. 2011), which is associated with a genetic predisposition to various CNS tumours (Ahronowitz, Xin et al. 2007). Details of other fine-mapped candidate genes are shown on Table 1-3.

Table 1-2. CGH studies on ependymomas identified common chromosomal aberrations in paediatric and adult ependymomas.

Paediatric	Loss	1p, 3, 6, 6q, 9p, 13q, 17, 22
	Gain	1q, 7 and 9
Adult	Loss	6, 10, 13q, 14q, 22, 22q
	Gain	2, 5, 7, 9, 12, 18, X

Table 1-3. aCGH studies enabled fine mapping of common gains and losses in epedymoma tumours according to CNS compartment and the genes associated with these genetic abnormalities.

Loss or Gain	**Chromosomal region**	**Tumour Location**	**Genes Associated**
Gain	1q23	Intracranial	*DUSP12, HSPA6*
Gain	1q31-32	Intracranial	*LAMININ, PRELP, GAC1, CHI3L1*
Gain	5p	Intracranial	*hTERT*
Loss	6q21-25	Posterior fossa	*AMD1, CDK11, SASH1, TCP1*
Gain	7	Spinal	*EGFR, TWIST1, HDAC9*
Loss	9p	Supratentorial	*CDKN2A, FREM1, C9orf24, KIAA116*
Gain	9q34	Supratentorial	*NOTCH1*
Loss	10q23	Spinal	*GRID1, MINPP1, TACC2, TUBGCP2*
Loss	17	Posterior fossa	*PRKCA*

Loss	22q11-13	Intracranial	*hSNF5/INI1, SULT4A, C22orf2, CBX7, RAC2, G22P1, MCM5*

Meta-analysis of the CGH data also found a higher prevalence of genomic alterations in adult ependymomas relative to their paediatric counterparts so that the average genomic inconsistency per tumour was 7.5 and 3.8, respectively (Kilday, Rahman et al. 2009). Additional tumour subtyping based on the number and diversity of observed chromosomal changes formed three separate subgroups: structural (little or partial genomic imbalances), numerical (13 or more whole chromosomal losses and gains, usually characteristic of adult ependymomas) and balanced (no chromosomal losses or gains, common in childhood ependymomas) (Dyer, Prebble et al. 2002). Out of the three subtypes, "structural" tumours showed the worst prognosis, which interestingly was the same profile generally adopted by recurring tumours. It is not fully understood why tumours with minimal genomic alterations have a predilection to induce unfavourable patient outcomes relative to those harbouring gross modifications. One theory suggests that since cancers partly mimic the behavior of undifferentiated healthy tissues, deregulation in cellular processes including diversification and self-renewal needs not to be drastic (Scotting, Walker et al. 2005). Therefore, any copy number alterations or mutations that subsequently afflict cells must have affected core oncogenes or tumour-suppressor genes that drive tumourigenesis solely in a spatio-temporal manner. Indeed, the shift to array CGH (aCGH) was an advantage due to its high-throughput and enhanced resolution for mapping small yet more complex alterations that are intrinsic to paediatric tumours (Modena, Lualdi et al. 2006).

1.2.4.2 Copy number-related gene deregulations in ependymoma

From a cohort of 204 tumour samples, Johnson, R. A., Wright et al. (2010) described 9 separate CNS region-specific subgroups based on their mRNA and miRNA expression profiles: supratentorial (A – D), spinal (E – F) and posterior fossa (G – I). Cataloguing the various copy number alterations (CNAs) in these tumours has elucidated gene expression signatures that were distinct to each CNS compartment such as spinal upregulation of chrosomosome 7, 9 and 12-related loci, downregulation in chrosomome 3, 9 and 22q for subgroup C and loss of 6q expression due to deletion in subgroup H. A number of these copy number-associated genes have been established as key ependymoma drivers that regulate processes involving proliferation (*EPHB2*) (Kayser, Nolt et al. 2008) and neural differentiation (*NOTCH1*) (Noisa, Lund et al. 2014) as well as the TSGs *PTEN* and *INK4A/ARF*.

A recent study performed extensive analysis of the CNAs that traverse the ependymoma landscape to elucidate putative genetic drivers of tumour development (Mohankumar, Currle et al. 2015). This study has identified 84 and 39 candidate oncogenes and TSGs respectively, which were more likely to be amplified (3.1x) and deleted (3.7x) across various malignancies according to the Cancer Genome Atlas (TCGA). *In vivo* work narrowed down the candidate oncogenes to 8 following DNA quantification from tumours that developed from oncogene transduction of NSCs (Table 1-4). Similarly, shRNA transduction of NSCs using a >4-fold increase threshold in shRNA sequences in at least two tumours identified 10 TSGs whose knockdown stimulated ependymoma development (Table 1-5).

Table 1-4. Novel ependymoma oncogenes identified in an *in vivo* screen (Mohankumar, Currle et al. 2015). **Key:** ** oncogenes discovered in supratentorial tumours where the *C11orf95-RELA* fusion gene is absent.

Oncogene	Location	Role	Reference
*ZNF668***	Cerebrum	Involved in chromatin relaxation during DNA repair in response to damage	(Hu, R., Wang et al. 2013)
*BCL7C***	Cerebrum	Forms complexes with SWI/SNF for chromatin modifications	(Kadoch, Hargreaves et al. 2013)
*RAB3A***	Cerebrum	Vesicular trafficking leading to cellular secretion	(Leenders, Lopes da Silva et al. 2001)
PRDX2	Cerebrum	Prevents apoptosis induced by oxidative stress	(Lu, Fu et al. 2014)
RTBDN	Cerebrum/ Spinal	Unknown	
AKT2	Cerebrum/ Hindbrain	Known effector of the PI3K signalling pathway	
TMEM129	Spinal	Unknown	
MRPS17	Hindbrain	Encodes for mitochondrial ribosomal protein	(Cavdar Koc, Burkhart et al. 2001)

Table 1-5. Novel ependymoma TSGs identified in an *in vivo* screen (Mohankumar, Currle et al. 2015).	
Novel ependymoma TSGs	**Established/putative TSGs**
ALD3HA1, ACTR1A, SNX6, ULK2, PCMT1	*DNA2, SUFU, STAG1, TET1, ST13*

1.2.5 Ependymoma tumour subgrouping

The enigmatic nature of ependymomas has been highlighted by factors including prognostic variability, inconsistent therapeutic outcomes and heterogeneous tumour behaviour despite manifesting histological similarities. Comprehensive surveying of the genomic landscape of ependymomas has elucidated tumour subgroups arising from the different CNS compartments (Pajtler, Witt et al. 2015) as summarised on Table 1-6.

1.2.5.1 C11orf95/RELA fusion gene

Parker, Mohankumar et al. (2014) employed whole genome sequencing (WGS) and RNA-Seq which identified a genomic anomaly mapping to chromosome 11q12.1-13.3. The random chromosomal rearrangements on this locus led to the fusion of the canonical NF-κB signalling effector, *RELA* gene to the functionally unknown *C11orf95* gene. This fusion gene was exclusive to supratentorial ependymomas, accounting for two thirds of tumours arising in this compartment. In their subsequent functional work, they found a preferential translocation of the fusion protein in the nucleus relative to wild-type RELA followed by an increase in NF-κB signalling and its downstream targets. Mice implanted with NSCs transduced with $RELA^{FUS1\text{-}RFP}$ potently formed ependymal tumours enriched for NF-κB target genes. Moreover, *C11orf95-RELA* negative tumours also contained *C11orf95*-related 'coding' fusion transcripts especially the *YAP1* and *MAML2* transcriptional regulators, suggesting that *C11orf95* could modulate the cellular dynamics of the associated transcription factors. YAP1 (YES-associated protein 1) is a target of the Hippo signalling pathway that control tissue growth and organ size (Zhao, B., Wei et al. 2007) whereas *MAML2* (Mastermind Like Transcriptional Coactivator 2) is a positive regulator of the Notch signalling pathway (Kitagawa 2016), whose activation has already been implicated in supratentorial tumours. However, their oncogenic impact relative to the *RELA* fusion is yet to be determined especially due to their infrequent appearance in supatentorial tumours.

1.2.5.2 Posterior fossa ependymomas

Studies have alluded to the intratumoural heterogeneity in posterior fossa (PF) tumours where two classifications have been described: Group A (PFA, common in infants and younger children that confers poor patient prognosis) and Group B (PFB, more

associated with older cohorts) (Witt, Mack et al. 2011, Mack, Witt et al. 2014, Hoffman, Donson et al. 2014, Wani, Armstrong et al. 2012). Analysis of gene expression profiles using grade II and III ependymomas from two separate cohorts (Toronto and Heidelberg) led to clustering of tumours into Group A (posterior fossa) and Group B (mixed posterior fossa and spinal) in which Group A manifested a significantly poorer prognosis compared to Group B (PFS = 24% vs 92%; OS= 48% vs 98%) (Witt, Mack et al. 2011). Group A also had an overrepresentation for more oncogenic processes including angiogenesis, MAPK signalling and EGFR signalling while Group B predominantly enriched for ciliogenesis. Molecular delineations between the two tumour groups were successively provided in two other studies using immunophenotyping (Hoffman, Donson et al. 2014) and expression level of 10 genes associated with survival (Wani, Armstrong et al. 2012) as parameters.

An extensive scrutiny of the genomic profiles of PFA tumours showed a more balanced genome relative to PFB tumours as characterised by a decreased rate in both Single Nucleotide Variations (SNVs) and recurrent mutations (Mack, Witt et al. 2014). These findings also reflected those genomes of other paediatric CNS tumours including medulloblastoma and neuroblastoma (Robinson, Parker et al. 2012, Pugh, Morozova et al. 2013), implicating the role of epigenetic mechanisms during tumourigenesis. Indeed, PFA tumours manifested a more CpG island methylator phenotype (CIMP) in contrast to the methylome of PFB tumours. CpG island methylations were particularly concentrated on genes that were silenced in a similar manner by the Polycomb repressive complex 2 (PRC2) in embryonic stem cells (ESCs), as indicated by the presence of H3K27me3 signatures on these genes. Therefore, epigenetic mechanisms through DNA methylation-mediated gene silencing presumably of TSGs and genes that regulate cell differentiation, are crucial towards disease pathology in PFA groups.

Recently, PFA tumours have shown further molecular heterogeneity when nine minor subtypes were identified within the two major tumour subgroups: PFA-1 and PFA-2 (Pajtler, Wen et al. 2018). Despite their histological similarities, PFA-1 and PFA-2 tumours along with their subtypes presented with unique molecular and clinical features which highlight individual disease entities (Table 1-7). PFA tumours were also shown to harbour missense mutations in the uncharacterized *CXorf67* gene. CXorf67's binding partners were found to be those that constitute the PRC2 complex, leading to a decrease in H3K27me3 levels which is typical of PFA ependymal tumours (Bayliss, Mukherjee et al. 2016).

The introduction of a detailed PF tumour subgrouping system enabled a better stratification of patients, which denotes a better indicator of prognosis and considers more suitable treatment approaches. For a tumour subgroup that historically conferred dismal patient outcomes, it is therefore imperative to extend its investigation in generating a representative model to validate these proposed causal molecular mechanisms.

Table 1-6. Summary of molecular and clinical details of the various compartment-specific ependymoma subgroups (Pajtler, Witt et al. 2015).

Compartment	**Subgroup**	**Genetics**	**Patient Survival**	**Other details**
Supratentorial	ST-EPN-RELA	Chromothripsis on chromosome 11 leading to the formation of the *C11orf95-RELA* fusion gene	Poor OS	Genes involved in cell cycle and migration, upregulation of NFκB and MAPK pathways
	ST-EPN-YAP1	Chromothripsis on chromosome 11 leading to the formation of the C11orf95-YAP1 fusion gene	Better patient survival	Increased cAMP/carbohydrate metabolism, dopamine signalling genes
	ST-SE	Balanced	Better patient survival	
Posterior fossa	PF-EPN-A	Balanced	Poor OS	Genes involved in cell cycle and migration, MAPK upregulation
	PF-EPN-B	Chromosome instability	Reduced OS relative to PF-SE	Genes involved in ciliogenesis
	PF-SE	Balanced	Better patient survival	High *KIT* expression, fatty acid metabolism
Spinal	SP-MPE	Chromosome instability	Better patient survival	
	SP-EPN	Chromosome instability and loss of 22q		Loss of *NF2* activity
	SP-SE	Loss of 6q		

Table 1-7 Clinical and molecular characteristics of the recently established PFA ependymoma subgroups and subtypes. (Pajtler, Wen et al. 2018)

PFA subgroup	PFA subgroup characteristics	PFA subtypes	PFA subtype-specific characteristics
PFA-1	- enriched for immune/inflammatory, angiogenesis and CNS patterning - local relapse - more associated with 1q gain, 10q loss, 22q loss - H3K27M mutations	PFA-1a	- H3F3A:p.K27M mutations - median age at diagnosis <2 years
		PFA-1b	
		PFA-1c	- poor PFS and OS - highest gain of 1q frequency (73.3%) - high frequency of 6q (23.3%) and 10q (27.9%) loss - median age at diagnosis >5 years
		PFA-1d	- poor PFS and OS
		PFA-1e	- poor PFS and OS - median age at diagnosis <2 years
		PFA-1f	- highest H3K27M mutation frequency (69%) - no CXorf67 expression - median age at diagnosis >5 years
PFA-2	- enriched for cilia functioning - distant relapse - whole chromosome gains (chr. 2, 8, 9, 11 and 19)	PFA-2a	- median age at diagnosis <2 years
		PFA-2b	
		PFA-2c	- better PFS and OS - lowest gain of 1q frequency (0%) - high expression of the OTX2 transcription factor

1.2.6 Ependymoma prognostic markers

Apart from defining the underlying molecular mechanism that drive tumourigenesis, clinical care could also benefit from defining an array of biomarkers that would confer prognostic significance. Retrospective studies have already determined a few markers, some of which are outlined in Table 1-8, including the well-characterised 1q gain which was associated with poor prognosis (Kilday, Rahman et al. 2009). Nevertheless, there is still a need to validate the prognostic relevance of some of these markers in a separate and larger patient cohort.

Table 1-8. Retrospectively identified prognostic markers in paediatric ependymoma.

Biomarker	Prognostic feature	Outcome	Reference
p53	Immunohistochemical positivity	Reduced PFS (p< 0.001) and OS (p= 0.0015)	(Zamecnik, Snuderl et al. 2003)
Bcl-2	Immunohistochemical positivity	Reduced PFS and OS (p< 0.001)	
p14ARF	Labelling index <10%	Reduced PFS (p< 0.001) and increased tumour recurrence (p= 0.0003)	(Korshunov, Golanov et al. 2002)
Tenascin	Immunohistochemical positivity	Reduced PFS (p= 0.0004)	(Korshunov, Golanov et al. 2000)
p27/Kip1	Labelling index <20%	Reduced PFS (p= 0.01)	
EGFR	Immunohistochemical positivity	Reduced PFS (p= 0.009)	
Survivin	High expression levels	Poor patient outcome (p= 0.003)	(Preusser, Wolfsberger et al. 2005)
Chromosome 1q	Gain	Poor patient outcome	(Kilday, Rahman et al. 2009)

Promising results have also been provided using Ki-67 proliferation indices whose increase was associated with poor patient outcome (Figarella-Branger, Civatte et al. 2000). The NSC marker Nestin and EVI1 transcription factor have also been presented as prognostic markers mainly for intracranial ependymomas (Milde, Kleber et al. 2011,

Koos, Bender et al. 2011). A separate study has proposed that hypoxic factors would also offer objective markers of disease outcome (McLendon, Lipp et al. 2015). Indicators of hypoxia would thereby support the use of histological grading to determine patient survival as hypoxia is typical of high grade tumours; a feat that was rejected initially due to subjectivity concerns and confounding variables. An independent study has also put forward the prognostic value of the PI3K signalling pathway in ependymoma (Rogers, Mayne et al. 2013). This survival cascade was shown to be activated in 72% of primary ependymomas which conferred a poorer progression free survival (PFS).

1.3 The PI3K pathway

The phosphatidylinositol (PtdIns) family of lipids is a minor component of eukaryotic cell membranes that are often subject to phosphorylations. Addition of phosphate groups to these membrane-bound lipids forms phosphoinositide species, which participate in cell signalling, lipid signalling and vesicular trafficking (Minogue, Waugh et al. 2006, Clayton, Minogue et al. 2013). Many malignant transformations are usually characterised with a series of signalling transductions often stimulated by the presence of phosphoinositides. The phosphoinositide 3-kinase (PI3K) pathway, in particular, presents a classic example of phosphoinositide-induced signalling cascade whose effects are contributory to the many hallmarks of cancer known today (Fresno Vara, Casado et al. 2004, Fruman, Chiu et al. 2017).

The PI3K pathway is a key survival signalling response that is frequently activated in many cancers including breast (Miller, Rexer et al. 2011), colorectal (Danielsen, Eide et al. 2015) and gliomas (Holand, Salm et al. 2011). Activation of the PI3K pathway regulates an array of biological processes such as cell metabolism, proliferation and motility (Cantley 2002) (Figure 1-3). Canonical PI3K signalling is typically initiated upon the binding of signalling molecules including growth factors and cytokines to receptor tyrosine kinases (RTKs), inducing its dimerisation and autophosphorylation of the intracellular domains (Engelman, Luo et al. 2006). This usually prompts the recruitment of Class I PI3K enzymes onto the plasma membrane where it catalyses the phosphorylation of Phosphotidylinositol (4,5)-bisphosphate (PIP_2) to Phosphotidylinositol (3,4,5)-trisphosphate (PIP_3); a process that is negatively regulated by the PTEN phosphatase. PIP_3 acts as a docking site for the Ser/Thr protein kinase AKT, whose activation by PDK1 and PDK2 (mTORC2) leads to the transduction of signal to downstream effectors (Sarbassov, Guertin et al. 2005, Manning, Toker 2017). As a major survival cellular pathway, much of research has focused on deciphering its biological influence towards tumourigenesis and its promise as a chemotherapeutic target to treat a broad spectrum of malignancies (Fruman, Chiu et al. 2017).

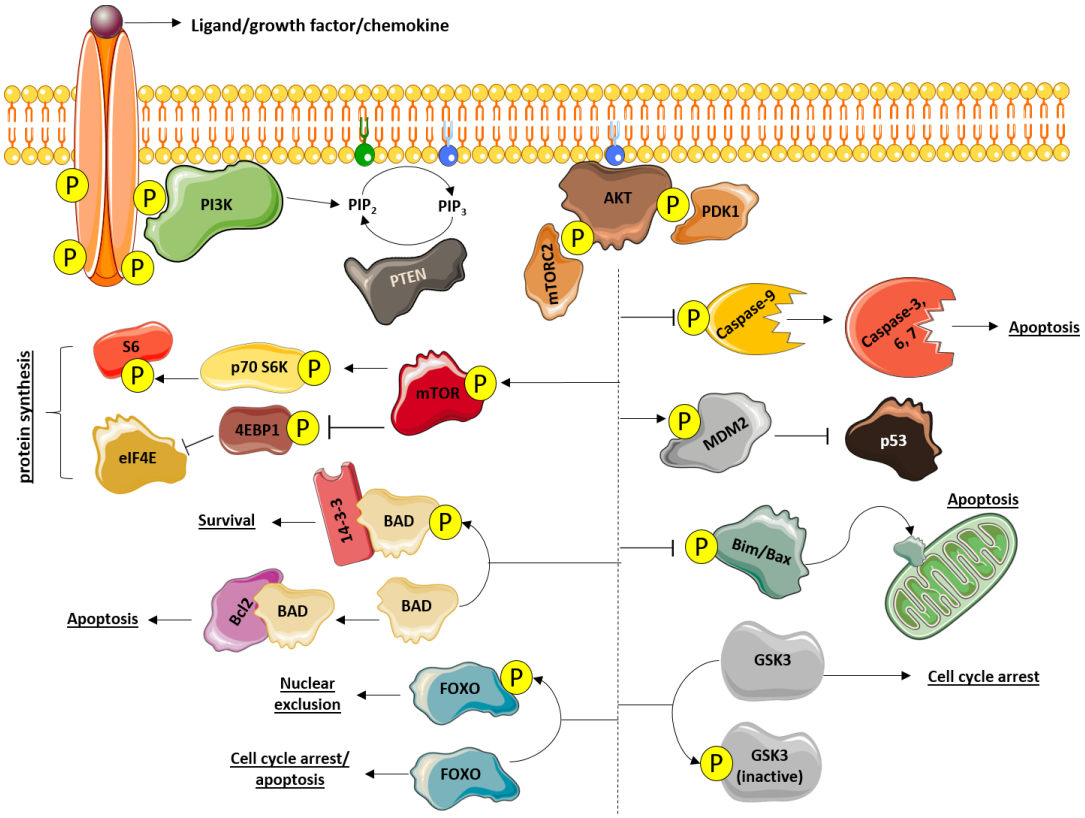


Figure 1-3 Activation of the PI3K enzyme leads to the phosphorylation of PIP_2 to PIP_3, which leads to recruitment of AKT to the plasma membrane. AKT activation following phosphorylation by PDK1 and mTORC2 enables transduction of signal to downstream targets to promote cellular processes including cell proliferation, survival and metabolism.

1.3.1 PI3K enzyme isoforms

PI3Ks are a family of lipid kinases, whose multifunctional roles have been observed in different eukaryotes (Vanhaesebroeck, Leevers et al. 1997). These enzymes are heterodimers consisting of a catalytic subunit and regulatory subunit that use PtdIns as substrates. The PI3K enzymes are divided into three classes based on their structure and substrate specificity. Class I PI3Ks are the most commonly studied and known activators of the canonical PI3K signalling pathway. This class is further subdivided into two subclasses: Class IA and IB. Class IA PI3Ks are characterised by a p110 catalytic subunit and a p85 regulatory subunit. There are three catalytic isoforms belonging to this subclass: p110α *(PIK3CA)*, p110β *(PIK3CB)* and p110δ *(PIK3CD)*, which interact with several p85 isoforms encoded by *PIK3R1* (p85α alongside its known splice variants, p55α and p50α), *PIK3R2* (p85β) and *PIK3R3* (p55γ) (Engelman, Luo et al. 2006). Class IB PI3Ks consist of a p110γ *(PIK3CG)* catalytic subunit, which forms complexes with either p101 *(PIK3R5)* or p87 *(PIK3R6)* regulatory subunits. For these Class I enzymes,

interaction of the regulatory subunit induces an inhibitory effect on the catalytic activity which is relieved upon the activation of cell surface receptors. Class I PI3Ks display some tissue-specific expression patterns so that the p110α and p110β isoforms are ubiquitously expressed in normal tissues whereas p110δ and p110γ are mainly localised in leukocytes (Okkenhaug, Vanhaesebroeck 2003). Evidence from mouse models showed loss of p110α or p110β resulted in early embryonic mortality (Bi, Okabe et al. 1999, Bi, Okabe et al. 2002) whereas p110δ- or p110γ-deficient mice had immune deficits (Sasaki, Irie-Sasaki et al. 2000, Okkenhaug, Bilancio et al. 2002).

Class II PI3Ks are monomeric kinases that exist in 3 isoforms: PI3K-C2α, PI3K-C2β and PI3K-C2γ. Their biological role remains elusive but they are known to preferentially phosphorylate PtdIns and PtdIns(4)P (phosphatidylinositol 4-monophosphate) (Arcaro, Zvelebil et al. 2000). Whether the phosphorylation of these lipid molecules has tumourigenic significance is yet to be elucidated but studies have shown an involvement in several cancer-related functions including angiogenesis (Yoshioka, Yoshida et al. 2012) as well as cell growth and survival (Elis, Triantafellow et al. 2008).

Class III PI3Ks are the least understood in this family of lipid kinases with one known isoform, VPS34. It facilitates the phosphorylation of PtdIns to PtdIns(3)P (Phosphotidylinositol 3-phosphate) and usually dimerises with another cell membrane component called VPS15 *(PIK3R4)* (Araki, Ku et al. 2013). This dimer forms the core of Complexes I and II which are implicated in the regulation of autophagy and vacuolar protein sorting pathways, respectively, as demonstrated in yeast-based studies (Volinia, Dhand et al. 1995, Kihara, Noda et al. 2001). More recent findings have highlighted the presence of analogous functions in higher organisms (Jaber, Zong 2013) where in addition, Class III PI3Ks have also been involved in the activation of the mTOR signalling pathway following changes in nutrient availability (Backer 2008).

1.3.2 AKT isoforms

AKT, also known as Protein Kinase B (PKB), is a Ser/Thr protein kinase which acts as the primary effector of the canonical PI3K signalling pathway. There are three known mammalian isoforms of AKT namely *AKT1*, *AKT2* and *AKT3*, which share a high degree of homology (~80%) (Vanhaesebroeck, Alessi 2000). Despite their structural similarities, studies have characterised AKT isoform-specific physiological roles as well as differential expression patterns. AKT1 and AKT2 are globally expressed while AKT3 is mainly expressed in brain, cardiac and kidney tissues (Koseoglu, Lu et al. 2007). *In vivo* studies demonstrated embryonic lethality in AKT1/AKT2 KO mice (Peng, Xu et al. 2003),

while AKT3 KO led to issues in brain development (Tschopp, Yang et al. 2005). AKT2 also presented a role in regulation of insulin signalling and development of diabetes (Cho, Mu et al. 2001). Non-overlapping functions between AKT isoforms were also validated in cancer studies such as AKT2's involvement in migration which is negatively regulated by AKT1 (Irie, Pearline et al. 2005). This was substantiated in a separate study where AKT2 is more likely to be recruited to the membrane in regions where focal adhesions are formed than AKT1 (Arboleda, Lyons et al. 2003). Despite their intrinsic differences, all isoforms are equally activated by canonical PI3K signalling and have implied oncogenic roles in a context-dependent manner.

1.3.3 Downstream targets and PI3K signalling crosstalk

The PI3K signalling pathway has a wide range of downstream targets that are regulated to support normal and healthy cell functioning. Characterisation of its complex network has elucidated multiple mechanisms that account for the diverse cellular behaviours, many of which have been deregulated in human diseases such as cancer. This section briefly outlines a subset of these PI3K/AKT pathway targets and their molecular impact during tumourigenesis.

1.3.3.1 The mTOR signalling pathway

The mTOR signalling pathway is a common direct target of AKT following activation of the PI3K pathway. mTOR (mammalian target of rapamycin) is a protein kinase that preferentially phosphorylates its substrates on serine or threonine residues. Following activation of canonical PI3K signalling, AKT negatively regulates a heterodimeric GTPase-activating protein (GAP) called TSC (tuberous sclerosis) 1/2 complex. This prevents the hydrolysis of GTP that is bound to the Rheb protein thus maintaining its active GTP-bound state (Inoki, Li et al. 2003). Rheb-GTP then interacts with mTOR to activate it, prompting multiple proteins to assemble with mTOR to form either the mTORC1 or mTORC2 complex (Figure 1-4).

The mTORC1 complex is composed of four proteins, alongside mTOR, which include Raptor, mLST8, PRAS40 and DEPTOR (Peterson, Laplante et al. 2009). mTORC1-mediated signalling is associated with anabolic processes, particularly lipogenesis through regulation of the sterol regulatory element binding protein 1 (SREBP1) (Porstmann, Santos et al. 2008) and protein synthesis. Formation of the protein synthetic machinery involves mTORC1 targeting of the p70S6 kinase which phosphorylates the S6 ribosomal protein to commence protein translation. mTORC1 also phosphorylates the eIF4E (eukaryotic translation initiation factor 4E) whose role is to

trigger the formation of translation pre-initiation complexes on the newly transcribed mRNA prior to protein synthesis (McKendrick, Morley et al. 2001). It further phosphorylates eIF4EBP1 (eukaryotic translation initiation factor 4E-binding protein 1) to prevent its sequestering effect on the eIF4E proteins thus ensuring that translation takes place (Jiang, Coleman et al. 2003).

mTORC1 also serves as a sensor for changes in nutritional availability (Howell, Manning 2011) in a mechanism that is yet to be understood. In the event of ATP or nutrient depletion, an increase in intracellular AMP activates the AMP-dependent protein kinase (AMPK) (Hardie 2007) which phosphorylates the TSC1/2 complex. This stimulates its GTPase activity leading to the formation of the inactive Rheb-GDP form and consequent loss of mTOR signalling. One effect of mTOR signalling inhibition is an upregulation in autophagic responses. The absence of the mTORC1 complex relieves the inhibitory effect on the ULK1/Atg13/FIP2000 kinase complex (Alers, Loffler et al. 2012) which is necessary for the maturation of autophagolysosomes that mediate the degradation of intracellular components. This establishes a recycling mechanism where components could then be reused for further cellular purposes. Other functions associated with mTORC1 signalling involve mitochondrial metabolism (Cunningham, Rodgers et al. 2007) and peroxisome proliferator-activated receptor-γ (PPARγ) (Kim, J. E., Chen 2004) transcription factors.

In contrast, the mTORC2 is a complex of six proteins: three of which are also mTORC1-associated proteins (mTOR, DEPTOR, mLST8) with the rest being mTORC2 specific (Rictor, mSIN1, Protor-1). Unlike the well-characterised role of mTORC1 signalling, mTORC2-mediated processes are less understood. In a study by Sarbassov, Guertin et al. (2005), mTORC2 was necessary for the full activation of the PI3K/AKT signalling axis. It phosphorylates AKT on Ser473, which alongside Ser308 phosphorylation by phosphoinositide-dependent kinase 1 (PDK1) enables signal transduction to downstream effectors that mediate cell survival and proliferation. This was supported by another study where incomplete activation of AKT due to loss of mTORC2 activity enhanced the activity of the forkhead box O-subfamily (FOXO) transcription factors (Calnan, Brunet 2008), particularly FOXO1 and FOXO3, by maintaining its dephosphorylated form. The serine-threonine protein kinase SGK1 was also found to be a downstream target of the mTORC2 complex (Yan, Mieulet et al. 2008). Activation of SGK1, which shares sequence homology with AKT, was shown to promote survival responses in cells (Mikosz, Brickley et al. 2001) and withdrawal of mTORC2 signalling induces a fall in SGK1 basal activity. Other studies have also suggested the implication of mTORC2 in cytoskeletal structuring, particularly through the activation of PKC and

consequently its associated targets (Jacinto, Loewith et al. 2004, Angliker, Ruegg 2013, Sen, Xie et al. 2014).

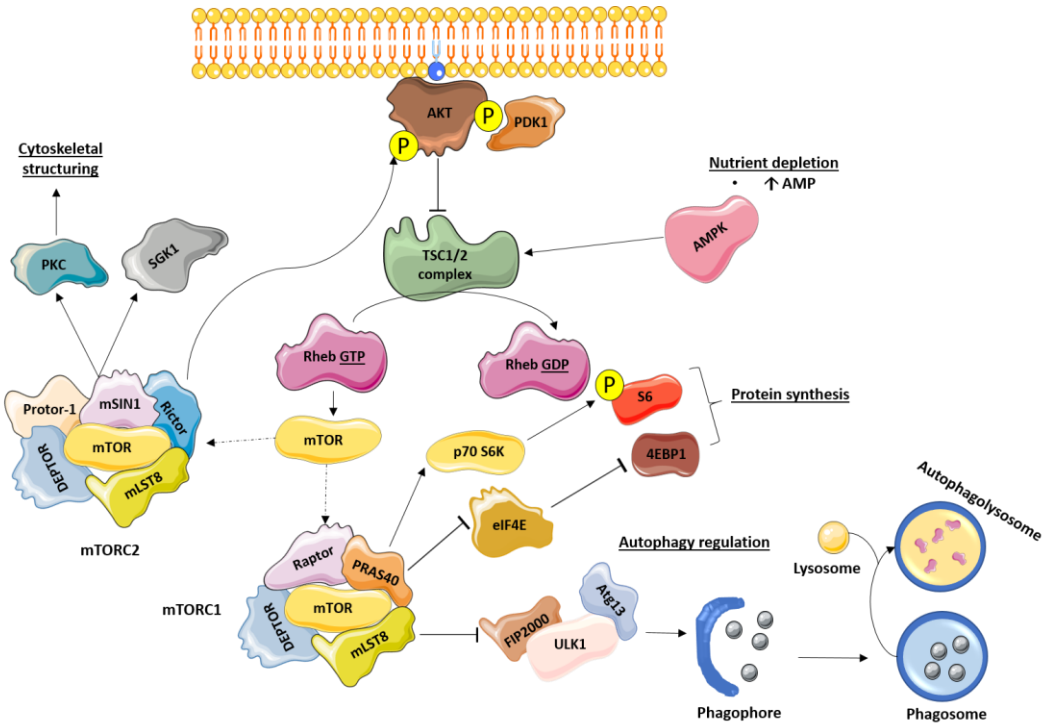


Figure 1-4 AKT activates the mTOR signalling pathway through the negative regulation of the TSC1/2 complex. Proteins assemble with mTOR to form either the mTORC1 or mTORC2 complex. mTORC1 is known to regulate processes such as protein synthesis and autophagy. mTORC2's function is less understood but is implicated in the full activation of AKT and cytoskeletal structuring.

1.3.3.2 The Wnt pathway

The highly conserved Wnt signalling pathway regulates a number of embryogenic processes such as determination of cell fate, proliferation and migration (Garcin, Habib 2017). Deregulated Wnt signalling has also been reported in cancer development, highlighting its clinical importance as a pharmaceutical target (Tai, Wells et al. 2015). The PI3K/AKT pathway could activate the Wnt signalling pathway by phosphorylating Glycogen Synthase Kinase 3β (GSK3β) to inhibit it (Figure 1-5). This negatively regulates the activity of the Destruction complex consisting of GSK3β, Axin and Adenomatous polyposis coli (APC), causing β-catenin to accumulate and induce transcription of target genes (e.g. *MYC* and Cyclin-D1, *CCND1*) following nuclear translocation (Cross, Alessi et al. 1995). GSK3β is also inhibited by the p70S6 kinase as a result of signalling through the mTOR pathway (Zhang, H. H., Lipovsky et al. 2006). Interestingly, the loss of GSK3β preserves mTOR signalling since it works in conjunction with AMP Kinase (AMPK) to activate the TSC1/2 complex which causes formation of the inactive Rheb-GDP and prevents activation of mTOR prior to the formation of mTORC complexes (Kwiatkowski, Manning 2005). Moreover, the inhibitory effect of the mTOR pathway on autophagic

responses prevents the degradation of Dsh (Gao, Cao et al. 2010), thus stimulating β-catenin transcription of genes.

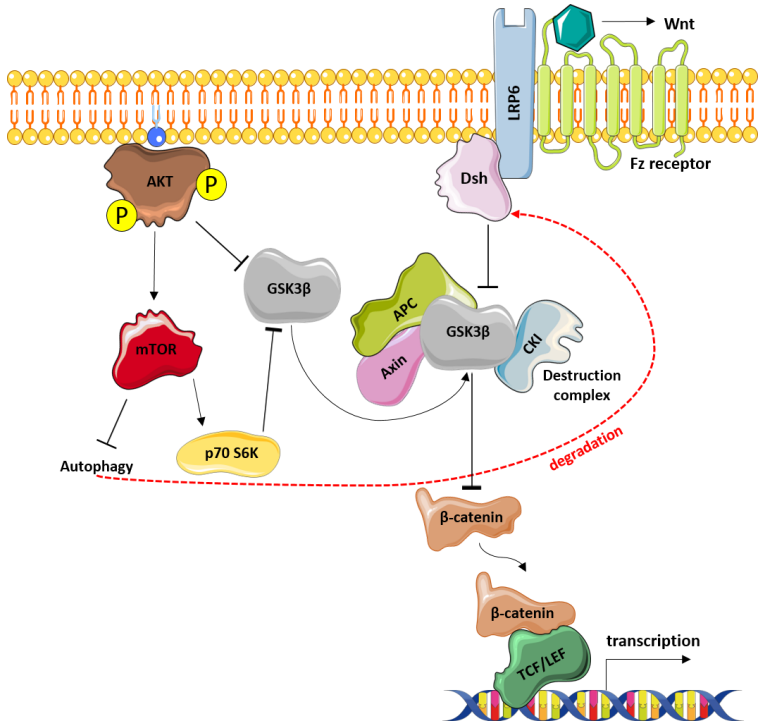


Figure 1-5 AKT negatively regulates GSK3β which is a component of the Destruction complex in the Wnt signalling pathway. The downregulation in its function leads to the stabilisation of β-catenin and increase in expression of target genes. Activation of the mTOR pathway through the p70S6 kinase negatively regulates GSK3β as well as the inhibition of autophagy-mediated degradation of the Dsh protein.

1.3.3.3 The NF-κB pathway

Gene expression of the NF-κB family of transcription factors is vital for mediating stress-related responses as well as regulating autoimmune functions following bacterial or viral antigen presentation (Wullaert, Bonnet et al. 2011). The most ubiquitously expressed form of NF-κB in many cells is the p65-RELA/p50 heterodimer (Oeckinghaus, Ghosh 2009). NF-κB is normally sequestrated in the cytoplasm by IκB proteins. IKKα has been shown to be a downstream target of AKT (Bai, Ueno et al. 2009). AKT activates IKKα by phosphorylating Thr-23, causing it to target IκB towards proteolytic degradation and consequently releasing NF-κB from physical sequestration. This increases the expression of NF-κB target genes that are usually involved in cell growth and proliferation (Guttridge, Albanese et al. 1999, Piva, Belardo et al. 2006) (Figure 1-6). Activation of the NF-κB pathway in cancers could therefore be considered as a protective mechanism particularly when exposed to the physiological stressors such as those from an inflammatory response.

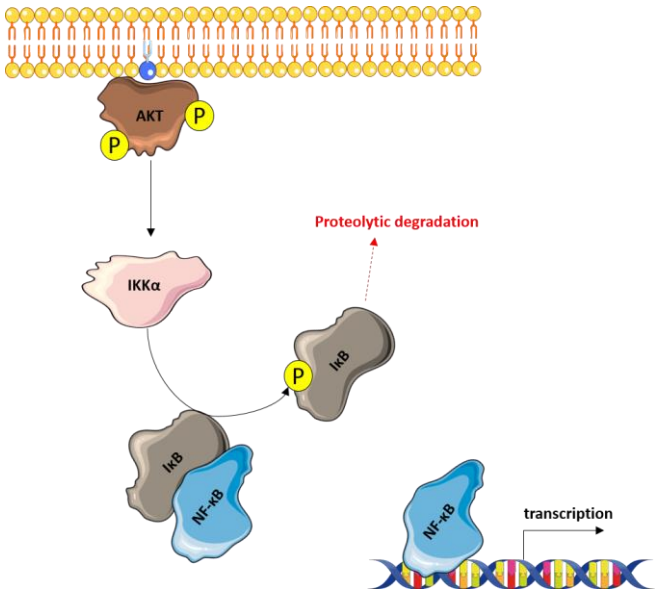


Figure 1-6 AKT regulates IKKα proteins, which in turn phosphorylate IκB. When phosphorylated, IκB is targeted towards proteolytic degradation thus relieving its sequestering effect on NF-κB and allowing its translocation into the nucleus to initiate gene expression.

1.3.3.4 The MAPK/ERK pathway

The Mitogen Activated Protein Kinase (MAPK) pathway is a protein kinase signalling cascade that regulates biological processes associated with growth, proliferation and cell survival (Mebratu, Tesfaigzi 2009). The overlapping functions between the MAPK/ERK and PI3K/AKT pathways have alluded to the possible modes of inter-pathway crosstalks that would consequently contribute towards tumourigenesis. Following activation of RTKs, docking proteins such as GRB2 would bind to phosphotyrosines in the intracellular domain of RTKs through their SH2 domain, which in turn would recruit a guanine nucleotide exchange factor (GEF) called mSOS through its SH3 domains. The resulting GRB2/mSOS complex stimulates GDP to dissociate from Ras to allow GTP binding to activate it. Ras-GTP binds and activates the Raf kinase, initiating the phosphorylation cascade from MEK to MAPK to its downstream targets (Figure 1-7). The PI3K pathway can influence MAPK signalling in various ways. One study showed that AKT-facilitated phosphorylation of Raf inactivates it, causing a reduction in MAPK signalling output (Zimmermann, Moelling 1999). Several studies have elucidated the significance of this crosstalk on cell differentiation (Reusch, Zimmermann et al. 2001) and chemotherapeutic outcome (Lee et al., 2008). Interestingly, it has been demonstrated that inhibition of Raf by PI3K/AKT was also necessary for cellular transformation (Cheung, M., Sharma et al. 2008). Another crosstalk highlighted in a different study showed that Rheb-GTP, which activates the mTOR pathway, could also interact with Raf to regulate its activity (Yee, Worley 1997).

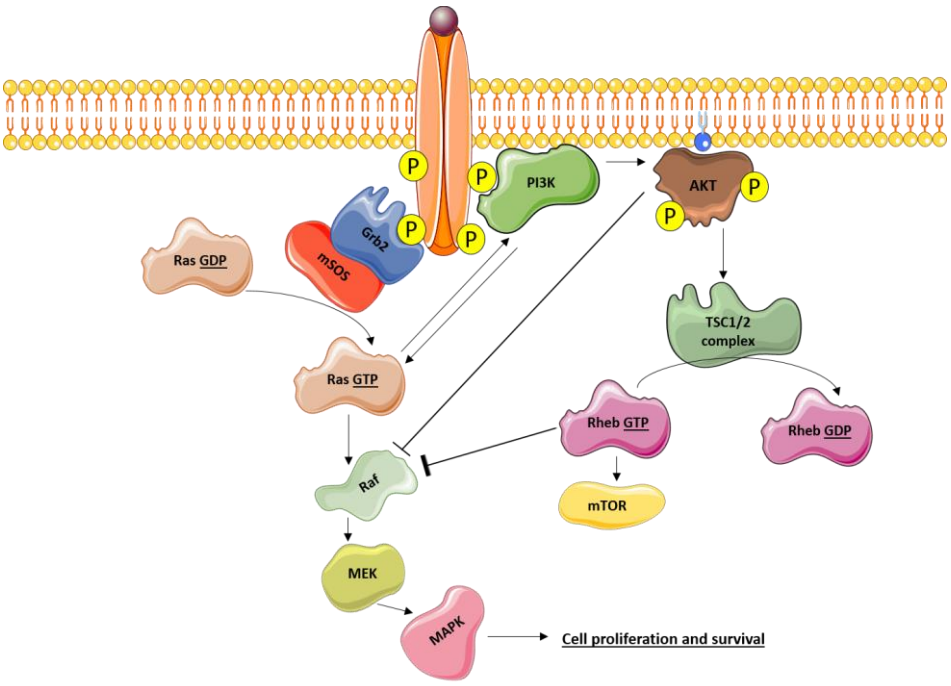


Figure 1-7 The MAPK pathway is another survival signalling pathway that is commonly activated alongside the PI3K pathway. The PI3K pathway can also regulate MAPK signalling through the regulation of Ras-GTP by PI3K as well as the inhibition of Raf by both AKT and Rheb-GTP.

1.3.3.5 Forkhead box proteins (FOXO)

Signalling through the PI3K pathway negatively regulates the activity of the FOXO family of transcription factors. Phosphorylation of FOXOs by AKT triggers their sequestration from the nucleus by binding to 14-3-3 proteins (Van Der Heide, Hoekman et al. 2004). This also targets FOXOs towards degradation by the Ubitquitin Proteosome Pathway (UPP) (Matsuzaki, Daitoku et al. 2003). FOXO activity is also regulated by other kinases including CDK2 and IKK (Huang, Regan et al. 2006, Huang, Tindall 2011). Increased FOXO activity exerts its tumour suppressive effects through promotion of cell cycle arrest and apoptosis (Greer, Brunet 2005). Indeed, the role of FOXO as a negative regulator of tumourigenesis has been demonstrated in many solid and haematological malignancies (Modur, Nagarajan et al. 2002, Seoane, Le et al. 2004, Kikuchi, Nagai et al. 2007).

1.3.3.6 Regulators of cell cycle

The PI3K pathway imposes a stringent control over cell cycle progression by regulating factors that facilitate transition between cell cycle phases. For instance, activation of the PI3K pathway inhibits the activity of several members of the Cip/Kip family such as $p27^{kip1}$ (Sekimoto, Fukumoto et al. 2004) and $p21^{cip1}$ (Heron-Milhavet, Franckhauser et al. 2006). Cip/Kip proteins induce cell cycle arrest by suppressing the

functioning of cyclin dependent kinase (CDK)/cyclin complexes in contrast to the Ink4a family of proteins which competitively bind to CDK4 and CDK6 (Sherr, Roberts 1999) with cyclin D. It is also interesting that the expression of these cyclin dependent kinase inhibitors (CDKi) could be facilitated by FOXO. In one study, loss of FOXO activity resulted in a downregulation of p27 expression (Medema, Kops et al. 2000) whereas $p15^{Ink4b}$- and $p19^{Ink4d}$-associated cell cycle arrest was mediated by FOXO (Katayama, Nakamura et al. 2008). FOXO could also promote cell cycle arrest by expressing members of the Retinoblastoma (Rb) family of proteins (Kops, Medema et al. 2002) and Bcl-6 which acts as a transcriptional repressor of the cyclin D2 (*CCND2*) gene (Fernandez de Mattos, Essafi et al. 2004). Since most of these impede CDK4/6-cyclin D activity, an arrest at the G_1/S phase of the cell cycle is observed. This usually involves the hypophosphorylation of the Rb protein which consequently sequesters members of the E2F family of transcription factors (e.g. E2F1) that are responsible for the expression of genes required to progress through the cell cycle (Martelli, Livingston 1999) (Figure 1-8).

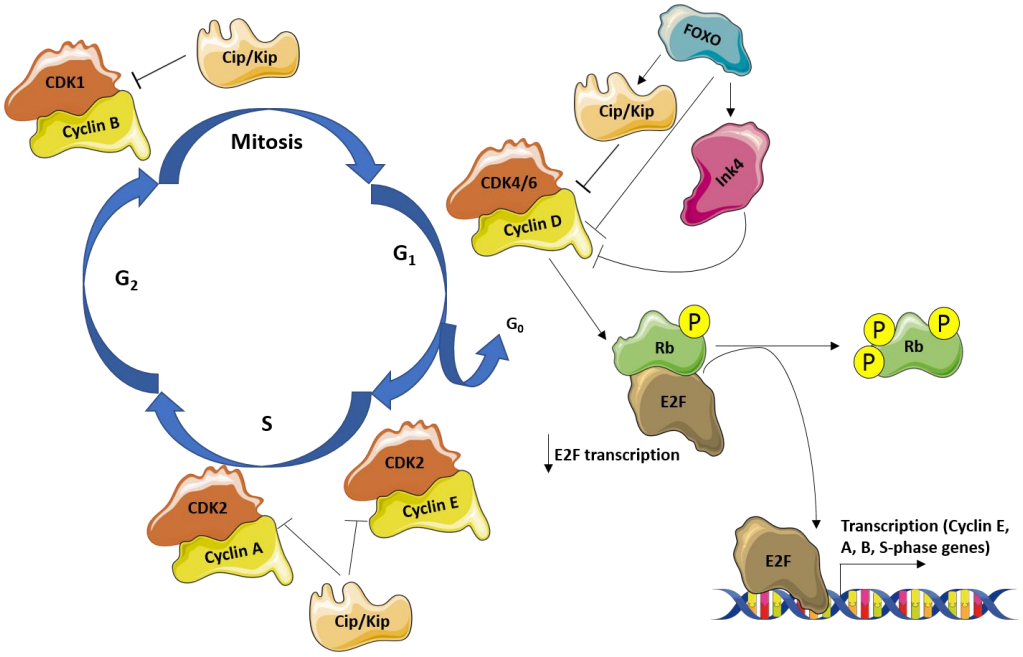


Figure 1-8 Activation of the PI3K pathway negatively regulates the cell cycle, partly through the inactivation of FOXO proteins. FOXO is usually associated with increased expression of intracellular cell cycle inhibitors such as the Cip/Kip (CDK/cyclin inhibitors) and Ink4 (CDK4/6-specific inhibitors) proteins whose functions ultimately induce cell cycle arrest. One of the affected proteins following loss of CDK4/6-cyclin D activity is Rb. In its hypophosphorylated state, Rb binds to E2F transcription factors to prevent their translocation into the nucleus where they initiate expression of genes necessary to proceed through the cell cycle. The cells become arrested at G_1/S as a result.

1.3.3.7 Regulators of cell survival

The PI3K pathway often inhibits cell death programs, particularly apoptosis, by negatively regulating their respective molecular drivers. Among the downstream substrates of AKT are pro-apoptotic proteins such as the Bcl-2 BH3-only protein BAD whose phosphorylation on Ser136 signals for 14-3-3-mediated sequestration from the mitochondria where it would normally be localised (Zha, Harada et al. 1996, Datta, Dudek et al. 1997). AKT also activates the E3 ubiquitin ligase, MDM2 whose role is to polyubiquitinate p53 to target it towards proteasomal degradation (Mayo, Donner 2001). As a result, expression of p53 targets including other pro-apoptotic members of the Bcl-2 gene family (e.g. Bax and PUMA) is suppressed (Yu, Z., Wang et al. 2009). Further survival influences of the PI3K pathway include downregulation of FOXO-targets including *FasL* and *BCL2L11* (Bim) (Huang, Tindall 2007), which are known mediators of apoptosis. An increase in pro-apoptotic proteins leads to binding to anti-apoptotic proteins that are located on the outer membrane of the mitochondria. This changes the permeability of mitochondrial membrane, releasing apoptotic factors including Smac/Diablo and Cytochrome c to initiate the sequential activation of the caspase-family of proteases, which facilitate intracellular degradation (Adrain, Creagh et al. 2001) (Figure 1-9).

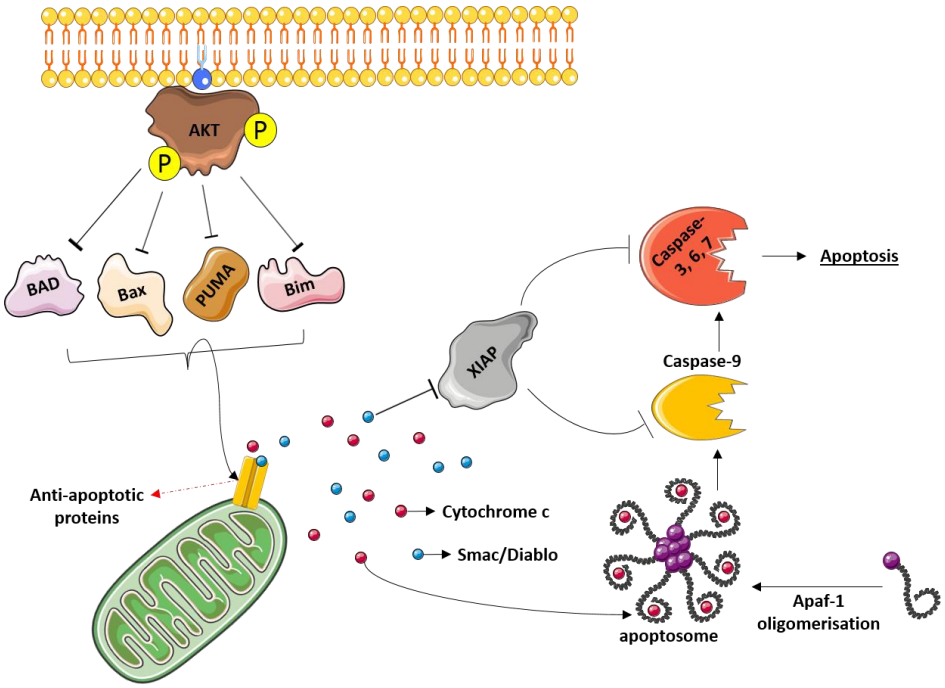


Figure 1-9 PI3K signalling negatively regulates activation of apoptosis. Inhibition of pro-apoptotic proteins, through AKT phosphorylation, prevents formation of channels with anti-apoptotic proteins localised in the mitochondrial outer membrane. In effect, Smac/Diablo and Cytochrome c are not released. Smac/Diablo inhibits the X-linked inhibitor of apoptosis protein (XIAP) which blocks the activity of caspases. Cytochrome c forms complexes with the oligomerised Apaf-1 proteins to form the apoptosome which instigates the cleavage of caspases that mediate intracellular degradation.

1.3.4 Aberrant activation of the PI3K pathway in cancers

Genomic studies have identified that genes encoding for various components of the PI3K signalling pathway are often mutated somatically or in the germ line resulting in its constitutive activation and subsequent development of malignancies (Vahidnezhad, Youssefian et al. 2016). Such mutations, which will be highlighted in this section, have been characterised in a broad spectrum of cancers including breast, leukaemias and gliomas (Millis, Ikeda et al. 2016).

1.3.4.1 Alterations in Class I catalytic subunits

Increased Class I PI3K enzymatic activity, leading to increased signalling output has been implicated in tumourigenesis (Thorpe, Yuzugullu et al. 2015). Enhanced PI3K activity has been shown to arise from genetic mutations in all structural domains of the enzyme. In the *PIK3CA* (p110α) gene, there are mutational hotspots identified in several cancers which usually result in an increased catalytic activity of the enzyme. These notable activating mutations include E542K and E545K located in the helical domain while H1047R is mapped onto the kinase domain, all of which have been confirmed to possess transforming capabilities (Isakoff, Engelman et al. 2005, Kang, Bader et al. 2005). In one systematic review (Karakas, Bachman et al. 2006), cancers such as breast and liver were found to have a high mutation frequency implicating the presence of additional *PIK3CA* mutations that affect other structural domains of the enzyme. It is further highlighted that such mutations would alter the enzyme's overall structure to recapitulate that of an active conformation (Burke et al., 2012). Unlike p110α, mutations in other Class I PI3K enzymes in cancer are not as common albeit they have copy number gains which typically lead to their upregulation (Thorpe et al. 2015). *In vitro* evidence has demonstrated these isoforms' oncogenic properties when overexpressed in cells with each having distinct modes of upstream activation and regulation of downstream processes (Kang, Denley et al. 2006).

Indeed, copy-number related upregulation of Class I PI3K has been identified in a proportion of solid tumours. These include p110δ in gliomas (Luk, Piekorz et al. 2012), p110γ in medulloblastoma (Guerreiro, Fattet et al. 2011) and p110α in lung and ovarian cancers (Okudela, Suzuki et al. 2007, Kolasa, Rembiszewska et al. 2009). Immunohistochemical data in one study showed a significant correlation between copy number gain and increased expression profile of Class I enzymes (Cui, Cai et al. 2014), which was also found to be related with poor prognosis.

1.3.4.2 Alterations in Class I PI3K regulatory subunits

The p85 regulatory subunit and its related isoforms are essential in negatively regulating the kinase activity of Class I PI3K enzymes, thus implicating a potential source of aberrant PI3K functioning and subsequent development of cancers. *PIK3R1* (p85α) mutations, for instance, have been discovered in several malignancies including endometrial cancer (Cheung, L. W., Hennessy et al. 2011) and glioma (Brennan, Verhaak et al. 2013). Mutational hotspots have been specifically mapped to the iSH2 (inter-Src homology 2) domain of the subunit (Jaiswal, Janakiraman et al. 2009) which directly binds to p110. Downregulation of *PIK3R1* as a result of a missense mutation was also reported in colorectal cancer (Cheung, L. W., Mills 2016) while this presented as a significant prognostic factor in breast cancer (Cizkova, Vacher et al. 2013). The result from these p85α mutants is often an increased PI3K activity despite still being able to form a stable heterodimer with p110. One study further demonstrated a more pronounced cancer phenotype in renal cell carcinoma following reduced *PIK3R1* expression, suggesting a possible link to tumour grade and progression (Lin, Y., Yang et al. 2015). Mutations in the *PIK3R2* gene, encoding for the p85β regulatory subunit, have also been determined although at a less frequent rate. Unlike p85α, p85β increases PI3K enzyme activity as validated by work on mouse models (Gonzalez-Garcia, Carrera 2012). Further enhancement of PI3K functioning from basal rate was observed as a result of some of these *PIK3R2* mutations, which consequently favour tumourigenesis (Cheung, L. W., Hennessy et al. 2011).

1.3.4.3 Alterations in Class II and III PI3K enzymes

As discussed in section 1.3.1, there has been little work into exploring the oncogenic role of Class II PI3K enzymes. In one study on GBM, *PIK3C2B* was amplified in a subset of tumours which was linked to an increase in PIK3C2B mRNA levels (Knobbe, Reifenberger 2003). Genomic surveillance also revealed other somatic mutations on *PIK3C2B* yet their biological effects remain undetermined (Kind, Klukowska-Rotzler et al. 2017). The oncogenic relevance of Class II PI3Ks was further supported in another *in vivo* study, in which reduction of *Pik3c2a* (PI3K-C2α) activity suppressed tumour growth as an effect of compromised blood vessel formation (Yoshioka, Yoshida et al. 2012).

Similar to Class II PI3Ks, there is scarcity in research regarding the contribution of Class III PI3K enzymes towards tumour development. Recent evidence showed that VPS34 can activate mTOR signalling through downregulation of TSC2 whose induction of the inactive Rheb-GDP form consequently prevents the formation of mTORC complexes (Mohan, Shen et al. 2016). In the same study, the authors demonstrated that inhibition of the mTOR pathway reverses the VPS34's transforming effects *in vitro*.

However, VPS34-mediated activation of the mTOR pathway is of a non-canonical manner and understanding its own unique signalling network would therefore help determine how this could be further exploited from therapeutic point of view.

1.3.4.4 Loss of PTEN

The lipid phosphatase activity of PTEN is an essential negative regulator of PI3K signalling activation as it catalyses the dephosphorylation of PIP_3 to PIP_2. Loss of PTEN activity is commonly found in many cancers as a mechanism for the deregulation of PI3K signalling. The *PTEN* locus, chromosome 10q23, is often subject to inactivating mutations and epigenetic silencing that leads to its downregulation during tumourigenesis (Song, Salmena et al. 2012). Carriers of *PTEN* mutations usually develop a condition called PTEN Hamartoma Tumour Syndrome (PHTS) which is subdivided into four disorders: Cowden syndrome, Bannayan-Riley-Ruvalcaba syndrome, PTEN-related Proteus syndrome and Proteus-like syndrome (Mester, Eng 2012). This autosomal dominant condition confers a predisposition to developing benign and malignant tumours, particularly breast, thyroid and endometrium (Tan, M. H., Mester et al. 2011). Somatic mutations have been identified across the gene sequence with some concentrating on a few mutational hotpots particularly those affecting Arg130, Arg173 and Arg233 (Song et al. 2012). Knockout of PTEN in mice recapitulates clinical characteristics of patients with PHTS (Stambolic, Tsao et al. 2000). Interestingly, evidence suggests that tumourigenesis following loss of PTEN is associated with the activity of p110β PI3K isoform instead of p110α (Jia, Liu et al. 2008, Ni, Liu et al. 2012), thus warranting the use of p110β-isoform specific inhibitors in this pathological context. On the other hand, reliance of PTEN loss on specific PI3K isoforms may actually be dependent on which isoform is predominantly expressed in tissue compartments. For instance, T-cell acute lymphoblastic leukaemia originates from p110δ and p110γ activity in thymocytes that lack PTEN activity (Subramaniam, Whye et al. 2012) while p110α is necessary for suprabasal cell viability of the epidermis in mouse models of PHTS (Wang, Q., Von et al. 2013).

1.3.4.5 Alternative activation of the PI3K pathway during cancer development

Maintenance of PI3K signalling in cancer also comes from external signalling cues that directly regulate various components of the PI3K pathway. For instance, small GTPases can directly activate Class I PI3K enzymes. Ras mutations are potent oncogenic drivers found in about 25% of human malignancies (Hobbs, Der et al. 2016). Such mutations confer a defect in GTP hydrolysis thus maintaining its active GTP-bound state. In cancers driven by mutant Ras, its physical binding with Class I PI3K enzymes was observed through the Ras binding domain (RBD) in a manner similar to wildtype Ras. *In vivo* models of lung cancer and leukaemia have demonstrated the importance of this

interaction in sustaining tumourigenic responses (Castellano, Sheridan et al. 2013, Gritsman, Yuzugullu et al. 2014) (Castellano et al., 2013; Gritsman et al., 2014). Moreover, it was also found that activating *KRAS* mutations were linked with increased AKT functioning in Wilms tumours (Polosukhina, Love et al. 2017) as reflected by earlier studies on other cancers. Furthermore, *in vitro* evidence highlighted the unique properties of p110β during cellular transformation where its activation required binding to other small GTPase proteins such as RAC1 and CDC42 (Fritsch, R., de Krijger et al. 2013). In one study, RAC1 and CDC42 expression was shown to stimulate angiogenesis and advanced TNM (tumour, lymph node and metastasis) staging in breast cancer (Ma, J., Xue et al. 2013).

PI3K signalling can also be stimulated through the action of G-Protein Coupled Receptors (GPCRs) (Figure 1-10) (Murga, Laguinge et al. 1998). Interestingly, GPCRs could use Rho GTPases to activate p110β PI3K signalling (Fritsch et al. 2013). Conversely, it has been shown that the interaction of the G-protein's $G_{\beta\gamma}$ subunits with the PI3K's regulatory subunit consequently stimulates AKT-mediated regulation of downstream processes including cell cycle and apoptosis (Murga, Laguinge et al. 1998, Schwindinger, Robishaw 2001, Goel, Phillips-Mason et al. 2002). One study has alluded to the putative oncogenic role of GPCRs where these were identified to be upregulated in various cancers through gene expression analysis (Li, S., Huang et al. 2005). However, it is also put forward that activation of PI3K signalling is dependent upon the cell type, environmental cues as well as the GPCR involved. Coupling of GPCR activation with PI3K signalling may not necessarily stimulate tumourigenicity suggesting that this interaction is modulated on a context-dependent basis (Bar-Shavit, Maoz et al. 2016).

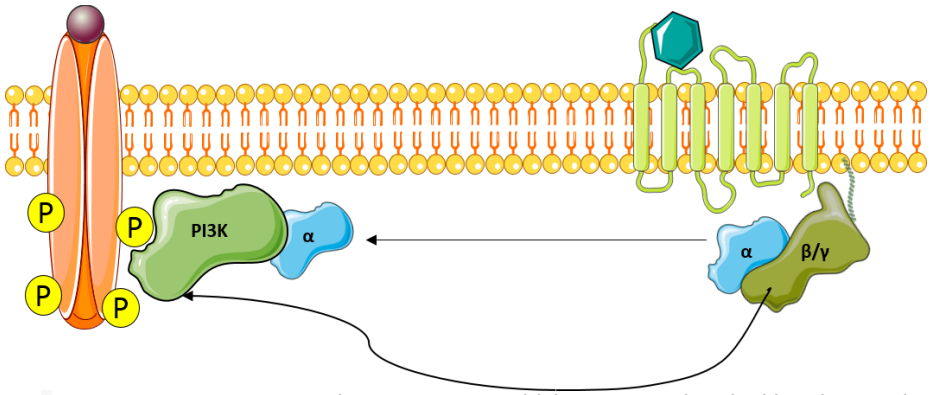


Figure 1-10 GPCRs are a 7-transmembrane receptor which are associated with a heterotrimeric G-protein. Usually upon its activation, the α-subunit dissociates from the β/γ subunits where it activates several targets including the PI3K enzyme. Studies have also shown that the β/γ subunits can also interact with the PI3K enzyme to activate the PI3K/AKT signalling node.

1.4 Activation of PI3K signalling in paediatric brain tumours

Studies have suggested the PI3K pathway as a potential prognostic marker and therapeutic target in several paediatric brain tumours (Faury, Nantel et al. 2007, Pollack, Hamilton et al. 2010, Rodriguez, Scheithauer et al. 2011, Rogers, Mayne et al. 2013). Activation of PI3K signalling in these tumours has been associated with mutations and alterations in several components of the pathway. The commonly mutated *PIK3CA* gene has been identified in several cases of paediatric high grade glioma (pHGG) (Gallia, Rand et al. 2006) and diffuse intrinsic pontine glioma (DIPG) (Grill, Puget et al. 2012, Wu, G., Diaz et al. 2014). *PIK3CA* mutations were also found in medulloblastomas (Robinson, Parker et al. 2012)but these tumours usually harbour amplification in genes encoding for Class I PI3K enzymes which often lead to their overexpression (Guerreiro, Fattet et al. 2011, Northcott, Shih et al. 2012, Shymanets, Prajwal et al. 2013). Decrease in *PTEN* activity was identified in medulloblastoma as a result of inactivating mutations, copy number loss and epigenetic silencing (Hartmann, Digon-Sontgerath et al. 2006, Parsons, Li et al. 2011). Aberrations in pHGG on the 10q locus, encompassing *PTEN,* have also been reported (Diaz, Baker 2014). Another study has described genetic alterations in genes encoding Class II PI3K enzymes (*PIK3C2B* and *PIK3C2G*) in pHGG but at low frequencies (Paugh, Qu et al. 2010). Moreover, it is postulated that PI3K pathway activation is a consequence of increased RTK activity in several paediatric brain tumours. In a few cases of pHGG, the adult-specific *EGFRvIII* mutation has been shown alongside copy number-associated EGFR upregulation (Pollack, Hamilton et al. 2006, Wu, G., Diaz et al. 2014). Interestingly, DIPG has a predilection for PDGFRα upregulation whose involvement has been evident during glioma formation in *in vivo* studies (Jackson, Garcia-Verdugo et al. 2006, Calzolari, Malatesta 2010). A subset of DIPG also contains activating point mutations in the *PDGFRA* gene but it is predominantly found in non-brainstem pHGG (Paugh, Qu et al. 2010). Other alterations in RTKs which are of clinical interest include the FGFR family in paediatric low grade glioma (pLGG) (Zhang, J., Wu et al. 2013), insulin- and insulin-like growth factor receptors in atypical teratoid/rhabdoid tumours (ATRT) (Arcaro, Doepfner et al. 2007) and neurotrophin receptor lesions in pHGG (Wu, G., Diaz et al. 2014).

Pharmacological inhibition of the PI3K/AKT/mTOR pathway has shown anti-tumourigenic effects against many paediatric brain tumours, suggesting biological dependence on its mitogenic effects. However, targeting the pathway is proved more useful as part of a combination strategy due to its cytostatic effects as indicated in several pre-clinical studies (Segerstrom, Baryawno et al. 2011, Cage, Chanthery et al. 2015, Agliano, Balarajah et al. 2017). Indeed, a few clinical trials have already assessed the efficacy of co-treatments involving PI3K pathway inhibitors to treat CNS tumours

(Speranza, Nowicki et al. 2016, Zhao, H. F., Wang et al. 2017). There are still clinical challenges that impede the therapeutic success of these inhibitors including drug delivery across the blood-brain barrier (Groothuis 2000, Wen, Lee et al. 2012, Heffron, Ndubaku et al. 2016), elucidation of compensatory signalling mechanisms (Mantamadiotis 2017) as well as the prospective long term cognitive effects in these young patients (Moore 2014).

1.4.1 PI3K signalling in paediatric ependymoma

Comprehensive molecular and cellular profiling of ependymomas has documented low frequency genetic alterations that would activate the PI3K pathway. These include loss of *PTEN* copy number as well as the amplification of *AKT2* (Johnson, R. A., Wright et al. 2010, Mohankumar, Currle et al. 2015). CNS compartment-specific gene expression profiles also alluded to other possible means of inducing signalling in ependymoma such as the upregulation of members of the EphB-Ephrin and Notch signalling pathways in supratentorial tumours (Taylor, Poppleton et al. 2005). Eph-mediated signalling is considered the largest signal transducer amongst RTK families (Lisabeth, Falivelli et al. 2013) whose activation involves cell-cell interaction resulting in a bidirectional signalling effect between cells. Ephrins could potentially mediate activation of the PI3K pathway in ependymoma as observed during endothelial cell proliferation and migration (Wiedemann, Jellinghaus et al. 2017). It is also possible for cross talks to occur between the Notch and PI3K pathways for instance through Notch-mediated PTEN suppression (Kim, S. J., Lee et al. 2016) as well as the dependence of Notch on PI3K signalling in evading apoptosis (Shepherd, Banerjee et al. 2013). Analysis of single nucleotide polymorphism (SNP) array data revealed rare copy-number gains in genes encoding for all three AKT isoforms and the AKT-activating enzyme PDPK1 but this did not increase the expression of the genes implicated (Johnson, R. A., Wright et al. 2010).

Rogers, Mayne et al. (2013) provided further evidence regarding PI3K pathway activation in paediatric ependymoma. Analysis of publicly available gene expression datasets has identified CNS compartment-specific transcriptional profiles, which were significantly enriched for the PI3K pathway. The genes that represented this enrichment involved those that participate in the PI3K/AKT signalling cascade as well as known downstream target genes. They found that the PI3K pathway was activated in a higher percentage of supratentorial tumours, relative to those arising from the posterior fossa and spinal regions as demonstrated by a higher expression profile of PI3K pathway-related genes and immunohistochemical data. Activation of the PI3K pathway also conferred prognostic significance, as it was associated with poor PFS. Treatment of

ependymoma cell lines with LY294002 and BKM120 showed a dose-dependent decrease in pAKT protein levels as well as a decrease in cell viability, suggesting that PI3K signalling regulates cell proliferation in ependymoma.

1.5 The PI3K/AKT/mTOR pathway as a therapeutic target

The PI3K pathway is central towards cell survival and proliferation. Its frequent activation in many cancers makes it a prime chemotherapeutic target. Successful efforts have been shown into developing inhibitors that target multiple nodes of the PI3K/AKT/mTOR signalling axis with many of these undergoing clinical trials.

1.5.1 Inhibiting the PI3K enzyme

Two of the known first generation PI3K enzyme inhibitors are Wortmannin and LY294002, which have also shown specificity for other PI3K-related kinases. However, evaluation of drug potencies identified wortmannin as being more superior over LY294002 despite having a shorter half-life (Marone, Cmiljanovic et al. 2008). Clinical progression of these drugs was limited by toxicity and solubility issues which prompted the necessity to improve their pharmacological performance. This led to the introduction of second generation of PI3K enzyme inhibitors. For instance, PX-866 and PWT-458 are wortmannin derivatives that can inhibit all PI3K isoforms and have demonstrated anti-tumourigenic effects in various mouse cancer models (Yu, K., Lucas et al. 2005, Koul, Shen et al. 2010) yet only PX-866 has been tested in clinical trials where recipients displayed stable disease with gastrointestinal-related adverse effects (Hong, Bowles et al. 2012). Conjugation of the RGD targeting peptide onto LY294002 produced the hydrophilic SF1126 inhibitor which enables binding to integrins found in many tumour cells. This preferentially results in the accumulation of the drug in tumours (Cleary, Shapiro 2010) where it can target Class I PI3K enzymes. The drug has shown anti-tumourigenic and anti-angiogenic effects in preclinical studies of glioma and prostate cancer (Garlich, De et al. 2008). SF1126 has entered Phase I of clinical trials in which patients with advanced solid tumours and B-cell malignancies also showed stable disease with various gastrointestinal issues (Mahadevan, Chiorean et al. 2012).

For many pharmaceutical companies, the aim is also to restrict drug effects only towards PI3K activity functioning which some of the earlier inhibitors such as wortmannin and LY294002 have failed to achieve. The Novartis compound BKM120 (Buparlisib) is a pan-class I PI3K inhibitor with reduced affinity for other members of the PI3K-related kinase (PIKK) family (Massacesi, Di Tomaso et al. 2016). Its anti-tumourigenic effects have been tested in various malignancies including breast cancer (Hu, Y., Guo et al.

2015), colorectal cancer (Yang, S., Li et al. 2017) and lymphoma (Civallero, Cosenza et al. 2015), in which activated PI3K pathway was generally identified as a factor towards chemoresistance. BKM120 has also been tested pre-clinically against CNS tumours for which drug delivery would not be problematic due to its ability to cross the blood-brain barrier (BBB) (Wen, Lee et al. 2012). *In vitro* studies using GBM cell lines showed a reduction in cellular growth independent of their PTEN or EGFR status (Koul, Fu et al. 2012). Orthotopic mouse models also manifested a decrease in tumour vascularisation and migration following treatment with BKM120 (Speranza, Nowicki et al. 2016) as well as synergistic effects when combined with temozolomide (TMZ) (Maira, Pecchi et al. 2012). BKM120 is currently undergoing clinical testing in various solid tumours with stable disease observed as the best response (Wu, Y. L., Zhang et al. 2016). To date, there have been clinical studies which assessed the efficacy of BKM120 in GBM as a single therapy (NCT01339052) or in combination with other drugs such as carboplatin and lomustine (NCT01934361).

PI3K and mTOR share a high degree of sequence homology, which enabled the development of PI3K/mTOR dual inhibitors. These agents present an advantage of circumventing the negative feedback that takes place along the PI3K/AKT/mTOR signalling axis following inhibition of the pathway (see section 1.5.4.1) thus enabling a more efficient suppression of the pathway. BEZ235 (Dactolisib) is an orally active PI3K/mTOR dual inhibitor which displayed anti-proliferative properties against pre-clinical cancer models including breast and colorectal (Serra, Markman et al. 2008a, Roper, Richardson et al. 2011). The drug entered clinical trials in 2006 to investigate its efficacy against advanced solid tumours (NCT00620594). Clinical trial recipients diagnosed with advanced solid tumours showed good tolerance to BEZ235 with stable disease manifestations (Peyton, Ahnert et al. 2011). Several studies have been undertaken to determine the drug's utility as a monotherapy or part of a combination in malignancies such as metastatic breast cancer, (NCT01495247), leukaemias (NCT01756118) and prostate (NCT01634061). GDC-0980 (Apitolisib) is another PI3K/mTOR dual inhibitor which potently induced cytotoxicity *in vitro* in breast, prostate and lung cancers at a nanomolar range (Wallin, Edgar et al. 2011). Participants diagnosed with advanced solid tumours in a Phase I study displayed anti-tumourigenic effects albeit only modest (Dolly, Wagner et al. 2016). Its excellent pharmacokinetic and pharmacodynamic properties have prompted further evaluation of its clinical utility when combined with other drugs including trastuzumab and paclitaxel (Wen, Lee et al. 2012).

Although they have shown to delay disease progression in a clinical setting, multi-isoform PI3K enzyme inhibitors still have sub-optimal efficacies with a relatively increased

rate of adverse effects (Bendell, Rodon et al. 2012a, Sarker, Ang et al. 2015). In order to address such issues, isoform specific targeting was introduced as a strategy since it is becoming more evident that several tumours have a proclivity for certain isoform activity. This is particularly valid in tumours that harbor *PIK3CA* mutations, leading to a constitutively active p110α. BYL719 (Alpelisib) is a p110α inhibitor that was produced from its parent compound, A66 which in turn was derived from the pan-PI3K inhibitor PIK-93 (Wang, X., Ding et al. 2015). *In vitro* studies on neuroendocrine tumours demonstrated that BYL719 inhibited cell viability following G_1/S arrest, as displayed by the drug's predecessors (Nolting, Rentsch et al. 2017). Single treatment of nasopharyngeal carcinoma cells with BYL719 also resulted in cell cycle arrest as well as apoptosis; such effects were enhanced when combined with MAPK pathway inhibitors and cisplatin, highlighting a potential therapeutic strategy (Wong, Ma et al. 2015). A recent Phase I study demonstrated BYL719 potency against wild-type and mutant *PIK3CA* breast cancers (Mayer, Abramson et al. 2017)with Phase II and III studies underway which see BYL719 as part of a combination treatment. Indeed, preclinical studies showed that mutations and amplifications in *PIK3CA* are indicators for drug sensitivity whereas loss of PTEN confers resistance (Fritsch, C., Huang et al. 2014). There are also prospects of specifically targeting the p110α isoform to impede angiogenesis as its activation mediates VEGF signalling which ultimately leads to endothelial cell migration (Graupera, Guillermet-Guibert et al. 2008). Preferential targeting of the p110δ isoform was deemed ideal for treating many autoimmune diseases and haematological malignancies as its signalling is vital towards immune-related cells including T-cells, B-cells and neutrophils (Patton, Garden et al. 2006). CAL101, a potent p110δ inhibitor, is an approved treatment by the United States Food and Drug Administration (FDA) for B-cell malignancies, as shown by the favourable patient outcomes in Phase I and II trials (Wang, X., Ding et al. 2015). It has also shown clinical value in patients with chronic lymphocytic leukaemia (CLL) when combined with rituximab compared to a placebo treatment (Fruman, Rommel 2014). Studies have indicated the role of CAL101 in reducing circulating chemokines that trigger CLL chemotaxis, migration to the lymphatics and subsequent disease progression (Hoellenriegel, Meadows et al. 2011). Akin to other reported isoform-specific inhibitors, inhibition of p110δ mainly produces cytostatic responses yet it is postulated that their mechanism of action involves attenuation of external survival signalling through reduced chemokine expression whilst abrogating subsequent survival responses.

1.5.2 Inhibiting AKT

As the primary effector of the canonical PI3K pathway, inhibiting AKT remains an attractive approach in suppressing PI3K signalling in cancers. Allosteric inhibitors are a class of AKT-directed agents that induce their effects by binding to a non-catalytic site on the enzyme. For instance, many of these inhibitors interact with the pleckstrin homology (PH) domain of AKT, which usually prevents its localisation to the cell membrane (Meuillet 2011). The allosteric AKT inhibitor perifosine is currently in Phase I/II of clinical trials to evaluate its therapeutic potential against a number of malignancies. The drug has already shown efficiency as a single treatment in Waldenström's macroglobulinemia (Ghobrial, Roccaro et al. 2010) and sarcomas (Gills, Dennis 2009). Other clinical tests have reported that perifosine was well tolerated by patients with both solid and haematological malignancies but dose-limiting toxicities ranging from nausea and diarrhoea to neutropenia and anaemia were still evident (Van Ummersen, Binger et al. 2004, Bendell, Nemunaitis et al. 2011). To augment its chemotherapeutic potential, recent preclinical studies are investigating perifosine as part of a combination treatment which would also circumvent feedback loops within the PI3K/AKT/mTOR signalling axis. For instance, combining perifosine with the mTOR inhibitor rapamycin increased apoptotic and autophagic responses in multiple myeloma *in vitro* as well as prolonged the survival of *in vivo* mouse models (Cirstea, Hideshima et al. 2010). The same treatment regime yielded similar results in *in vitro* and *in vivo* studies for GBM (Pitter, Galban et al. 2011) and non-small cell lung cancer (Ma, Z., Zhu et al. 2012). Various structural modifications in emerging allosteric AKT inhibitors led to the development of alkylphospholipids, sulfonamides and purine-based agents that equally target the enzyme's PH domain (Nitulescu, Margina et al. 2016); many of which have potently exhibited dose-dependent anti-proliferative effects both *in vitro* and *in vivo*.

ATP-competitive inhibitors, unlike their allosteric counterparts, directly bind to the enzyme's AKT catalytic site to inactivate it. The pyrrolopyrimidine AKT inhibitor AZD5363 has shown a good pharmacological profile which reduced tumour growth in a breast cancer xenograft model (Addie, Ballard et al. 2013) and manifested similar responses in multiple solid tumours including gynaecological, colorectal and lung (Hyman, Smyth et al. 2017). Phase I and II trials have already taken place to investigate its clinical utility in cancer patients (Crabb, Birtle et al. 2017, Banerji, Dean et al. 2018). GDC-0068 (Ipatasertib) is another ATP-competitive AKT inhibitor whose potency has been demonstrated in all three isoforms and a low binding affinity for other related kinases including PKA (Blake, Xu et al. 2012). In another study, GDC-0068 prevented downstream AKT signalling in several tested cancer cell lines which ultimately produced a cytotoxic effect (Lin, J., Sampath et al. 2013). They further demonstrated GDC-0068

sensitivity in cancer xenograft models and to some extent, independent of their mutation status which included PTEN loss and PIK3CA alterations. Patients with solid tumours in a recent clinical study showed stable disease and incomplete response as the best outcome following treatment with GDC-0068 (Saura, Roda et al. 2017). Further active trials are ongoing to assess GDC-0068 as part of a combination therapy for breast cancer (NCT02301988) and prostate cancer (NCT03072238). Pan-AKT inhibition offers the prospect of eliminating compensatory AKT signalling from other isoforms should one isoform just be targeted thus ensuring a complete inhibition of downstream PI3K signalling. However, these inhibitors also increase the risk of off-target effects especially against kinases belonging to the same family as AKT which would give rise to potential clinical adverse effects; an aspect that is arguably not as severe with the employment of AKT allosteric inhibitors (Yun 2010).

1.5.3 Targeting mTOR

Rapamycin was the earliest agent discovered to inhibit mTOR which was initially employed as an anti-fungal and immunosuppressive agent but was later found to have tumour suppressive properties (Sehgal 2003). Interestingly, its mechanism of action only targets the mTORC1 complex due to its binding to the FK506-binding protein-12 (FKB12) which is exclusive to mTORC1 activity. Rapamycin has since become a structural template for the development of analogues which are equally efficacious yet having far more superior pharmacological profiles.

Everolimus and temsirolimus are two known rapalogues that have shown potent anti-neoplastic effects and favourable outcomes in several clinical studies including pancreatic (Yao, J. C., Shah et al. 2011) and metastatic breast cancer (Royce, Osman 2015). One notable cancer that these rapalogues are used as part of the treatment regime is renal cell carcinoma (RCC). As demonstrated by the favourable tolerance in patients in clinical trials, everolimus and temsirolimus have since been employed as a first-line treatment for RCC (Hudes, Berkenblit et al. 2009, Motzer, Escudier et al. 2010). Other studies have also suggested the combination of these rapalogues with RTK inhibitors in treating these tumours, having shown an overrepresentation for mTOR and VEGF signalling processes during disease pathogenesis (Rini, Atkins 2009). Rapalogues have also been evaluated in several clinical trials as a treatment option for CNS tumours including paediatric recurrent/non-recurrent progressive low grade glioma (NCT01734512), DIPG (NCT03355794) and recurrent/progressive ependymoma (NCT02155920). Currently, everolimus is a clinically recognized treatment for subependymal giant cell astrocytoma (SEGA) (Franz, Belousova et al. 2014), which is

the main cause of mortality in children with Tuberous sclerosis complex (TSC) (Roth, Roach et al. 2013). Indeed, rapalogues confer therapeutic benefits particularly against many CNS tumours which were characterised with PI3K/AKT pathway mutations that would hyperactivate downstream targets including mTOR signalling (see section 1.4)

However, rapalogues only prevent the mTORC1 cascade and not mTORC2 which is an issue due to the negative feedback that leads to the reactivation of AKT signalling upstream. Dual mTORC1/2 inhibitors are drawing interest as a therapeutic strategy to address this issue as well as exploit mTOR's primary role in cell growth and metabolism. PP242 (Torkinib) is an ATP-competitive mTOR kinase inhibitor that potently activates autophagic responses following suppression of mTORC1/2 complexes (Feldman, Apsel et al. 2009, Zhou, J., Tan et al. 2013). PP242 has previously shown to suppress induction of several hallmarks of cancer such as proliferation and metastasis in pre-clinical studies including gastric cancer (Xing, Zhang et al. 2014), bladder cancer (Zhang, Z., Zhang et al. 2016) and GBM (Neil, Shannon et al. 2016). The orally bioavailable OSI027 mTORC1/2 dual inhibitor has also shown potent cytotoxic effects in a panel of tested cancer cell lines characterised with an activated PI3K/AKT signalling pathway (Bhagwat, Gokhale et al. 2011). The same study also reported a more efficient reduction in tumour growth in xenograft models of cancer following monotherapeutic administration of OSI027, relative to rapamycin. Phase I trials have just been finished in patients with advanced solid tumours or lymphoma (NCT00698243), but findings are yet to be disclosed. Most mTORC1/2 inhibitors are still in pre-clinical testing and have yet to be assessed in patient trials. While they have shown some therapeutic promise using *in vitro* and *in vivo* models, factors such as drug tolerance and dose-limiting toxicities remain uncertain.

1.5.4 Resistance mechanisms to PI3K pathway inhibitors

Despite presenting as an attractive target for cancer treatment, clinical responses to inhibition of the PI3K pathway have been disappointing. The intricacy behind PI3K signalling is inundated with various feedback loops and inter-pathway cross talks which give rise to emerging resistance mechanisms, thus accounting for the sub-optimal patient outcomes observed in many of these studies.

1.5.4.1 Reactivation of the PI3K pathway

One major caveat of upstream inhibition of the PI3K pathway is the upregulation of RTK expression as mediated paradoxically by activation of FOXO transcription (Figure 1-11), having previously discussed their role as tumour suppressors. This was

demonstrated in several malignancies including breast (Serra, Markman et al. 2008b) and prostate (Carver, Chapinski et al. 2011) cancer. It was further showed that the increase in RTK activity is also caused by the loss of mTORC1-mediated negative regulation following subsequent suppression of mTOR signaling (Chandarlapaty, Sawai et al. 2011). This mechanism is highlighted especially in the activation of insulin and insulin-like growth factor receptors (IGFR). PI3K inhibition consequently reduces mTORC1 signalling following loss of mTOR activity, resulting in a downregulation of p70S6 kinase activity which eliminates the inhibitory effect on the IRS (insulin receptor substrate). As a result, the IRS can interact with the PI3K enzyme which stimulates the reactivation of downstream signalling. It is also highlighted that this in turn would augment mTOR signalling, which involves the formation of mTORC2 complexes. mTORC2 is recruited to the membrane and is crucial for the complete activation of AKT. Therefore, the increase in RTK activity leads to an overall saturation of downstream signalling cascades including the PI3K pathway.

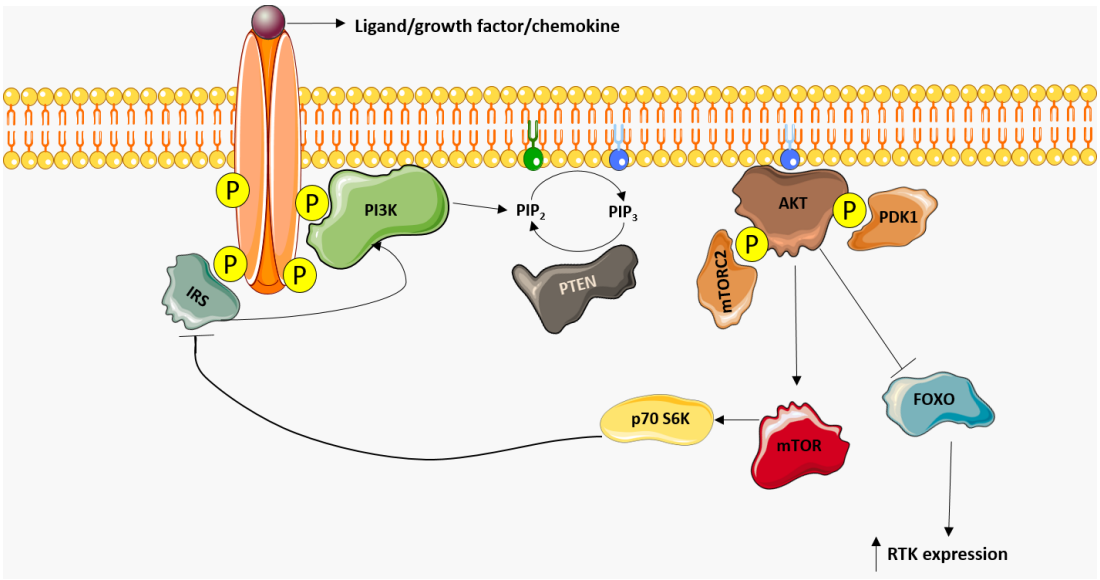


Figure 1-11 Inhibition of the PI3K pathway leads to the activation of FOXO proteins. FOXOs have been shown to upregulate the expression of RTKs which leads to the reactivation and potential saturation of cell signalling pathways including the PI3K cascade. The consequential loss of mTOR signalling following PI3K pathway inhibition also alleviates the inhibitory effect of p70S6 kinase on IRS proteins which then stimulates the activation of the PI3K enzyme.

Biphasic inhibition of the PI3K signalling pathway through the use of PI3K/mTOR dual inhibitors is a strategy that would minimise the formation of feedback loops that may underlie resistance towards PI3K pathway agents. Incidentally, one study has described a less explored mechanism that undermines the effects of PI3K/mTOR dual inhibition which involved the JAK/STAT signalling pathway (Britschgi, Andraos et al. 2012). They

found an increase in expression of interleukin-8 (IL-8) in metastatic breast cancer cells following treatment with BEZ235. IL-8 activated the chemokine (CXC motif) receptor 1 (CXCR1) which consequently stimulated signalling through the JAK2/STAT5 pathway. JAK2 can associate with PI3K through its SH2 domain which stimulates its activity thus reactivating the PI3K/AKT pathway (Figure 1-12). However, the prospect of this as a general resistance mechanism towards PI3K/mTOR inhibitors in cancers is yet to be elucidated. Nevertheless, studies have shown that JAK2/STAT5 signalling can reactivate the PI3K cascade through methods such as interaction with the Epidermal growth factor receptor (EGFR) (Yamauchi et al., 1997) and IRS proteins (Gual, Baron et al. 1998), which are both positively regulated in response to the suppression of the PI3K pathway. Therefore, such findings support cancer treatments that include both JAK2 and PI3K inhibitors (Bartalucci, Tozzi et al. 2013, Fiskus, Verstovsek et al. 2013).

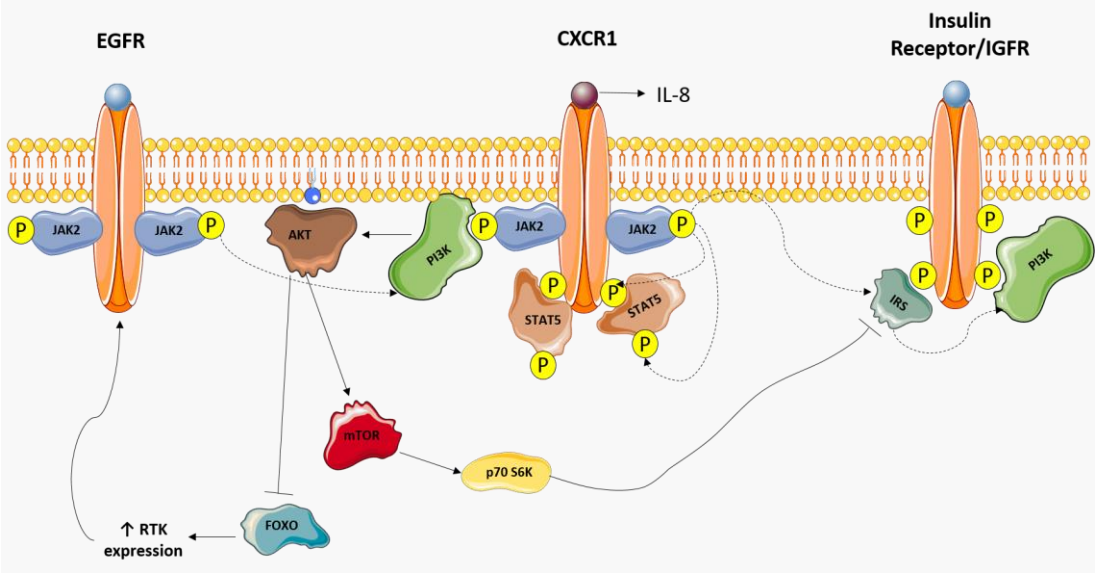


Figure 1-12 Britschgi, Andraos et al. (2012) showed that the CXCR1 receptor activates the JAK2/STAT5 signalling pathway following an upregulation of IL-8, as a result of treatment with BEZ235. JAK2 binds to the SH2 domain of the PI3K enzyme, leading to its activation. JAK2 could also reactivate the PI3K pathway through its association with EGFR or IRS proteins.

1.5.4.2 Activated parallel signalling pathways

The capability of the PI3K signalling cascade to facilitate resistance mechanisms also originates from the various cross talks it has with several other survival pathways. Interaction between the PI3K and MAPK pathways is one of the commonly reported cross talks in cancer which regulate downstream substrates (e.g. GSK3β, c-Myc and BAD) to promote cell survival, growth and viability (Mendoza, Er et al. 2011). One study showed that the activation of the MAPK pathway, which in turn can also reactivate the PI3K pathway through Ras (Castellano, Downward 2011), was observed in response to treatments with rapalogues (Carracedo, Ma et al. 2008). Loss of mTOR signalling

downregulates p70S6 kinase activity thus relieving the inhibitory effect on IRS scaffold proteins. While this could reactivate the PI3K pathway as mentioned in the last section, IRS could also serve as a docking site for the GRB2/mSOS complex (Buday, Egan et al. 1994) which in turn triggers the MAPK cascade (see section 1.3.3.4). Moreover, elevated surface expression of RTKs due to PI3K inhibition also enhances output from the MAPK signalling pathway.

Activation of the Wnt signalling pathway has also been associated with resistance to PI3K pathway inhibition. This is particularly highlighted in cancers driven by Wnt signalling where there is an increase in β-catenin expression of target genes (Pai, Carneiro et al. 2017). In fact, high β-catenin could synergise with active FOXO3a as a result of PI3K/AKT suppression to promote tumour progression. Despite the latter's well-documented role as a tumour suppressor, the combined effects of β-catenin and FOXO3a resulted in a shift in transcriptional program that favours invasion and metastasis (Tenbaum, Ordonez-Moran et al. 2012). Another study also demonstrated upregulation of Wnt signalling following inhibition of the PI3K pathway in breast cancer (Tzeng et al., 2015). Treatment of cells with the pan-PI3K inhibitor GDC-0941 resulted in the phosphorylation of the LRP co-receptor, preceded by the induction of various Wnt ligand expressions. Indeed, there have been treatments involving combinations of PI3K and Wnt pathway inhibition emerging which could potentially produce therapeutic prospects in many cancers (Arques et al., 2016; Solzak et al., 2017).

1.5.4.3 Incomplete inhibition of the PI3K pathway

The tumour suppressive properties of PI3K pathway inhibitors have been evident in several pre-clinical models of cancers but the overall therapeutic responses to these agents have been modest. It was suggested that incomplete inhibition of the PI3K pathway could be attributed to these findings. For instance, treatment of *PIK3CA*-mutant breast cancer cells with the p110α-inhibitor BYL719 resulted in a decrease in AKT phosphorylation but mTORC1 signalling was still observed. Sensitivity to BYL719 was only restored when co-treated with the rapalogue everolimus (Elkabets, Vora et al. 2013). A similar study showed that despite the reduction in phospho-AKT levels in response to PI3K inhibition, no cell cycle arrest was observed in certain *PIK3CA*-mutant breast cancer cell lines (Vora, Juric et al. 2014). Combining PI3K suppression with inhibitors of AKT, mTOR or cell cycle effectively overcame the resistance leading to a reduction in cell viability. It is therefore suggested that in human trials, PI3K pathway inhibitors are administered at doses which would minimise patient adverse effects. However, these doses may restrict the drug's capability to adequately suppress PI3K signalling thus decreasing the efficiency of PI3K pathway inhibitors in these studies.

1.6 Rationale, aims and hypothesis

Understanding the molecular basis of ependymomas is crucial to identify prognostic markers, prospective therapeutic targets and molecular drivers that contribute towards tumourigenesis. This project focused on investigating the biological significance of the PI3K pathway towards disease pathogenesis, having identified its activation in a high percentage of primary ependymomas (Rogers, Mayne et al. 2013). Since paediatric ependymomas also manifest a relatively poor prognosis with few effective adjuvant therapies, a need for alternative treatment strategies has been emphasised. Therefore, this project also evaluated the prospect of targeting the PI3K pathway as a therapeutic approach to treat ependymomas.

Signalling through the PI3K pathway is essential towards cell survival and viability. Its involvement in progression of many cancers has been reported, making it a prospective target for treating such malignancies. The activation of the PI3K signalling in ependymoma implicates its pathological significance towards tumour biology. It is therefore hypothesised that the PI3K pathway regulates cellular processes that favour ependymoma tumourigenesis. Its inhibition would then be detrimental towards tumour survival thus highlighting a prospective treatment strategy that could be considered as being clinically beneficial. There were three distinct aims to support the rationale that was outlined for this study. These included:

1.) Investigation of the PI3K pathway as a regulator of survival in ependymoma
   - Observed whether inhibition of PI3K signalling could reduce cell viability of other established ependymoma cell lines
   - Determined if cell viability reduction is due to cytotoxic or cytostatic responses to PI3K inhibition
   - Determined whether the inhibition of canonical PI3K/AKT signalling cascade facilitated the biological processes observed in ependymoma

2.) Identification of downstream targets of the PI3K pathway
   - Employed microarray technology to differentiate gene expression profiles of ependymoma cells before and after PI3K pathway inhibition
   - Identified biological functions that were enriched in the genes that were differentially expressed following PI3K pathway inhibition
   - Suggested a potential molecular mechanism that lead to the regulation of the identified biological functions

- Pinpointed processes that could be targeted pharmacologically in combination with PI3K pathway inhibition

3.) Experimental validation of the cellular processes presented in the gene expression data and identifying its relevance from a clinical perspective
    - Functionally verified the proposed molecular mechanism that would regulate the significantly enriched biological functions identified in ependymoma post-PI3K pathway inhibition
    - Evaluated whether targeting the PI3K pathway can enhance the effects of conventional chemotherapies in ependymoma as predicted by the gene expression data

CHAPTER 2. MATERIALS AND METHODS

2.1 Cell culture and cell based assays

2.1.1 Origin of cell lines and cell culture

The cell lines used in this project were derived from patients' tumour samples whose clinical details are outlined below in Table 2-1. Establishment of the BXD1425-EPN cell line involved injection of primary tumour cells in immune deficient mice, which were subtransplanted prior to mechanical dissociation. DKFZ-EP1 cells form as a monolayer but were originally derived from neurospheres following enrichment for stemness of isolated patient samples. EPN1, EPN8 and EPN12A cells, on the other hand, were established at the Children's Brain Tumour Research Centre (CBTRC) from fresh tumours from pathology or surgery which were subsequently dissociated using an enzyme cocktail. Growth was closely monitored until passage 5 before banking. Currently, collaborations between leading European scientists which subsequently make up BIOMECA (Biological Markers for Ependymomas in Children and Adolescents) are investigating an array of biomarkers that can potentially be used for disease stratification as well as support diagnostic and prognostic purposes in ependymoma patients. Some of these biomarkers have previously been implicated with ependymoma pathogenesis or cancer development in general including 1q gain, Tenascin-C, C11orf95-RELA and -YAP1 fusion genes, ABCB1, BLBP ERCC5, hTERT mRNA, EZH2 and CDNK2.

All cell lines were cultured as a monolayer and were incubated in a standard humidified 5% CO_2-air incubator at 37ºC. Dulbecco's Modified Eagle Medium (DMEM, Thermofisher Scientific) supplemented with 10% foetal bovine serum (FBS) (GE Healthcare) was used to culture BXD-1425EPN and DKFZ-EP1 cell lines and 15% FBS in DMEM for EPN1, EPN8 and EPN12A cell lines. Maintenance of cell lines also included frequent mycoplasma testing using MycoAlert™ detection kit (Lonza). Other cell lines used in this project were UW228-3 (non-ependymoma cell line) cultured in Dulbecco's Modified Eagle Medium: Nutrient Mixture F-12 (DMEM/F12, Thermofisher Scientific) supplemented with 10% FBS and 1% L-glutamine (Sigma-Aldrich) and MCF7 (human breast adenocarcinoma cell line) (Soule, Vazguez et al. 1973) cultured in RPMI-1640 Medium (Sigma-Aldrich) supplemented with 10% FBS.

Table 2-1. Clinical and *in vitro* characteristics of the different ependymoma cell lines used in this project.

Cell line	Patient details	Tumour characteristics	Doubling time (hours)	Cellular appearance	Other details
BXD-1425EPN (Yu, L., Baxter et al. 2010)	9 year old, male	Supratentorial, recurrent anaplastic ependymoma (Grade III)	23 ± 1.23	Cells adopt the typical epithelial cell morphology but they tend to be triangular or satellite-like in shape, with their cytoplasmic processes often extending into thin spindle-like formations as it reaches ~80% confluency. Cells are arranged in a circular pattern resulting in "lumen-like" patches *in vitro.*	• RELA fusion positive *(determined by Western Blot).* • Earliest established passage used is around passage 60 with growth rate remaining unchanged even after passage 100.
DKFZ-EP1 (Milde, Kleber et al. 2011)	18 year old, female	Supratentorial, primary anaplastic ependymoma (Grade III)	116.3 ± 9.83	Cells are adherent but resemble the parental neurospheres from which these were derived from. They appear smaller and circular in shape, in contrast to the other ependymoma cell lines.	• RELA fusion positive *(determined by Western Blot).* • Growth rate in culture is variable so most experiments were performed between passages 15-20.

EPN1 (Hussein, Punjaruk et al. 2011)	22 year old, male	Supratentorial, recurrent ependymoma (Grade II)	203.3 ± 3.33	Cells adopt the typical epithelial cell morphology in culture but these cells grow to form a more regular structure as if a “tight” monolayer will be formed with continued passaging, unlike BXD-1425EPN, EPN8 and EPN12A cells which appear to grow on top of each other.	• RELA fusion positive *(determined by DNA methylation array profiling).* • Slow growing cell line which becomes more prominent around passages 25-30.
EPN8	1.5 year old, male	Posterior fossa, anaplastic ependymoma (Grade III),	Details not available	Cells have a comparable appearance as BXD-1425EPN in which they tend to grow on top of each other; with long and extensive cytoplasmic processes. Cells also form circular patterns to form “lumen-like” structures especially when reaching ~80% confluency.	• Posterior fossa Group A *(determined by DNA methylation array profiling).* • Grows up to around passage 15 before proliferative rate declines.
EPN12A	0.5 year old, female	Posterior fossa, anaplastic ependymoma (Grade III)	40.81 ± 1.88		• Manifests an increased growth rate until it reaches around passage 20.

2.1.2 Sub-culturing monolayer cells

Cell lines were routinely sub-cultured when they reach 70-80% confluency. Media was aspirated followed by washing of adherent cells with Hank's Balanced Salt Solution (HBSS, Thermo Scientific). 2 ml of 1x Trypsin-EDTA (TE) Buffer (Sigma-Aldrich) was added to each flask before incubating at 37^{o}C until the cells fully detached. The Trypsin-EDTA was neutralised using the respective growth media and the cell suspension was divided into individual flasks according to their observed growth rate.

2.1.3 Cell pelleting

Having harvested the cells as depicted on section 2.1.2, the cell suspension was transferred in a 15 ml Falcon tube and was centrifuged at 162 *x g* for 5 minutes. The media was discarded and the pellet was resuspended in 1 ml of phosphate saline buffer (PBS) in a 1.5 ml Eppendorf tube. The tubes were centrifuged at 700 *x g* for 5 minutes. The supernatant was discarded and the pellet was stored in -80^{o}C for future processing.

2.1.4 Cell counting

Cell pellets were prepared as depicted on section 2.1.3. The pellet was resuspended in 1 ml of cell culture media. 10 µl of the cell suspension was mixed with 10 µl of trypan blue stain 0.4% (NanoEntek) in a 1:2 dilution. 10 µl of the mixture was carefully applied onto a chamber of an EVE Cell Counting Slide (NanoEntek). The slide was inserted with the sample side in first into the EVE Automated Cell Counter (NanoEntek). The image's resolution on the screen was adjusted, as represented on the manufacturer's protocol. The cells were counted and the value related to the viable ones was used to prepare cell suspension dilutions prior to seeding.

2.1.5 Preparation of cell line stocks

Cells were harvested (see section 2.1.2), centrifuged at 162 *x g* for 5 minutes and the supernatant was discarded as depicted in section 2.1.3. The pellet was resuspended in FBS containing 10% dimethyl sulfoxide (DMSO, Sigma). 1 ml aliquots were transferred into cryovials in which cell concentrations were kept at about 1 x 10^{6} cells/ml. Cryovials were transferred to a freezing container (Nalgene) and stored at -80^{o}C for at least 24 hours before transferring in liquid nitrogen.

2.1.6 Resuscitation of frozen cells from liquid nitrogen

Frozen stocks of cell lines were removed from long-term storage in liquid nitrogen and were rapidly thawed in a 37ºC waterbath. The cell suspension was slowly dispensed into a 25cm^2 tissue culture flask containing 5 ml of pre-warmed growth media. The cells were incubated in a standard humidified 5% CO_2-air incubator at 37ºC for 24 hours to allow cellular attachment to the flask. Media was subsequently replaced, reducing DMSO toxicity and removing unattached cells in the process.

2.2 Bacterial culture

2.2.1 Plasmid constructs

The GFP plasmid construct used in this project consists of the 700 bp GFP gene insert with a RCAS (A) vector backbone (Addgene, RCAS GFP #13878) (Chen, C. M., Smith et al. 1999). Other details of this plasmid are outlined in Appendix 1. Following transfection into ependymoma cells, expression of GFP proteins was visualised to determine the transfection efficiency.

2.2.2 Culturing and plasmid preparation

A sterile loop was used to inoculate bacterial samples from the stab culture provided by the company onto agar plates (Appendix 2) which contained 100 µg/ml of ampicillin (Thermofisher Scientific). The plates were incubated overnight at 37ºC. Single colonies produced on the agar plate were picked and inoculated in 5 ml of Luria Broth (LB) (Appendix 3), and were incubated at 37ºC for 8 hours with vigorous agitation to produce a starter culture. 200 µl of each starter culture was inoculated in 100 ml of LB before incubating for a further 12 hours at 37ºC with vigorous agitation. The bacterial cultures were pelleted at the end of the incubation through centrifugation at 6000 *x g* at 4ºC for 15 minutes. The resulting pellets were processed using Qiagen Maxi Kit, following the manufacturer's protocol, to extract the plasmid constructs. The plasmid DNA was eluted in TE Buffer (10 mM Tris•Cl, pH 8.5) and was quantified using the Nanodrop 2000 (Thermofisher Scientific). An ideal plasmid DNA concentration for transfection was set to at least 500 ng/µl with a 260/280 ratio of ~1.8 as a threshold to consider the sample as high quality.

2.2.3 Lipofectamine™-mediated transfection

2.2.3.1 Transfection optimisation

BXD-1425EPN cells were seeded in duplicate into 24-well plates at densities of 4 x 10^4, 6 x 10^4 and 1 x 10^5 cells per well. For a classical forward transfection, the plates were incubated at 37ºC in a 5%-CO_2 air incubator to allow the cells to settle. For each duplicate, two Lipofectamine™ 3000 Reagent (Thermofisher Scientific) volumes were used, 0.75 and 1.5 µl which were diluted in 25 µl of Opti-MEM™ medium (Thermofisher Scientific). 25 µl of Opti-MEM™ medium containing 1 µg of GFP plasmid DNA was added to each Lipofectamine™ dilution. The complex was incubated at room temperature for 20 minutes before adding directly into the appropriate wells. The cells were incubated for 24 – 48 hours before visualising GFP expression using the Zeiss Axiovert S100 inverted fluorescence microscopy. GFP-filtered (excitation at 475 nm) and brightfield images were taken using Axiovision v4.8.2.0. These images were superimposed onto each other using GNU Image Manipulation Program (GIMP) v2.10 to provide a visual representation of the transfection efficiency. ImageJ v1.52a was used to count the number of GFP-transfected and total number of cells per captured image and determine the transfection efficiency.

2.2.4 Nucleofector™-mediated transfection

The Nucleofector™ technology employs electroporation to enable high transfection efficiencies in a vast array of cells including primary cells, stem cells and hard to transfect cell lines. It involves a series of pre-set programs which when coupled with one of the kit's Nucleofector solutions would achieve successful introduction of DNA with low mortality rates.

2.2.4.1 Nucleofector™ set-up

Cells were cultured for at least two days and confluency was maintained at 70-85% prior to harvesting. Before proceeding with the experiment, the media routinely used for maintenance of cells and RPMI-1640 media were conditioned in a 5%-CO_2 air incubator at 37ºC for at least an hour. Cells were harvested as described in section 2.1.2 and counted using an EVE Automated Cell Counter (NanoEntek). 5 x 10^5 cells were pelleted for Nucleofection™. The supernatant was removed and the pellet was resuspended in 100 µl of Nucleofection™ solution consisting of either L- or V- solution and reaction supplement (Lonza) in a 4.5:1 ratio. During optimisation, 2 µg of the provided pmaxGFP® Vector was added to the suspension. 100 µl of the cell suspension was carefully transferred into a certified cuvette before inserting it into the Nucleofector™ II (Amaxa Biosystems) cuvette holder and running the following programs: A-020, T-020, T-030 and X-001. 500 µl of pre-conditioned RPMI-1640 media was added into the same

cuvette followed by incubation for 10 minutes at 37ºC. The sample was transferred into a 6-well plate containing 1.5 ml of the pre-conditioned cell culture media using the specialised pipettes supplied in the same kit. The plate was incubated for 24 hours in a 5%-CO_2 air incubator at 37ºC.

2.2.4.2 Determining optimal Nucleofector™ conditions

Imaging of GFP-transfected cells and manual determination of transfection efficiency was performed as outlined in section 2.2.3.1. Wells containing viable cells were harvested and pelleted. The pellet was resuspended in propidium iodide (PI) diluted in 500 µl of PBS/1% BSA (Bovine serum albumin) in a 1:20 ratio. The samples were transferred into FACS tubes and were arranged around a carousel in a Beckman Coulter FC500 Flow Cytometer System. The resulting LMD files were analysed using WEASEL Flow Cytometry Software v3.0. Gating was performed on a forward versus side scatter density plot to exclude debris in the analysis, and was subsequently performed on a forward scatter height versus forward scatter area density plot to incorporate single cell populations only. Using a double parameter density plot, a summary of the overall state of the cells in a sample was shown having factored in positive PI staining in conjunction with GFP expression. The resulting flow cytometry profile was divided into quadrants to differentiate viable from non-viable cells as well as identify those that harbor GFP fluorescence thus indicating a transfection efficiency and percentage cell viability.

2.3 MTT viability assays

The MTT cell viability assay measures metabolic activity in cells according to colorimetric changes (MTT Cell Proliferation Kit, Roche). The assay depends on the reduction of the yellow tetrazolium MTT salt, 3-(4,5-dimethylthiazol-2-yl)-2,5-diphenyltetrazolium bromide, by NAD(P)H-dependent cellular oxireductase enzymes from metabolically active cells into purple insoluble formazan crystals which can then be spectrophotometrically analysed. A higher absorbance measure correlates with increased cell viability.

2.3.1 MTT assay standard protocol

Cells were harvested as described in section 2.1.2 and were counted using an EVE Automated Cell Counter (NanoEntek). Cells were plated in triplicate in a 96-well plate at a seeding volume of 100 µl per well and incubated overnight in a 5%-CO_2 air incubator at 37ºC. Media was also added to three extra wells to serve as a blank control. The media was aspirated from all wells and was replaced with media containing drugs. The plate was incubated for 72 hours in a 5%-CO_2 air incubator at 37ºC. Following

incubation with the drug, 10 µl of MTT reagent was added to each well. Incubation at 37^{o}C for 4 hours enabled the formation of the purple formazan crystals in the wells. Subsequently, 100 µl of MTT solubilisation reagent was added to each well to dissolve the formazan crystals. The plate was incubated at 37^{o}C overnight. Absorbance was read using a FLUOSTAR plate reader (BMG labtech instruments) at 560 nm with 650 nm reference wavelength. The raw data was extracted using the Omega software (BMG labtech instruments). The values were corrected by subtracting the mean blank reading before converting these as a percentage viability relative to the vehicle control. The percentage viability values were plotted against the drug concentration used to determine the cell viability trend in response to drug treatments.

2.3.2 Standard curve

To determine the seeding density to be used for each cell line in the MTT assay, a standard curve was initially generated. Cells were harvested as described in section 2.1.2 and counted using an EVE Automated Cell Counter. Cells were plated in triplicate in a 96-well plate using the following seeding densities: 500, 1000, 5000, 10 000, 15 000 cells at a seeding volume of 100 µl per well. Three wells containing media only were also established. The cells were incubated for 96 hours in a 5%-CO_2 air incubator at 37^{o}C. After incubation, the subsequent MTT assay steps were performed as described in section 2.3.1. Absorbance was read using a FLUOSTAR plate reader (BMG labtech instruments) at 560 nm with 650 nm reference wavelength. The raw data was extracted using the Omega software (BMG labtech instruments). The mean absorbance values were plotted against the various seeding densities to create a cell growth curve. For all subsequent MTT assays, the seeding densities used for each cell line were chosen from when the cells were in an exponential growth phase.

2.3.3 Cell seeding

The optimum seeding densities used per well in a 96-well plate format, for all subsequent MTT assays as identified from the standard curve analyses described in section 2.3.2, were: BXD-1425EPN (7000 cells), DKFZ-EP1 (7000 cells), EPN1 (6000 cells), EPN8 (2500 cells), EPN12A (3000 cells), MCF7 (5000 cells) and UW228-3 (1000 cells). Cells were seeded in triplicate in a final volume of 100 µl per well and were allowed to attach overnight before drug treatment.

2.3.4 Drug treatment

Details of the drugs used in the MTT assays in this project are outlined in Table 2-2.

Table 2-2. Details of the various drugs used for various experimental set-ups in this project.

Drug/Reagent (Company)	Solvent used for reconstitution	Stock concentration
BKM120 (AdooQ® Bioscience)	DMSO	10 mM
Perifosine (Invivogen)	H_2O	108 mM
GDC-0068 (AdooQ® Bioscience)	DMSO	10 mM
Chloroquine (CQ) (Sigma-Aldrich)	H_2O	100 mM
AS1842856 (Merck Millipore)	DMSO	14 mM
Paclitaxel (Sigma-Aldrich)	DMSO	1 mM
Cisplatin (Accord)	H_2O	3.33 mM
Gemcitabine (Sigma-Aldrich)	H_2O	20 mM
Epidermal growth factor (EGF) (Sigma Aldrich)	H_2O	1 mg/ml

Cells were seeded in triplicate and were treated with drugs as outlined in Table 2-3. Vehicle controls were also set up per treatment according to the preparation of the highest drug concentration using the appropriate solvent used to reconstitute the drug (i.e. water or DMSO). Drug treatments involving CQ, AS1842856, paclitaxel, gemcitabine and cisplatin were set up in combination with BKM120 whose purposes are summarised in Table 2-4. For CQ and AS1842856 combination treatments with BKM120, these drugs were first set up individually to determine any dose-limiting toxicities. For co-treatments involving paclitaxel, gemcitabine and cisplatin, their IC_{50} values were first determined before combining with BKM120 IC_{50}-based concentrations for each cell line. Two concentrations above and three concentrations below (increasing and decreasing, respectively, each time by double) the IC_{50} value for each drug per cell line were used as a combination strategy, giving a fixed ratio in individual set-ups. The media in all the wells was substituted with the necessary drug treatment and the cells were incubated with the drugs at 37ºC for 3 days before performing the MTT assay endpoint as described in section 2.3.1.

Table 2-3. Single drug treatment of ependymoma and control cells, to determine the IC_{50} value following a 72 hour MTT viability assay.

Key:

******* indicates that the cell line was treated with the specified drug using the same concentrations as the other cell lines.

--- indicates that the specified drug was not used to treat this cell line.

Drug/Reagent	Cell line						
	DKFZ-EP1	**BXD1425-EPN**	**EPN1**	**EPN12A**	**EPN8**	**UW228-3**	**MCF7**
BKM120	0.1, 0.5, 1, 5 μM				**---**	**---**	**---**
Perifosine	5, 10, 25, 50 μM				**---**	*******	**---**
GDC-0068	5, 10, 25, 50 μM				**---**	**---**	*******
Paclitaxel	---	0.39, 0.78, 1.56, 3.13, 6.25, 12.5, 25, 50, 100, 250, 500 nM			**---**	**---**	**---**
Cisplatin	---	0.10, 0.20, 0.39, 0.78, 1.56, 3.13, 6.25, 12.5, 25, 50, 100 nM			**---**	**---**	**---**
Gemcitabine	---	0.20 0.39, 0.78, 1.56, 3.13, 6.25, 12.5 nM 0.025, 0.05, 0.1 0.5, 1, 5, 10, 20 μM			**---**	**---**	**---**

Table 2-4. The various combination treatments involving BKM120 used in this project. The CQ drug concentration used was fixed throughout the entire experimental set-up, irrespective of the cell line used and the concentration of AS1842856 used was limited to three different drug concentrations. **Key:** ***Treatments were dependent on the calculated IC_{50} values per drug for each cell line. BKM120 concentrations used were also adjusted relative to the individually determined IC_{50}.

BKM120 in combination with…	**Purpose**	**Cell line**			
		BXD-1425EPN	**DKFZ-EP1**	**EPN1**	**EPN12A**
CQ	Inhibition of autophagy activated by PI3K pathway inhibition; concentration used is 5 μM	✓	✓	✓	✓
AS1842856	Inhibition of the active unphosphorylated FOXO1 following PI3K pathway inhibition; concentrations at 200 nM, 100 nM, 50 nM	✓	X	✓	✓
***Paclitaxel**	Inhibit G2/M processes in combination with PI3K pathway inhibition.	✓	X	X	✓
***Gemcitabine**	Inhibit S-phase processes and combine DNA damage with PI3K pathway inhibition.	X	X	X	✓
***Cisplatin**	Combine DNA damage with PI3K pathway inhibition.	✓	X	X	✓
EGF	Pulse activate the PI3K pathway following incubation of cells in serum free media (SFM); final concentration used is 50 ng/ml.	✓	✓	✓	✓

2.3.5 IC_{50} estimation

Dose response curves were generated using GraphPad Prism v7.04. The percentage cell survival was plotted against the drug concentrations and non-linear regression analysis was performed to estimate IC_{50} values from the curves generated.

2.3.6 Analysis of effects of BKM120 treatment combinations

The MTT assay data for the BKM120 only treated cells and those treated with BKM120 in combination with either CQ or AS1842856 were analysed using GraphPad Prism v7.04. The dose response curves produced by both single and combination treatments were compared using a two-way ANOVA to determine whether there was a significant difference in the cell viability between these treatment conditions. Moreover, BKM120 co-treatments with the three standard chemotherapies (see Table 2-4) were analysed using CompuSyn v1.0 which is based on the Chou-Talalay method (Chou 2010) to determine whether such treatments produce synergistic, antagonistic or additive effects in ependymoma cells. The absorbance values for the individual drugs as well as for the previously highlighted combinations were subtracted from 1 to obtain the percentage inhibition per treatment point. For each analysis, the values for the BKM120/chemotherapy combination and the corresponding individual treatment were input into the CompuSyn program. This enables the quantification of dose-effect relationships of each drug and when combined with other agents according to the principles of the mass-action. This results in the deduction of combination indices (CI), which pertain to the overall outcome of the drug combination treatment. The consequent CI values obtained from the drug combination analysis and their general effects are outlined in Table 2-5.

Table 2-5. Effects of drug interaction based on the combination index (CI) identified by the Chou-Talalay analysis.

CI value	Effect
< 0.10	Very strong synergism
0.10 – 0.30	Strong synergism
0.30 – 0.70	Synergism
0.70 – 0.85	Moderate synergism
0.85 – 0.90	Slight synergism
0.90 – 1.10	Nearly additive
1.10 – 1.20	Slight antagonism
1.20 – 1.45	Moderate antagonism
1.45 – 3.30	Antagonism
3.30 – 10.00	Strong antagonism
> 10.00	Very strong antagonism

2.4 Cell death assays

2.4.1 LDH assay

Lactate dehydrogenase (LDH) activity is used to quantitatively measure the amount of cellular cytotoxicity (Sigma-Aldrich). LDH is a cytosolic enzyme that is released into the supernatant when cells undergo cytolysis following a particular treatment. LDH catalyses the oxidation of lactate to pyruvate which also results in the reduction of the coenzyme NAD ($NADH + H^+$). $NADH + H^+$ is then used to reduce the yellow tetrazolium salt into the red formazan salt, which can be measured spectrophotometrically. Consequent colorimetric changes are therefore proportional to the amount of cell death induced.

2.4.1.1 Cell density optimisation

Cells were harvested as described in section 2.1.2 before pelleting in a 15 ml falcon tube through centrifugation at 162 *x g*. The cell pellet was resuspended in assay medium consisting of DMEM (Thermofisher Scientific) supplemented with 1% FBS (GE Healthcare) and 1% Penicillin/Streptomycin (Sigma-Aldrich) and cells were counted using an EVE Automated Cell Counter (NanoEntek). A cell concentration of 2×10^6 cells/ml was prepared. 100 µl of assay medium was added to each of the wells labelled in Figure 2-1. 100 µl of the prepared cell suspension was then added to wells A1-F1, effectively producing a final cell count in these wells of 1×10^5 per well following a 1:2 dilution. With a multi-channel pipette, 100 µl was removed from wells A1-F1 and was transferred to the

wells in column 2 (A2-F2) and these were then thoroughly mixed. This process was repeated across the plate to perform a serial dilution until column 8. The aspirated 100 µl from column 8 was discarded and assay media only was added in wells A9-C9. The plate was incubated in a 5%-CO_2 air incubator at 37ºC for 96 hours. After incubation, 5 µl of lysis solution was added in the wells designated as high controls followed by incubation for a further 15 minutes. A reaction mixture was prepared consisting of the LDH kit's catalyst diluted in the dye solution in a 1:45 ratio. 100 µl of the reaction mixture was added to each well before incubating for 10 minutes at room temperature whilst protecting from light. 50 µl of stop solution was added to all wells and was shaken at 300 rpm using the Orbital Incubator SI500 (Stuart) for 10 seconds. The plate was read using a FLUOSTAR plate reader (BMG labtech instruments) at an absorbance wavelength of 490/492 nm with >600 nm as a reference wavelength. The raw data was extracted using the Omega software (BMG labtech instruments). The triplicates were averaged and background value obtained from the media only wells was subtracted from all the calculated averages. For each cell concentration, the difference between the high and low controls was determined. The cell concentration that showed the greatest difference between the high and low measurements were considered the optimal seeding density in the LDH experiments.

	1	2	3	4	5	6	7	8	9	10	11	12
A	$1x10^5$	$5x10^4$	$2.5x10^4$	$1.25x10^4$	$6.25x10^3$	$3.1x10^3$	$1.6x10^3$	781	Media only			
B	$1x10^5$	$5x10^4$	$2.5x10^4$	$1.25x10^4$	$6.25x10^3$	$3.1x10^3$	$1.6x10^3$	781	Media only			
C	$1x10^5$	$5x10^4$	$2.5x10^4$	$1.25x10^4$	$6.25x10^3$	$3.1x10^3$	$1.6x10^3$	781	Media only			
D	$1x10^5$	$5x10^4$	$2.5x10^4$	$1.25x10^4$	$6.25x10^3$	$3.1x10^3$	$1.6x10^3$	781				
E	$1x10^5$	$5x10^4$	$2.5x10^4$	$1.25x10^4$	$6.25x10^3$	$3.1x10^3$	$1.6x10^3$	781				
F	$1x10^5$	$5x10^4$	$2.5x10^4$	$1.25x10^4$	$6.25x10^3$	$3.1x10^3$	$1.6x10^3$	781				
G												
H												

Figure 2-1 Ependymoma cell density optimisation set up for LDH cell death assays. Each column showed a specific cell count with which Rows A-C were allocated as low controls while Rows D-F corresponded with high controls. Column 9 only contained assay media. **Key:** **Low Control**, **High Control.**

2.4.1.2 Drug treatment

The optimised seeding densities for the ependymoma cell lines were: BXD-1425EPN and DKFZ-EP1 (7000 cells), EPN1 (6000 cells) and EPN12A (5000 cells). Cells were seeded in triplicate in assay media. Triplicate wells were also prepared for the low and high measurements. 100 µl of assay medium was added to 6 wells for background and substance only triplicate controls. The plate was incubated overnight in a 5%-CO_2 air incubator at 37ºC to allow the cells to settle. On day 2, the media in all wells was replaced with the appropriate vehicle or varying BKM120 concentrations. Assay media was added to the background wells. The highest BKM120 concentration used (5 µM) in the experiment was added to the substance only wells. The plate was incubated for a further 72 hours at 37ºC prior to detection and analysis.

2.4.1.3 Detection and analysis

For the detection of LDH-mediated cytotoxicity, the protocol used was the same as that outlined in the LDH assay cell density optimisation in section 2.4.1.1. The triplicates for each condition were averaged and the background value was subtracted from these averages. Cytotoxicity was calculated for each drug concentration using the equation:

$$Cytotoxicity = \frac{(experimental\ value - low\ control)}{(high\ control - low\ control)}\ x100$$

One-way ANOVA was used to determine significant changes in LDH activity in each drug concentration relative to the vehicle control.

2.4.2 Cell cycle analysis using flow cytometry

2.4.2.1 Establishing cell seeding density using alamarBlue™ assay

Optimisation for sample preparation of cell cycle analysis was performed using the alamarBlue™ cell viability assay (Invitrogen) to determine appropriate seeding densities that relate to a proliferative rather than lag phase. It employs the blue resazurin compound, which is reduced into the red resorufin compound upon entry into living cells. The amount of red resofurin compound was established using absorbance-mediated endpoint measurement.

Cells were harvested and pelleted as outlined in sections 2.1.2 and 2.1.3, respectively. The pellets were resuspended in SFM and counted using an EVE Automated Cell Counter (NanoEntek). Cells were seeded in 25 cm^2 cell culture flasks at

a final volume of 5 ml using the following densities: 5 x 10^3, 1 x 10^4, 2 x 10^4, 5 x 10^4, 8 x 10^4 and 1.6 x 10^5 cells/ml. A media only containing 25 cm^2 flask was also set up as a blank. The cells were incubated in a 5%-CO_2 air incubator at 37^{o}C overnight. The media in all of the flasks was replaced with cell culture media corresponding to the cell line being optimised (see section 2.1.1) and was incubated for a further 24 hours (also extended to 72 hours for BXD-1425EPN cells). After incubation, 500 µl of alamarBlue^{TM} reagent was added to each flask before a 2-hour incubation at 37^{o}C. 100 µl of the supernatant from each flask was added in triplicate on a 96-well plate and was read using a FLUOSTAR plate reader (BMG labtech instruments) with an excitation wavelength of 544 nm and emission wavelength of 590 nm. The raw data was extracted using the Omega software (BMG labtech instruments). Triplicates were averaged and the mean background value was subtracted from these. The absorbance values were plotted against the cell density. Cell densities were picked where the cells were at a proliferative state in conjunction to a confluency of ~70% prior to the addition of the alamarBlue^{TM} reagent.

2.4.2.1 Cell seeding and drug treatment

BXD-1425EPN, EPN1 and EPN12A cells were seeded in SFM with a final volume of 5 ml in 25 cm^2 flasks overnight at 37^{o}C at a density of 8 x 10^4, 6 x 10^4 and 8 x 10^4 cells/ml, respectively following standard curve analysis with alamarBlue^{TM} assays. BXD-1425EPN cells were seeded at 5 x 10^4 cells/ml for a 72-hour drug treatment. After incubation in a 5%-CO_2 air incubator at 37^{o}C overnight, media was replaced with the corresponding media containing either DMSO (vehicle) or different concentrations of BKM120 (0.5, 1 and 5 µM). An untreated (media only) condition was added as a toxicity control for the DMSO treatment. The flasks were incubated for 24 or 72 hours in a 5%-CO_2 air incubator at 37^{o}C.

2.4.2.2 Sample preparation

The cells were harvested as detailed in section 2.1.2 and collected in a 15 ml falcon tube. The samples were centrifuged at 300 *x g* for 5 minutes and the supernatant was discarded. The pellet was washed in 500 µl PBS and fixed in 4.5 ml of cold 70% ethanol for 2 hours. The samples were centrifuged at 300 *x g* for 5 minutes before thoroughly decanting the ethanol. The pellet was suspended in 5 ml PBS then centrifuged at 300 *x g* for 5 minutes. After decanting the supernatant, the pellet was resuspended in 1 ml PI staining solution (PBS with 0.1% (v/v) Triton X-100 (Sigma-Aldrich), 10 µg/ml PI (Invitrogen), 100 µg/ml DNase-free RNAse A (Sigma-Aldrich) and was protected from light at room temperature for 30 minutes.

2.4.2.3 Detection and analysis

The samples were transferred into FACS tubes and arranged around a carousel in a Beckman Coulter FC500 Flow Cytometer System. Fluorescence for PI bound to DNA was measured using an excitation wavelength at 536 nm and emission at 617 nm. The resulting LMD files were analysed using WEASEL Flow Cytometry Software v3.0. Gating was performed in order to select cells contained within a certain region on the resulting scatter plot using characteristics including cell size and granularity for cell cycle analysis. This was implemented on a forward versus side scatter density plot which excluded debris that were detected in the samples. Gating was also undertaken in a forward scatter height versus forward scatter area density plot which related to single cell populations only. Using a single parameter histogram, a cell cycle profile was produced. Induced cell cycle fit was applied onto the profiles to quantify cell populations in various cell cycle phases (Sub-G_0, G_0/G_1, S-phase, G_2/M, Super G_2). A two-way ANOVA was used to determine significant differences in cell numbers per drug treatment relative to the vehicle control in each cell cycle phase.

2.5 Protein-based assays

2.5.1 Western blot

2.5.1.1 Drug treatment

The following protocol is relevant for the investigation of PI3K pathway inhibition following BKM120 treatment (see section 3.2.1), AKT inhibitor treatment (see section 3.2.6) and analysis of FOXO activation (see section 5.2.1). Cells were seeded in SFM in duplicates in a 6-well plate format with a seeding volume of 2 ml. The seeding densities for the different cell lines were: 1.5 x 10^5 (BXD-1425EPN), 1.8 x 10^5 (DKFZ-EP1), 1.8 x 10^5 (EPN1) and 1.5 x 10^5 (EPN12A) cells per well. Prior to drug treatment, the cells were allowed to settle for 24 hours. BKM120 was diluted in SFM at a final concentration of 0.5, 1 and 5 µM. DMSO was also diluted in SFM as a control. The media was replaced with the appropriate drug containing media before incubating for 50 minutes at 37^{o}C. EGF was added to the drug containing media at a concentration of 50 ng/ml to activate intracellular signalling pathways. The cells were then incubated for a further 10 minutes at 37^{o}C. At the end of the incubation, the wells were washed with HBSS and 200 µl of 1x TE Buffer was added in each well. 1 ml of media was used to stop the trypsinisation process and cells for each duplicate treatment were collected in 1.5 ml Eppendorf tubes. The tubes were centrifuged at 700 *x g* for 5 minutes and the supernatant was subsequently removed before storing the cell pellets at -80^{o}C. Preparation of cells for Perifosine and GDC-0068 western blot analysis (see section 3.2.6) was performed in the same way except that only BXD-1425EPN cells were investigated (5 x 10^4 cells per well). The drug concentrations

used for both Perifosine and GDC-0068 treatments were 5, 10 and 25 μM as well as the vehicle control.

Western blot analysis relating to autophagy (see section 3.2.4), apoptosis (see section 3.2.3.2) and investigation of Rb-mediated cell cycle arrest mechanism (see section 5.2.3) follow the following drug treatment protocol. Cells were seeded in SFM in 6-well plates using the same seeding densities as described previously. After 24 hours of incubation at 37^{o}C, the media was replaced with normal or tumour media containing either DMSO, 0.5, 1 or 5 μM BKM120. The cells were incubated with the drugs for another 24 hours. At the end of the incubation, the media for each drug treatment was transferred in a 15 ml Falcon tube to collect any cells that had detached. The wells were washed with HBSS and 200 μl of 1x TE buffer was added to each well for trypsinisation. 1 ml of media was used to inhibit the trypsinisation process and pool the duplicate wells together before combining with the appropriate Falcon tubes containing the media that was collected prior to cell harvesting. The tubes were centrifuged at 162 *x g* for 5 minutes. After discarding the supernatant, the pellet was resuspended in 1 ml PBS and transferred into 1.5 ml Eppendorf tubes followed by centrifugation at 700 *x g* for 5 minutes. The supernatant was removed before storing the pellet at -80^{o}C.

2.5.1.1 Protein lysate preparation

Lysis buffer was made by diluting protease cocktail stock (Promega) in protease cocktail buffer (Appendix 4) in a 1:50 ratio. Cell pellets were dissociated in 25 μl of lysis solution and incubated on ice for 20 minutes. The samples were centrifuged at 15 900 *x g* for 30 minutes at 4^{o}C. The supernatant containing the protein lysate was transferred to a fresh Eppendorf tube before storing at -80^{o}C.

2.5.1.2 Protein quantification

The concentration of proteins extracted from cell pellets was determined using a Bradford assay. In this assay, a set of samples with known BSA concentrations was used as a basis for establishing the concentration of protein lysates. To create the BSA standards, red Coomassie Brilliant Blue G-250 protein assay dye (Bio-Rad) was diluted 1:4 using distilled water. 0.5, 2.5, 5, 7.5, 10, 15 or 20 μl of 2 mg/ml BSA were each added to 1 ml of diluted protein assay dye. 2 μl of each protein lysate were also added to 1 ml of diluted protein assay dye. In addition, a blank control was prepared consisting of just the diluted protein assay dye. 200 μl of each BSA concentration and diluted protein lysate was added in triplicate to a 96-well plate. The triplicate wells containing just the diluted protein assay dye served as a blank for background normalisation. Absorbance was read using a FLUOSTAR plate reader (BMG labtech instruments) at 595 nm, using 570 nm as

a reference wavelength. The raw data was obtained using the Omega software and a standard curve was plotted on Microsoft Excel for the various BSA absorbance values to create a linear equation (y= mx+c). This was used to identify the concentration of the protein lysates being assayed.

20 µg of protein was transferred into fresh Eppendorf tubes before adding 20% sample buffer containing 1:20 β-mercaptoethanol. The samples were boiled at 99^{o}C for 3 minutes to denature the proteins and allow an overall negative charge to encapsulate whole protein structures. The tubes were then centrifuged at 15 900 *x g* for 1 minute after which the samples are stable at room temperature (RT).

2.5.1.3 Gel preparation and electrophoresis

Gel preparation and electrophoresis were performed using the Mini-Protean Tetra Cell kit (Bio-Rad). A casting frame was used to affix a 1.5 mm spacer plate with a glass short plate. This was subsequently clamped into a casting stand where it was also pressed onto a rubber footing forming a sealed cavity between the two plates. Distilled water was put into the cavity for 10 minutes to ensure that any leakage was minimal.

A 15% lower (resolving) gel (Appendix 5) was prepared. The mixture was poured into the cavity made by the two plates to a level 1.5 cm below the top of the short plate. A layer of 70% ethanol was added on top of the gel to exclude any air pockets as well as prevent the gel mixture from evaporating as it set for one hour. The ethanol was fully discarded and was replaced with an upper (stacking) gel (Appendix 5). A 15 lane 1.5 mm comb (Bio-Rad) was placed into the space containing the upper gel to create the loading wells where the processed samples are dispensed. The upper gel was allowed to set for 45-60 minutes. Once set, the glass plates were gently removed from the casting frame and were assembled into the gel cassette, following the manufacturer's instructions. The whole cassette was lowered into a tank filled with electrode buffer (Appendix 6). The comb was gently removed ensuring that the wells were fully submerged in buffer. Any air bubbles in the wells were removed by ejecting buffer into the wells with a syringe. 7.5 µl of SeeBlue Plus2 Marker (Novax) was added to well 1 of the assembly in addition to the experimental samples. The gel was run at 140V for 90 minutes at RT.

2.5.1.4 Protein transfer

An 8.5 x 5.5 cm Amersham Hybond P membrane (GE Healthcare) was activated with methanol for 10 seconds before rinsing in water for 5 minutes. The membrane was subsequently put in transfer buffer (Appendix 6) for 10 minutes. The glass plates were separated and the upper gel was carefully trimmed before sliding the lower gel onto two

pieces of pre-soaked filter paper with two sponges underneath (*NB*. Ensure that this assembly was taking place on the black side of the cassette). The membrane was placed on top of the gel and a roller was used to eliminate any air bubbles that would impede protein transfer. Two more pre-soaked filter papers were placed on the membrane followed by two sponges. The assembly was clipped in place before putting in a transfer cassette. This was subsequently lowered into a transfer tank, which was then filled with transfer buffer. The transfer process was run at 25V overnight at 4^{o}C.

2.5.1.5 Antibody probing

At the end of the transfer process, the membrane was carefully removed from the assembly and blocked for 1 hour with 5% blocking solution consisting of 5% w/v milk powder in 1x TBS-T (Appendix 6) on a rocker. The membrane was rinsed twice with 1x TBS-T before incubating with the appropriate primary antibody (see Table 2-6 for antibody incubation details) After primary antibody probing, the membrane was washed twice with 5% blocking solution followed by 2X 10 minute in blocking solution and a 5 minute 1x TBS-T wash. The necessary species-specific HRP-conjugated secondary antibody (Cell Signalling Technology, CST) was diluted 1:2000 in 1x TBS-T and poured onto the membrane, to be incubated for 1 hour at RT. The secondary antibody solution was discarded followed by 2X rinse with blocking solution. The membrane was washed 2X 10 minutes with blocking solution followed by a 5 minute 1x TBS-T wash. A final 5 minute 1x TBS wash was performed on the membrane before proceeding with enhanced chemiluminescence (ECL) detection.

2.5.1.6 Enhanced chemiluminescence (ECL) detection

Luminol and enhancer solution (ECL kit, GE Healthcare) were mixed at a 1:1 ratio before pouring onto the membrane, which was placed on a piece of saran wrap. The mixture was spread across the membrane to fully cover it and incubated at RT for 5 minutes. The membrane was then wrapped in the saran wrap. The membrane was placed in an x-ray cassette for transport into the dark room. The membrane was exposed to film (Kodak biomax) for variable times to detect protein bands. The film was soaked in some Ilford PQ developing solution (diluted 1:100 in distilled water) until the bands begin to emerge. To stop the developing process, the film was subsequently rinsed with stopping solution. The ladder markers, present on the membrane, were indicated onto the film as a basis for identifying protein bands of interest. The membrane was stored in 1x TBS at 4^{o}C for future probing.

2.5.1.7 Membrane stripping

Previously probed membranes were stripped in order to remove any bound antibodies and minimise any non-specific protein detection before the next antibody could be added. The membrane was washed with stripping buffer (Appendix 6) twice for 10 minutes. 2X 10 minute PBS washes were performed followed by 2X 5 minute washes with 1x TBS-T before starting the blocking process outlined in section 2.5.1.5.

Table 2-6 Antibodies used in Western blot analysis including the species type, dilution and length of incubation.

Antibody	Supplier	Species	Protein size (kDa)	Dilution	Incubation
pAKT	Cell Signalling Technology	Rabbit	60	1:1000	1 hour at RT
AKT	Cell Signalling Technology	Mouse	60	1:2000	1 hour at RT
pS6	Cell Signalling Technology	Rabbit	32	1:2000	1 hour at RT
S6	Cell Signalling Technology	Mouse	32	1:1000	1 hour at RT
Caspase 3	Cell Signalling Technology	Mouse	17, 19, 35	1:1000	Overnight at 4ºC
p62	R&D Systems	Mouse	62	1:3000	1 hour at RT
pRb	Cell Signalling Technology	Rabbit	110	1:1000	Overnight at 4ºC
Rb	Cell Signalling Technology	Mouse	110	1:1000	Overnight at 4ºC
pFOXO1	Cell Signalling Technology	Rabbit	82	1:1000	Overnight at 4ºC
FOXO1	Cell Signalling Technology	Rabbit	78-82	1:1000	Overnight at 4ºC
pFOXO3a	Cell Signalling Technology	Rabbit	97	1:1000	Overnight at 4ºC
FOXO3a	Cell Signalling Technology	Mouse	82-97	1:1000	Overnight at 4ºC
GAPDH	R&D Systems	Mouse	37	1:50 000	1 hour at RT

2.5.2 Luciferase assay

Luciferase reporter assays were employed to measure E2F-mediated gene expression in ependymoma cells in response to inhibition of the PI3K pathway. These experiments and its outcomes were discussed in detail on section 5.2.4.2.

2.5.2.1 Nucleofection™ of constructs

The E2F reporter construct, constitutively expressing firefly luciferase (positive control) and non-inducible firefly luciferase (negative control) constructs were purchased from SABiosciences. The constructs were transfected through Nucleofection™ in a similar way as described with the GFP plasmid constructs in section 2.2.4.1. For luciferase assays, there were some alterations made to the protocol to prevent overloading the transfection system's reaction. 5 x 10^5 BXD-1425EPN cells were pelleted and resuspended in 100 µl Nucleofection™ solution. 1 µg of the appropriate luciferase construct was added to the reaction mix. This was transferred into a specialised cuvette and the X-001 program was used for the transfection (see 5.2.4.1 for optimisation results). 500 µl of pre-conditioned RPMI-1640 media was added into the cuvette and incubated at 37ºC for 10 minutes. The samples were carefully transferred into a 15 ml falcon tube containing 4.5 ml pre-conditioned cell culture media. The diluted cell suspension was mixed and dispensed into a sterile reservoir. Using a multi-channel pipette, 100 µl of the diluted cell suspension was added to a 96-well plate before incubating in a 5%-CO_2 air incubator at 37ºC overnight. 12 wells were each allocated to cells transfected with either the E2F reporter construct or the negative control construct. Three wells were set up for cells transfected with the positive control construct. This essentially puts the cell density at an estimated 10 000 cells per well. Cell culture media was also added to three further wells for background controls. As part of the optimisation, cells transfected with the positive control construct was observed for GFP expression using the Zeiss Axiovert S100 inverted fluorescence microscope to ensure that transfection via Nucleofection™ was successful despite alterations made to the manufacturer's protocol.

2.5.2.2 Drug treatment and detection

The dual-Luciferase® Reporter Assay System (Promega) was used to quantify changes in luciferase readouts in transfected cells following drug treatment. The media in the E2F reporter transfected wells was removed after overnight incubation and replaced with either vehicle or BKM120 (0.5, 1 or 5 µM). The positive control, negative control and blank wells were replaced with fresh cell culture media. The plate was incubated again for 24 hours in a 5%-CO_2 air incubator at 37ºC. The media was discarded at the end of the incubation and the wells were washed with PBS twice to remove any residual media

that may have interfered with the reading. 5x Passive Lysis Buffer (PLB) was diluted in distilled water before adding 30 µl to all wells to lyse the cells. The plate was rocked at room temperature for 15 minutes while protected from light. 100 µl of reconstituted Luciferase Assay Reagent II was then added to each well. The reaction solution was mixed using a multi-channel pipette before transferring 125 µl into a white solid 96-well plate. Luciferase output was determined using a FLUOSTAR plate reader (BMG labtech instruments). A lens filter was used for luminescence readings with the following conditions: 0.1 second settling time, 2.0 second measurement interval time and Gain measurement at 3600. 100 µl of Stop & Glo® reagent (50x Stop & Glo® Substrate diluted in Stop & Glo® Buffer) was added in each well followed by a second reading to obtain the Renilla luciferase readout. The luciferase and renilla values were averaged then corrected for background noise by subtracting the corresponding mean blank value. Each mean luciferase value was divided by their corresponding mean Renilla luciferase value for normalisation. A one-way ANOVA was performed to determine significant differences in luciferase expression of BKM120 treated cells relative to the vehicle control.

2.6 Microarray expression

2.6.1 Cell seeding and treatment

BXD-1425EPN and EPN1 cells were harvested as described on section 2.1.2 and pelleted by centrifugation at 162 *x g* for 5 minutes. The pellet was resuspended in SFM and cells counted using the EVE Automated Cell Counter (NanoEntek). The cells were seeded in 6-well plates at a seeding density of 1.5 x 10^5 and 1.8 x 10^5 for BXD-1425EPN and EPN1 cells, respectively, in a final volume of 2 ml before incubating at 37^{o}C in a 5%-CO_2 air incubator overnight. After incubation, the media was replaced with media containing either DMSO or 2.5 µM (BXD-1425EPN) or 4.5 µM (EPN1) BKM120. The cells were re-incubated in a 5%-CO_2 air incubator at 37^{o}C for 24 hours. Duplicates were also prepared for each drug concentration.

2.6.2 RNA extraction

The wells were washed with HBSS and 200 µl of 1x TE Buffer was added in each well to trypsinise the cells. 1 ml of media was used to stop the trypsinisation process and cells for each duplicate treatment were collected in 1.5 ml Eppendorf tubes. The tubes were centrifuged at 700 *x g* for 5 minutes and the supernatant was subsequently removed. RNA was extracted from cell pellets using the *mir*VANA™ miRNA isolation kit (Invitrogen), using an altered version of the manufacturer's protocol. The pellet was disrupted by adding 300 µl of Lysis/Binding Buffer. 30 µl of miRNA Homogenate Additive was added

to the suspension, which was vortexed and then left on ice for 10 minutes. 300 µl of Acid-Phenol:Chloroform was added to the sample, which was vortexed and then centrifuged for 5 minutes at 10 000 *x g*. The upper aqueous phase was transferred into a fresh Eppendorf tube, noting down the estimated volume collected. 1.25 x volumes of 100% ethanol were added to each sample. Up to 700 µl of the mixture was pipetted onto a filter cartridge affixed into a collection tube then centrifuged for about 15 seconds at 10 000 *x g*. This process was repeated for any left over mixture, discarding the flow through each time in the process. 700 µl of miRNA Wash Solution 1 was added to the cartridge and centrifuged for 15 seconds. The flow through was discarded. 500 µl of Wash Solution 2/3 was added and centrifuged for 10 seconds at 10 000 *x g*. Flow through was discarded and Wash Solution 2/3 step was repeated before a final one minute centrifugation step having discarded the flow through from the previous spin. The cartridge was placed in a fresh collection tube after which 100 µl of pre-heated (95^{o}C) nuclease-free water was added to the cartridge filter. The tube was centrifuged for 30 seconds at 10 000 *x g* to elute the RNA. The RNA concentration was quantified using a Nanodrop 2000 (Thermofisher Scientific) with a desired concentration of at least 100 ng/µl, and a 260/280 ratio of ~2.0.

2.6.3 Quality control and microarray run

RNA quality control and all transcriptomic protocols were performed by Prof. Sean May's research group at the Nottingham Arabidopsis Stock Centre (NASC), Sutton Bonington, University of Nottingham. RNA quality was evaluated using the Agilent RNA 6000 Nano Kit (Integrated Sciences) with results processed using the Agilent 2100 Expert Software as mediated by the Agilent 2100 Bioanalyzer instrument, according to the manufacturer's instructions. This generated a RIN (RNA Integrity Number) score out of 10, using >7 as a threshold. Total RNA from three biological repeats of the vehicle and drug treated samples for each cell line were hybridised on GeneChip^{TM} Human Gene 2.1 ST Array (Affymetrix), following the manufacturer's instructions for sense cDNA synthesis, fragmentation and hybridisation. Microarray hybridisation was processed by the GeneChip® 3000 System (Affymetrix). The resulting gene expression profile *CEL* files were analysed using Partek® Genomics Suite 6.6 software. Quality control measures included chip surface surveying for damages, labeling and calculation of 3' probe set to 5' probe set ratio as an indication for the quality of the microarray data. An expression matrix post-hybridisation was generated using Robust Multi-array Average (RMA). The intensity signals from the array were represented as a value that was background corrected, $\log^2$ transformed and quantile normalised followed by linear model fitting through the normalised data to determine the expression level per probe on the array.

2.6.4 Gene expression analysis

2.6.4.1 Gene ontology analysis

Differentially expressed genes (DEGs) were identified using a t-test and fold change calculations. A threshold of ±2 fold-change and an unadjusted p-value of <0.05 were used as cut offs. Gene ontology (GO) enrichment analysis of cell line specific DEGs, for biological and molecular functions, was performed using Partek® Genomics Suite. Additional GO analysis was performed using DAVID Bioinformatics Resources 6.8 (Huang da, Sherman et al. 2009) and Gene Ontology Enrichment Analysis and Visualization Tool (GOrilla) (Eden, Navon et al. 2009a). On the DAVID platform, the official gene symbols of the 202 DEGs identified on the microarray work (see section 4.2.3.2) were manually uploaded as a gene list using *Homo sapiens* as an annotated species. The functional annotation chart was then used under the Gene Ontology category for analysis. GOrilla was mainly used for the upregulated genes within the 202 ependymoma DEGs. *Homo sapiens* was set as the organism and two unranked lists of genes were processed: target set (26 upregulated genes) and background set (29,605 gene probes on the microarray). Biological process was used as the ontological function to be analysed.

2.6.4.2 Gene network analysis

The list of overlapping DEGs between the two cell lines was queried into STRING v10.5 to establish protein-protein interactions using a high confidence interaction score (0.700). The resulting STRING network was imported into Cytoscape v3.6.1 as a framework to consequently produce a visual map of these interactions. The add-on Cytarget LINKER app was used to superimpose gene regulatory factors, particularly transcription factors, onto the genetic map using Regulatory Interaction Networks (RegINS): TFe and ENCODE.

2.6.4.3 Transcription factor enrichment analysis

The list of overlapping DEGs between the two ependymoma cell lines was processed into Gene Set Enrichment Analysis (GSEA) (Subramanian, A., Tamayo et al. 2005). Under the motif gene sets function, computation of transcription factor target (TFT) overlaps was undertaken to determine common upstream *cis*-regulatory motifs which signify prospective binding sites for transcriptional elements that regulate expression of these DEGs. The top 100 transcriptional regulators were elucidated using an FDR q-value of <0.05 as a cut off. Further analysis of related transcription factors was performed using the Cytoscape genetic map following application of the TFe and ENCODE RegINS as functional packages of the software. Identification of transcription factors of interest on

the map allows isolation of “neighbouring” target genes in support of the findings obtained from GSEA analysis.

CHAPTER 3. FUNCTIONAL EFFECTS OF CANONICAL PI3K/AKT/mTOR SIGNALLING IN EPENDYMOMA

3.1 Introduction

Activation of the PI3K pathway in 72% of primary ependymomas suggests a significant role in disease pathogenesis (Rogers, Mayne et al. 2013). Since the pathway is known to be a crucial regulator of cell viability and survival, its inhibition represents a potential therapeutic approach in large patient cohorts. It has been shown that inhibition of the PI3K pathway induces tumour suppressive effects by reducing cellular processes such as cell proliferation, growth and metabolism (Manning, Cantley 2007). However, responses towards PI3K pathway inhibition are usually cancer-specific with treatments mostly conferring either cytostaticity or cytotoxicity. For instance, PI3K pathway inhibition has been known to arrest cells at the G_1/S phase of the cell cycle (Fekete, Santiskulvong et al. 2012, Dan, Okamura et al. 2012) while others have demonstrated an increase in cell death responses (Tsuruta, Masuyama et al. 2002, Hu, Y., Guo et al. 2015), with apoptosis being the common mechanism. Loss of PI3K signalling also upregulates autophagic responses whose role promotes the isolation and breakdown of intracellular components which are usually reused by the cell for anabolic purposes. However, its activation presents a dual function that could either favour survival due to this recycling process or stimulate cell death as a result of extensive degradation (Zakeri, Melendez et al. 2008). Autophagy-mediated cell death (Type II cell death) therefore introduces an alternative cytotoxic mechanism that could arise from PI3K pathway inhibition.

Since the PI3K pathway regulates a broad range of downstream targets that promote a series of cellular responses, it is essential to characterise those functions that are specific to ependymoma pathogenesis. Inhibition of the PI3K pathway in ependymoma cells would establish whether loss of these functions negatively impacts tumourigenesis thus providing an indication of its mechanism of action as a chemotherapeutic target. In this study, the pan-class I PI3K inhibitor BKM120 was used as a primary tool to suppress PI3K signalling in a panel of patient-derived ependymoma cells. Inhibition of the PI3K pathway using BKM120 has been shown to reduce cell viability of many cancers *in vitro* such as medulloblastoma (Zhao, P., Hall et al. 2017), sarcoma (Anderson, Park et al. 2015) and acute lymphoblastic leukaemia (ALL) (Pereira, Machado-Neto et al. 2015). Preliminary data has also demonstrated that BKM120-mediated inhibition of PI3K signalling in two ependymoma cell lines resulted in a reduction

in viability (Rogers, Mayne et al., 2013). Further experimental data is necessary to elucidate the cellular processes that underlie these findings in ependymoma.

This chapter continues from the findings that were put forward by Rogers and colleagues with an aim to functionally establish how the PI3K pathway promotes survival and viability in ependymoma. In this chapter, the following aspects were investigated:

- whether PI3K pathway inhibition also leads to a reduction in cell viability in these additional ependymoma cell lines.
- whether the reduction in cell viability is caused by cell death or inhibition of cell proliferation.
- the mechanism that would underlie cell death if shown to be an effect of BKM120.
- autophagy (and its effects) as a regulated downstream target of the PI3K/AKT/mTOR signalling axis.
- whether the responses induced in ependymoma is mediated through canonical PI3K/AKT signalling.

3.2 Results

3.2.1 Treatment of ependymoma cells with BKM120 resulted in a decrease in PI3K/mTOR signalling pathway

Three supratentorial (BXD-1425EPN, DKFZ-EP1, EPN1) and one posterior fossa-derived (EPN12A) ependymoma cell lines were seeded in serum-free media for 24 hours. Subsequently, they were treated with various BKM120 concentrations for one hour before activating cell signalling through a 10-minute pulse treatment of EGF. Immunoblotting against pAKT and pS6 were performed to determine the status of PI3K/AKT/mTOR signalling. Probing for total AKT and S6 were also done as well as GAPDH which controlled for sample loading. According to the western blot data, there was a gradual reduction in the expression levels of pAKT and pS6 with increasing BKM120 concentration which was indicative of a loss of PI3K and mTOR signalling in these cells (Figure 3-1). Expression of AKT and S6 remained constant irrespective of the drug concentration, demonstrating that total protein concentrations were not affected by BKM120 treatment.

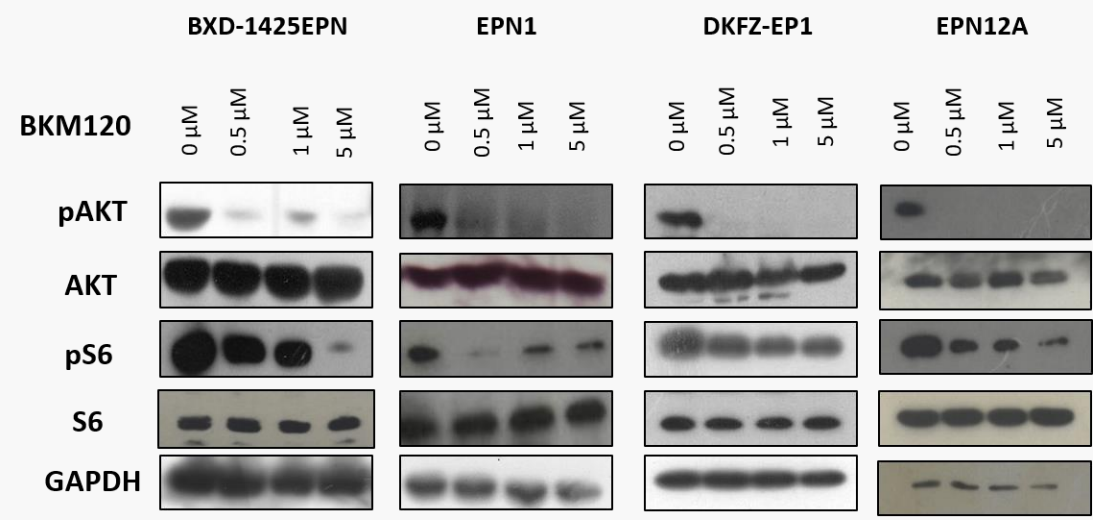


Figure 3-1 Ependymoma cells were seeded in serum free media (SFM) for 24 hours, treated with BKM120 for one hour followed by a pulse activation of the PI3K pathway using EGF for 10 minutes. Western blot analysis was performed to determine changes in phosphorylated AKT and S6 levels in addition to the total AKT and S6 levels following BKM120 treatment of ependymoma cell lines. GAPDH levels were also determined to ensure equal loading of proteins per lane (n=3).

3.2.2 Treatment with BKM120 decreased viability of ependymoma cells

MTT viability assays in response to BKM120 treatment were undertaken on BXD-1425EPN and EPN1 cells by Rogers, Mayne et al. (2013), with IC_{50} values determined to be within clinical range (~4 µM) (Bendell, Rodon et al. 2012b). These assays were repeated on DKFZ-EP1, EPN12A and one additional posterior fossa-derived cell line EPN8 to establish whether BKM120 could also reduce the viability of these cells thereby maintaining a consistent effect. BKM120 treatment significantly reduced the viability of all additionally tested ependymoma cell lines relative to vehicle controls (***$p<0.001$) in a dose-dependent manner after a 72 hour incubation (Figure 3-2). BKM120 IC_{50} values were determined in all cells through non-linear regression analysis. The MTT raw data previously obtained for BXD-1425EPN and EPN1 were re-analysed alongside the findings for the other three tested cell lines to maintain consistency in the project's data interpretation. Re-calculated BKM120 IC_{50} values were 2.1 and 4.2 µM for BXD-1425EPN and EPN1, respectively, which reflected those determined by Rogers et al. (2013). The IC_{50} values determined for the other cell lines were also within clinical range (DKFZ-EP1: 2.8 µM, EPN8: 1.5 µM, EPN12A: 1.0 µM) thus suggesting its efficacy against both supratentorial and posterior fossa tumours.

Since Rogers and colleagues also highlighted that a higher proportion of supratentorial tumours have activated PI3K signalling relative to posterior fossa tumours, it was subsequently investigated whether there was a significant difference in BKM120 responses between ependymomas from the two anatomically distinct CNS

compartments. Cell viability trends following BKM120 treatment were compared using corrected two-way ANOVA multiple comparisons testing. First, the viability trends of cell lines belonging to each compartment were compared against each other to evaluate any significant variances in BKM120 responses per region but showed no significant differences in the interaction of their cell viability trends (supratentorial cell lines p= 0.260, posterior fossa cell lines p= 0.273). Next, cross-comparisons of the supratentorial and posterior fossa cell viabilities were carried out. A significant difference in responses to BKM120 treatment was shown between the supratentorial and posterior fossa cells (Table 3-1), apart from BXD-1425EPN versus EPN8 (p= 0.131). This difference mainly related to the posterior fossa cells generally manifesting a more profound inhibitory profile as a result of BKM120 treatment. These results suggest that BKM120 could potently inhibit the PI3K pathway in both supratentorial and posterior fossa tumours, with the latter group potentially displaying increased sensitivity based on their inhibitory profiles.

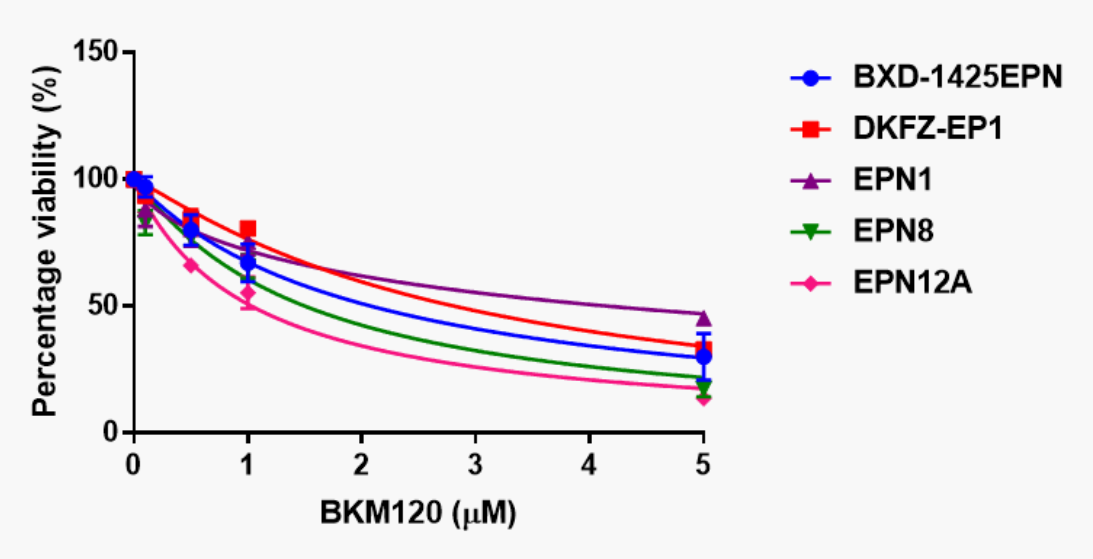


Figure 3-2 MTT viability assays. Treatment of supratentorial and posterior-fossa derived ependymoma cell lines with BKM120 for 72 hours significantly reduced cell viability with IC_{50} values determined at ≤ 4 μM using non-linear regression analysis (n= 3).

Table 3-1 Multiple comparisons test of supratentorial and posterior fossa ependymoma cell lines to determine significant differences in inhibition of cell viability following BKM120 treatment. (**p<0.01, ***p<0.001) (**Key: Supratenorial cell line; Posterior fossa cell line**)

Comparison		Adjusted p-value	Summary
BXD-1425EPN	EPN8	0.1310	ns
	EPN12A	0.0090	**
DKFZ-EP1	EPN8	0.0030	**
	EPN12A	0.0002	***
EPN1	EPN8	0.0060	**
	EPN12A	0.0003	***

3.2.3 PI3K pathway inhibition and cell death in ependymoma

One of the effects of inhibiting the PI3K pathway is stimulating cell death responses. Several cancer studies have demonstrated the cytotoxic effects of BKM120 treatment including in medulloblastoma (Zhao, P., Hall et al. 2017) and gliomas (Foster, Jane et al. 2015). Having established a decrease in ependymoma cell viability post-BKM120 treatment, subsequent work aimed to determine whether this was attributed to the activation of cell death responses.

3.2.3.1 BKM120 significantly induced cell death in one out of the four tested ependymoma cell lines

LDH assays were used to quantify the amount of cytotoxicity produced by BKM120 treatments in ependymoma cells. Data was presented as the inverse function of the amount of cytotoxicity produced so that the percentage viability was indicated instead following treatment of ependymoma cells with BKM120 (Figure 3-3). Incubation of ependymoma cells with BKM120 for 72 hours showed that only BXD-1425EPN cells resulted in a significant decrease in cell viability but with a 5 μM treatment dose (***p<0.001) (Figure 3-3A). However, these findings conferred no clinical relevance since the induced response was beyond the peak plasma concentration put forward for BKM120 (~4 μM) (Bendell et al., 2012). The significant increase in LDH activity attributed in this treatment condition may have been caused by the overwhelmingly toxic effect of treating such a high BKM120 concentration in these cells, which makes this finding only a proof of concept for cell death induction. No further significant LDH activity increase was detected in the other cell lines suggesting that no cell death was induced by BKM120. From these results, it could not be concluded that cell death was the likely cause of the reduction in cell viability observed in the MTT assays.

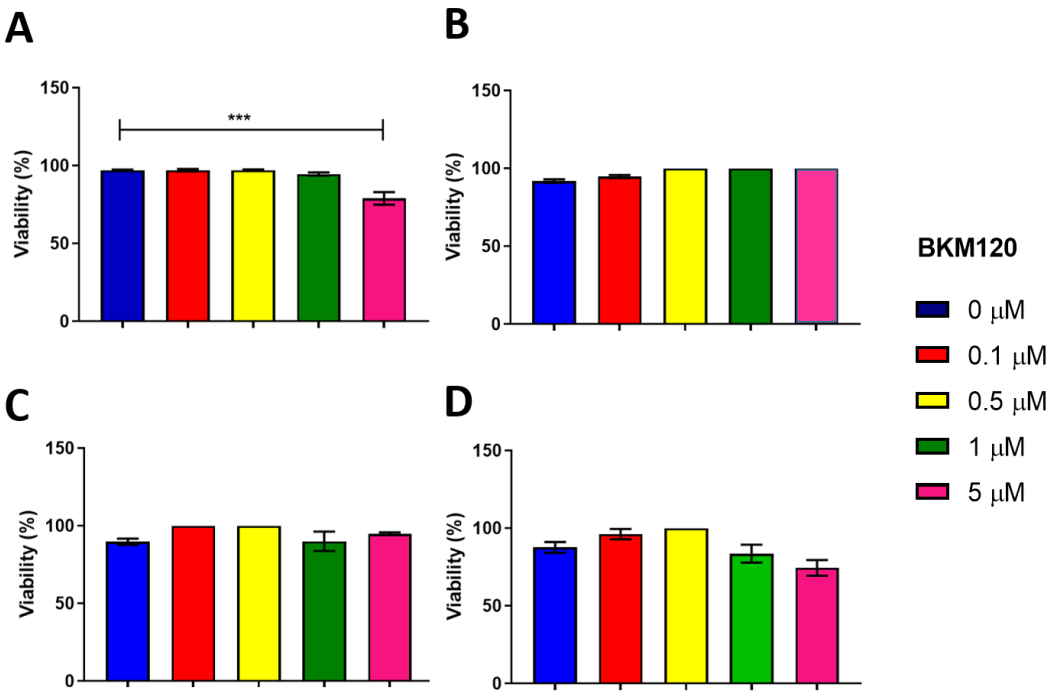


Figure 3-3 LDH cytotoxicity assays quantified cell death responses in (A) BXD-1425EPN, (B) DKFZ-EP1, (C) EPN1, (D) EPN12A cells following treatment with various concentrations of BKM120 for 72 hours (n=3). Only the treatment of BXD-1425EPN cells with 5 μM BKM120 showed a significant increase in LDH activity post-BKM120 treatment (***p<0.001). Values were presented with the standard error of the mean and analysed using one-way ANOVA (n=3).

3.2.3.2 BKM120 did not induce caspase-3 cleavage in ependymoma cells

Apoptotic cell death is the most commonly studied cell death mechanism following PI3K pathway inhibition (Yea, Fruman 2013). Upregulation of pro-apoptotic proteins and sequential cleavage of inactive pro-caspases consequently lead to the degradation of intracellular components and manifestation of apoptotic hallmarks. Using cleaved caspase-3 as a marker, it was investigated whether treatment of ependymoma cells with BKM120 induced apoptosis.

Ependymoma cells were incubated with various concentrations of BKM120 for 24 hours. As depicted in Figure 3-4A, increasing drug concentration detected no cleaved caspase-3 proteins (17 and 19 kDa) across the panel of cell lines at the end of the 24-hour incubation, suggesting that BKM120 did not induce any apoptotic responses. To mimic the MTT assay conditions, BXD-1425EPN cells were treated with BKM120 for 72 hours prior to immunoblotting (Fig. 4B). However, even prolonged drug incubation did not result in caspase-3 cleavage implying that reduction in cell viability post-72 hour BKM120 treatment was not due to activation of apoptosis. The western blot data also supports the LDH data that cell death was not a functional consequence of BKM120 treatment in ependymoma.

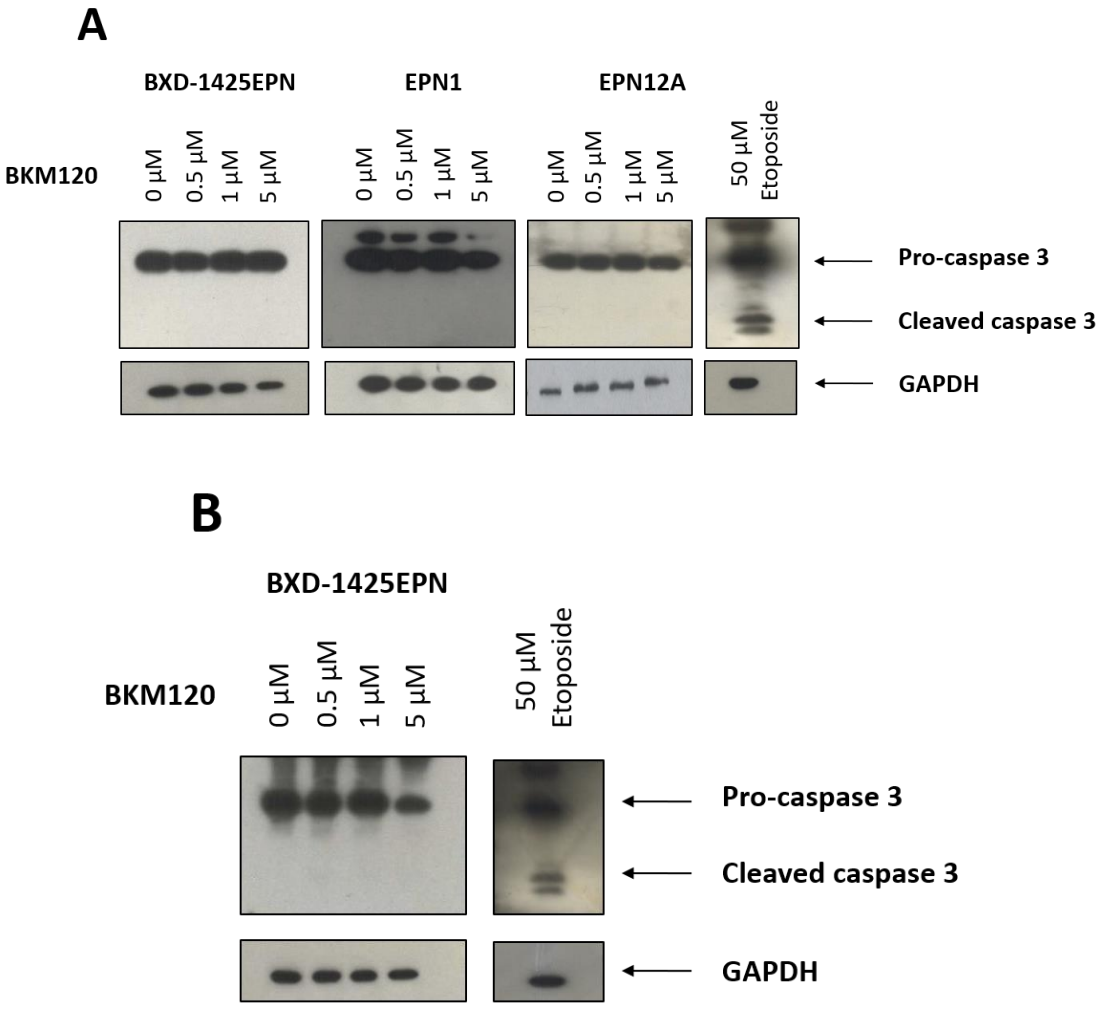


Figure 3-4 (A) Ependymoma cells were treated with BKM120 for 24 hours prior to caspase-3 probing. (B) BKM120 treatment was also extended to 72 hours for BXD-1425EPN cells. BXD-1425EPN cells treated with 50 µM etoposide served as a positive control as this resulted in cleavage of pro-caspase 3 to produce bands of 17 and 19 kDa. No bands pertaining to cleaved caspase-3 were detected in BKM120-treated ependymoma cells. Data is representative of at least three independent repeats.

3.2.3.3 BKM120 arrested cell cycle at G_0/G_1 phase in ependymoma cells

BKM120-mediated inhibition of the PI3K pathway in ependymoma did not induce cell death, suggesting that it only produces cytostatic effects. To further investigate this, flow cytometry was employed to determine whether BKM120 does induce cytostaticity rather than cytotoxicity in three ependymoma cell lines: BXD1425-EPN, EPN1 and EPN12A. After a 24-hour incubation with BKM120 (Figure 3-5), cell cycle analysis showed a significant increase in cell population in the G_0/G_1 phase of the cell cycle with increasing BKM120 concentration for all cell lines (**$p<0.01$). A significant decrease in S-phase cell population was also observed (**$p<0.01$). No accumulation of cells in the Sub-G_0 phase was seen, signifying no induction of cell death responses. BKM120 treatment also resulted in a significant decrease in EPN12A cell number at the G_2 phase after 5 µM

treatment (*p<0.05). Furthermore, cell cycle analysis was also completed for a 72 hour BKM120 treatment for BXD-1425EPN cells (Figure 3-6). Cell cycle profiles of BXD-1425EPN cells treated with BKM120 for 72 hours did not recapitulate a dose-dependent increase in cell population at the G_0/G_1 phase of the cell cycle with no significant change in the proportion of cells at any phase following drug treatment. Furthermore, the lack of cells in the Sub-G_0 phase further indicates that no cell death was induced. Therefore, these findings demonstrated that BKM120 treatment did not have a cytotoxic effect in ependymoma cells which further validates the LDH and caspase-3 immunoblot data. Instead, a cell cycle arrest at G_0/G_1 was found.

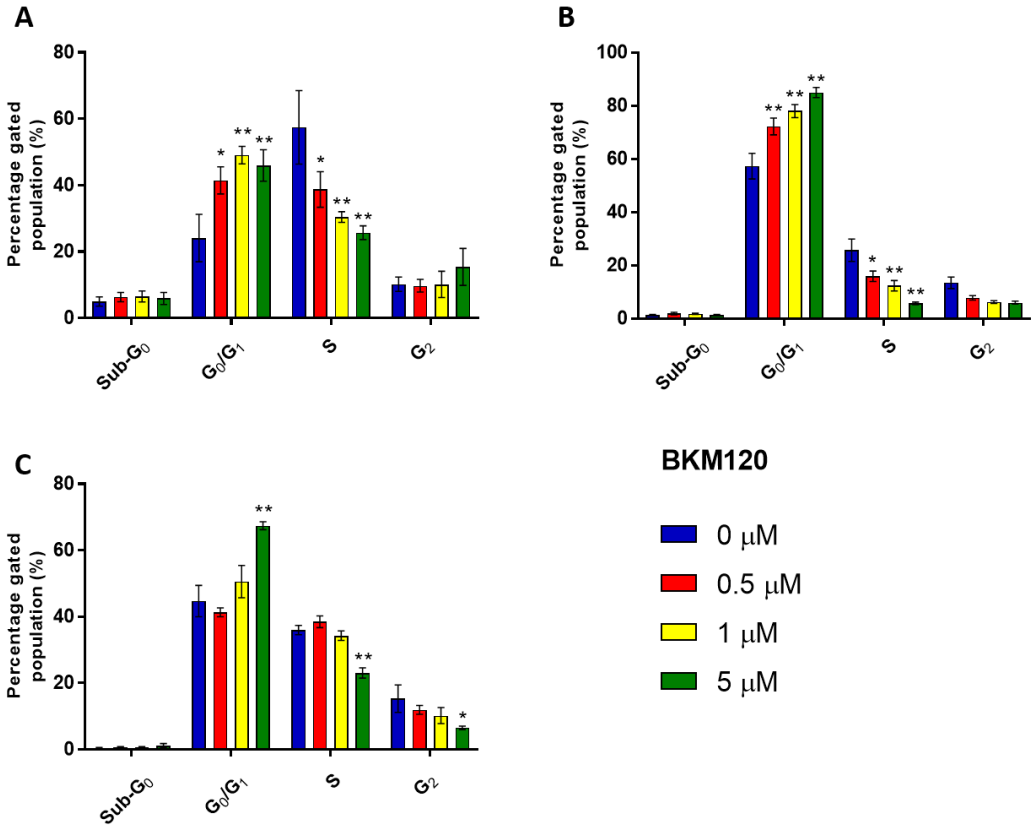


Figure 3-5 (A) BXD-1425EPN, (B) EPN1, (C) EPN12A cells were treated with BKM120 for 24 hours. Following PI3K inhibition, a significant increase in cell population was found in the G_0/G_1 phase of the cell cycle whilst simultaneously showing a decrease in the other phases. No dose-dependent increase in cell number was observed in the Sub-G_0 phase, suggesting the significant absence of cell death. Comparisons were made relative to the vehicle control per cell cycle phase (**p<0.01, *p<0.05). Statistical analysis on at least three independent repeats per cell line was performed using two-way ANOVA.

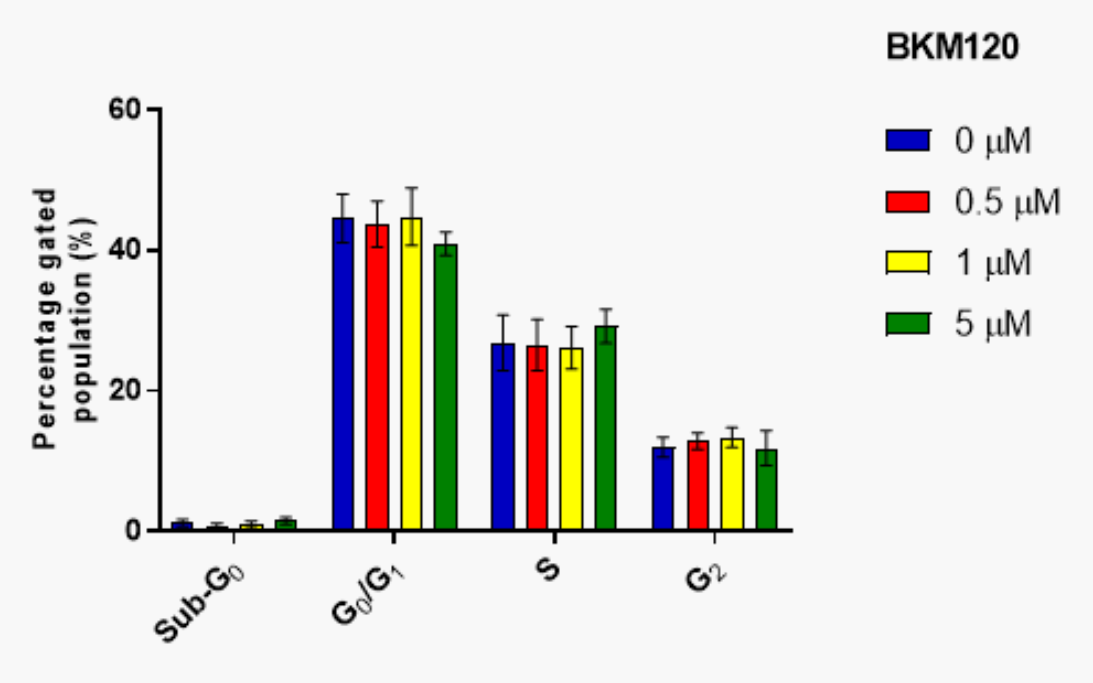


Figure 3-6 Cell cycle profile of BXD-1425EPN cells treated with BKM120 for 72 hours. No significant increase in cell number in G_0/G_1 phase was identified following drug treatment relative to the vehicle control based on a two-way ANOVA analysis. The decrease in cell number in the other cell cycle phases was also absent alongside the lack of cells in the Sub-G_0 phase. Data was presented with the SEM and is representative of three independent repeats.

3.2.4 Investigating autophagy as a cell death mechanism in ependymoma

Section 1.3.3.1 highlighted that autophagy is negatively regulated by the mTOR pathway, which is a direct target of the canonical PI3K pathway. Inhibition of the PI3K/AKT/mTOR signalling axis activates the autophagic machinery, which mediates intracellular degradation and consequent recycling of components for *de novo* synthesis and cellular homeostasis (Todde, Veenhuis et al. 2009). Interestingly, extensive autophagic responses have been proposed as an alternative avenue in stimulating cell death (Type II cell death) (Zakeri, Melendez et al. 2008) which highlights its bifunctional role in promoting survival as well as inducing cytotoxicity. In this chapter, the possibility of autophagy as a cell death mechanism was also explored simultaneously with the investigation of apoptotic responses following suppression of the PI3K pathway in ependymoma.

3.2.4.1 BKM120 resulted in a decrease in p62 levels in ependymoma cells

Probing for the multifunctional p62 protein was carried out to determine if reduction of PI3K/AKT/mTOR signalling in ependymoma would alleviate the inhibitory effects on autophagy. p62 serves as an autophagic marker due to its association with polyubiquitinated cargoes that are targeted for degradation (Cohen-Kaplan, Ciechanover

et al. 2016) thus resulting in a decrease in intracellular levels following activation of autophagy. Results showed that treatment of ependymoma cells with BKM120 for 24 hours led to a decrease in intracellular p62 levels in a dose-dependent manner (Figure 3-7), implying the formation of autophagolysosomal complexes to mediate its degradation. This demonstrated the role of PI3K signalling in negatively regulating autophagy in ependymoma, highlighting a potential survival effect of the pathway by preventing unnecessary cellular self-degradation.

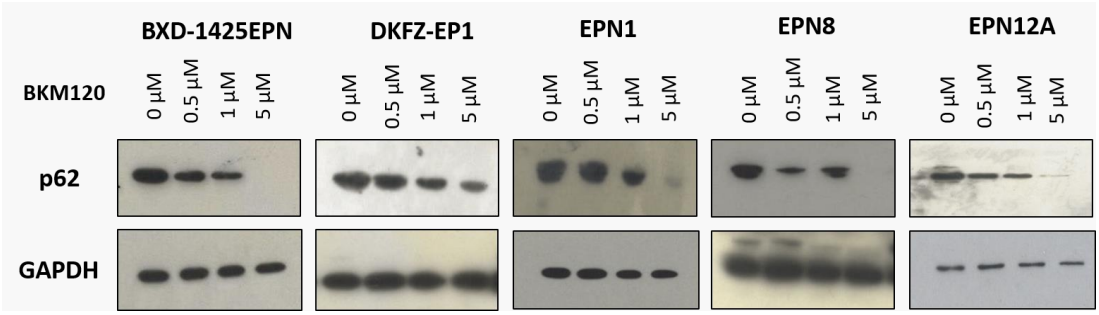


Figure 3-7 Ependymoma cells were treated with BKM120 for 24 hours followed by probing for p62 expression to determine activation of autophagic responses in ependymoma cells. Loss of p62 expression demonstrates degradation of associated cargo proteins by pre-formed autophagolysosomal complexes (n= 3).

3.2.4.2 Treatment of ependymoma cells with chloroquine inhibited BKM120-mediated autophagy

Historically, studies have perceived autophagy as a pro-survival mechanism due to its intrinsic recycling system. However, it is argued that excessive autophagy may be instrumental towards cellular crisis and ultimately, cell death. This work aimed to elucidate whether activation of autophagy, following PI3K inhibition, conferred cytotoxicity or cytoprotection in ependymoma.

Chloroquine (CQ), an anti-malarial agent, is a known inhibitor of autophagy by altering lysosomal pH which inactivates enzymatic activities necessary for degradation (Homewood, Warhurst et al. 1972). BXD-1425EPN and DKFZ-EP1 cells were treated with two CQ concentrations (5 and 20 µM) to determine dose-limiting toxicities that could be considered for further analyses. Results showed that cells tolerated a treatment of 5 µM after which a decline in cell viability was observed, attributing to possible off-target effects (*$p<0.05$) (Figure 3-8). To validate CQ's role as an autophagy inhibitor, BXD-1425EPN cells were incrementally treated with CQ in combination with 5 µM BKM120. Probing for p62 showed no BKM120 dose-dependent decrease in intracellular level proving that CQ potently reversed the effects of BKM120-induced autophagy (Figure 3-9).

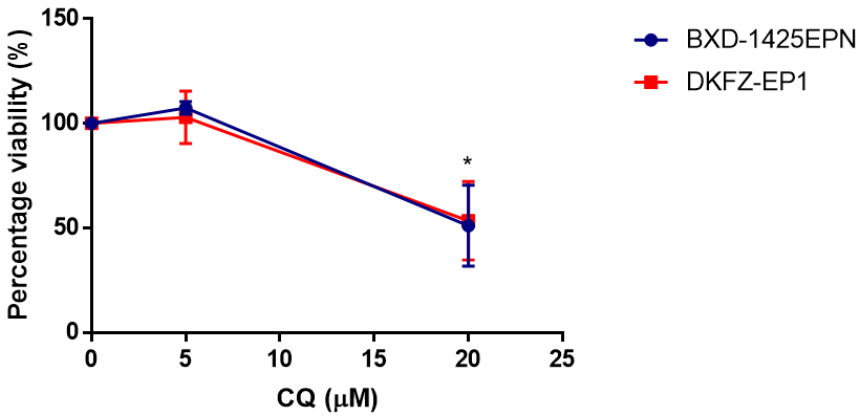


Figure 3-8 MTT viability assay of CQ only treated BXD-1425EPN and DKFZ-EP1 cells (n= 3) for 72 hours. Data was presented with standard error of the mean and changes in percentage viability relative to the vehicle control for each cell line was statistically analysed with one-way ANOVA.

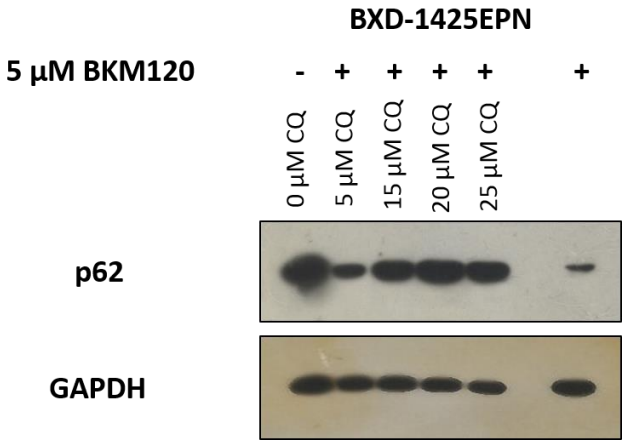


Figure 3-9 BXD-1425EPN cells were treated with 5 μM BKM120 in combination with 5, 15, 20 and 25 μM CQ for 24 hours to determine if CQ could inhibit BKM120-mediated activation of autophagy. Increasing CQ concentration with BKM120 treatment resulted in augmented p62 expression, suggesting autophagy inhibition. Lysate from a single 5 μM BKM120 treatment was also run in parallel for comparison of band density. The p62 expression from this treatment was lower as expected due to BKM120-mediated activation of autophagy. The no BKM120/CQ treatment condition relates to an active PI3K signalling with which autophagy is negatively regulated, preventing p62 proteins from being degraded.

3.2.4.3 BKM120 and CQ combination treatment showed no significant changes in cell viability

As previously shown in section 3.2.4.2, CQ treatment reverses the activating effect of BKM120 on autophagy. MTT viability assays were performed to ascertain whether autophagy inhibition induced cytotoxic or cytoprotective effects in ependymoma cells. Cells were treated with various concentrations of BKM120 with or without 5 µM CQ for 72 hours. Cell viability trends between the two treatment conditions were compared to see whether CQ-mediated inhibition of autophagy would improve or worsen the effects of BKM120, based on any significant shifts in the viability curves (Figure 3-10). Despite showing a general increase in cell viability predominantly in the supratentorial cell lines in response to BKM120/CQ co-treatments relative to monotherapeutic BKM120 treatments, this was statistically significant only for EPN1 cells (two-way ANOVA, *p<0.05) (Figure 3-10C) which suggests that autophagic responses conferred a cytotoxic effect in these cells. However, the lack of consensus in these results meant that autophagy may not necessarily produce a cytotoxic effect in ependymoma. So far, whether there is biological relevance in the activation of autophagy towards ependymoma pathogenesis is yet to be clarified.

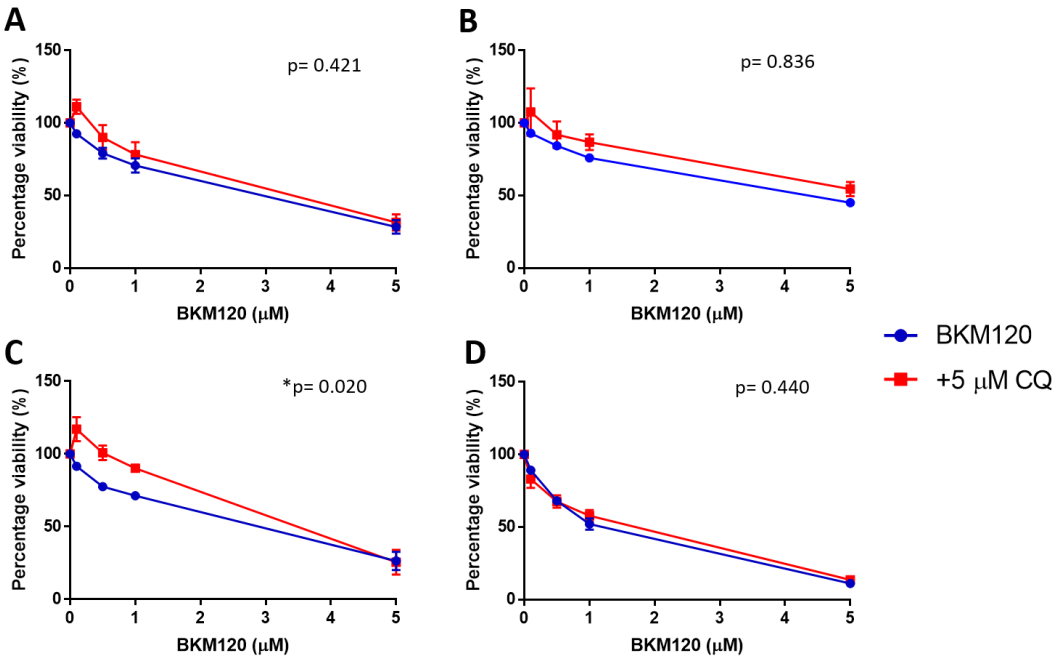


Figure 3-10 MTT viability assay of (A) BXD-1425EPN, (B) DKFZ-EP1, (C) EPN1, (D) EPN12A cells treated with 0, 0.1, 0.5, 1, 5 µM BKM120 only and in combination with 5 µM CQ for 72 hours. Data is representative of at least three independent repeats and cell viability trends of both treatment conditions were analysed using two-way ANOVA. A significant difference in the cell viability between BKM120/CQ combination and BKM120 single treatment was only shown for EPN1 cells (*p<0.05). This was associated with an increase in cell viability following inhibition of autophagy, suggesting that it conferred cytotoxicity in these cells.

3.2.5 Inhibition of mTOR signalling activates autophagy in ependymoma

Negative regulation of autophagic responses is commonly instigated by the activation of the mTOR signalling pathway. To investigate this hypothesis, pharmacological inhibition of the mTOR pathway was used to demonstrate whether this could directly regulate autophagy in ependymoma cell lines. Ependymoma cells were treated with various concentrations of the rapalogue, Temsirolimus (TMS) for 24 hours. Immunoblot data showed a decrease in pS6 levels with increasing drug concentration representing inhibition of the mTOR signalling pathway. Probing for p62 protein post-TMS treatment also showed a decrease in expression levels indicating the presence of autophagic responses (Figure 3-11). These findings highlighted that the mTOR pathway serves as a negative regulator of autophagy in ependymoma as well as implicating its role in potentially bridging the same inhibitory effect from upstream PI3K signalling.

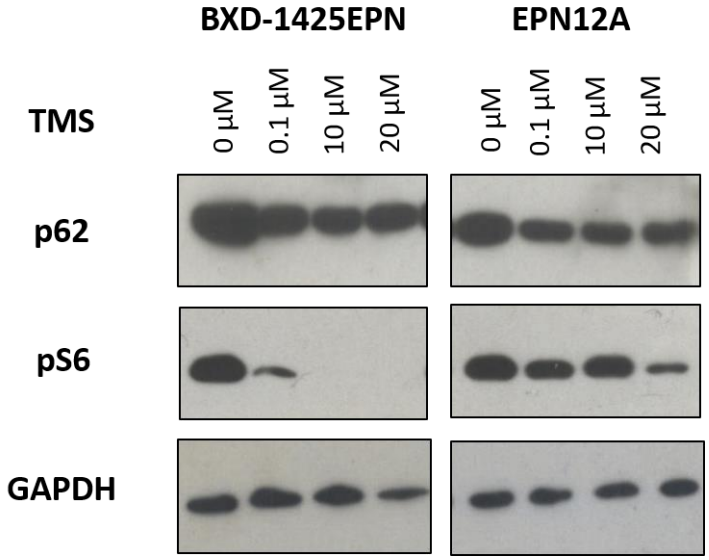


Figure 3-11 Inhibition of the mTOR signalling pathway in BXD-1425EPN and EPN12A cells was performed through treatment with TMS for 24 hours. Subsequent immunoblotting for both p62 and pS6 showed a decrease in expression levels suggesting activation of autophagy following a decrease in mTOR signalling output, respectively, in these cells because of drug treatment (n=2).

3.2.6 Investigating whether BKM120 inhibition in ependymoma was mediated through the canonical PI3K/AKT signalling node

Canonical PI3K signalling involves the activation of AKT as the primary effector that transduces the signal to downstream targets of the pathway. However, stimulation of AKT-independent mechanisms has also been elucidated which could produce survival responses that mimic those of AKT-mediated signaling (Qiu, Kung 2000, Lang, Strutz-Seebohm et al. 2010). Having observed the biological effects of PI3K inhibition using the PI3K inhibitor BKM120, this project aimed to evaluate if loss of AKT functioning could recapitulate the same outcomes as directly inhibiting PI3K enzyme activity.

3.2.6.1 Perifosine did not reduce ependymoma cell viability

Ependymoma cells were treated with the allosteric AKT inhibitor, perifosine to evaluate if this leads to a reduction in cell viability. After a 72-hour incubation with the drug, there was no significant decrease in cell viability across the panel of tested ependymoma cell lines relative to the vehicle control. However, perifosine was effective at decreasing the viability of the medulloblastoma cell line UW228-3 with a calculated IC_{50} of 14.3 μM (***$p<0.001$) (Figure 3-12A), suggesting that the drug was active. If perifosine was not able to reduce ependymoma cell viability, it is possible that the PI3K pathway was not inhibited following drug treatment. In order to test this, immunoblotting was performed against pAKT in response to treatment with perifosine. Cells were treated with perifosine for one hour followed by pulse activation of the pathway with EGF for 10 minutes to avoid saturation of intracellular signalling pathways. Results showed that treatment with perifosine caused a decrease in pAKT levels, suggesting that AKT was inhibited. There was also a reduction in the total AKT levels after drug treatment for an hour (Figure 3-12B), which is an effect found to arise from using AKT inhibitors as highlighted in one study (Fu, Kim et al. 2009). This data suggests that the cells may have displayed resistance towards the inhibitory effects of perifosine. However, it is also possible that the reduction in ependymoma cell viability following PI3K pathway inhibition may not have been mediated in an AKT-dependent manner which implicates the potential involvement of non-canonical PI3K signalling.

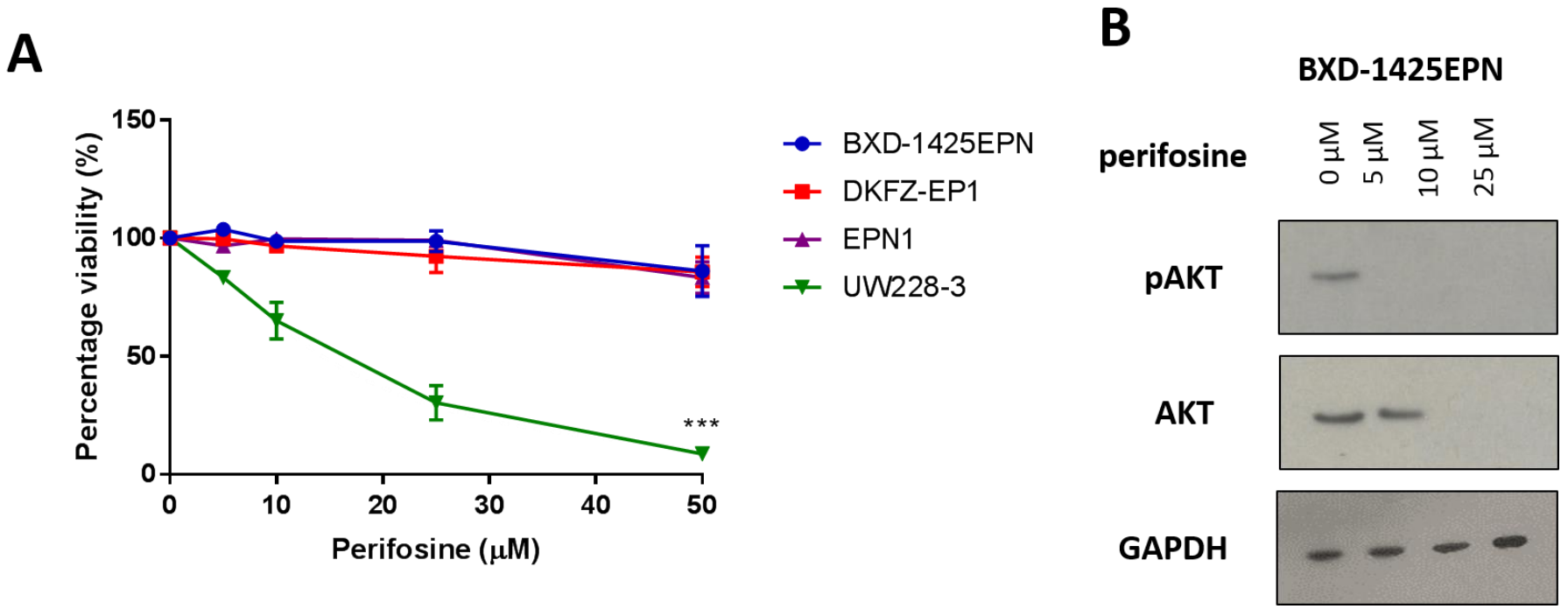


Figure 3-12 (A) MTT viability assay of ependymoma cells post-72-hour treatment with perifosine. UW228-3 served as a positive control whose IC_{50} for perifosine was determined using non-linear regression analysis (n=3). Statistical analysis of changes in percentage viability over the treatment course was performed using two-way ANOVA Dunnett's multiple comparisons test. (B) BXD-1425EPN cells were treated with perifosine for an hour followed by EGF-mediated pulse activation of the PI3K pathway. Probing for pAKT as well as total AKT was performed to determine the inhibitory effects of perifosine on the pathway. No samples were obtained for UW228-3 cells, as these did not tolerate the conditions used for sample preparation.

3.2.6.2 GDC-0068 did not reduce ependymoma cell viability

To further test whether activation of the canonical PI3K/AKT signalling was associated with the cellular responses observed in ependymoma, an alternative inhibitor whose mechanism of action is different to perifosine was employed to inhibit AKT activity. Treatment of ependymoma cells with GDC-0068 was considered as this drug directly targets the AKT catalytic site to suppress its functioning. However, a 72 hour treatment with GDC-0068 also did not decrease the viability of the various tested ependymoma cell lines while it caused a significant reduction for the breast cancer cell line MCF7 (***$p<0.001$) relative to the vehicle control. MCF7's IC_{50} for GDC-0068 was 3.2 μM, which was higher (1.88 μM) than that determined by Lin, J., Sampath et al. (2013) (Figure 3-13A). The same one-hour drug treatments were performed on BXD-1425EPN cells to monitor GDC-0068's capacity to inhibit the PI3K pathway. Western blot data indicated that GDC-0068 treatment resulted in an increase in intracellular pAKT levels, which is an expected finding for inhibiting AKT activity using a catalytic site-directed AKT inhibitor as highlighted by Lin et al. (2012). Interestingly, GDC-0068 induced a decrease in the expression of total AKT levels in a manner similar to perifosine (Figure 3-13B). This could also be explained by the same effect highlighted by Fu, Kim et al. (2009) regarding the use of AKT inhibitors and the consequent impact on AKT protein turnover. Moreover, it is not understood how an increase in AKT phosphorylation could simultaneously occur with a decrease in total AKT levels following treatment with GDC-0068. While this could have resulted from an inefficient membrane stripping issue prior to re-probing with AKT antibodies, further scrutiny is required to explain any underlying mechanism that could account for this. Nevertheless, results from the GDC-0068 treatments were also not able to conclude whether ependymoma cells generally display reduced sensitivity to AKT inhibitors or if responses were mediated by non-AKT effectors of PI3K signalling hence the inefficiency of pharmacologically targeting AKT. Further functional techniques which involve direct manipulation of AKT expression are required to associate the classical PI3K/AKT signalling node with ependymoma survival and viability.

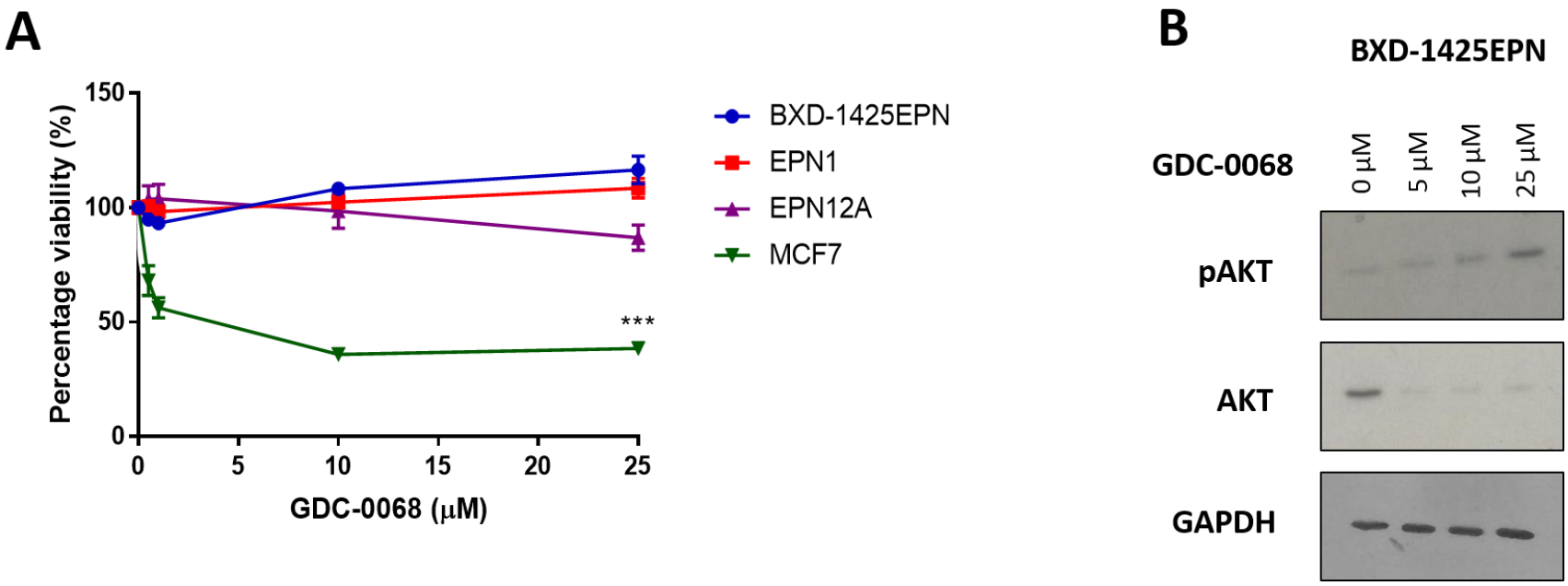


Figure 3-13 (A) MTT viability assay of ependymoma cells post-72 hour treatment with GDC-0068. MCF7 was used as a positive control whose IC_{50} was determined using non-linear regression analysis (n= 3). Statistical analysis of changes in percentage viability over the treatment course was performed using two-way ANOVA Dunnett's multiple comparisons test. (B) BXD-1425EPN cells were treated with GDC-0068 for an hour followed by probing against pAKT and total AKT levels to determine PI3K pathway inhibition. No MCF7 samples were obtained for Western blot analysis as these cells did not tolerate the conditions used for sample preparation.

3.3 Discussion

In continuation of the work published by Rogers, Mayne et al. (2013), functional experiments were initially carried out on a panel of established ependymoma cell lines to investigate how these tumours would respond to the inhibition of the PI3K pathway with the aim of understanding its impact on disease pathogenesis and whether it presents itself as a prospective target for therapeutic purposes. The key findings on this chapter showed that BKM120 treatment inhibited the PI3K pathway across the panel of tested ependymoma cell lines, as indicated by the reduction of pAKT and pS6 levels. The inhibition of the PI3K pathway resulted in a significant decrease in ependymoma cell viability, in which there was suggestive increased sensitivity to BKM120 in the posterior fossa-derived cell lines. BKM120 did not stimulate cell death in ependymoma but an arrest was observed at the G_0/G_1 phase of the cell cycle, implicating an induction of a cytostatic rather than a cytotoxic effect. A reduction in p62 levels was also shown following treatment with either BKM120 or the rapalogue TMS, suggesting that inhibition of the PI3K/AKT/mTOR signalling axis activated autophagic responses in ependymoma. BKM120/CQ co-treatments showed no significant difference in the cell viability trend when compared to BKM120 only treatment. Currently, it is undetermined which of the dual roles of autophagy is biologically relevant in ependymoma. Finally, treatment of ependymoma cells with either an allosteric or an ATP-competitive AKT inhibitor did not reduce the cell viability. Therefore, it is yet to be elucidated whether AKT was involved in mediating BKM120 responses in ependymoma or if the cells were resistant to the inhibitory effects of AKT-directed agents.

3.3.1 The canonical PI3K pathway and its subsequent effects in ependymoma

According to Rogers, Mayne et al. (2013), activation of the PI3K pathway was identified in higher proportions of supratentorial tumours relative to those originating from other CNS compartments. In this project, it was investigated whether there were differences in responses to PI3K pathway inhibition among ependymomas arising from different locations. Rogers and colleagues have shown that treatment of two supratentorial cell lines, BXD-1425EPN and EPN1, showed a reduction in cell viability in response to BKM120 treatment with IC_{50} concentrations determined to be within clinical range (Bendell, Rodon et al. 2012b). A repeat of these experiments on another supratentorial (DKFZ-EP1) and two posterior fossa cell lines (EPN8 and EPN12A) also resulted in overall cell viability reduction whose IC_{50} values were also within clinical range. The BKM120-mediated reduction in ependymoma cell viability also coincided with the loss of PI3K/AKT/mTOR signalling as shown by the dose-dependent decrease in pAKT and pS6 protein levels in all tested ependymoma cells. Therefore, it is assumed that the

negative effects of PI3K pathway suppression do not discriminate between tumours of the supratentorium or posterior fossa. Pre-clinical studies in other cancers support this conjecture in which targeting of the PI3K pathway generally manifests congruent results across disease subtypes (Lynch, McEwen et al. 2016), implicating the potential advantage of these inhibitors as a universal treatment for paediatric ependymomas irrespective of location as well as subgroup-specific clinical differences.

However, analysis of the interaction in the different kill curves showed that there was a significant difference between the cell viability trends of supratentorial and posterior fossa ependymoma cells. Based on the MTT data, the posterior fossa ependymoma cells manifested a shift in the inhibitory profile with which lower IC_{50} values were identified thus insinuating increased sensitivity to BKM120 relative to the supratentorial cell lines. The fact that ependymomas arising in both CNS compartments were responsive to the inhibitory effects of BKM120 within clinical thresholds suggests that testing the effects of PI3K pathway inhibitors could even potentially be extended to tumours arising from the different sub-groups. One could further argue that the differences in treatment responses between the supratentorial and posterior fossa cell lines could be attributed to the distinct molecular signatures characterised in these anatomically discrete tumours (Pajtler, Witt et al. 2015). While the PI3K pathway was not implicitly recognised as a molecular feature for ependymoma classification, its clinical value is highlighted especially for prognostic purposes and stratifying patients based on their prospective therapeutic outcomes.

It was subsequently investigated whether similar responses could be obtained if AKT was inhibited. Repression of AKT activity not only functions as an alternative method to block PI3K signalling but it also validates whether cellular functions in ependymoma are facilitated through a canonical route. Two classes of AKT inhibitors were used to suppress AKT in ependymoma. These were perifosine (allosteric AKT inhibitor) and GDC-0068 (catalytic site-directed AKT inhibitor), whose anti-tumourigenic efficacy has been identified against pre-clinical models including high grade gliomas (Lin, J., Sampath et al. 2013, Becher, Millard et al. 2017). However, treatment of ependymoma cells with either perifosine or GDC-0068 showed no significant decrease in cell viability relative to their respective positive control cell lines. Yet according to the western blot analysis, both drugs showed indications that AKT was inhibited in ependymoma cells which would have potentially abrogated PI3K signalling and reduced cell viability.

3.3.1.1 Predicaments with BKM120 treatment and AKT inhibition of the PI3K pathway

BKM120 is considered as one of the most clinically advanced PI3K pathway inhibitors (Janku 2017) that can suppress the activity of all class I isoforms. Its ability to cross the BBB also emphasises another advantage in evaluating its effects in ependymoma. However, studies have shown that BKM120 also possesses off-target effects by binding to tubulin sub-units to destabilise microtubule polymerisation (Brachmann, Kleylein-Sohn et al. 2012). The authors demonstrated this by engineering MCF7 cells to overexpress a constitutively active AKT, with which resistance was conferred towards the PI3K inhibitor pictilisib but were sensitive to BKM120 treatments especially at concentrations above 1 μM. Since ependymoma cells were treated at concentrations of >1 μM, it is possible that the anti-tumourigenic effects of BKM120 may have been mediated by irregularities in microtubule treadmilling rather than through the inhibition of the PI3K pathway. If this was the case, an arrest at the G_2/M phase of the cell cycle should have been observed as reported by other studies regarding the consequences from BKM120 treatment (Koul, Fu et al. 2012, Lonetti, Antunes et al. 2014, Civallero, Cosenza et al. 2015). However, G_2/M arrest was not identified in the cell cycle analysis, suggesting that the reduction in ependymoma cell viability following BKM120 treatment may not be associated with issues in microtubule polymerisation.

It is possible that BKM120 impedes ependymoma cell viability by inhibiting other downstream effectors of the PI3K pathway which are independent from AKT functioning. The involvement of a non-canonical PI3K signalling in promoting cellular responses in ependymoma would therefore account for the observed lack of tumour suppressive efficiency of AKT inhibitors in this project. Studies have shown that there are alternative non-AKT effectors of the pathway that can equally transduce signals to downstream targets after PI3K activation. For instance, SGK kinases could serve as an AKT surrogate (Lang, Strutz-Seebohm et al. 2010) with earlier studies demonstrating inactivation of FOXO transcription factors through phosphorylation to promote cell survival (Brunet, Park et al. 2001). An earlier study has functionally demonstrated a decrease in SGK activity as a result of LY294002 treatments while its kinase output was further enhanced following transient transfection of a constitutively active p110 PI3K subunit (Park, Leong et al. 1999). Bruton's tyrosine kinase (BTK), a non-RTK intracellular kinase involved in B- and T-lymphocyte signalling, is another downstream PI3K effector that was presented as a putative pharmacological target due to its oncogenic role (Qiu, Kung 2000, Molina-Cerrillo, Alonso-Gordoa et al. 2017).

However, the likelihood of ependymomas conferring resistance to AKT-targeted agents could not be ruled out. Indeed, the downside of inhibiting AKT in cancers could be associated with feedback loops that result in various resistance mechanisms that limit the efficiency of these agents (see section 1.5.4). One notable study by Chandarlapaty, Sawai et al. (2011) explained that AKT inhibition led to an upregulation of RTK, which would consequently lead to the reactivation of the PI3K pathway. It is also argued that PI3K inhibition, relative to AKT, is less likely to stimulate these feedback loops due to it being more upstream in the pathway. Since it possesses a much broader range of targets than AKT, loss of PI3K activity would produce a more potent anti-tumourigenic effect. The notion of resistance to AKT inhibitors may actually be the underlying reason for the sub-optimal clinical responses in patients. This was highlighted in a human-based study which involved medulloblastoma, neuroblastoma and ependymoma patients who only displayed progressive to no response as the best outcome (Becher, Millard et al. 2017).

3.3.1.3 Future work for the investigation of canonical PI3K/AKT signalling in ependymoma

It was hypothesised that signaling through the PI3K pathway is essential towards ependymoma viability therefore its targeting presents an attractive therapeutic strategy to suppress tumourigenesis. Despite demonstrating that BKM120 resulted in a significant reduction in cell viability in conjunction with loss of signalling output from the PI3K/AKT/mTOR axis, the effects were not repeated when AKT inhibitors were employed in subsequent experimental work. Currently, more evidence is required to support whether the cellular effects seen following BKM120 treatment of ependymoma cells were mediated by the loss of canonical PI3K signalling pathway. In order to address this, several experimental plans were proposed for future investigations to uphold the pathological relevance of the PI3K pathway in ependymoma and maintain its potential as a chemotherapeutic target to treat these tumours.

According to the findings of Brachmann, Kleylein-Sohn et al. (2012), it is likely that the BKM120 treatments in this project have resulted in off-targeting due to concentrations used for the various experiments. To address this, it is necessary to investigate as a follow up whether BKM120 treatment influenced microtubule polymerisation in ependymoma cells at these concentration ranges. Furthermore, if BKM120's effects were mediated through a non-canonical pathway then future work would also consider investigating the biological relevance of non-AKT effectors in stimulating cellular responses in ependymoma. For instance, the phosphorylation state of SGK and BTK kinases could be analysed following BKM120 treatment. Inhibition of these

kinases could also be undertaken to determine whether this would cause a decrease in ependymoma cell viability.

The failure of either an allosteric or an ATP-competitive AKT inhibitor to significantly inhibit cell viability necessitated the use of other approaches to functionally characterise the effects of loss of AKT activity. To rule out any unaccounted off-targeting associated with a pharmacological-mediated inhibition of the PI3K pathway, direct manipulation of AKT expression would be a more suitable method. Two experimental techniques were suggested to undertake this work in the future. The first approach was to employ siRNA-mediated knockdown of all three AKT isoforms. Three different siRNA probes are used to target the different AKT isoforms followed by quantitatitve real-time PCR (qRT-PCR) to detect successful loss of transcripts. MTT assays would be performed subsequently to measure if any reduction in cell viability is induced following multiple AKT isoform knockdowns. The other proposed approach towards this work was the transfection of ependymoma cells with plasmid constructs that would encode for either a constitutively active AKT or a dominant-negative form of AKT. A constitutively active AKT would hyperactivate the PI3K pathway which would consequently block the effects of pathway inhibitors. No reduction in cell viability is therefore predicted post-drug treatment. In contrast, a dominant-negative form of AKT would essentially suppress the pathway in a manner similar to drug-mediated inhibition thus effectively decreasing cell viability. Once optimised, functional assays such as cell death and cell cycle analysis will be carried out to support the current data regarding the role of the PI3K/AKT signalling axis in stimulating ependymoma cell processes.

If cellular responses were then proven to be associated with activation of the conventional PI3K/AKT signalling axis, several pathway inhibitors could be used to see if these would maintain the effects observed from treatment with BKM120. Indeed, MTT viability experiments have previously been performed on several ependymoma cell lines using the PI3K/mTOR dual inhibitor BEZ235 as well as an array of mTOR inhibitors including TMS and everolimus. Pursuing an experimental plan similar to the ones performed in this project using these inhibitors would support the conclusions drawn so far regarding the role of the PI3K pathway in ependymoma pathogenesis.

3.3.2 Functional investigation of cellular responses in ependymoma post-BKM120 treatment

3.3.2.1 Induction of cell death

The PI3K pathway is a principal regulator of cell survival responses. Having shown a reduction in ependymoma cell viability in response to BKM120 treatment, it was hypothesised that this was due to the induction of cell death following suppression of PI3K signalling. Apoptosis is the most commonly attributed cell death mechanism in many drug treatment studies during which a cascade of caspase activation takes place resulting in the degradation of intracellular components. Studies have determined that PI3K pathway inhibition could induce cells to undergo apoptosis through the upregulation of certain apoptotic factors (Brachmann, Hofmann et al. 2009, Lonetti, Antunes et al. 2014, Zhao, P., Hall et al. 2017). However, no apoptotic responses were stimulated by BKM120 treatment in ependymoma cells based on the absence of cleaved caspase-3 proteins. Indeed, BKM120-mediated inhibition of PI3K pathway produced no cytotoxic effects in ependymoma, albeit cytostaticity was observed as the treatment primarily arrested cells in the G_0/G_1 phase of the cell cycle. From these results, it was concluded that triggering cell death did not account for the reduction in ependymoma cell viability. These findings contrasted with other studies in which hallmarks of cell death were identified following suppression of PI3K signalling in cancers such as medulloblastoma (Frasson, Rampazzo et al. 2015) and breast (Hu, Y., Guo et al. 2015)(Hu et al., 2015). Instead, the results in this chapter were consistent with the reported cytostatic effects in several studies in which PI3K pathway inhibition prevented G_1 exit into the S-phase of the cell cycle (Collado, Medema et al. 2000, Dan, Okamura et al. 2012, Wong, Ma et al. 2015). Based on these results, it could be concluded that PI3K pathway inhibition as a sole therapeutic approach in ependymoma is insufficient. If such findings did reflect clinical outcomes, one would argue that PI3K pathway inhibitors are best employed for mediating disease stabilisation rather than a primary line of treatment following surgery or radiotherapy. PI3K pathway inhibition as part of a treatment combination would be a more plausible strategy when aiming for complete tumour eradication. However, it is premature to assume at this point whether administration of PI3K pathway inhibitors in patients would be sub-optimal. Further work is imperative to fully understand the anti-tumourigenic effects of these drugs before translation into patient-based trials.

In this project, three lines of evidence were presented that supported BKM120-mediated cytostaticity rather than cytotoxicity in ependymoma. However, several experimental proposals could also be considered to further strengthen the current conclusions made regarding the role of PI3K pathway in regulating cell death in ependymoma. For instance, characterising apoptotic cell death solely depended on the

cleavage of caspase-3 when the process incorporates a multitude of factors that bring about such a response. Arguably, caspase-3 activation is a classic marker for apoptosis but there are also other effector caspases which have shown some degree of functional redundancy such as caspase-6 and caspase-7 (Walsh, Cullen et al. 2008). The interplay between these caspases in terms of which has a superior role over the other is yet to be elucidated but it is thought to be dictated by several factors such as their expression levels, turn-over rates and context-dependent cellular states. Determining the changes in intracellular expression of relevant apoptotic substrates such as Bid and PARP would have also revealed a clearer notion of the presumed destruction occurring within the cell due to PI3K pathway inhibition. Depiction of any hallmarks of cell death could have also been achieved at the morphological level by adopting cell staining and imaging approaches to visualise physical changes in cells post-treatment.

Cell death assays that use parameters such as LDH activity and amount of DNA released also raise further issues in investigating drug induced cell death mechanisms. Given that these assays lasted 72 hours, it is questioned whether this endpoint would actually reflect the amount of cell death that was stimulated. It could be suggested that cell death measurement using this timeframe may not be suitable if the parameter being examined was actually present at an earlier stage of the experiment. Therefore, multiple endpoints for these cell death assays could be investigated to increase the likelihood of capturing cell death induction. Although cell cycle analysis addressed this issue by examining profiles at 24 and 72 hours, there were also some technical limitations that could be focused on such as the loss of samples as a result of preparation and guarantees in successful collection of dead cells whose adhesive properties necessary for pelleting may not be as efficient as the viable ones. One way to improve the robustness of these experiments is the inclusion of a positive control such as etoposide-treated BXD-1425EPN cells which has been shown to induce apoptotic cell death in previous works.

3.3.3.2 Activation of autophagy

Autophagy is known for its protective mechanism whose activation is stimulated by cellular stress or the presence of an adverse environmental cue to maintain survival. However, there are certain physiological instances that prolong autophagy thus inducing cellular crisis and consequently, increased mortality (Zakeri, Melendez et al. 2008, Kroemer, Levine 2008). Autophagy was investigated in this project to determine which of its dual roles is relevant towards ependymoma biology.

This study has demonstrated that treatment of ependymoma cells with BKM120 resulted in a reduction in expression of the autophagy marker p62, indicating its

degradation that is facilitated by autophagic responses. When ependymoma cells were treated with TMS, there was a reduction in both pS6 and p62 levels in a dose-dependent manner suggesting that the PI3K/AKT/mTOR axis is a direct regulator of autophagy in ependymoma. At this point, it is unknown whether activation of autophagy in ependymoma following inhibition of the PI3K pathway confers a cytoprotective or is detrimental towards cellular survival. Having demonstrated that the PI3K/AKT/mTOR pathway is a negative regulator of autophagy, it was subsequently investigated how the viability of BKM120-treated ependymoma cells was influenced following the inhibition of autophagy responses. Co-treatment of ependymoma cells with BKM120 and the anti-malarial agent CQ showed no decrease in intracellular p62 levels according to western blot analysis, which indicated that CQ reversed the activation of autophagy by BKM120. However, MTT assays showed that the effects of this combination were only significant in EPN1 cells where an increase in cell viability was found thus implicating that activation of autophagy conferred cytotoxicity. Since these results were not recapitulated in the other tested cell lines, it means that the role of autophagy still remains ambiguous. According to the MTT assay, it is put forward that inhibition of the autophagy had no general impact on ependymoma cell viability, which suggests that autophagy induction may be irrelevant towards ependymoma pathogenesis. Further work is needed to delineate which of the dual role of autophagy is producing a genuine effect in ependymoma upon its activation.

Although, it remains an interesting direction for the project to further investigate the role of autophagy in ependymoma biology considering its previous implication as a fundamental regulator of oncogenic processes (White 2015). So far, evidence has shown that PI3K pathway inhibition generally did not induce cell death in ependymoma which implies that activation of autophagy is less likely to have cytotoxic effects. If autophagy presents as a pro-survival mechanism in ependymoma then one may argue that its inhibition could circumvent yet another resistance mechanism arising from PI3K suppression. Therefore, this would advocate the rationale for suppressing autophagy in conjunction with the inhibition of the PI3K pathway. Since the MTT assay of BKM120/CQ co-treatments did not significantly establish autophagy's cytoprotective role in ependymoma, alternative functional approaches could be considered to further support this hypothesis in future studies. For instance, if inhibition of autophagy through treatment with CQ did induce a cytotoxic effect in ependymoma then this could be measured through cell death assays or cell cycle analysis.

Finally, it is also worth noting that the CQ concentration used in these experiments was 6 times above the reported plasma peak concentration with an average half-life of 3 days (Walker, Dawodu et al. 1983). It could therefore be highlighted that these

experiments would have only served as a proof of concept to understand whether autophagy confers cytotoxicity or cytoprotection in ependymoma. The ranges considered in these experiments would otherwise be deemed clinically irrelevant as they might induce adverse effects when administered to patients.

3.3.3 Conclusion

This chapter focused on the functional work to determine the role of the PI3K pathway in promoting survival in ependymoma. It also sought to associate these cellular responses to the activation of the canonical PI3K/AKT signalling axis, rather than through external non-AKT mediated processes that are also found downstream of the PI3K enzyme. Treatment of ependymoma cells with BKM120 resulted in inhibition of the PI3K pathway and consequently induced a reduction in ependymoma cell viability. Cell death responses were not shown, but an arrest at the G_0/G_1 phase of the cell cycle was observed instead, suggesting that PI3K inhibition produces a cytostatic as opposed to a cytotoxic effect. Treatment with BKM120 or TMS also activated autophagic responses in ependymoma, demonstrating the role of the PI3K/AKT/mTOR signalling axis as a negative regulator of autophagy but its biological effect in ependymoma cells is yet to be determined. Targeting of AKT in ependymoma using either an allosteric or ATP-competitive inhibitor did not reduce cell viability in a manner similar to BKM120. With this, it remains unclear whether there are other non-AKT mediators of PI3K pathway-related responses in ependymoma or these cells displayed resistance to the AKT inhibitors.

3.4 Summary of chapter findings

- BKM120 inhibited the PI3K/AKT/mTOR signalling axis in ependymoma as indicated by the reduction of pAKT and pS6 expression levels.

- BKM120 treatment resulted in a dose-dependent decrease in ependymoma cell viability with the calculated IC_{50} values reflecting peak plasma concentrations (≤4 μM).

- BKM120 did not stimulate cell death in ependymoma as signified by three lines of evidence: lack of LDH activity with increasing BKM120 dosage, absence of cleaved caspase-3 from western blot analysis and no accumulation of cells in Sub-G_0 following cell cycle analysis.

- Ependymoma cells were arrested in the G_0/G_1 phase of the cell cycle signifying BKM120 induced a cytostatic instead of a cytotoxic effect.

- Activation of autophagy was observed in ependymoma following BKM120 inhibition of the PI3K pathway.

- Treatment of ependymoma cells with TMS resulted in downregulation of the mTOR pathway and subsequent activation of autophagy in ependymoma, indicating that mTOR signalling negatively regulates autophagic processes downstream of PI3K signalling.

- Inhibition of autophagy, induced by BKM120, by co-treating with CQ showed no significant changes in cell viability. At present, the biological relevance of autophagy in ependymoma is yet to be understood.

- Allosteric and catalytic site targeting of AKT in ependymoma using perifosine and GDC-0068, respectively, failed to reduce cell viability. Further work is required to determine whether these findings are due to drug resistance or other non-AKT effectors involved in promoting PI3K pathway-related responses in ependymoma.

CHAPTER 4. GLOBAL ELUCIDATION OF DOWNSTREAM TARGETS OF THE PI3K PATHWAY IN EPENDYMOMA

4.1 Introduction

Exploring the vast PI3K signalling network provides an opportunity to better understand the underlying biology of ependymal tumours. If considered as a promising target, it is necessary to be familiarised with the complex molecular circuitry of the PI3K pathway which consists of various feedback loops and inter-pathway cross talks that may be attributed to resistance mechanisms. The previous results chapter has demonstrated that BKM120-mediated inhibition of the PI3K pathway reduces ependymoma cell viability and induces biological responses that limit survival. In order to understand the cellular events that induce such tumour behaviours, it is essential to explore the dynamic changes in downstream signalling affected by the inhibition of the PI3K pathway.

Transcriptomic analysis following drug treatment is a common approach in investigating tumour biological mechanisms and the implications of pharmacological targeting. One notable work by Pei, Liu et al. (2016) incorporated gene expression data to characterise the molecular events that stimulate medulloblastoma growth in response to histone deacetylase (HDAC) inhibitors. Gene expression profiles showed overrepresentation of FOXO1 targets and concurrently, increased activity of FOXO1 itself. They further deduced that inhibition of the PI3K pathway would synergise with HDAC inhibitors since FOXO1 is a known downstream target of the PI3K pathway. In a separate study by Shats, Gatza et al. (2013), gene expression analysis enabled the delineation of the E2F1 transcription factor's tumour suppressive role in which, through the co-regulation of FOXO proteins, expression of apoptotic cell death genes was identified when cells were exposed under mitogen-deficient conditions. The authors further highlighted that FOXO/E2F1-mediated gene expression could also be activated in response to PI3K inhibitors or histone deacetylase inhibitors (HDACi). It was later proposed that this transcriptional program conferred favourable prognosis since loss of FOXO/E2F1 signalling axis was associated with a more aggressive phenotype.

In this chapter, microarray technology consisting of various gene probes that best represent the human genome was employed to determine changes in ependymoma transcriptional profiles post-BKM120 treatment. Enrichment analysis of significant differentially expressed genes (DEGs) was used to elucidate biological trends that related

to disease pathology as well as serve as a putative therapeutic target that could be combined with PI3K pathway inhibition.

The aims of this chapter were:

- To establish the changes in transcriptional profile following inhibition of the PI3K pathway
- To identify biological functions that could be attributed to disease pathogenesis through gene ontology (GO) enrichment analyses
- To determine the regulation of these significant DEGs thus providing a candidate molecular mechanism that induce cellular responses
- To identify relevant therapeutic targets that could potentially be exploited in conjunction with inhibition of the PI3K pathway and subsequently be investigated in follow up experiments

4.2 Results

4.2.1 Sample preparation for transcriptomic analysis

The previous chapter has indicated that tumours arising in the posterior fossa regions may display increased sensitivity PI3K pathway inhibitors, relative to its supratentorial counterparts. However, Rogers, Mayne et al. (2013) have shown that a higher percentage of supratentorial tumours displayed PI3K pathway activation relative to posterior fossa and spinal ependymoma. On the basis of these findings, it was presumed that the biological effects of signaling through the PI3K pathway on ependymoma pathogenesis would be better understood if the molecular profile of supratentorial tumours was investigated further. In this project, transcriptomic analysis was performed on two supratentorial cell lines, BXD-1425EPN and EPN1; both of which have shown a significant decrease in cell viability following BKM120 treatment within clinical range as indicated by their calculated IC_{50} values. Initially, the cells were seeded in serum-free media overnight then treated with either DMSO (vehicle) or BKM120 for 24 hours, in three independent biological repeats. Probing against pAKT was performed with BXD-1425EPN cells to confirm if the conditions used for sample preparation inhibited PI3K signalling. Results showed that these conditions resulted in a reduction in pAKT levels with increasing drug concentration suggesting that PI3K signalling was inhibited post-BKM120 treatment (Figure 4-1).

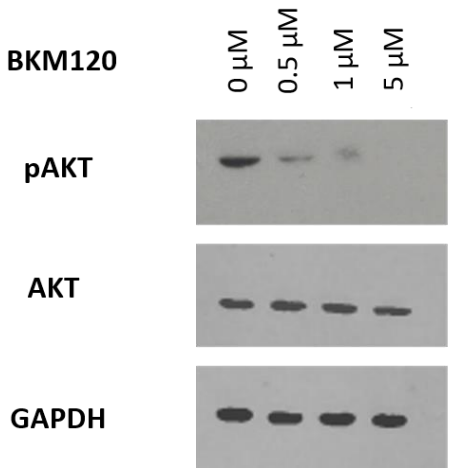


Figure 4-1 Western blot analysis to determine the treatment conditions suitable for the preparation of ependymoma samples for the transcriptomics experiments using BXD-1425EPN cells. 24 hour treatment with BKM120 of cells seeded in serum free media resulted in a decrease in pAKT levels, indicating loss of PI3K signalling. GAPDH was used as a loading control.

As a proof of concept, an MTT assay (n=1) was performed to see whether shortening the incubation period to 24 hours could decrease viability compared to vehicle treatment (Figure 4-2). This was necessary to ensure that the inhibition of PI3K signalling would still induce a different biological response relative to vehicle controls despite a shorter treatment duration. There was an observable dose-dependent decrease in cell viability implicating a differential cellular response that might be instigated by changes in downstream signalling events relative to vehicle treatment. Therefore, it was concluded that the 24-hour treatments were sufficient to inhibit the PI3K pathway and consequently induce changes at the transcriptomic level.

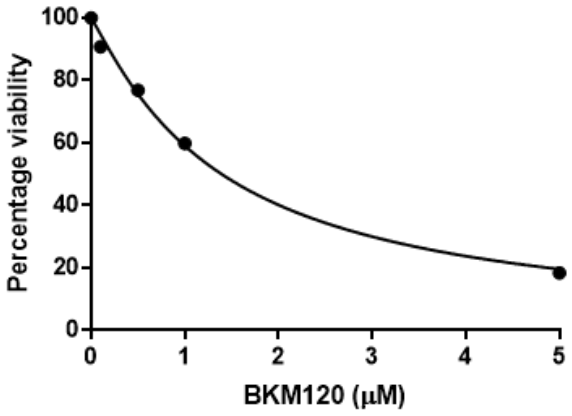


Figure 4-2 MTT assay results of BXD1425-EPN cells treated with BKM120 for 24 hours. No statistical analysis was performed as the data represents one repeat, though a decrease in cell viability was observed with increasing drug concentration.

4.2.2 Quality control (QC)

4.2.2.1 Screening for integrity of extracted RNA samples showed high quality in preparation for microarray hybridisation

Total RNA was extracted from BXD1425-EPN and EPN1 cells treated with either DMSO or BKM120 (2.5 and 4.5 μM, respectively, based on their previously determined IC_{50} values) for 24 hours. Three biological repeats were prepared per treatment condition for each cell line. Before performing the microarray hybridisation, RNA obtained from all samples were evaluated to determine their quality using the 28S:18S rRNA ratio as a reference. According to the electropherogram generated for the various RNA samples, two distinct peaks were shown corresponding to the two principal mammalian rRNA species, 28S and 18S. The electropherogram traces also showed little RNA degradation as indicated by the absence of peaks in the region between the 18S and 5S peaks (also known as the fast area) This was further supported by the assigned RNA integrity number (RIN) of >9.5 for most of the samples (out of a maximum score of 10) (Table 4-1). However, the quality of two EPN1 samples seemed to have been compromised based on the inconsistency in their electrophoretic profiles (Lanes 11 and 12 on Figure 4-3). Furthermore, the Agilent software allocated a RIN score of N/A to these samples as a warning regarding the accuracy of this value. A visual inspection of their electropherograms (n= 3 of vehicle and n= 1 of 4.5 μM BKM120 on Figure 4-4B) was warranted in order to evaluate whether these samples were still eligible for array hybridisation. Despite indications of some degree of degradation, the 18S and 28S peaks of these samples were still considered “strong” thus allowing the microarray run to be performed as planned.

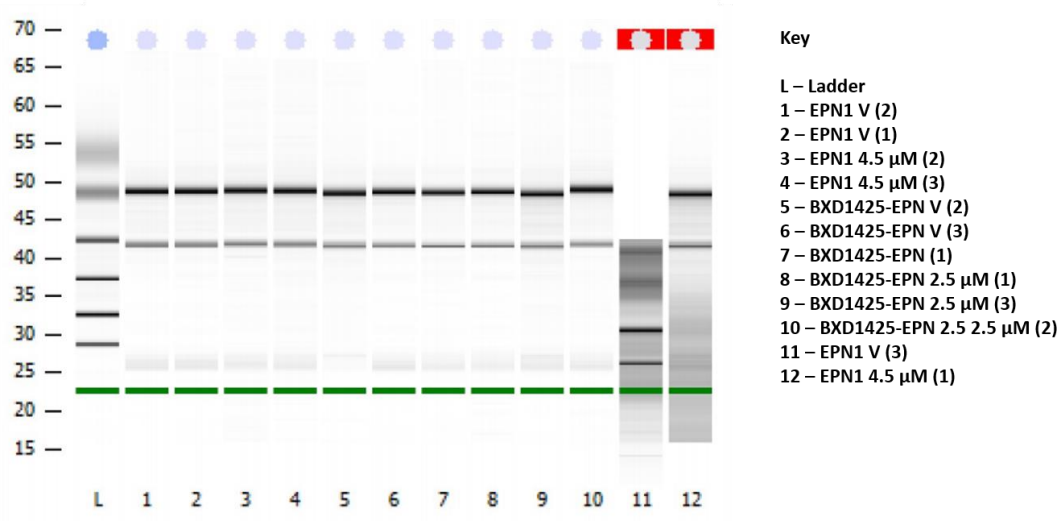


Figure 4-3 Electrophoretic profile of BXD1425-EPN and EPN1 samples as part of quality control prior to microarray hybridisation. The two distinct bands correspond to the 28S and 18S rRNA species which are predominantly found in mammals.

Table 4-1 RIN Scores for the various RNA samples used for microarray hybridisation to indicate their quality as determined by Agilent 2100 Expert Software.

Sample	RIN Score
BXD-1425EPN Vehicle (n=1)	10
BXD-1425EPN Vehicle (n=2)	9.8
BXD-1425EPN Vehicle (n=3)	10
BXD-1425EPN BKM120 2.5 µM (n=1)	10
BXD-1425EPN BKM120 2.5 µM (n=2)	10
BXD-1425EPN BKM120 2.5 µM (n=3)	9.7
EPN1 Vehicle (n=1)	10
EPN1 Vehicle (n=2)	10
EPN1 Vehicle (n=3)	N/A
EPN1 BKM120 4.5 µM (n=1)	N/A
EPN1 BKM120 4.5 µM (n=2)	10
EPN1 BKM120 4.5 µM (n=3)	9.9

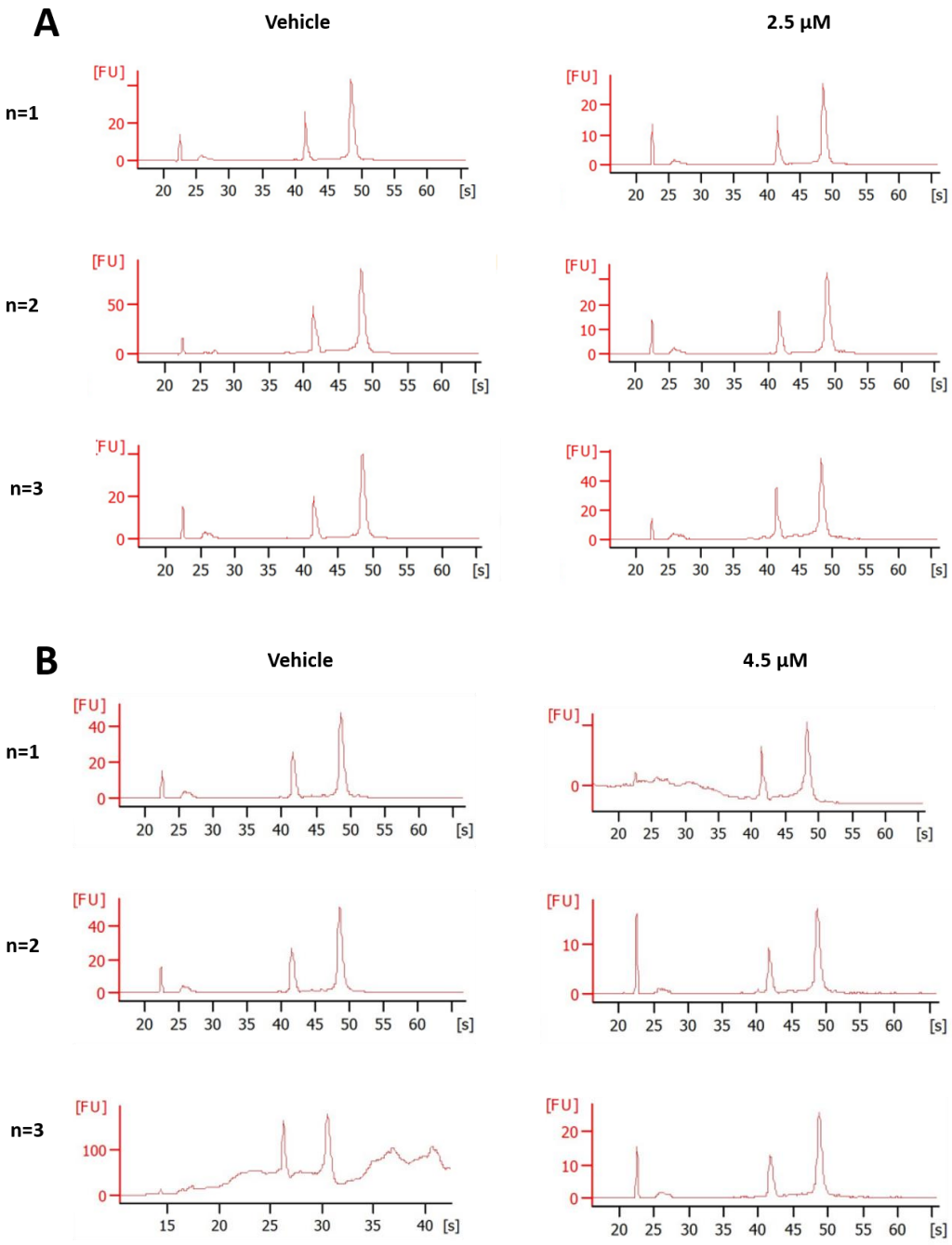


Figure 4-4 Electropherogram traces of all (A) BXD1425-EPN and (B) EPN1 samples used for microarray hybridisation. An ideal profile, usually signifying a RIN score of ~10, would have two peaks relating to the 18S and 28S rRNA mammalian species. A small peak also forms on the extreme left of the trace pertaining to the 5S rRNA. The region between the 5S and 18S peaks relates to the fast area on which a low absorbance profile would indicate minimal RNA degradation.

4.2.2.2 Differences in gene expression observed between treated and untreated ependymoma cells were due to BKM120 treatment

Prof. Sean May's group at the Nottingham Arabidopsis Stock Centre (NASC), University of Nottingham, performed the subsequent microarray experiments following initial quality control measures. Total RNA from each sample was hybridised on the GeneChip™ Human Gene 2.1 ST Array (Affymetrix). For these gene expression experiments, it was expected that there would be significant differences in the transcriptomic profiles between the treated and untreated samples. However, differences may arise from various factors including random and systematic errors, making the data unreliable. A Sources of Variation plot, which graphically represents the influence of each factor on experimental validity, was used to rule out any of these external errors as principal contributor of variation. Analysis showed that the mean signal-to-noise ratio of all microarray gene probes was higher for the drug treatment factor in comparison to errors (Figure 4-5) for both BXD1425-EPN and EPN1 cells, implicating that the significant variation between the two different experimental conditions originated from the type of treatment instead of errors introduced into the experiments.

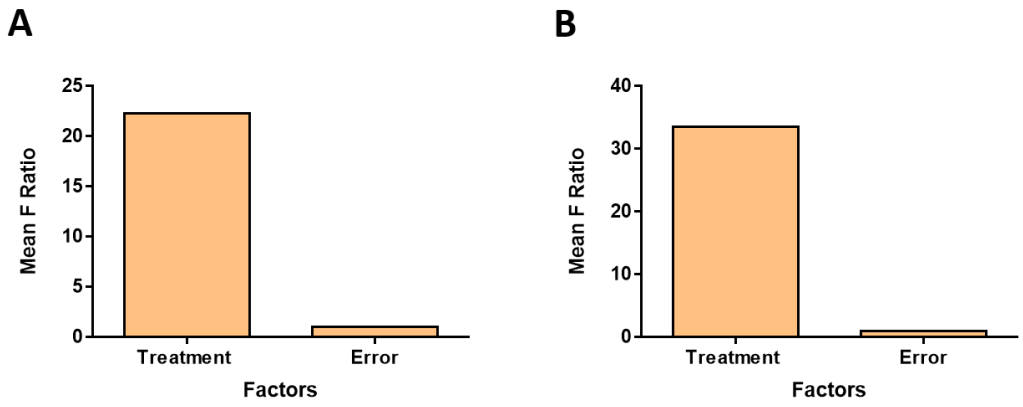


Figure 4-5 Sources of variation plot to assess the origin of variability in the experimental conditions considered in the microarray hybridisation. For both (A) BXD1425-EPN and (B) EPN1 sample batches, a higher signal-to-noise ratio was observed in treatment suggesting that the differences in expression levels were less likely to result randomly from extraneous errors.

4.2.2.3 BKM120 or DMSO treated BXD1425-EPN and EPN1 cells have distinct transcriptional profiles

Having established that the differences between the samples were significantly attributed to the type of treatment performed, analysis was continued by summarising the total variance within the dataset to elucidate treatment-specific transcriptional patterns. Unsupervised compression of multiple data points following microarray hybridisation through Principal Component Analysis (PCA) demonstrated distinct clustering of the

different treatment groups of each cell line (Figure 4-6). For each treatment condition, the variances between the three independent repeats were presented, culminating in four separate groups representing BKM120 and vehicle treatment for both BXD1425-EPN and EPN1 cells. These results suggest that treatment of ependymoma cells with BKM120 resulted in transcriptomic differences in relation to vehicle treated ependymoma cells. The lack of overlap between the drug treated and vehicle treated conditions with their corresponding counterparts in the other cell line might be due to intrinsic variability between the two cell lines used.

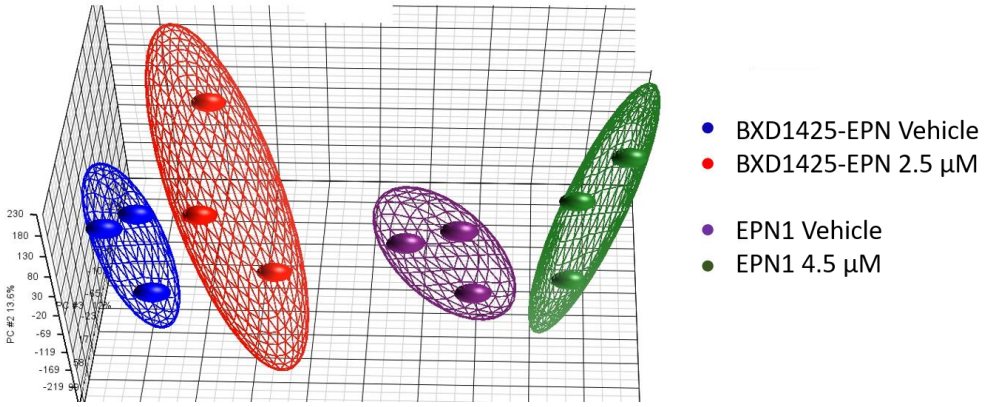


Figure 4-6 PCA plot to summarise the variation between the treatment conditions in each cell line. Four different groups were identified signifying the cell line-specific differences in the expression profile for vehicle and drug treated samples.

4.2.3 Functional enrichment of differentially expressed genes (DEGs) in BKM120 treated ependymoma cells

4.2.3.1 Biological enrichments in BXD-1425EPN and EPN1 cells in response to inhibition of the PI3K pathway

Processing of data following microarray hybridisation determined an expression level of each given probe per treatment condition in the individual cell line used. In order to determine significant DEGs between vehicle treated and drug treated groups in each cell line, one-way ANOVA with an unadjusted $p < 0.05$ was performed using Partek® Genomics Suite. A fold change of ±2 was also added as a threshold to filter out other genes from the final list of DEGs. Prior to this, it was found that adjusting the p-value to accommodate for false positives resulted in no significant genes for the BXD-1425EPN datasets hence disregarding this method during the analysis of the gene expression array data. Cell line-specific gene probe fold changes and their significance in treated cells relative to untreated cells are summarised on the volcano plot on Figure 4-7. The subsequent statistical analysis has generated a total of 366 and 790 significant

differentially expressed gene probes (appendix 7 and 8) in BXD-1425EPN and EPN1 cells, respectively.

The list of significant gene probes obtained in BXD-1425EPN and EPN1 cells were analysed using the GO functionality within Partek® Genomics Suite to identify enriched biological processes. Any processes with an enrichment score of >1 was considered significant. The analysis was performed at different levels so that the data was presented initially with the broadest GO terms and eventually branching out to more specific cellular functionalities. GO analysis of the 366 BXD-1425EPN-specific DEGs showed an enrichment for cell proliferation processes as well as those relating to growth and metabolism (Figure 4-8). Further scrutiny of cell proliferation processes manifested enrichment for mechanisms associated with regulation of cell cycle and division (Figure 4-9) thus supporting previous data regarding the main cellular effects of PI3K pathway inhibition in ependymoma. Interestingly, it also highlighted enrichment for inner cell mass and neural precursor proliferation (Figure 4-10) which are commonly associated with CNS development arising from stem cell activity (Guillaume, Johnson et al. 2006). Furthermore, roles in synaptic plasticity and homeostatic processes were also enriched which would allude to potential mechanisms of CNS maintenance (Figure 4-11). Enrichment of GO terms for EPN1 DEGs also found those that govern cell division and proliferation were significantly enriched (Figure 4-12). Detailed analysis of these molecular events also determined processes that are potentially associated with CNS maturation and functioning as well as osteoblast proliferation, which is more ascribed to bone development (Figure 4-13). GO analysis of BXD1425-EPN and EPN1 DEGs also identified enrichment for response to an abiotic stimulus (external or environmental cues/insults), which is BKM120 treatment in this case (Figure 4-14). Detailed evaluation of responses to abiotic stimulus was only shown for EPN1 cells where identified processes included responses to radiation and DNA damage, which are common effects of cellular stress induced by abiotic stimuli (Figure 4-15).

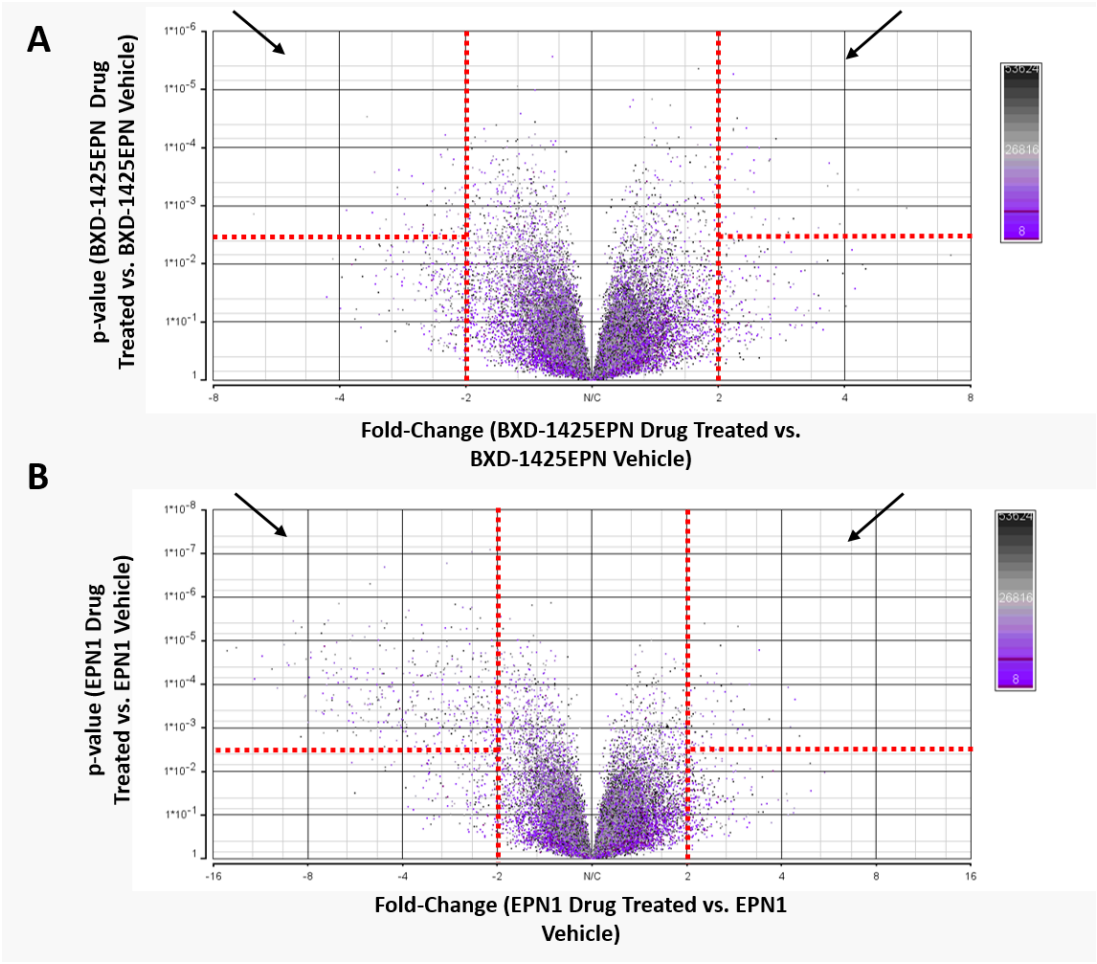


Figure 4-7 Volcano plot graphically representing the fold changes and p-values of the different microarray gene probes in (A) BXD-1425EPN and (B) EPN1 cells following BKM120 treatment. Using the threshold of unadjusted $p<0.05$, ±2 fold change (one-way ANOVA), 366 and 790 significant differentially expressed probes were identified in BXD-1425EPN and EPN1 cells respectively, which were represented by the quadrants indicated by the arrows on the plot above.

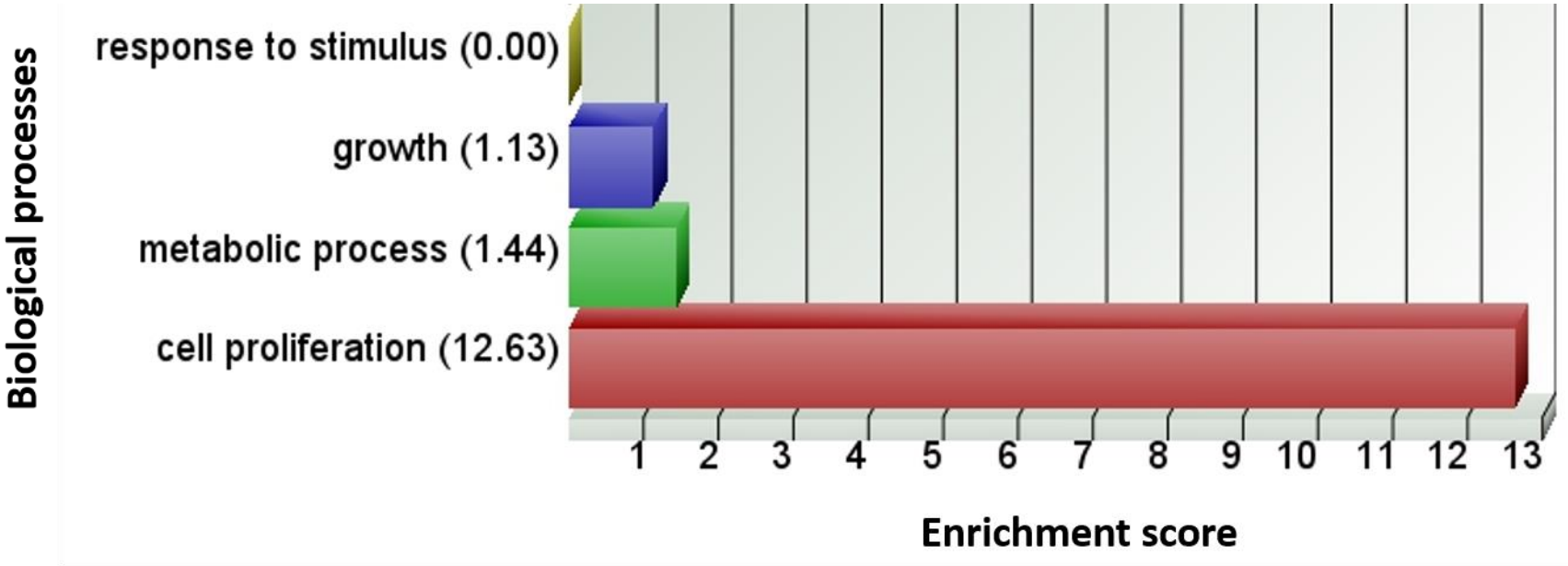


Figure 4-8 Partek®-mediated gene enrichment analysis of BXD1425-EPN samples showed an overrepresentation of processes related to cell proliferation as well as cell growth and metabolism. The analysis showed the highest enrichment score that was achieved for this group of cellular processes where a score of more than 1 was considered a significant biological response to inhibition of the PI3K pathway.

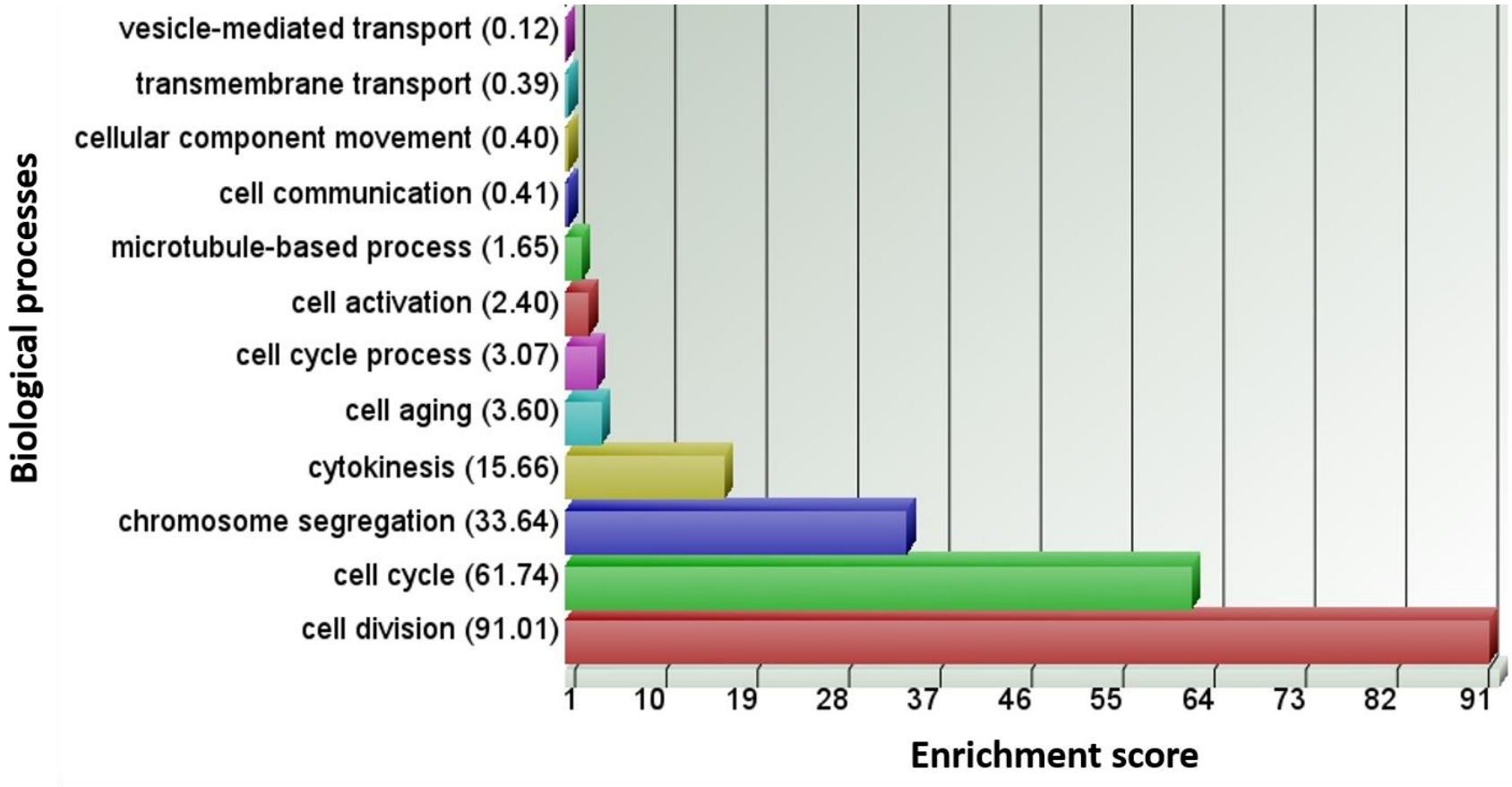


Figure 4-9 Detailed analysis of the cell proliferation processes in BXD1425-EPN further identified sub-functions particularly cell cycle and cell division as induced by BKM120 treatments.

Table 4-2 Elucidation of genes associated in each biological enrichment that was significantly identified in BXD1425-EPN cells and their expression status following treatment with BKM120.

Biological process	Total no of genes	Upregulated genes	Downregulated genes
Microtubule-based process	1	---	*GTSE1*
Cell activation	1	*PDGFRA*	---
Cell cycle process	1	---	*PHGDH*
Cell aging	2	*NOX4*	*CDK1*
Cytokinesis	8	---	*AURKB, BIRC5, ESPL1, INCENP, KIF20A, KIF23, PLK1, PRC1*
Chromosome segregation	14	---	*BIRC5, CASC5, CENPF, ESPL1, HJURP, INCEP, NDC80, NEK2, NUF2, SGOL1, SGOL2, SKA1, SKA3, SPC25*
Cell cycle	42	---	*ASPM, AURKB, BORA, CCNF, CDC20, CDCA2, CDCA3, CDK1, CDKN3, CEP55, CHAF1B, CKS2, CLSPN, CBF4B, DLGAP5, FAM83D, FANCD2, FOXM1, GSG2, H2AFX, HJURP, KIF11, KIF20B, KIFC1, MKI67, NCAPG, NCAPG2, NCAPH, NDC80, NUSAP1, OIP5, PRC1, PSRC1, SKA3, SPAG5, SUV39H1, TICRR, TIMELESS, TPX2, UBE2C, UBE2S, ZWINT*

Cell division	46	---	*ASPM, BIRC5, BORA, BUB1, CASC5, CCNA2, CCNB1, CCNB2, CCNF, CDC20, CDC7, CDCA2, CDCA3, CDCA8, CDK1, CENPE, CENPF, CEP55, CKS2, FAM83D, KIF11, KIF20B, KIF2C, KIFC1, MAD2L1, NCAPG, NCAPG2, NCAPH, NDC80, NEK2, NUF2, NUSAP1, OIP5, PSRC1, SGOL1, SGOL2, SKA1, SKA3, SPAG5, SPC24, SPC25, TIMELESS, TPX2, UBE2C, UBE2S, ZWINT*

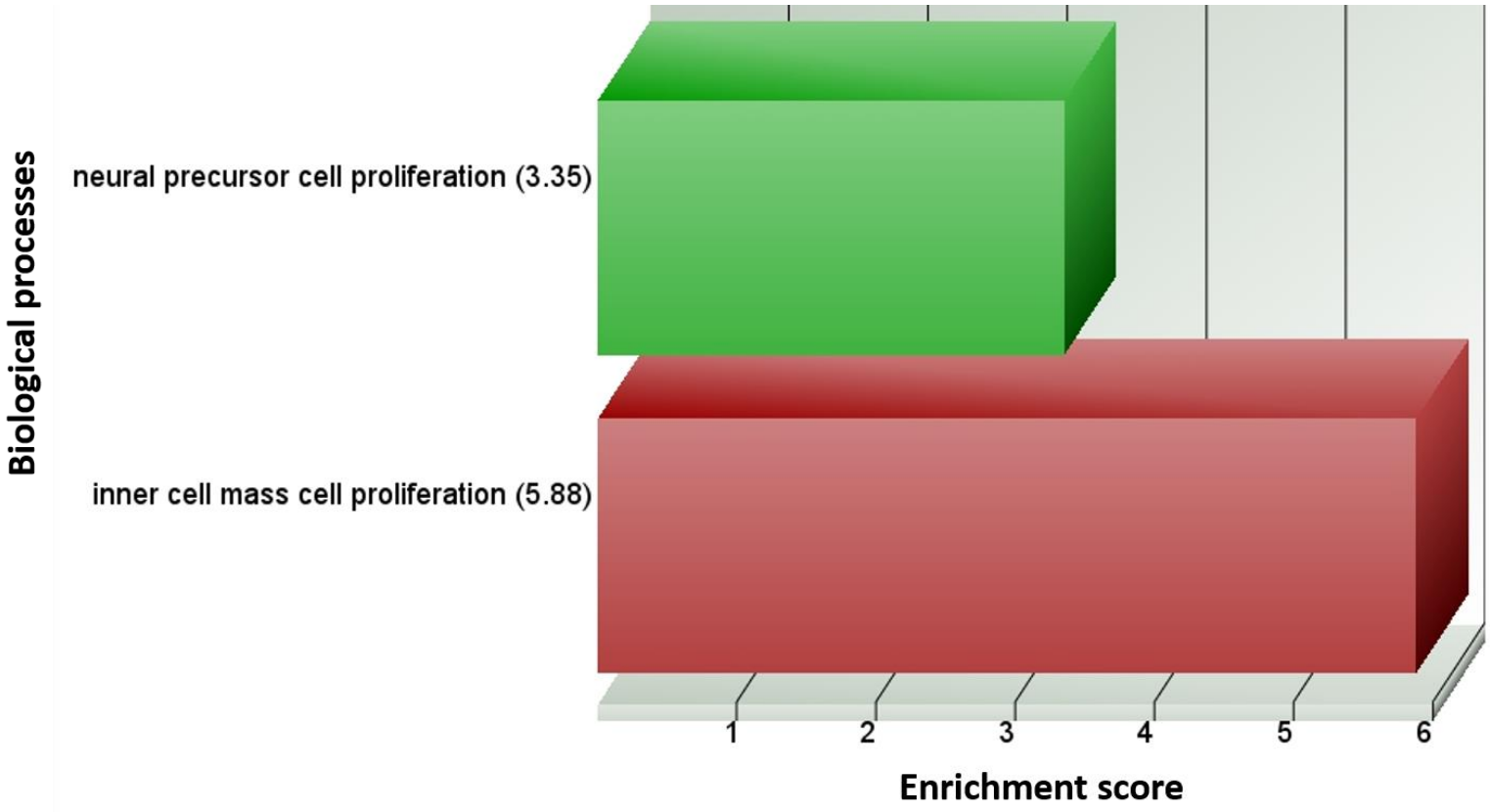


Figure 4-10 Additional cell proliferation sub-functions identified by Partek® Genomics Suite in BKM120-treated BXD1425-EPN cells were stem cell-related functions necessary for CNS formation.

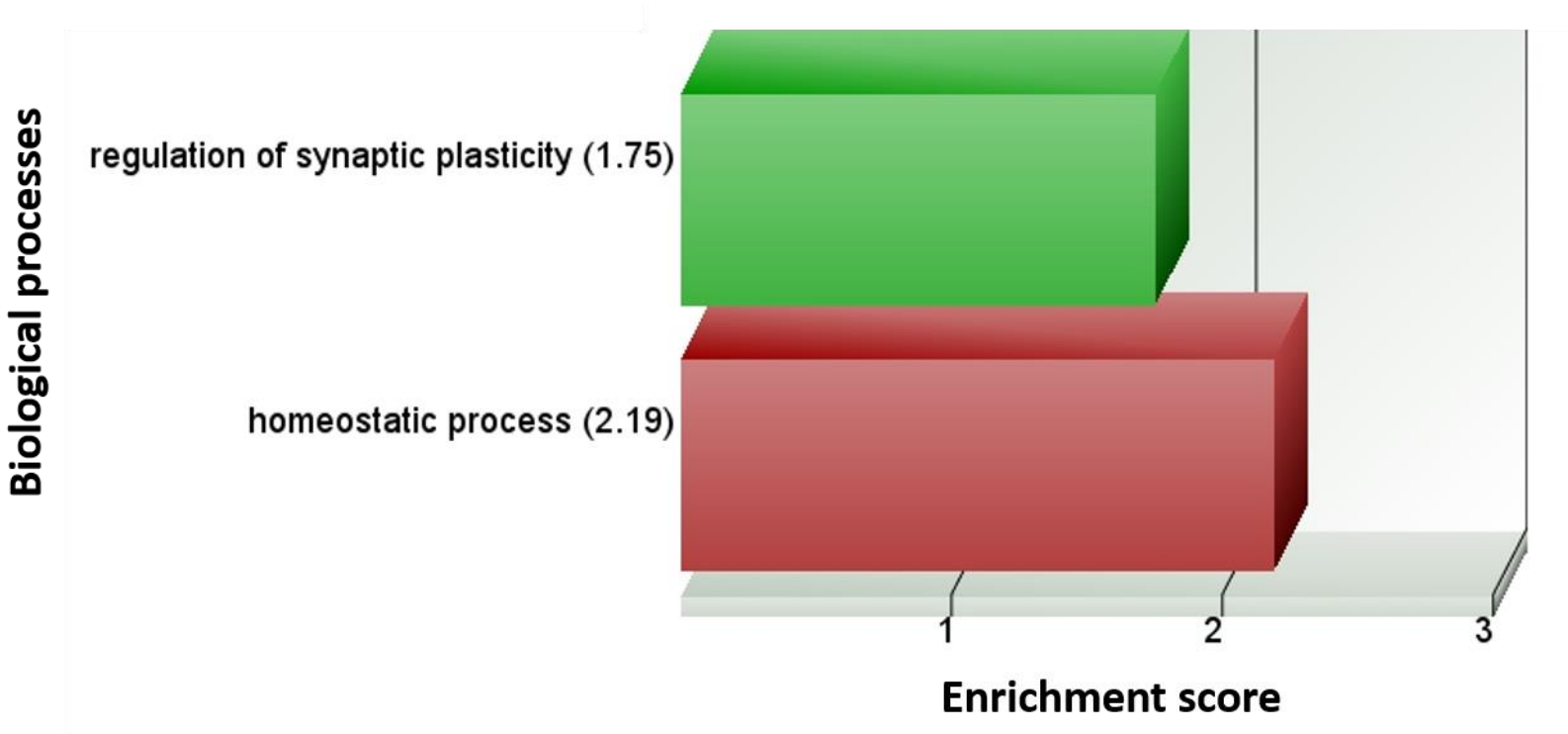


Figure 4-11 In conjunction with functions that relate to CNS formation, BKM120 treatment of BXD1425-EPN cells also enriched for processes that ensure maintenance and preservation of neurological activities.

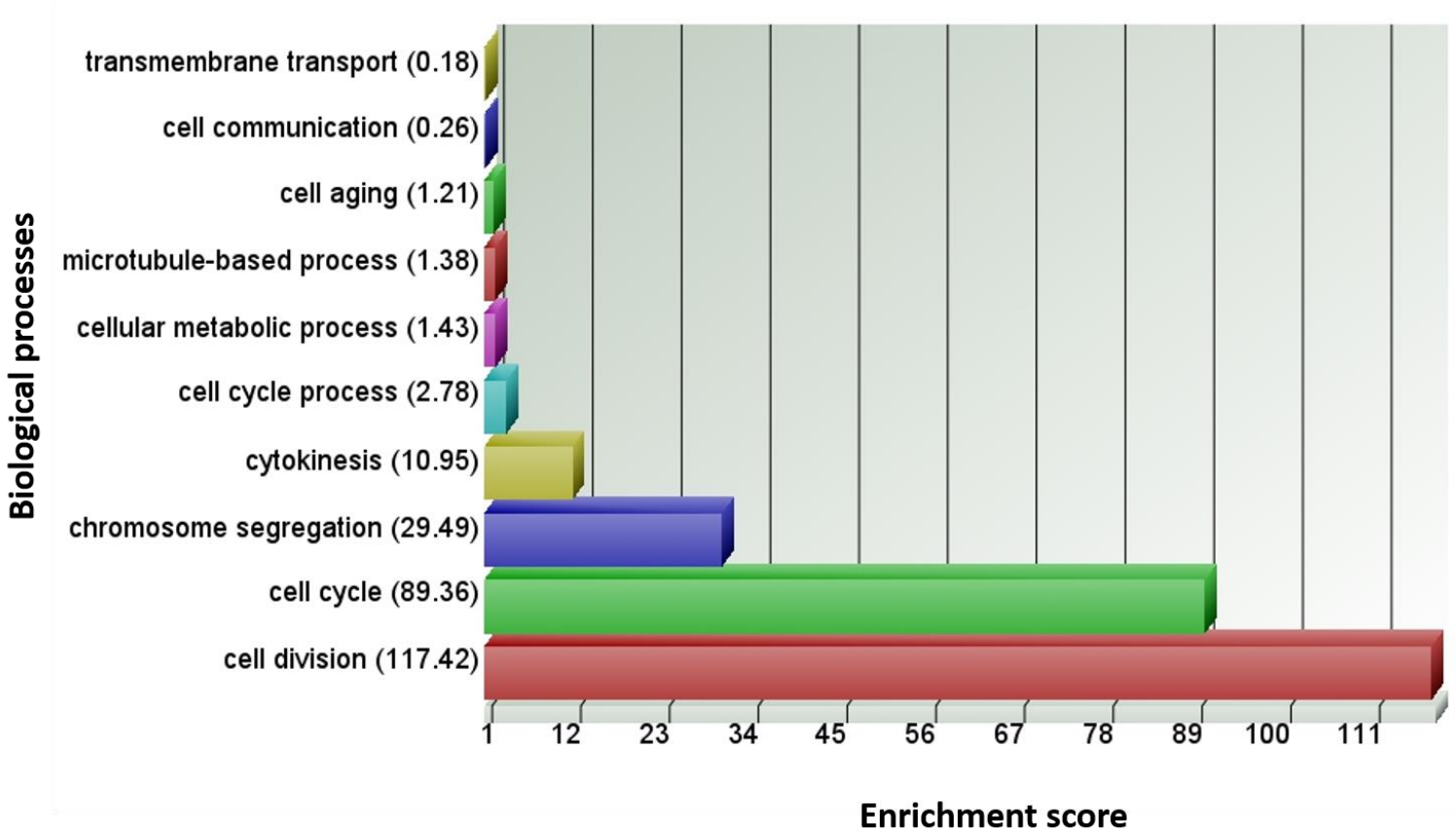


Figure 4-12 BKM120 treatment of EPN1 cells also led to an overrepresentation of cell cycle-related functions, signifying the importance of the PI3K pathway in regulating cell proliferation in ependymoma.

Table 4-3 Elucidation of genes associated in each biological enrichment that was significantly identified in EPN1 cells and their expression status following treatment with BKM120.

Biological process	Total no of genes	Upregulated genes	Downregulated genes
Cell aging	1	---	*CDK1*
Microtubule-based process	3	---	*GTSE1, TUBA1A, TUBA1B*
Cellular metabolic process	1	---	*BLM*
Cell cycle process	1	---	*PHGDH*
Cytokinesis	9	---	*AURKB, BIRC5, ESPL1, INCENP, KIF20A, KIF23, PLK1, PRC1*
Chromosome segregation	20	---	*NIRC5, BRCA1, CASC5, CENPF, CENPH, CENPO, DSN1, ESPL1, HJURP, INCENP, NDC80, NEK2, NUF2, PTTG1, SGOL1, SGOL2, SKA1, SKA3, SPC25, TOP2A*
Cell cycle	78	*CHMP1B*, *GAS1*	*ANLN, ASPM, AURKA, AURKB, BORA, BRCA1, BRCA2, BUB1B, CCNF, CDC20, CDCA2, CDCA3, CDCA5, CDK1, CDK2, CDKN3, CEP55, CHAF1A, CHAF1B, CKAP2, CKS1B, CKS2, CLSPN, DBF4B, DLGAP5, DSCC1, DTYMK, E2F8, ESCO2, FAM83D,*

			FANCD2, FANCI, FOXM1, GSG2, H2AFX, HAUS5, HAUS6, HAUS8, HELLS, HJURP, KIF11, KIF20B, KIFC1, LIN9, MCM2, MIS18A, MIS18BP1, MKI67, MTBP, NASP, NCAPD2, NCAPD3, NCAPG, NCAPG2, NCAPH, NDC80, NUSAP1, OIP5, PRC1, PSRC1, RACGAP1, SASS6, SKA3, SMC2, SMC4, SPAG5, SUV39H1, SUV39H2, TICRR, TIMELESS, TP73, TPX2, UBE2C, UBE2S, UHRF1, ZWINT
Cell division	86	*CHMP1B*	*ASPM, AURKA, BIRC5, BORA, BUB1, BUB1B, CASC5, CCNA2, CCNB1, CCNB2, CCNE1, CCNE2, CCNF, CDC20, CDC25A, CDC25C, CDC6, CDC7, CDCA2, CDCA3, CDCA5, CDCA8, CDK1, CDK2, CENPE, CENPF, CENPH, CENPJ, CENPO, CEP55, CKS1B, CKS2, DSN1, ERCC6L, FAM83D,*

			FBXO5, HAUS5, HAUS6, HAUS8, HELLS, KIF11, KIF20B, KIF2C, KIFC1, KNTC1, LIG1, MAD2L1, MAPRE1, MASTL, MCM5, MIS18A, MIS18BP1, NCAPD2, NCAPD3, NCAPG, NCAPG2, NCAPH, NDC80, NDE1, NEK2, NUF2, NUSAP1, OIP5, PSRC1, PTTG1, SGOL1, SGOL2, SKA1, SKA3, SMC1A, SMC2, SMC4, SPAG5, SPC24, SPC25, TIMELESS, TPX2, TUBA1A, TUBA1B, UBE2C, UBE2S, ZWILCH, ZWINT

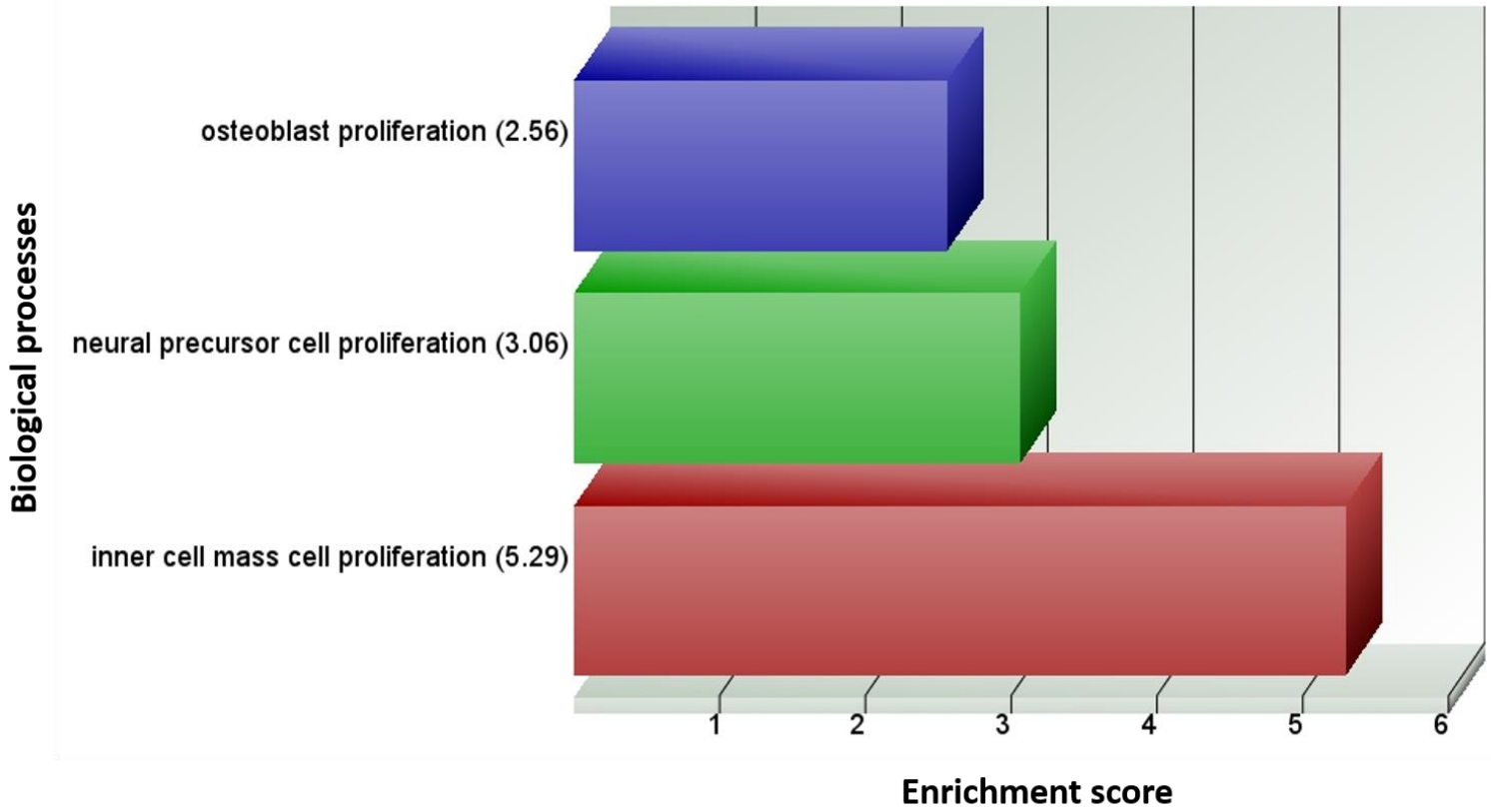


Figure 4-13 Similar to BXD1425-EPN cells, there was an enrichment for CNS stem cell activity in EPN1 cells which is mainly relevant during CNS maturation. Interestingly, BKM120 treatment of EPN1 cells also affected osteoblast-related proliferations which suggest neuronal-osteogenic cross talks for the latter's differentiation and functioning.

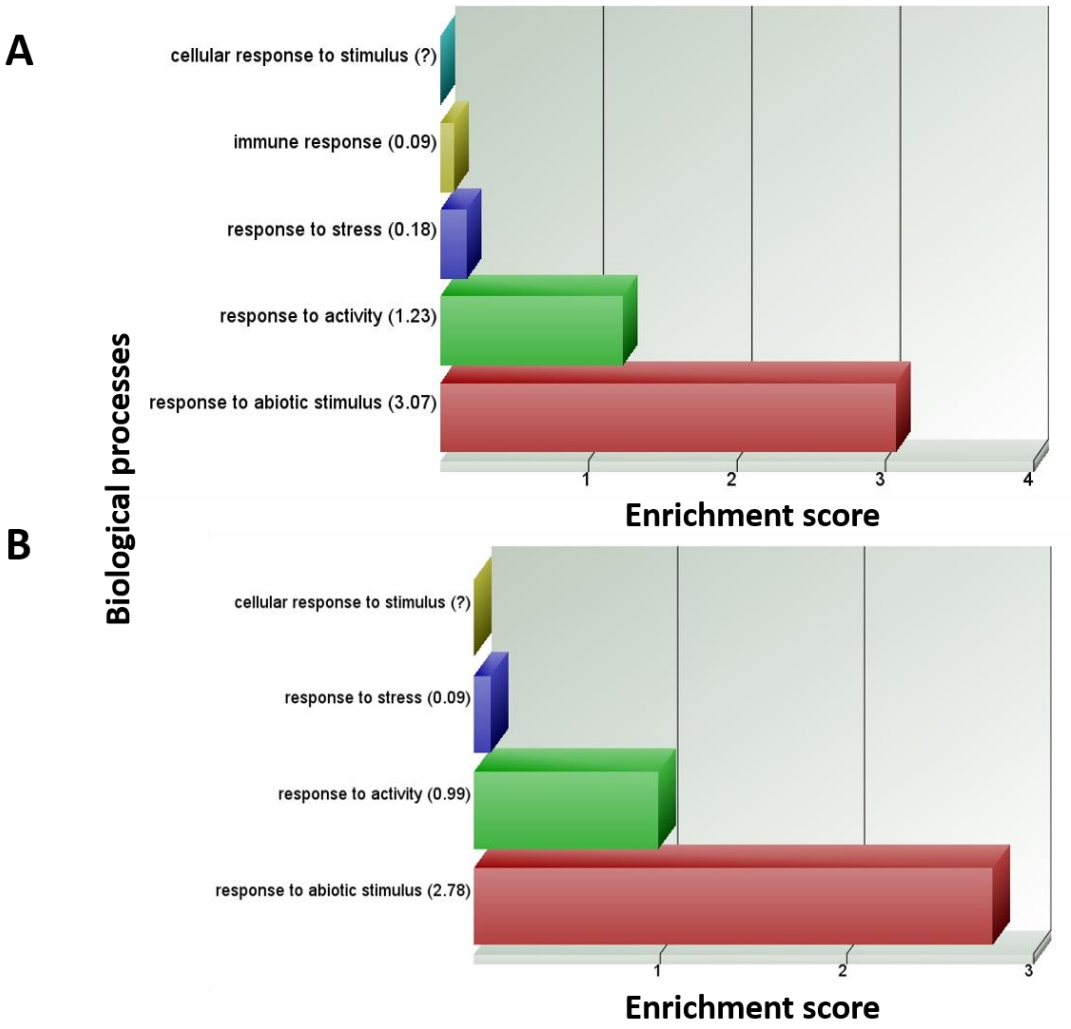


Figure 4-14 Inhibition of the PI3K pathway in (A) BXD1425-EPN and (B) EPN1 cells induced appropriate cellular responses that attend to the effects of extensive exposure to an abiotic stimulus, which in this case was BKM120 treatment.

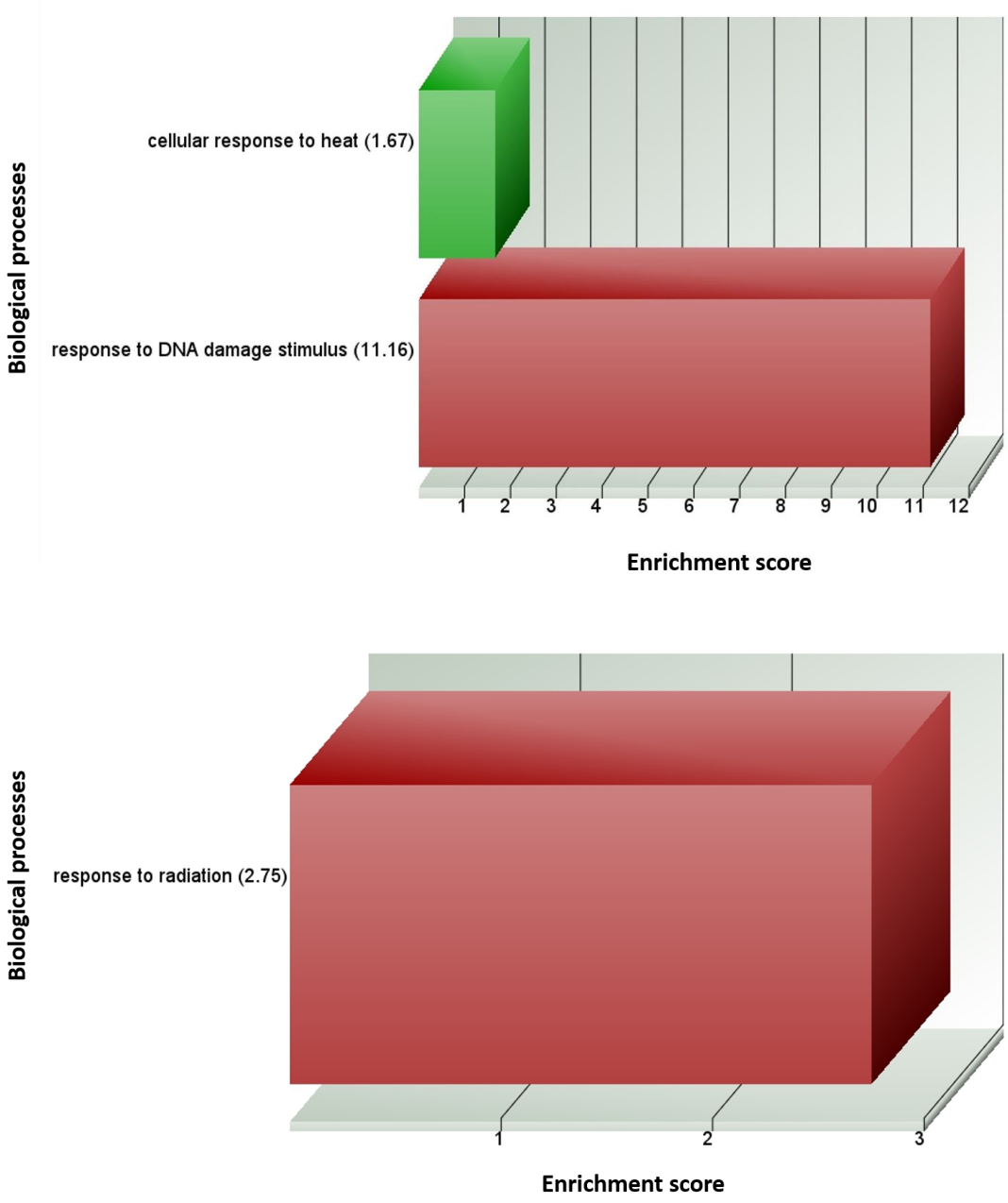


Figure 4-15 Detailed analysis of the response to abiotic stimulus to further elucidate any associated underlying biological processes was only available for the EPN1 dataset. The identified processes were mostly involved with reversing the effects of radiation and any impending DNA damage, implicating the role of the PI3K pathway in maintaining genomic integrity in ependymoma.

4.2.3.2 Biological enrichment analysis for common DEGs between BXD-1425EPN and EPN1 cells

Individual GO analysis of BXD1425-EPN and EPN1 cells has identified several biological enrichments, especially cell cycle related functions in response to BKM120 treatment. In order to pinpoint processes which were commonly affected by PI3K pathway inhibition in both BXD-1425EPN and EPN1 cells, overlapping genes from the individual DEG lists for each cell line were identified using Partek® Genomics Suite. A total of 202 overlapping DEGs were found between the two tested cell lines (Figure 4-16). In order to assess whether this overlap was significant, a hypergeometric test was performed. This test assumes random sampling of genes from a known list of genes without replacement. The hypergeometric test factors in the number of genes in set A (n_1) and set B (n_2), the commonly shared genes between the two sets (m) and the full set of probes incorporated on the microarray (n). The test was performed using the online microarray analysis and other bioinformatics tools function available on nemates.org where this overlap in the significant DEGs between the two ependymoma cell lines was found to be significant (***$p<0.001$) therefore transcriptomic changes observed were likely to be shared effects of the BKM120 treatment. Enrichment analysis for the 202 common DEGs was performed using DAVID Bioinformatics Resources 6.8 (Huang da, Sherman et al. 2009). GO analysis of the 202 common DEGs through DAVID reflected earlier findings with more detailed functional annotations that were not disclosed by Partek® software analysis. Such functions covered several events that take place in the progression through the cell cycle including G_1/S and G_2/M transitions, DNA replication and dynamic cytoskeletal organisation (Table 4-4). Interestingly, the majority of the genes involved in regulating these processes were downregulated as a result of BKM120 treatment, implicating its principal role in controlling cell cycle in ependymoma. These findings also presented further evidence that suppression of the PI3K pathway in ependymoma cells only produced cytostatic effects as demonstrated by previous work in this project.

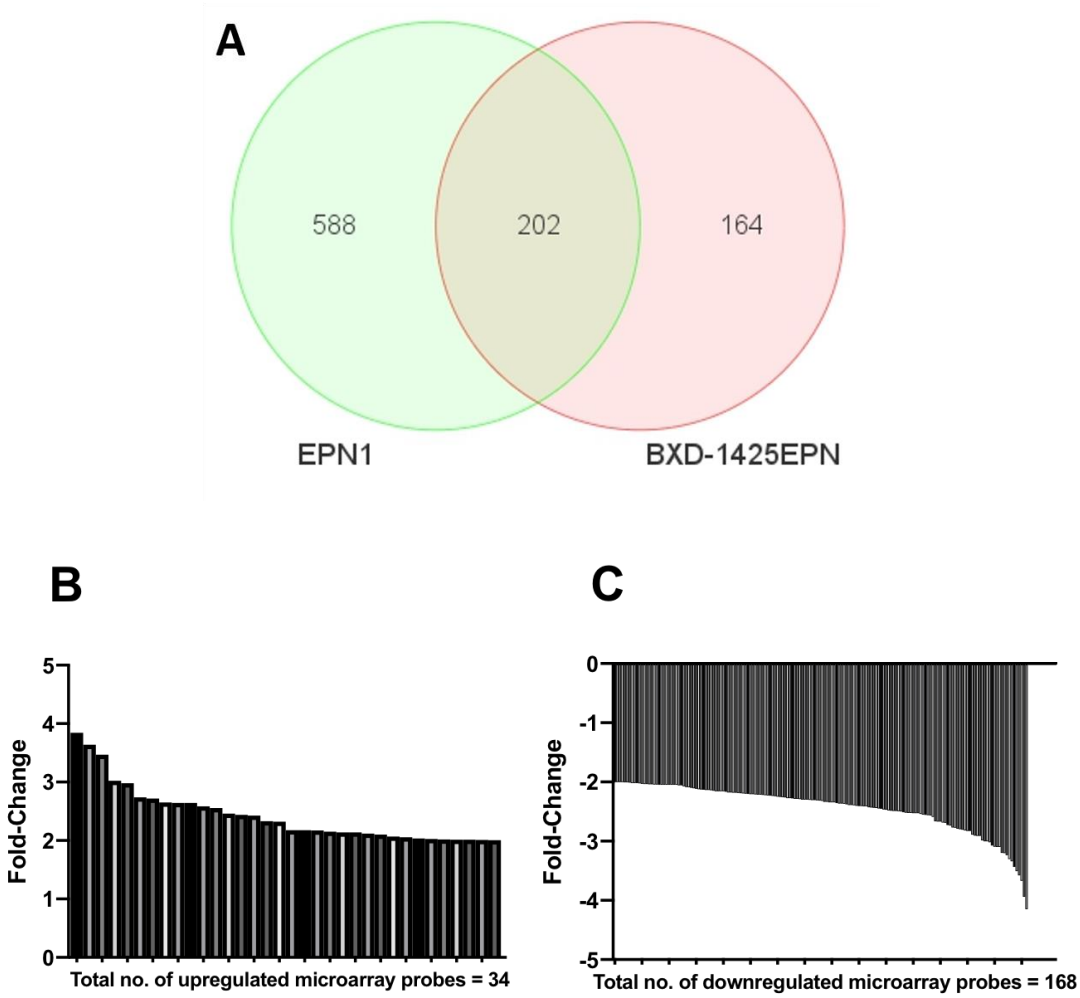


Figure 4-16 (A) Post-microarray hybridisation identified 790 and 366 gene probes, which were differentially expressed following BKM120 treatment relative to vehicle control in EPN1 and BXD-1425EPN cells, respectively. 202 gene probes overlapped between the two cell lines signifying the commonly differentially expressed probes in response to BKM120-mediated PI3K inhibition. Out of the 202 overlapping gene probes, (B) 34 gene probes were upregulated (FC ≥2) while (C) 168 gene probes were downregulated (FC ≤2).

Table 4-4. Top biological processes regulated by the 202 overlapping genes in BKM120-treated BXD1425-EPN and EPN1 cells, as identified by DAVID Bioinfomatics Resources. The p-values shown were corrected for multiple testing. Genes associated per GO Term are outlined in appendix 10.

GO Term	Upregulated genes	Downregulated genes	Total no. of genes	P-value (Benjamini)
Cell division	0	46	46	1×10^{-36}
Sister chromatid cohesion	0	22	22	1.7×10^{-20}
Chromosome segregation	1	16	17	1.7×10^{-16}
Microtubule-based movement	0	12	12	1.5×10^{-8}
DNA replication	0	13	13	1.2×10^{-6}
G_2/M transition of mitotic cell cycle	0	12	12	2.8×10^{-6}
Cell proliferation	1	16	17	1.1×10^{-5}
Spindle organisation	0	6	6	1.2×10^{-5}
DNA repair	0	13	13	7.1×10^{-5}
G_1/S transition of mitotic cell cycle	0	9	9	1.5×10^{-4}
Cytokinesis	0	7	7	1.6×10^{-4}
DNA replication initiation	0	5	5	3.7×10^{-3}
Double-strand break repair via break-induced replication	0	3	3	1.4×10^{-2}
Cerebral cortex development	0	5	5	2.3×10^{-2}
DNA biosynthetic process	0	4	4	2.4×10^{-2}
Protein localisation to kinetochore	0	3	3	4.4×10^{-2}

4.2.3.3 GO analysis of upregulated genes resulting from PI3K pathway inhibition

A small subset of the 202 common DEGs elucidated in both BXD-1425 and EPN1 cells showed upregulation following BKM120-mediated inhibition of the PI3K pathway. A total of 25 genes were upregulated (FC ≥2, $p<0.05$) in response to BKM120 treatment (Table 4-5). When these were analysed using DAVID, the GO terms identified were predominantly related to regulation of PI3K signalling, chromatin remodelling and regulation of DNA binding prior to transcription. However, the corrected p-values for these findings were found to be non-significant ($p>0.05$). To address the matter regarding a smaller gene list being considered for GO analysis, the Gene Ontology Enrichment Analysis and Visualisation Tool (GOrilla) (Eden, Navon et al. 2009b) was used. The positively regulated DEGs were compared against the full microarray background gene list in order to characterise the molecular involvement of this gene set within the vast system of higher-level processes that are typically active within the species (i.e. *Homo sapiens*) the analysis was based on. Enrichment for molecular functions of these genes showed these to be key contributors to several cellular pathways, whose activity may potentially be affected by the inhibition of the PI3K pathway in ependymoma (Table 4-6). One implicated signalling cascade was the MAPK pathway, another survival signalling pathway involved in tumourigenesis (Bradham, McClay 2006, Dhillon, Hagan et al. 2007). Two of the genes associated were *PDGFRA* (encoding for the platelet-derived growth factor receptor alpha) and *NEK10* (encoding for a Ser/Thr kinase that also participates in cell cycle regulation). Interestingly, some of these upregulated genes are also involved in the positive regulation of the PI3K pathway including *IRS2,* an adaptor protein encoding gene for the recruitment of pathway components, which could interact with the PI3K enzyme to activate it. Three microRNAs: *MIR221*, *MIR222*, *MIR21*, could target *PTEN* transcripts for degradation (Pezzolesi, Platzer et al. 2008, Garofalo, Quintavalle et al. 2012) which eliminates the negative regulation of PI3K pathway thus enhancing its signalling. Based on these results, the use of MAPK pathway inhibitors and RTK-specific agents in conjunction with PI3K pathway inhibition could be proposed as a potential treatment approach for ependymoma. However, supplementary functional experiments are required in order to verify whether these functions identified in the analyses truly represent cellular events post-PI3K pathway inhibition in ependymoma.

Table 4-5. List of genes commonly upregulated in BXD1425-EPN and EPN1 following inhibition of the PI3K pathway. Gene functions were characterised using GeneCards® Human Gene Database.

Gene	P-value	Function
KLHL24	0.000278137	- component of the E3 ubiquitin ligase complex, serves as substrate receptor.
NEK10	0.000462696	- confers a transferase activity, particularly phosphorylation events
SLC16A6	0.00241123	- involved in transmembrane transportation of monocarboxylate compounds
FBXO32	0.00168214	- F-box containing protein that participates in protein-protein interaction, leading to ubiquitination of targets.
SPRY2	0.00635531	- mediates negative feedback during the signalling of many RTKs
SAT1	0.0000698	- possesses an acetyltransferase activity which is necessary for maintenance of cellular polyamine levels
TMEM198B	0.000158854	- a pseudogene that encodes for a transmembrane protein which has a putative role in Wnt signalling
MIR21	0.0198514	- a microRNA-encoding gene known to have oncogenic effects by knocking down phosphatases that negatively regulate survival pathways including the PI3K pathway
CREBRF	0.000167935	- confers a DNA binding function which regulates transcription especially that of CREB3 in response to unfolded proteins in the cell's endoplastic reticulum
TCP11L2	0.00171849	- function unknown; paralogous to *TCP11L1* associated with a disease called Unilateral or Bilateral Cryptorchidism
PDGFRA	0.00210782	- belongs to the platelet-derived growth factor receptor family that instigates several cellular pathways including the PI3K pathway upon activation
DTWD1	0.016678	- function unknown

MIR222	0.0115479	- a microRNA-encoding gene associated with epithelial tumours; increases cell proliferation and inhibits apoptosis
SLC35E2	0.0000457	- encodes for a solute carrier and involved in transport of undisclosed cellular material
AKAP12	0.0423462	- regulates Protein Kinase A (PKA) activity, signalling and localisation
IRS2	0.00136869	- encodes for the insulin receptor substrate 2 that mediates recruitment of downstream effectors of insulin or insulin-like growth factor signalling in particular.
JMY	0.0000503	- potentiates p53-mediated processes such as apoptosis when translocated in the nucleus; involved in actin dynamics when localised in the cytoplasm
MIR635	0.0134862	- a microRNA encoding gene with documented tumour suppressive properties
SNORD116-5	0.0364146	- a small nucleolar RNA that is non-coding whose downregulation has shown links with Prader-Willi Syndrome
HDAC5	0.00544163	- a histone deacetylase that promotes heterochromatinisation and gene expression silencing.
CTHRC1	0.0189626	- modulates collagen deposition particularly during vascularisation
MIR221	0.0113575	- a microRNA-encoding gene with oncogenic properties; works in conjunction with *MIR222*
INO80B	0.00552233	- involved in chromatin remodelling which consequently affects processes such as transcription and DNA replication
SNORD90	0.0459707	- encodes for non-coding RNA molecule; function is yet to be elucidated
SLC4A7	0.00219481	- transports sodium and bicarbonate ions across the cell membrane to regulate visual and auditory sensory transmissions

Table 4-6. Enrichment of positively regulated genes in ependymoma for biological functions following inhibition of the PI3K pathway using GOrilla programme.

GO Term	FDR q-value	Enrichment Score	Genes
Positive regulation of AKT signalling	1.18×10^{-4}	37.74	*MIR221, MIR222, IRS2, MIR21, SPRY2, PDGFRA*
Negative regulation of angiogenesis	1.51×10^{-3}	31.66	*MIR221 MIR222, MIR21, SPRY2, HDAC5*
Regulation of ERK1 and ERK2 cascade	1.24×10^{-4}	19.37	*NEK10, MIR221, MIR222, MIR21, SPRY2, PDGFRA*
Regulation of cell migration	6.01×10^{-3}	8.23	*MIR221, MIR222, IRS2, MIR21, SPRY2, HDAC5, PDGFRA*

4.2.4 Transcription factors involved in the regulation of DEGs in BKM120 treated ependymoma cells

Characterisation of the transcriptional machinery that regulates the expression of the 202 common DEGs further characterises how PI3K pathway-related biological responses were stimulated in ependymoma. Gene Set Enrichment Analysis (GSEA) (Subramanian, A., Tamayo et al. 2005) was used to identify transcription factors that regulate the expression of these genes through computation of shared upstream *cis*-regulatory sequences. The top 10, out of the 31, most significant transcription factors are listed in Table 4-7. One of the identified transcription factors on this analysis was E2F1, a known regulator of the cell cycle whose target genes include those involved in the G_1/S transition of the cell cycle. In order to visualise the interaction between the 202 common DEGs, a genetic map was produced using STRING v10.5 and Cytoscape v3.6.1. TFe and ENCODE RegIns were employed to add onto the network various transcription factors associated with regulating these genes. Analysis of 'neighbouring' targets has identified 13 genes transcriptionally regulated by E2F1 including *CDK1*, *CENPL* and *DBF4* (Figure 4-17) whose expression profiles were also reduced and involvement were implicated in various cell cycle processes (see appendix 9). These findings suggest that PI3K pathway inhibition may decrease E2F1 transcriptional activity in ependymoma leading to downregulation of cell cycle genes and consequently promoting cell cycle arrest. Interestingly, the Cytoscape interaction map also found two more members of the E2F

family of transcription factors, E2F4 and E2F6, which were not identified in the GSEA analysis. Both transcription factors were shown to be involved in controlling a subset of the ependymoma DEGs. Selection of neighbouring targets for E2F4 identified 64 genes whereas E2F6 interacted with 6 genes (Figure 4-18), most of which were implicated in cell cycle progression and division. These analyses suggest a multi-faceted regulation of cell cycle genes in ependymoma involving several members of the E2F family.

Table 4-7. Analysis of upstream *cis*-regulatory sequences using Gene Set Enrichment Analysis (GSEA) in the 202 DEGs identified significantly associated transcription factors involved in the regulation of these genes. (**Key** **:- refers to redundancy in description of a similar transcription factor outlined prior to).

Gene Set Enrichment for transcriptional regulation	P-value (Benjamini)	Other description
GATTGY_NFY_Q6_01	1.01×10^{-19}	Nuclear transcription factor Y binds to the highly conserved M5 GATTGGY motif (CCAAT box); cell cycle regulator with potential implications in various human diseases (Ly, Yoshida et al. 2013).
KRCTCNNNNMANAGC_ UNKNOWN	1.30×10^{-11}	Binds to the highly conserved M120 KRCTCNNNNMANAGC motif, usually located around the gene's transcription start site; no known class of transcription factors associated.
E2F1_Q3	2.91×10^{-7}	Belongs to the class of Fork head/winged helix transcription factors; binds to the consensus motif of TTTXXCGC (X could be G or C) (Slansky, Farnham 1996).
NFY_Q6	4.6×10^{-7}	**
E2F1_Q6	1.53×10^{-6}	**
E2F_Q3	9.38×10^{-6}	**
E2F_Q6	9.38×10^{-6}	**
E2F_Q4	9.38×10^{-6}	**
E2F1DP1_01	9.38×10^{-6}	Belongs to the DP family of proteins; forms heterodimers with E2F1 (Rabinovich, Jin et al. 2008).
E2F1DP2_01	9.38×10^{-6}	**

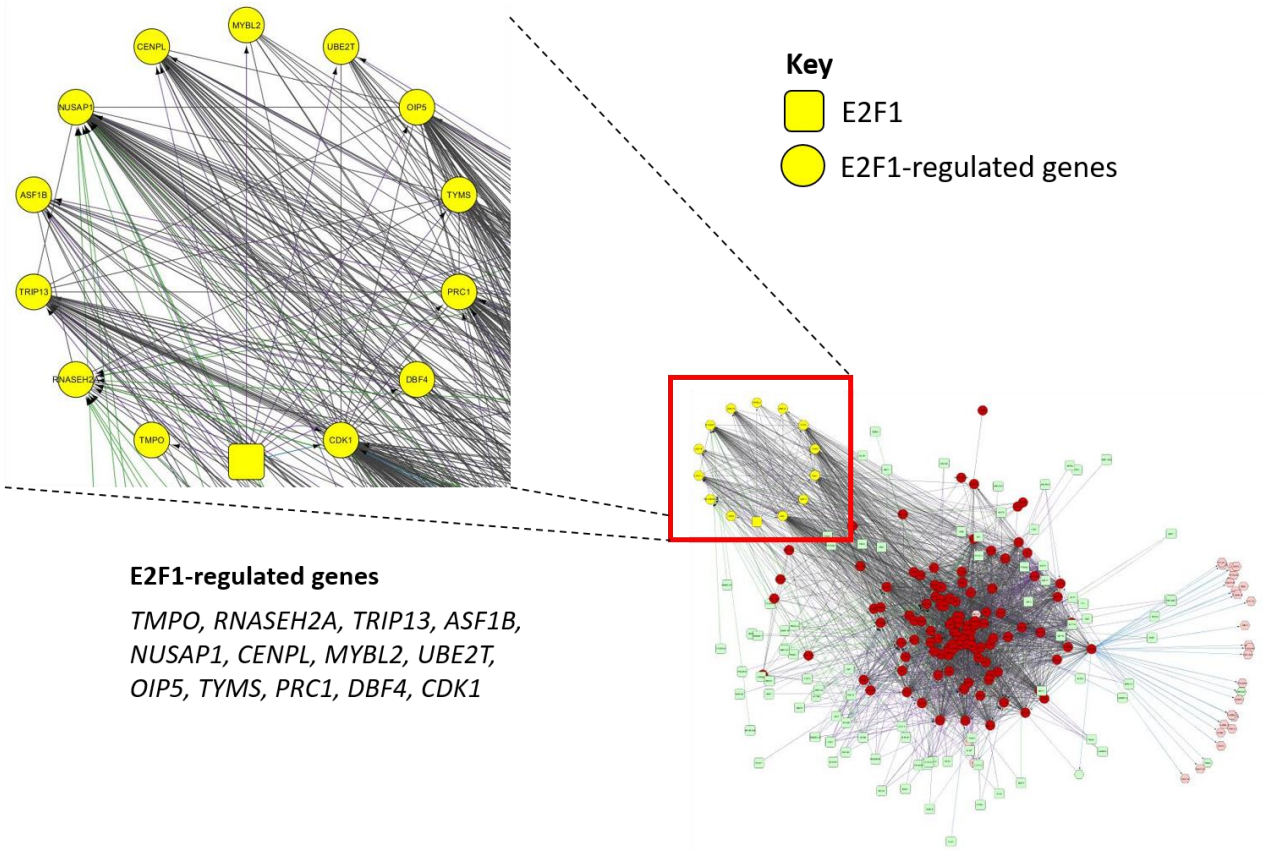
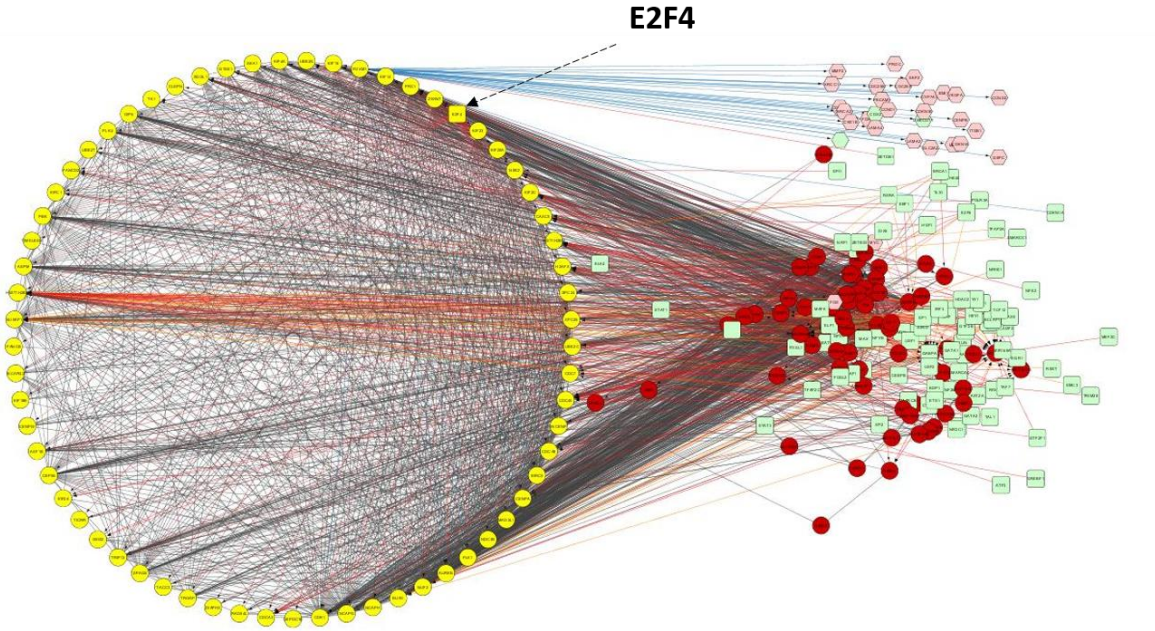


Figure 4-17 Interaction map of the 202 elucidated ependymoma DEGs (indicated by the red circles) alongside the various transcription factors that regulate these as extracted from TFe and ENCODE RegIns (indicated by the green squares and pink circles) was produced using STRING and Cytoscape. From this, analysis of 'neighbouring' targets of E2F1 (yellow square) has identified 13 genes (yellow circles) which were then clustered and highlighted in a circular layout on the map. These genes, which were also listed above, showed a reduction in expression and were enriched for cell cycle functions thus supporting cell cycle arrest as a cellular response to BKM120 treatment.



E2F4 related genes

ASF1B, ASPM, AURKB, BIRC5, BUB1, CASC5, CDC45, CDC7, CDCA3, CDCA8, CDK1, CENPA, CENPW, CEP55, CLSPN, DEPDC1B, DIAPH3, FANCB, FANCD2, FOXM1, GSG2, GTSE1, H2AFX, HIST1H2BC, HIST1H2BM, INCENP, KIF14, KIF15, KIF18B, KIF20A, KIF23, KIF24, KIF2C, KIF4A, KIFC1, MAD2L1, NCAPG, NCAPG2, NCAPH, NDC80, NEK2, NUF2, NUSAP1, OIP5, PBK, PLK1, PLK4, PRC1, RAD54L, SGOL1, SKA1, SPAG5, SPC24, SPC25, TACC3, TICRR, TIMELESS, TK1, TRIP13, TROAP, UBE2C, UBE2S, UBE2T, ZWINT

Figure 4-18 Querying of the genetic interaction map for other E2F transcription factor members pinpointed E2F4 as a regulator of a subset of the ependymoma DEGs. Clustering analysis of E2F4-related factors identified 64 genes which predominantly showed a downregulation in expression as well as enrichment for cell cycle functions.

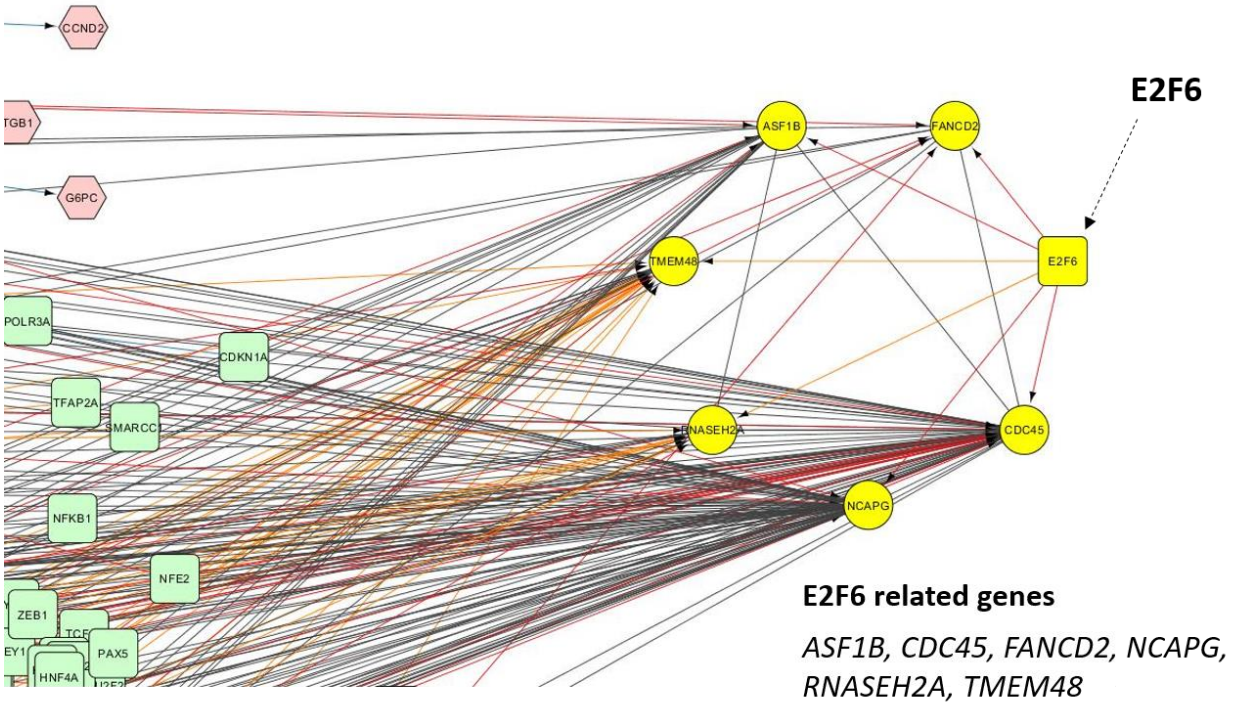


Figure 4-19 A comprehensive survey of the Cytoscape gene interaction map has pinpointed E2F6, another member of the E2F family of transcription factors. Analysis of 'neighbouring' targets of E2F6 has identified six genes which also enriched for cell cycle processes.

4.3 Discussion

It has been demonstrated in the previous chapter that BKM120-mediated inhibition of the PI3K pathway restricted ependymoma growth and viability. In this chapter, gene expression changes in ependymoma were analysed following BKM120-mediated inhibition of the PI3K pathway to identify molecular functions that could be related to promoting survival and viability. By employing microarray technology in this study, a broader indication of the therapeutic impact of inhibiting the PI3K pathway in ependymoma was gained. It also enabled the exploration of the vast PI3K signalling network to pinpoint nodes that could be further exploited therapeutically in ependymoma in conjunction with inhibition of the PI3K pathway. In this study's transcriptomic analysis, a total of 202 common DEGs were significantly found between BXD-1425EPN and EPN1 cells. GO analysis showed an enrichment for cell cycle related processes whose implicated genes were downregulated in response to treatment with BKM120. No enrichment for cell death mechanisms was found which further supports that BKM120 only induced a cytostatic, instead of a cytotoxic response in ependymoma. Scrutiny of upstream *cis*-regulatory sequences of these DEGs showed E2F1 and its binding partners as significant transcriptional regulators of expression of these genes. Other biological processes that were downregulated following PI3K pathway inhibition include DNA repair responses and G_2/M-related functions such as spindle organisation, microtubule treadmilling and kinetochore functioning; all of which are crucial processes for maintaining survival and proliferation in cancers. GO analysis of the upregulated genes induced by BKM120 revealed a positive regulation of MAPK signalling and reactivation of the PI3K pathway, highlighting the potential of co-inhibiting both pathways as a possible mode of treatment for ependymoma.

4.3.1 Inhibition of BXD-1425EPN and EPN1 cells resulted in a downregulation of cell cycle processes

It was previously demonstrated that both BXD-1425EPN and EPN1 cells were responsive to the inhibitory effects of BKM120 and so it was essential to investigate common pathway mechanisms that stimulate ependymoma tumourigenesis. Treatment of BXD-1425EPN and EPN1 cells with BKM120 resulted in 366 and 790 significant differentially expressed gene probes, respectively, of which 202 were mutual to both cell lines. This overlap was found to be significant based on the hypergeometric test, suggesting BKM120-mediated inhibition of the PI3K pathway commonly affects regulation of these genes in the two tested cell lines. GO analysis of the 202 significant DEGs for biological enrichment showed an overrepresentation of cell proliferation and cell cycle-related processes. One of the identified GO terms linked to cell cycle following PI3K

pathway inhibition is that involved with G_1/S transition. The genes associated with this process showed a negative fold-change, which implicates an arrest at this phase of the cell cycle. These results supported the cell cycle analysis in Chapter 3 where BKM120 treatment caused an increase in cell population at G_0/G_1 while decreasing those in the other cell cycle phases. As discussed earlier, cytostaticity as exemplified by G_1/S cell cycle arrest is typical of pharmacological inhibition of the PI3K pathway where a lack of cytotoxic effect could also be found in many cancers (Serra, Markman et al. 2008a, Zhao, P., Hall et al. 2017, Ishikawa, Senba et al. 2018).

The PCA plot produced during QC analysis showed that while there was independent clustering of variables for DMSO and BKM120 treatment in both the BXD-1425EPN and EPN1 samples, there was also a lack in overlap in the different treatment conditions with their counterparts in the other cell line. The segregation of the DMSO and BKM120 transcriptomic clusters on the PCA plot was expected to indicate the difference between drug treated and untreated conditions. On the other hand, the absence of co-clustering of BKM120 and DMSO treated conditions for both cell lines suggested a difference in the cell lines' gene expression patterns which may be related to underlying tumourigenic differences despite both cell lines being derived from the supratentorial region. Initial GO analysis of each cell line's list of significant DEGs also indicated some disparities in biological enrichments such as response to DNA damage and radiotherapy being apparent only to EPN1. One may argue that these findings support the general notion that ependymomas are clinically distinct from each other despite their histopathological similarities but further work involving several other cell lines is necessary to substantiate this inference.

The conclusions made in this chapter could be strengthened by the inclusion of a posterior fossa-derived ependymoma cell line in future analyses. Addition of a posterior fossa cell line sample would have determined overlapping oncogenic mechanisms between the two compartmentally restricted tumours. This would potentially put forward a therapeutic strategy that could be generalised to both supratentorial and posterior fossa ependymomas. The benefit of such findings in the long term would address the issue of paucity of effective treatments for ependymoma which is partly related to efforts in tailoring therapeutic regimes to accommodate tumour differences in molecular signatures. Therefore, developing on this work presents putative clinical relevance particularly in alleviating the disappointing survival rates of patients belonging to the posterior fossa group A or harbouring *C11orf95-RELA* positive supratentorial tumours.

4.3.2 Downstream mechanism of cell cycle arrest in ependymoma post-PI3K pathway inhibition

GSEA analysis of the overlapping ependymoma DEGs showed E2F1 and its binding partners as significant transcription factors that regulate their expression. Surveying of the gene interaction map produced using STRING and Cytoscape has also identified two other members of the E2F transcription factor family, E2F4 and E2F6, whose functions would potentially be stimulated in parallel with E2F1. Clustering analysis following identification of 'neighbouring' targets for each E2F transcription factor has pinpointed genes which were enriched for cell cycle functions. These genes also showed a negative fold-change following BKM120 treatment thus supporting an E2F-mediated mechanism to facilitate cell cycle arrest in ependymoma.

E2F1, alongside E2F2 and E2F3a, belong to the group of E2F activators that ensure the progression of cell cycle (Takahashi, Rayman et al. 2000). Activity of all three E2Fs peaks during G_1/S transition and are equally capable of being sequestered by the Rb protein to prevent transcription of their target genes (see section 1.3.3.6) (Dimova, Dyson 2005). Since many of the cell cycle genes displayed a decrease in expression levels, it was hypothesised that E2F1-mediated transcription in ependymoma undergoes negative regulation through binding of E2F1 to Rb following inhibition of the PI3K pathway. Alternatively, the downregulation of cell cycle genes could have been facilitated by the activity of E2F4 and E2F6. Several findings have alluded to their roles as repressors of transcription through various mechanisms (Christensen, Cloos et al. 2005, Dimova, Dyson 2005). E2F4 forms complexes with an Rb-like protein called p130 which binds to promoters especially in quiescent cells to repress gene transcription (Takahashi, Rayman et al. 2000). Other studies have also demonstrated a role for E2F4 in cell cycle exit and differentiation (Persengiev, Kondova et al. 1999, Enos, Bancos et al. 2008). E2F6 is deemed to confer a similar transcriptional repressive mode of action especially having identified its association with the Polycomb group of proteins (Ogawa, Ishiguro et al. 2002), which are essential for chromatin remodelling. E2F6 can also confer anti-tumourigenic effects by targeting several tumour suppressor genes such as *BRCA1* (Oberley, Inman et al. 2003). Since many of the genes regulated by E2F1 according to this analysis also corresponded with the transcriptional program of E2F4 and E2F6, one would argue that downregulation of cell cycle genes in ependymoma could also be mediated through the action of E2F repressors, particularly E2F4 and E2F6, alongside the loss of E2F1 activity following BKM120 treatment.

Binding of the Rb protein to E2F transcription factors involves Rb in its hypophosphorylated state (Li, J. M., Hu et al. 1997), which is associated with the loss of

CDK4/6-cyclin D activity. Abrogation of CDK4/6-cyclin D functioning during G_1/S arrest could be mediated through several mechanisms including downregulation of *CCND1* transcription following activation of GSK3β (Shtutman, Zhurinsky et al. 1999), the stimulation of p53 activity(Ball, Lain et al. 1997, Chen, J. 2016) and expression of proteins that inhibit cell cycle progression (Sherr, Roberts 1999). Another known instigator of cell cycle arrest is the FOXO family of transcription factors which are activated due to a reduction in inhibitory phosphorylation following PI3K signalling suppression (Hay 2011). Under normal signalling conditions, FOXOs are phosphorylated which usually prompts nuclear exclusion and consequently decreasing transcriptional output of genes thus encouraging proliferation and viability. As depicted in sections 1.3.3.6 and 1.3.3.7, FOXOs predominantly act as a master regulator of tumour suppression by enhancing the activity of a broad range of targets including the Cip/Kip and Ink4 family of cell cycle inhibitor proteins which arrest cells particularly at the G_1/S phase (Zhang, X., Tang et al. 2011). Interestingly, several studies have also demonstrated that this cell cycle arrest could actually precede the induction of cell death (Georgakis, Li et al. 2006, Gong, Liao et al. 2012). One compelling reason is the PI3K pathway's negative regulation on several drivers of cell death especially those that mediate apoptotic responses, which is relieved following loss of signalling. However, gene expression data generated in this chapter suggests this was not the case in ependymoma since no enrichment for cell death mechanisms was identified during the analysis of the overlapping significant DEGs, coinciding with the results from chapter 3. Nevertheless, one may infer the significance of FOXO activity as a promoter of cell cycle arrest in ependymoma.

With these, it is postulated that cell cycle arrest in ependymoma is mediated through the activation of FOXO proteins post-PI3K pathway inhibition. Upregulation of FOXO targets including an array of cell cycle inhibitors consequently leads to a reduction in the activity of CDK4/6-cyclin D, which is essential during G_1/S transition. This results in the hypophosphorylation of Rb which increases its binding affinity to the E2F1 transcription factor, thus decreasing its transcriptional output in the process.

4.3.3 BKM120 treatment induced a reduction of expression in G_2/M-related genes in ependymoma

GO analysis of the ependymoma DEGs has also shown a reduction in processes that are typically stimulated during the G_2/M phase of the cell cycle including spindle organisation, kinetochore assembly for cohesion of sister chromatids and microtubule-based movements. Loss of these processes is indicative of the activation of several checkpoints in this stage of the cell cycle in response to BKM120 treatment which

prevents both G_2 exit into mitosis and completion of mitotic division. Two of the downregulated genes in ependymoma following BKM120-mediated inhibition of the PI3K pathway are *CDK1* and *CCNB1*. Since successful passage through the G_2/M cell cycle phase requires the activation of the CDK1/Cyclin-B complex (Pines, Hunter 1992), this finding further supports that G_2/M-associated checkpoints have been induced following treatment with BKM120. Indeed, several studies have suggested that the PI3K pathway could simultaneously regulate both G_1/S and G_2/M transitions of the cell cycle (Shtivelman, Sussman et al. 2002, Garcia, Kumar et al. 2006). In mammalian cells, PI3K/AKT activity fluctuates throughout the cell cycle during which a peak could be observed in the advent of G2/M transition (Kumar, Carrera 2007). It is also put forward that completion of mitotic division requires signalling input from the PI3K pathway (Roberts, Shapiro et al. 2002).

Signalling through the PI3K pathway has been contributory to resistance to conventional chemotherapy as it enables these checkpoints to be by-passed (Kandel, Skeen et al. 2002, Lal, Bae et al. 2009) thus continuing with the cell cycle without inducing cell death. In particular, resistance to taxol-based agents such as paclitaxel has been associated with upregulation of G_2/M processes which could circumvent spindle attachment checkpoints (Anand, Penrhyn-Lowe et al. 2003) prior to entering the last stages of the cell cycle. Therefore, it is hypothesised that PI3K pathway inhibition could enhance the effects of microtubule agents by targeting G_2/M processes. According to Atkinson, Shelat et al. (2015), the identification of centrosome cycle pathways as a target in ependymoma implicates the vulnerability of these tumours towards abrogation of G_2/M related processes. In a separate study, upregulation of kinetochore components was found in recurrent ependymal tumours (Peyre, Commo et al. 2010); a tumourigenic feature that contributes towards circumvention of spindle attachment checkpoints (Zhang, W., Mao et al. 2016) which would confer resistance to taxol-based agents. Therefore, combining PI3K pathway inhibition with taxol-based agents could possibly be exploited as a potential treatment approach in ependymoma especially at recurrences where disease management is much more challenging (Messahel, Ashley et al. 2009). Currently, there have been no reports that strongly suggest that paediatric ependymomas show reduced sensitivity to paclitaxel. If these tumours did display paclitaxel resistance, it is worth noting that the underlying resistance mechanism may not necessarily be associated with the activation of PI3K signalling unless proven functionally. Nevertheless, the fact that PI3K pathway inhibition resulted in a reduction in these cellular processes conveys a sound basis for investigating the enhancement of taxol-based agents' tumour suppressive effects in ependymoma.

4.3.4 BKM120 treatment induced a reduction of expression in DNA repair genes in ependymoma

Apart from enrichment in cell cycle-related processes, treatment of ependymoma with BKM120 also resulted in downregulation of DNA repair responses. It is interesting that this biological enrichment was only found in EPN1 when the gene expression data from the two ependymoma cell lines was analysed individually. However, this GO process was included under the broad term of 'responses to abiotic stimulus' which was relevant to both BXD-1425EPN and EPN1 cells. One possible reason for this discrepancy is that there may have been more genes detected in EPN1 cells relative to BXD-1425EPN cells that confer DNA repair functions hence its apparent detection only in the EPN1 dataset; but it does not necessarily mean that the enrichment for DNA repair responses is exclusive to EPN1 cells. The fact that DNA repair responses were identified as a significantly enriched molecular function in the overlapping DEGs suggests that this process is more likely to be a downstream event of the PI3K pathway in ependymoma. Since two different GO analysis platforms were used to elucidate the various DEG biological functions, such disparities in the post-transcriptomic results may be attributed to the algorithmic thresholds that were set in each program.

Nevertheless, the PI3K pathway is depicted as a major regulator of various DNA damage sensors, signalling effectors and transducers that mediate responses for repairing genomic lesions and restoring integrity to the DNA structure (Liu et al., 2014). Therefore, suppression of PI3K signalling would lead to elimination of DNA repair systems in ependymoma as signified by the microarray analysis. It is reasoned that signalling through the PI3K pathway may confer resistance to genotoxic agents following an amplification of DNA damage responses. It is then hypothesised that PI3K pathway inhibition leads to impairment of DNA repair pathways which would induce hypersensitivity to DNA damaging agents and consequently favour cell death responses due to genomic catastrophe (Chirnomas, Taniguchi et al. 2006, Michels, Vitale et al. 2013). Indeed, some of the identified downregulated DNA repair genes on the microarray have previously been associated with chemoresistance including *POLQ*, *FANCD2* and *PARPBP* (Wang, Y., Wiltshire et al. 2006, Adelman, Lolo et al. 2013, Long, J., Zhu et al. 2018). In support, several pre-clinical studies have demonstrated the advantage of inhibiting the PI3K pathway to enhance the effects of DNA damaging therapies in cancer (Bozulic, Surucu et al. 2008, Shi, Guo et al. 2017). At present, it seems a promising approach to inhibit PI3K signalling to augment the effects of genotoxic drugs in ependymoma due to the likelihood of a reduced DNA repair response.

4.3.5 The upregulated genes induced by BKM120 treatment in ependymoma

The PI3K signalling network also consists of feedback loops and inter-pathway crosstalks that consequently lead to sub-optimal outcomes towards PI3K pathway inhibitors (Garrett, Chakrabarty et al. 2011, Brown, Toker 2015). Analysis of the global transcriptomic signature of BKM120-treated ependymoma cells enabled identification of enriched cellular functions and processes that may potentially deny PI3K pathway inhibition from achieving its full therapeutic capacity. For this, the upregulated genes were evaluated to determine if these would augment certain functions that would negate the effects of repressing PI3K signalling.

GO analysis of the upregulated genes from the 202 overlapping DEGs showed enrichment for positive regulation of MAPK signalling as well as reactivation of the PI3K signalling, which was partly associated with miRNA-mediated gene silencing. Indications of MAPK activation following PI3K inhibition included the upregulation of *PDGFRA* and *NEK10* expression. *PDGFRA* encodes for platelet-derived growth factor receptor alpha, an RTK that undergoes ligand-induced dimerisation leading to the stimulation of various downstream signalling cascades including MAPK (Wang, Y., Pennock et al. 2004). MAPK signalling, similar to PI3K signalling, is another cell survival pathway associated with inducing the different hallmarks of cancer. One study showed that activation of PDGFRα in medulloblastoma consequently increased MAPK signalling and targeting the PDGFRα/MAPK signalling axis inhibited tumourigenesis *in vitro* as demonstrated by the decrease in migration rates (MacDonald, T. J., Brown et al. 2001). Similarly, activation of PDGFRα/MAPK signalling enhanced the transformation potential of gliomas (Ozawa, Brennan et al. 2010) and ensured survival of gastrointestinal stromal tumours (GISTs) (Subramanian, S., West et al. 2004). NEK10 belongs to the family of NIMA-related kinases which play a role in cell cycle control. Interestingly, NEK10 is more engaged in DNA damage repair responses that are usually triggered by abiotic stimuli such as UV irradiation (Moniz, Stambolic 2011). Environmental insults stimulate NEK10 to form complexes with Raf-1 and MEK-1, inducing the latter's activation and further propagation of downstream MAPK signalling. It is possible that treatment with a PI3K inhibitor provided the abiotic stimuli to stimulate MAPK signalling through NEK10, thus constituting a potential compensatory survival mechanism. Conversely, upregulation of *SPRY2* was also included in the MAPK regulation enrichment in BKM120-treated ependymoma cells yet its function contradicts the effects of MAPK signalling on ependymoma pathogenesis. SPRY2 acts as a tumour suppressor by negatively regulating RTK activity through its binding to the Grb2 adaptor protein (Hanafusa, Torii et al. 2002, Yim, Ghosh et al. 2015). Therefore, the effects of MAPK signalling in ependymoma following PI3K inhibition are yet to be clarified.

In addition, the increase in expression of the microRNAs *MIR221*, *MIR222* and *MIR21* following BKM120 treatment warrants further investigation as a regulator of the PI3K signalling pathway. These microRNAs are principally involved in the reactivation of the PI3K pathway. *MIR21* has been shown to target *PTEN* transcripts (Pezzolesi, Platzer et al. 2008), which effectively relieves inhibition on upstream cascades of the pathway. *MIR221* and *MIR222*, like *MIR21*, are known oncomiRs that were also upregulated in ependymoma following PI3K pathway inhibition. These share a high sequence homology and are usually co-expressed in vertebrates (Wurz, Garcia et al. 2010). *MIR221/MIR222* also target *PTEN* as well as other known downstream targets of the PI3K/AKT pathway leading to increased cell proliferation and survival (Garofalo, Quintavalle et al. 2012). In addition, their expression in various cancers has also contributed towards resistance to conventional chemotherapy (Magee, Shi et al. 2015), which implicates modulation of the microtranscriptome as a possible strategy for treating cancer. Without PTEN activity, PI3K signalling in ependymoma becomes sustained following activation of RTKs especially the upregulated PDGFRα. It would also uphold signalling from insulin- and insulin-like receptors since *IRS2* is also upregulated, which interacts with the PI3K enzyme to activate it (see section 1.5.4.1). Therefore, recognising the contributory role of miRNAs may present a novel and more effective approach in circumventing potential resistance mechanisms that may arise as a result of inhibiting the PI3K pathway.

4.3.6 Future work: analysis of trancriptomic profile at various timepoints

Analysis of ependymoma gene expression profile post-BKM120 treatment aimed to identify further cellular processes that might affect tumourigenesis. So far, results only confirmed what has been observed in the previous chapter in which there is a predominant enrichment for processes the prohibit growth and proliferation. This is likely due to the comparable timepoints that the treatments were conducted for both the experimental work in chapter 3 and the transcriptomic analysis. Although there were novel biological functions elucidated through this work including a downregulation in DNA repair systems and prospective activation of other signalling pathways which could be further investigated, it is also worth analysing the expression data of ependymoma cells that were pharmacologically treated for less than 24 hours. This would reflect the earlier changes at the transcriptomic level, in response to drug treatment, which may yield a more informative dataset that would account for the anti-tumourigenic effects of PI3K pathway inhibitors. This is especially relevant with the transcription of immediate early genes, which would have been omitted in the final analysis as their expression increases rapidly and transiently in response to environmental cues (Fausto, 2000). Immediate early genes

are important regulators of cell fate, growth and viability since they control the subsequent expression of late response genes which ultimately govern over the aforementioned cellular processes (Bahrami, Drablos 2016). Examples of late response genes include E2F transcription factors, cyclins and CDKs which have already been elucidated in this chapter's analysis. Many of these immediate early genes encode for transcription factors and DNA binding proteins including c-fos and c-jun, whose expression is maintained provided that there is constant growth factor and mitogenic signalling (O'Donnell, Odrowaz et al. 2012). It is also considered that these immediate early genes confer an oncogenic effect. If deemed to be essential factors in tumourigenesis then targeting their activity might be a potential strategy for improving disease outcomes. In this project, it could be suggested that downregulation of immediate early response genes may be achieved through the presence of PI3K pathway inhibitors. This would consequently affect the expression of many late response genes thus phenotypically manifesting as cell growth inhibition.

While it has already been put forward that the formation of Rb/E2F1 complexes would lead to suppression of cell growth, it is also argued that the anti-proliferative effect of BKM120 could be observed at an earlier phase through the negative regulation of several immediate early response genes. Since it has been demonstrated in the preceding chapter that incubation of ependymoma cells with BKM120 for one hour inhibits PI3K signalling, it is hypothesised that similar treatment conditions would also induce changes at the transcriptional level. As part of future work, analysis of expression levels in ependymoma in response to shorter drug incubation periods is performed. Through this, biological enrichments and other key molecular players which were not seen in the current data but could be of pathological significance might be captured.

4.3.7 Conclusion

Overall, the gene expression data robustly showed that PI3K inhibition only conferred cytostatic effects in ependymoma as signified by the downregulation of cell cycle genes as well as the lack of enrichment for cell death mechanisms. This further supports that PI3K pathway inhibitors are more ideal for stabilising disease rather than being considered as a first-line therapy. This also argues that PI3K pathway inhibition could be better exploited as part of a treatment combination. E2F1 and its binding partners were found to be significant regulators of expression of the different ependymoma DEGs following analysis of upstream *cis*-regulatory binding sequences. Loss of E2F1 transcription, presumably through Rb-mediated sequestration, was proposed as a mechanism for the induction of cell cycle arrest post-BKM120 treatment. Post-

transcriptomic analysis has also revealed several molecular enrichments, which highlighted avenues for promoting resistance to PI3K pathway inhibition (e.g. stimulation of MAPK and reactivation of PI3K signalling) as well as processes that could be exploited as part of a combination treatment (e.g. DNA repair responses and processes of G_2/M transition). Future work will include analysing gene expression patterns using different time points to elucidate any other biological processes or molecular targets that may significantly contribute towards disease pathogenesis.

4.4 Summary of chapter findings

- There were 202 overlapping significant DEGs identified between EPN1 and BXD-1425EPN cells, which generally showed a negative fold change thus suggesting a reduction in biologically enriched functions such as cell cycle processes, DNA damage response and several G_2/M-related processes.

- No enrichment for cell death mechanisms was identified in response to BKM120 treatment, which supports the cytostatic effect of inhibiting the PI3K pathway in ependymoma.

- Downregulation of DNA damage response and G_2/M-related processes following PI3K pathway inhibition may potentially enhance the tumour suppressive effects of DNA-damaging agents and taxol-based drugs, implicating a prospective combination treatment in ependymoma that could be further investigated.

- Enrichment of upregulated genes resulted in processes that stimulated MAPK signalling as well as reactivation of the PI3K pathway, which presented potential resistance mechanisms towards PI3K pathway inhibition. Suppressing both pathways was suggested as a therapeutic tactic for treating ependymoma.

- Analysis of upstream *cis*-regulatory sequences identified E2F1 and its binding partners as significant transcriptional regulators of the expression of ependymoma DEGs. E2F4 and E2F6 were further elucidated as potential co-regulators following comprehensive surveying of the Cytoscape gene interaction map. Loss of E2F1-mediated transcription was proposed to be an underlying mechanism for the reduction in expression of cell cycle genes and the subsequent induction of cell cycle arrest in ependymoma in response to BKM120 treatment.

CHAPTER 5. POST-TRANSCRIPTOMIC FUNCTIONAL ANALYSIS OF DOWNSTREAM PI3K PATHWAY TARGETS

5.1 Introduction

Gene ontology analysis of the differentially expressed genes in response to PI3K pathway inhibition has highlighted several enriched biological functions that may play a crucial role in ependymoma pathogenesis. Enrichment of the differentially expressed genes in ependymoma showed regulation of cell cycle progression as a significant biological process following BKM120 treatment. The genes involved were downregulated, which was suggestive of cell cycle arrest as supported by the results in chapter 3. This chapter aimed to functionally investigate the molecular mechanisms that promote cell cycle arrest in ependymoma in response to the suppression of PI3K signalling.

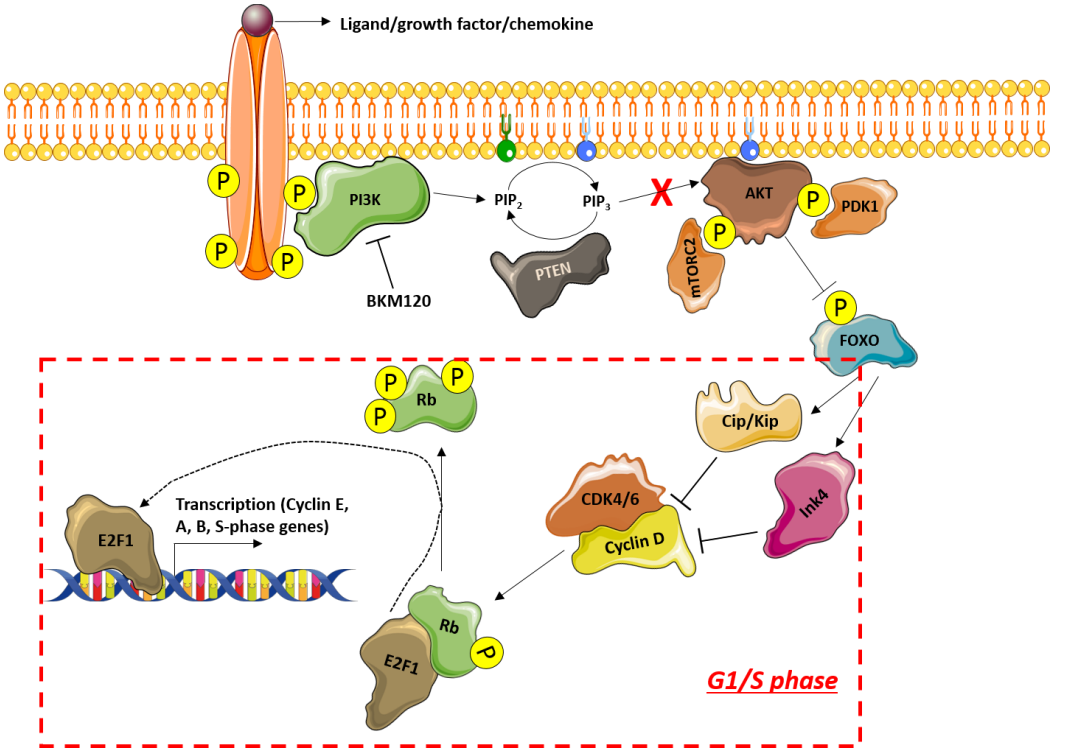


Figure 5-1 Proposed downstream mechanism for the induction of cell cycle arrest in ependymoma post-BKM120 treatment. BKM120 treatment inhibits PI3K/AKT signalling which activates FOXO, resulting in the expression of cell cycle inhibitors such as the Cip/Kip and Ink4 proteins. These inhibit CDK4/6-Cyclin D activity which results in Rb hypophosphorylation. Rb sequesters the E2F1 transcription factor, consequently decreasing its transcriptional output.

As discussed in chapter 4, it was proposed that PI3K pathway inhibition leads to the activation of FOXO family of transcription factors which consequently induces the formation of Rb/E2F1 complexes. Rb sequestration of E2F1 prevents the latter's

translocation into the nucleus thus decreasing its transcriptional output (Li, J. M., Hu et al. 1997) (Figure 5-1), as signified by the negative fold-change of its identified target genes on the microarray data. This study therefore investigated whether the cytostatic effects of PI3K pathway inhibition in ependymoma was mediated by the activation of FOXO proteins, resulting in the inhibition of the Rb/E2F1 pathway.

Studies have shown that activation of the PI3K pathway contributes towards the inefficiency of many chemotherapeutic drugs in cancer (West, Castillo et al. 2002, Brown, Toker 2015). Microarray analysis in the previous chapter identified a downregulation of several cellular processes, in response to PI3K pathway inhibition, which could potentially contribute towards resistance to conventional chemotherapy in ependymoma. These include DNA damage responses which could reduce the efficacy of genotoxic agents such as cisplatin and gemcitabine, and G_2/M-related processes which could limit the effects of taxol-based drugs such as paclitaxel. By eliminating these downstream, secondary responses through inhibition of PI3K signalling, it was postulated that the effects of these traditional anti-cancer agents could be enhanced in ependymoma. In this chapter, it was therefore tested whether combining PI3K pathway inhibition with paclitaxel, cisplatin and gemcitabine could exert synergistic effects in ependymoma cells thus suggesting a potential treatment modality for these tumours.

This work serves as a functional follow-up on the gene expression analysis presented in the previous chapter. It focused on investigating two research questions:

1. What is the underlying molecular mechanism that promotes cell cycle arrest in ependymoma following PI3K pathway inhibition?
    - AIM: To investigate if ependymoma cell cycle arrest is mediated by the activation of FOXO proteins, and the subsequent loss of E2F1 transcription in association with Rb hypophosphorylation.

2. Can PI3K pathway inhibition enhance the effects of common anti-cancer drugs in ependymoma?
    - AIM: To investigate whether BKM120 can synergise with the effects of paclitaxel, cisplatin and gemcitabine in ependymoma.

5.2 Results

5.2.1 Inhibition of the PI3K pathway led to loss of phosphorylation of FOXO1 but not FOXO3 in ependymoma

To investigate whether PI3K pathway inhibition in ependymoma activates FOXO proteins, the phospho-status of FOXO1 and FOXO3, whose roles were implicated in cell cycle arrest (Schmidt, Fernandez de Mattos et al. 2002a), was investigated. Western blot data showed that inhibition of the PI3K pathway for one hour resulted in a dose-dependent decrease in phosphorylation of FOXO1 but not FOXO3 in all the tested ependymoma cell lines (Figure 5-2). Levels of total FOXO3 were not affected by BKM120 treatment. Moreover, BKM120 did not change the total FOXO1 protein level expression in BXD-1425EPN cells but was interestingly increased in EPN1 and EPN12A cells. This data suggests that FOXO1 activity is directly regulated by the PI3K pathway in ependymoma cells, relative to FOXO3.

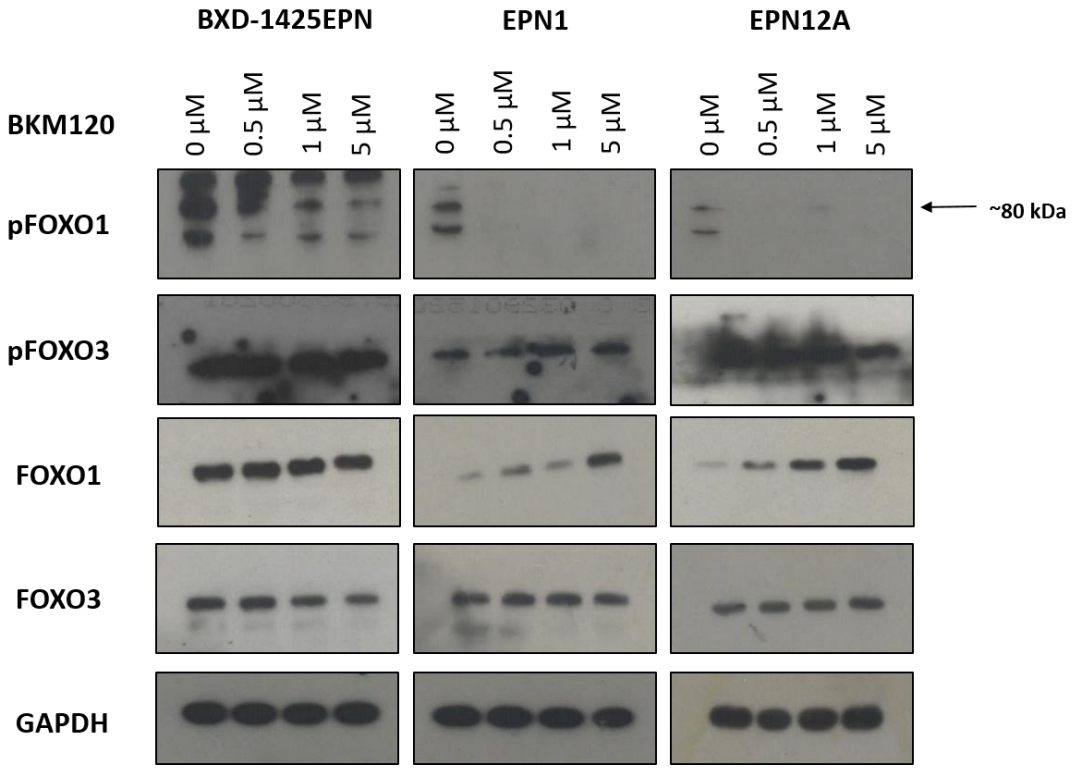


Figure 5-2 Western blot analyses of phosphorylated FOXO1 and FOXO3 in response to increasing doses of BKM120 after a one hour incubation. A reduction in expression of pFOXO1 (80kDa band) but not pFOXO3 was seen in a BKM120 dose-dependent manner across all the tested ependymoma cell lines. Probing against the total FOXO3 showed a constant expression in all cells whilst total FOXO1 expression increased, except in BXD-1425EPN cells, following BKM120 treatment. GAPDH was used as a loading control (n= 3).

5.2.2 Co-inhibition of FOXO1 did not increase cell viability in BKM120-treated ependymoma cells

So far, it was demonstrated that BKM120 treatment decreased FOXO1 phosphorylation, suggesting it is activated following PI3K inhibition and may potentially facilitate the reduction of ependymoma cell viability through induction of cell cycle arrest. It was subsequently investigated if loss of FOXO1 activity could rescue the inhibitory effects of BKM120 in ependymoma. FOXO1 activity was inhibited using the drug AS1842856 which confers a high affinity binding relative to other members of the FOXO family of transcription factors (Nagashima, Shigematsu et al. 2010). BXD-1425EPN, EPN1 and EPN12A cells were treated with various BKM120 concentrations in combination with increasing doses of AS1842856. MTT viability assays were performed, following incubation with the drugs, to determine whether FOXO1 inhibition could relieve the inhibitory effects of BKM120 (Figure 5-3). A two-way ANOVA was performed to determine whether there was a significant change in the overall cell viability trend with the addition of AS1842856 relative to the BKM120 only treatment. Results showed that there was no significant difference between the inhibitory curves of BKM120 only and BKM120/AS1842856 co-treatments in all three ependymoma cell lines. This indicates that AS1842856 treatment was not able to counteract the effects of BKM120 by increasing cell viability, as originally hypothesised. However, further functional work is necessary to determine whether FOXO1 plays a regulatory role in ependymoma cell cycle progression.

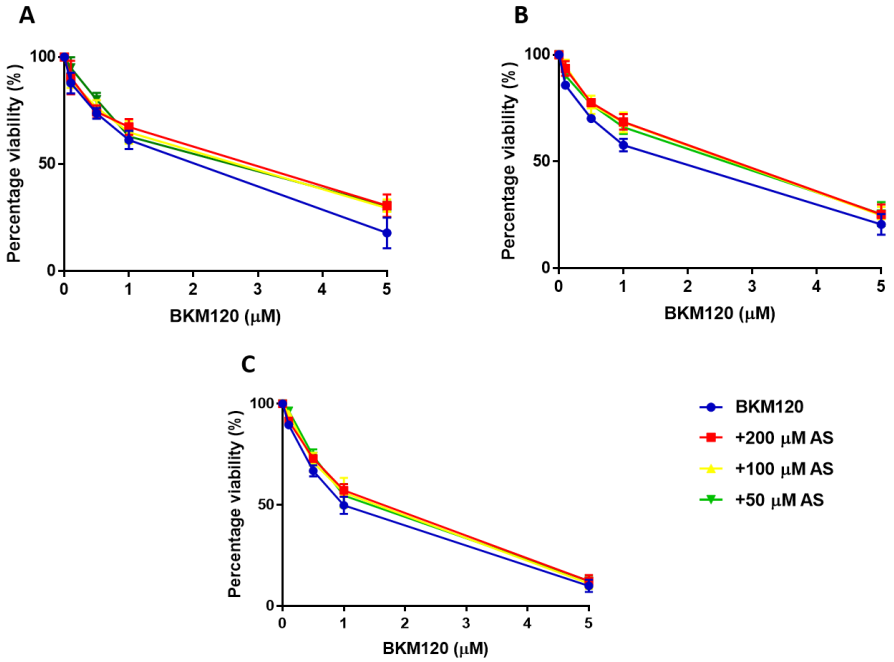


Figure 5-3 MTT assay results of (A) BXD1425-EPN, (B) EPN1 and (C) EPN12A cells treated with increasing BKM120 doses in combination with 200, 100 and 50 μM of the FOXO1 inhibitor, AS1842856, for 72 hours. No significant difference was shown in the inhibitory curves between BKM120 only treatment and when co-treated with various AS1842856 concentrations. Experiments were analysed using a two-way ANOVA Dunnett's multiple comparisons test (n=3).

5.2.3 Inhibition of the PI3K pathway led to loss of phosphorylation of Rb protein in ependymoma

G_1/S arrest is characterised by the hypophosphorylation of Rb causing it to bind and sequester the E2F1 transcription factor (Li, J. M., Hu et al. 1997), consequently decreasing the expression of genes necessary to progress through to the next cell cycle phase. The phospho-status of Rb was subsequently investigated to determine whether BKM120-mediated inhibition of the PI3K pathway in ependymoma results in loss of Rb phosphorylation, which would contribute towards cell cycle arrest. BXD-1425EPN, EPN1 and EPN12A cells were treated with various concentrations of BKM120 for 24 hours followed by immunoblotting against pRb and total Rb protein levels. Western blot analysis showed a decrease in Rb phosphorylation in a BKM120 dose-dependent manner in all tested ependymoma cell lines (Figure 5-4). Interestingly, there was also a decrease in total Rb protein in response to BKM120 treatment, an effect also seen in previous studies (Liu, Korc 2012, Vijayaraghavan, Karakas et al. 2017). This data suggests that regulation of Rb activity is a downstream effect of the PI3K signalling in ependymoma and may potentially influence cell cycle progression in ependymoma following BKM120 treatment.

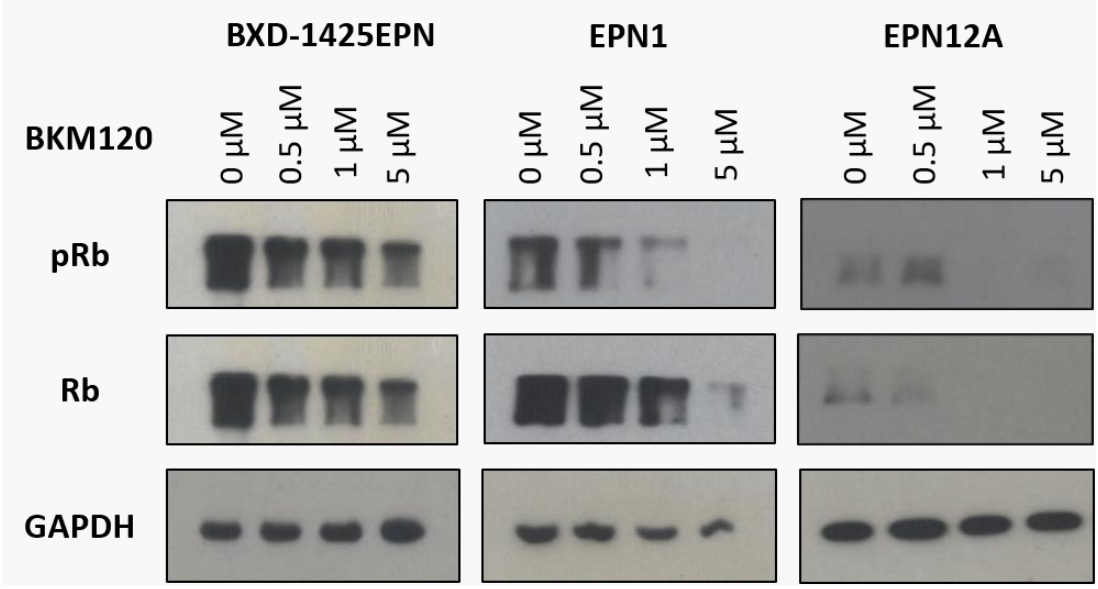


Figure 5-4 Immunoblotting of phosphorylated Rb showed a decrease in levels across the panel of tested ependymoma cell lines following a 24-hour incubation with BKM120. Probing against total protein levels of Rb also showed decrease in a dose-dependent manner. Experiments were representative of at least two biological repeats.

5.2.4 Investigation of E2F1 transcription as a downstream effector of PI3K signalling

The reduction in Rb phoshorylation increases its binding to the E2F1 transcription factor which minimises its activity and expression of target genes. Since BKM120 reduced Rb phosphorylation in ependymoma, it was investigated whether BKM120 subsequently reduced E2F1-mediated gene expression.

5.2.4.1 Transient transfection through Nucleofection™ was superior over Lipofectamine™-based approaches in ependymoma cells

Elucidation of E2F1 activity in ependymoma was performed through luciferase reporter assays using BXD-1425EPN cells. This involves cellular transfection of reporter constructs containing the luciferase gene sequence under the influence of an E2F promoter. To ensure a successful execution of the assays, two different transfection approaches were compared to identify the method with the best transfection efficiency: lipid-based (Lipofectamine™) or electroporation (Nucleofection™). First, GFP constructs were transfected into the cells using Lipofectamine™. During optimisation, various experimental factors were tested which are summarised on Table 1. Cells were visualised under brightfield and GFP-filtered modes before superimposing these images. GFP-expressing cells were manually counted alongside the total number of cells imaged to determine the transfection efficiency (Figures 5-5 – 5-7). Results showed that the best transfection efficiencies were achieved by transfecting 1 µg of plasmid DNA using either 0.75 or 1.5 µl of Lipofectamine™ reagent with a 24 hour incubation period at a seeding density of 80,000 – 100,000 cells per well (~30%) (Table 5-1). Next, GFP constructs were transfected using Nucleofection™ (Figure 5-8). Four different programs were tested in combination with L- and V-Solution (Table 5-2). Flow cytometry analysis demonstrated that the best transfection efficiency was achieved with the X-001 program and L-solution (72.5%). Propidium iodide staining for the same condition also showed high cell viability 89.7%) after Nucleofection™ (Figure 5-9). Therefore, Nucleofection™ using L-solution and the X-001 program was selected for downstream experiments.

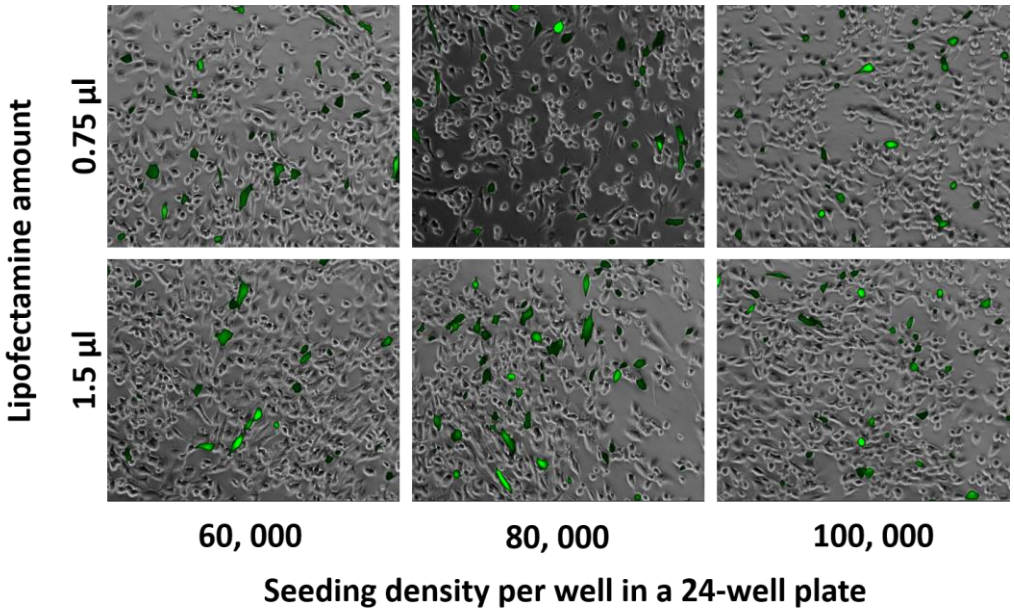


Figure 5-5 Transfection efficiency of 500 ng DNA incubated for 24 hours in BXD-1425EPN cells. 0.75 and 1.5 µL of Lipofectamine™ was used to transfect GFP constructs in three different seeding densities. GFP images were overlaid on brightfield images and cells were manually counted using ImageJ to determine transfection efficiencies.

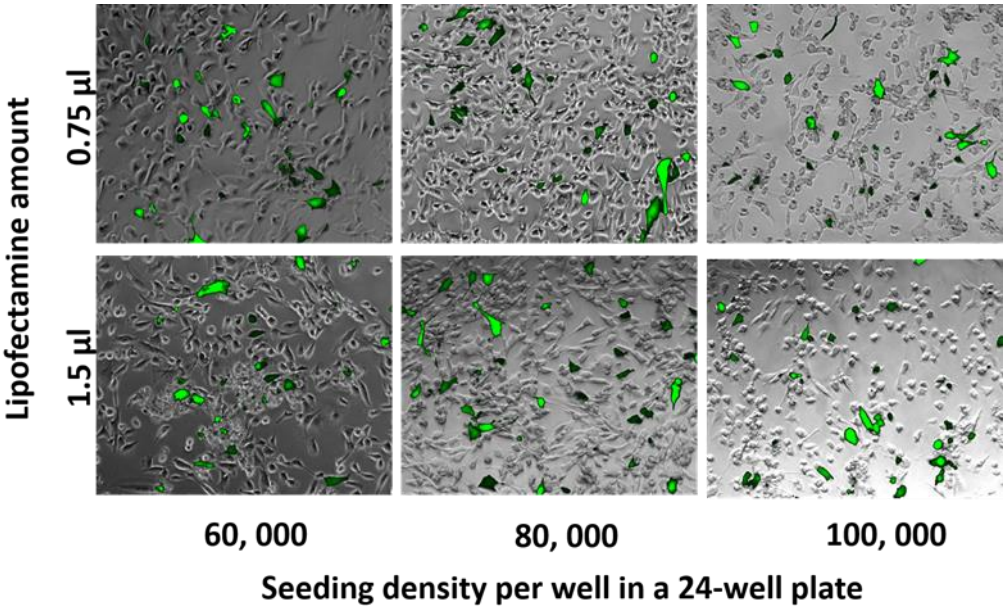


Figure 5-6 Transfection efficiency of 500 ng DNA incubated for 48 hours in BXD-1425EPN cells. 0.75 and 1.5 µL of Lipofectamine™ was used to transfect GFP constructs in three different seeding densities. Cells that were positive for GFP expression and the total number of cells were determined manually using ImageJ to calculate transfection efficiencies.

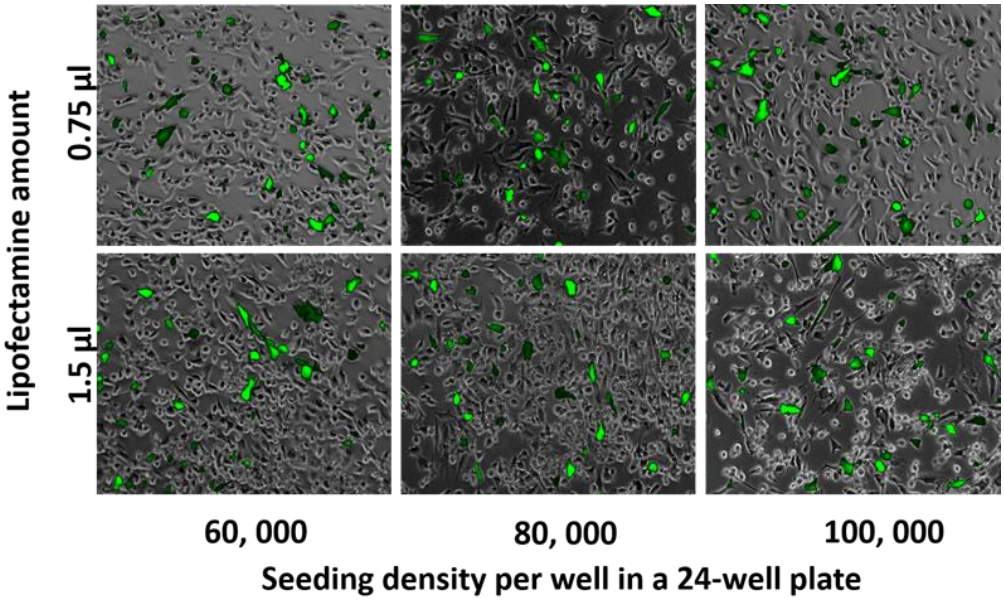


Figure 5-7 Transfection efficiency of 1 µg DNA incubated for 24 hours in BXD-1425EPN cells. 0.75 and 1.5 µL of Lipofectamine™ was used to transfect GFP constructs in three different seeding densities. Cells that were positive for GFP expression and the total number of cells were determined manually using ImageJ to calculate transfection efficitencies.

Table 5-1 Summary of transfection efficiencies of Lipofectamine™-mediated transfection of GFP plasmid constructs in BXD-1425EPN cells using various optimisation conditions.

Conditions	Cell count	Lipofectamine™ amount (µL)	Transfection efficiency (%)
500 ng of plasmid DNA; 24 hour incubation	60 000	0.75	10.86
		1.5	7.89
	80 000	0.75	10
		1.5	18.18
	100 000	0.75	9.69
		1.5	13.58
500 ng of plasmid DNA; 48 hour incubation	60 000	0.75	12.62
		1.5	11.98
	80 000	0.75	16.33
		1.5	10.94
	100 000	0.75	11.18
		1.5	8.25
1 µg of plasmid DNA; 24 hour incubation	60 000	0.75	22.03
		1.5	27.01
	80 000	0.75	27.78
		1.5	30.11
	100 000	0.75	22.12
		1.5	28.84

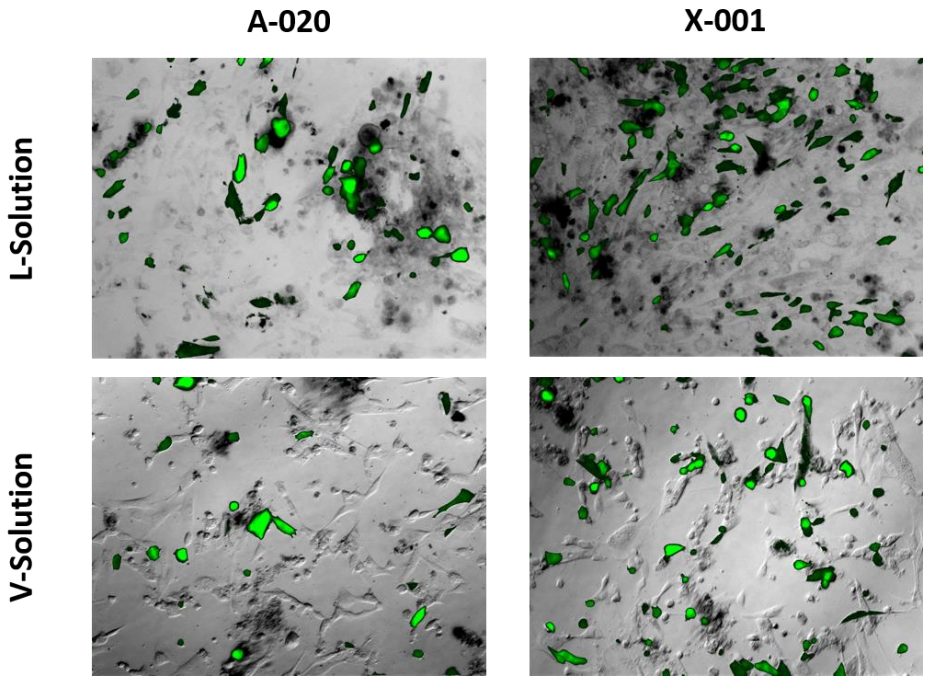


Figure 5-8 Fluorescence imaging of BXD1425-EPN cells transfected with pmaxGFP constructs using Nucleofection™ to determine conditions with optimal efficiency. Images were not taken for the T-020 and T-030 programs due to low cell tolerance leading to almost 100% mortality. Viable BXD-1425EPN cells were available for imaging with the A-020 and X-001 programs in combination with the L- and V-Solution.

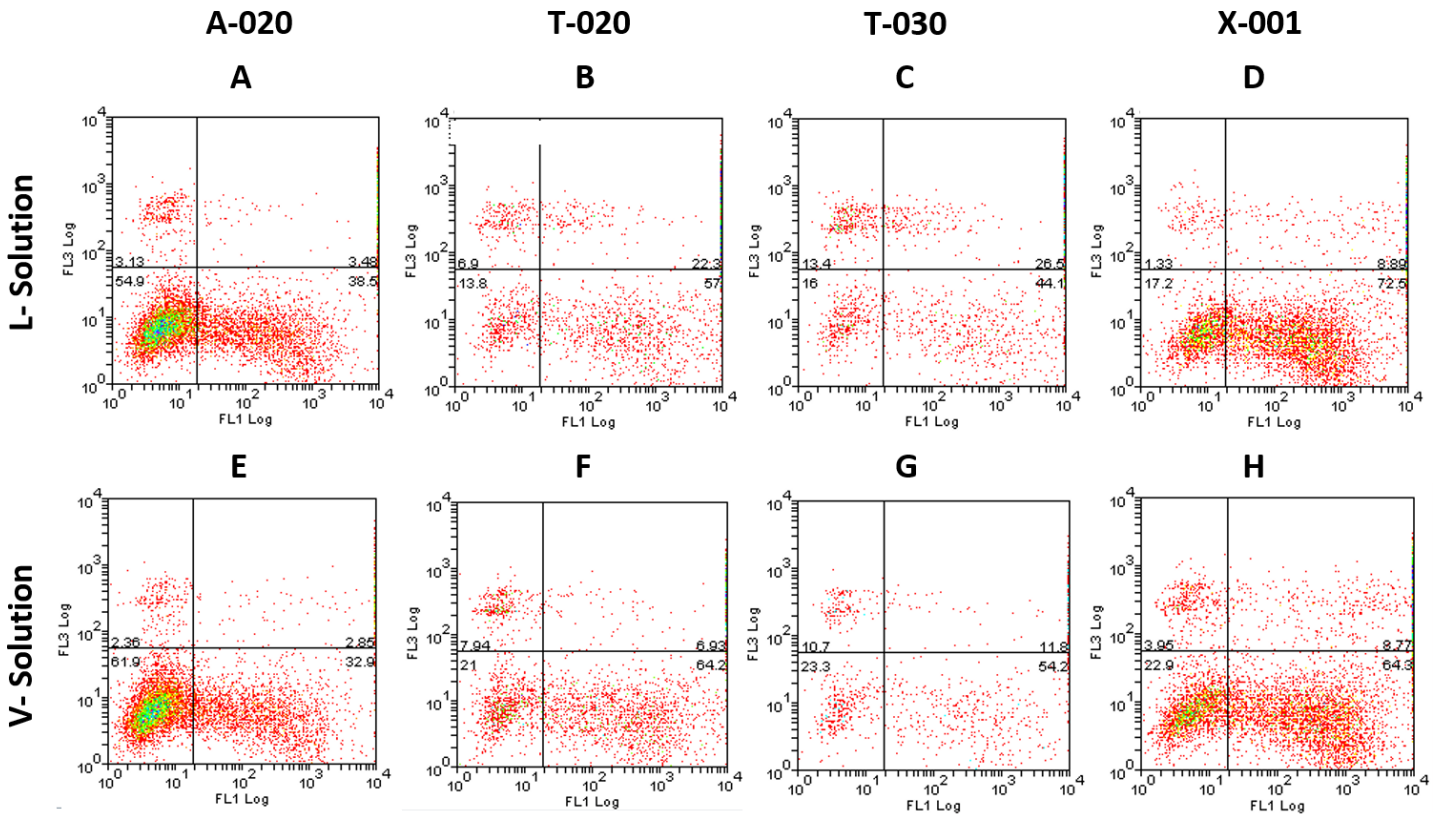


Figure 5-9 Flow cytometry analysis of propidium iodide stained BXD-1425EPN cells transfected with pmaxGFP constructs using Nucleofection™. Analysis for GFP expression and propidium iodide staining simultaneously determined the transfection efficiency as well as the viability post-Nucleofection™. The Nucleofection™ programs tested in combination with L- or V-solution were A-020, T-020, T-030 and X-001. The x-axis represents the level of GFP expression and the y-axis relates to degree of propidium iodide staining. Therefore, the bottom right quadrant in each result represents transfected viable cells. The percentage of cells detected per quadrant is indicated. The highest transfection efficiency was achieved using L-solution and the X-001 program.

Table 5-2 A summary of the flow cytometry analysis of propidium iodide-stained BXD-1425EPN cells transfected with pmaxGFP constructs using Nucleofection™. Results indicate the cell viability and transfection efficiency of each solution-Nucleofector™ program combination used during optimisation.

Solution	Program	Viable Cells (%)	Transfection efficiency (%)
L-Solution	A-020	93.4	38.5
	T-020	70.8	57.0
	T-030	60.1	44.1
	X-001	89.7	72.5
V-Solution	A-020	94.8	32.9
	T-020	85.2	64.2
	T-030	77.5	54.2
	X-001	87.2	64.3

5.2.4.2 Treatment with BKM120 did not significantly reduce E2F-mediated transcriptional activity in BXD-1425EPN cells

In order to test the hypothesis that cell cycle arrest in ependymoma was associated with loss of E2F1 transcription following PI3K inhibition, reporter constructs encoding for the firefly luciferase protein under the influence of an E2F promoter were transfected into BXD-1425EPN cells followed by treatment with BKM120 for 24 hours. Experimental controls included luciferase constructs with either a non-inducible minimal promoter or a constitutively expressing firefly luciferase. Luminescence reading at the end of the incubation for the positive control showed an approximately 13-fold increase in luciferase activity relative to the negative control, suggesting that transfection via Nucleofection™ was a feasible approach for these experiments (Figure 5-10A). Treatment of transfected cells with BKM120 showed a dose-dependent decrease in luciferase activity relative to the vehicle control but this change was found to be statistically insignificant ($p=0.31$) (Figure 5-10B). These results showed no conclusive evidence to attribute loss of E2F1 activity with cell cycle arrest in ependymoma. It would be worth repeating these experiments in other ependymoma cell lines to see if significant data could be obtained.

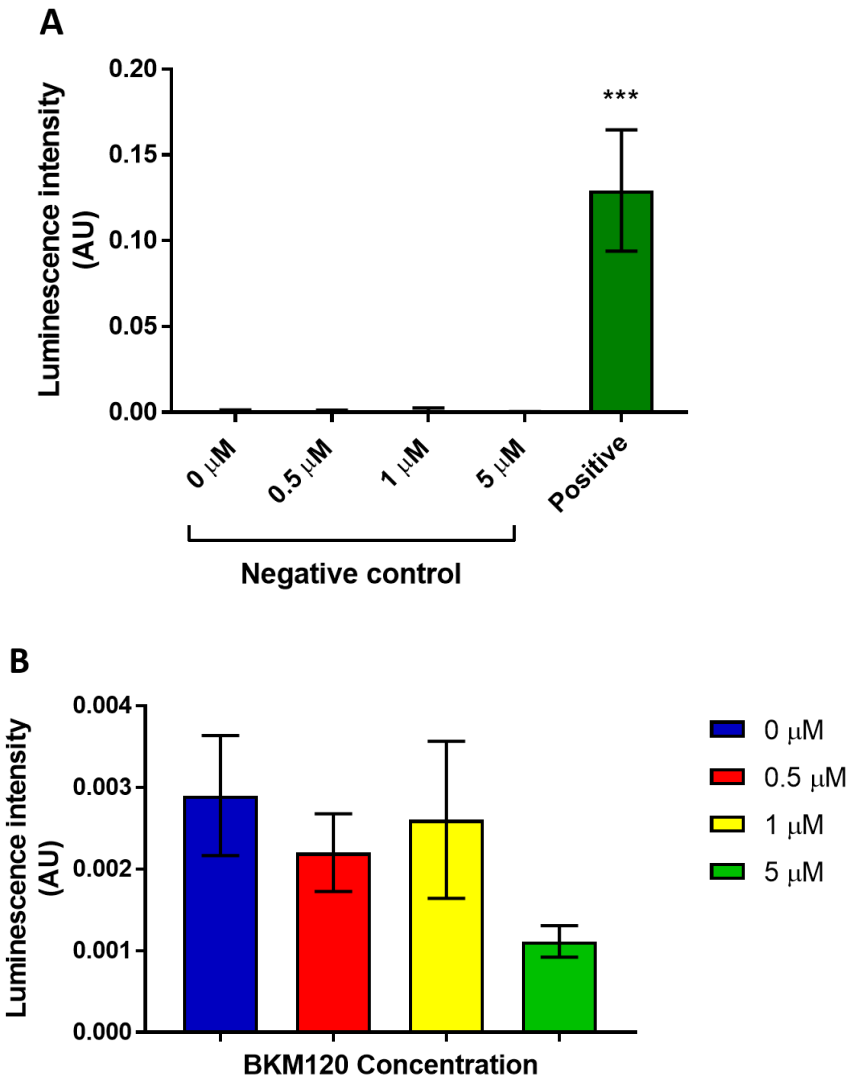


Figure 5-10 (A) Nucleofection™-mediated transfection of a constitutively expressing firefly luciferase (positive) construct in BXD1425-EPN cells showed a significant ~13-fold increase in luminescence arbitrary units (AU) compared to those transfected with a non-inducible minimal promoter (negative) construct (***p<0.001). (B) Transfection of BXD-1425EPN cells with E2F luciferase reporter constructs and treated with various BKM120 concentrations. No significant difference in luciferase reporter activity was found between untreated and BKM120 treated cells. Data was presented with the standard error of the mean and analysed using one-way ANOVA (n=3).

5.2.5 Identifying the potential value of combining PI3K inhibition with conventional chemotherapeutic drugs

Activation of the PI3K pathway is considered to be a significant contributing factor towards acquisition of resistance to conventional chemotherapy in cancer (West, Castillo et al. 2002, Brown, Toker 2015). Microarray analysis of BKM120-treated ependymoma cells has shown a downregulation of biological processes which have been previously related to a decrease in chemotherapeutic efficiency in other cancer studies. Therefore,

it was hypothesised that inhibition of the PI3K pathway would enhance the effects of conventional chemotherapies in ependymoma. This work would give an indication whether combining anti-cancer agents with PI3K pathway inhibition would be a more therapeutically beneficial approach in managing ependymomas.

The effects of combining BKM120 with paclitaxel, cisplatin and gemcitabine on ependymoma cell viability were investigated. These agents were selected based on the fact that certain cellular processes, found to be reduced by PI3K inhibition in ependymoma cells, can influence their efficiency. For these drug treatments, BXD-1425EPN and EPN12A cells were used. The IC_{50} for each drug was initially determined for each cell line using MTT viability assays. Combination experiments used a fixed ratio of the two drugs based on the calculated IC_{50} concentrations.

5.2.5.1 Investigating the effects of BKM120 and paclitaxel combination treatment in ependymoma

Paclitaxel is a microtubule stabilising agent that prevents depolymerisation causing inhibition of processes such as chromosome segregation and cytokinesis, which are often followed by the activation of spindle attachment checkpoints (Long, B. H., Fairchild 1994). It has been shown that the PI3K signalling pathway stimulates biological functions related to G_2/M transition which were previously suggested to overcome these checkpoints thus resulting in inefficient outcomes to paclitaxel treatments(Anand, Penrhyn-Lowe et al. 2003). Therefore, it was put forward that PI3K pathway inhibition could enhance the effects of paclitaxel treatments in ependymoma through the negative regulation of G_2/M processes.

BXD1425-EPN and EPN12A cells were treated with paclitaxel for 72 hours to determine an IC_{50} value for each, which were 42.16 nM and 14.8 nM, respectively (Figure 5-11A and 5-11B). These cells were then co-treated with BKM120 and paclitaxel at fixed concentration ratios based on their respective IC_{50} values for 72 hours followed by a MTT assay. To determine whether there was a significant difference in the cell viability trends between BKM120/paclitaxel combination and BKM120 or paclitaxel single treatments, a two-way ANOVA was performed. Analysis of the interaction between the inhibition curves of the different treatment conditions showed no significant difference in BXD-1425EPN cells ($p=0.06$). This was especially manifested by the BKM120/paclitaxel combination which showed a similar inhibitory profile as the BKM120 only treatment, suggesting that both treatments are equally effective in inducing an anti-proliferative effect in these cells (Figure 5-11C). In contrast to BXD-1425EPN cells, there was some variability in the inhibition curves between the BKM120/paclitaxel co-treatment and single treatment of

either BKM120 or paclitaxel with the EPN12A cells. Indeed, an overall significant interaction was found in EPN12A cells between BKM120/paclitaxel combination treatments relative to both BKM120 and paclitaxel single treatments (**p<0.01) (Figure 5-11D). A post-hoc Tukey's multiple comparisons test was performed to analyse if the overall significant interaction observed in EPN12A cells were due to actual significant differences arising from the individual comparison of the single BKM120 or paclitaxel treatments with the BKM120/paclitaxel co-treatment. These analyses showed that while there was a significant difference in the inhibition profile between BKM120 only and BKM120/paclitaxel treatment (*p<0.05), this was not found between paclitaxel only and BKM120/paclitaxel treatment (p=0.11). This suggests that the inhibitory effects of paclitaxel and BKM120/paclitaxel co-treatments on EPN12A cell viability were similar. Therefore, it is argued that combining BKM120 with paclitaxel conferred no significant therapeutic benefits relative to single treatments of paclitaxel in ependymoma.

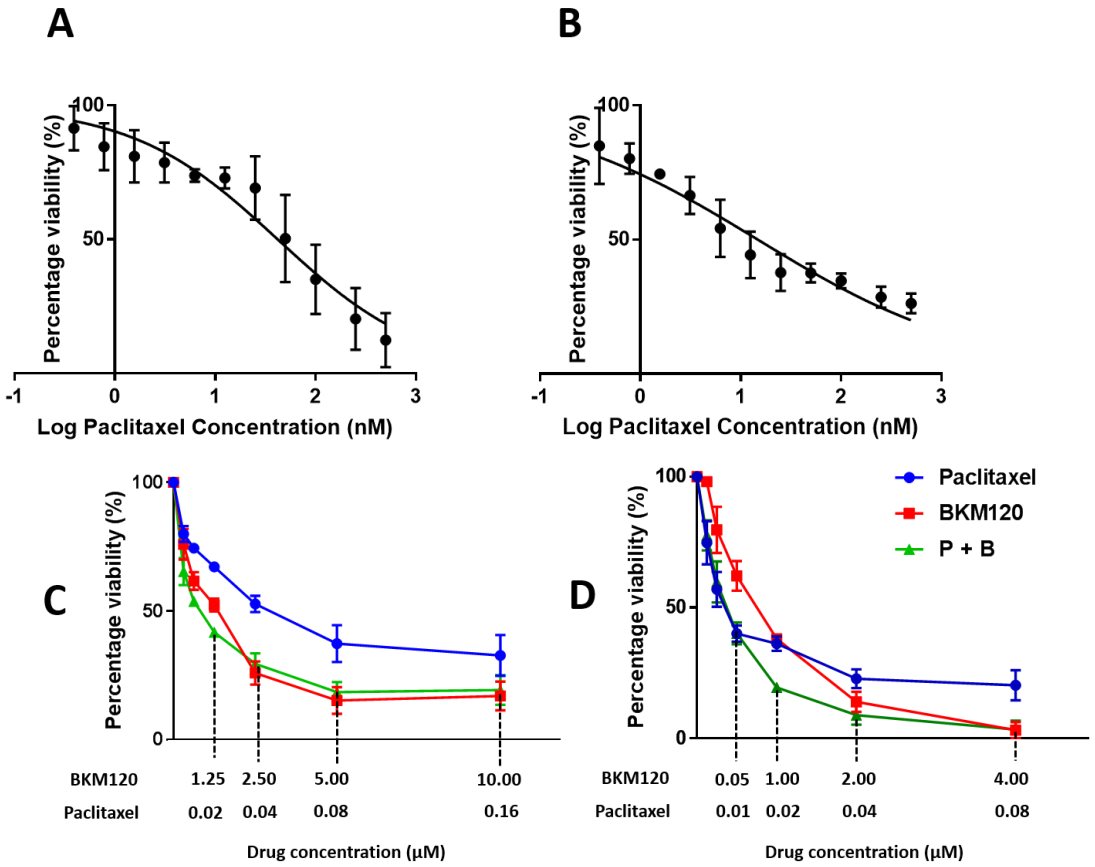


Figure 5-11 IC_{50} values of paclitaxel for (A) BXD1425-EPN and (B) EPN12A cells were determined using non-linear regression analysis. Paclitaxel concentrations were presented as their Log_{10} function. 72 hour MTT assay results for the BKM120 and paclitaxel single treatments, and BKM120/paclitaxel combination (P + B) in (C) BXD1425-EPN and (D) EPN12A cells showed no significant difference between the cell viability trends in all treatment conditions as determined using a two-way (post-hoc) ANOVA analysis.

5.2.5.2 Investigating the effects of BKM120 and cisplatin combination treatment in ependymoma

Cisplatin is a DNA-damaging agent that causes genomic lesions particularly DNA-DNA or DNA-protein cross-linkages (Eastman 1990), which would consequently instigate cell death responses. Circumvention of the effects of cisplatin usually involves the activation of multiple DNA repair systems in the cell that recruit an array of repair proteins to restore the integrity of the genome. Survival pathways including the PI3K pathway are fundamental towards stimulating this cascade of events, which arguably denies cisplatin from inducing its optimal therapeutic effect in many cancers (Sinnberg, Lasithiotakis et al. 2009, Zhang, Y., Bao et al. 2016). Analysis of the gene expression data from the previous chapter has shown an enrichment for DNA repair responses in the significant DEGs identified following PI3K inhibition. It was therefore hypothesised that PI3K pathway inhibition would lead to impairment of DNA repair pathways in ependymoma which would induce hypersensitivity to DNA damaging agents and consequently favour cell death responses due to genomic catastrophe(Chirnomas, Taniguchi et al. 2006, Michels, Vitale et al. 2013).

Similar to the paclitaxel experiment, IC_{50} values for cisplatin treatment were also obtained for BXD-1425EPN and EPN12A cells: 40.07 nM and 1.89 nM, respectively (Figure 5-12A and 5-12B). A two-way ANOVA showed that the cell viability trend of the BKM120/cisplatin combination did not significantly differ to that of the individual cisplatin or BKM120 treatments in BXD-1425EPN cells, suggesting that the overall cellular responses to either single or combination treatments were similar ($p=0.38$) (Figure 5-12C). In contrast, treatment of EPN12A cells with BKM120/cisplatin showed a significant difference in the overall cell viability profiles of the three treatment conditions (**$p<0.01$) (Figure 5-12D). Post-hoc tests indicated that this was due to a significant difference in viability reduction of BKM120/cisplatin combination treatments compared to cisplatin alone (***$p<0.001$). However, no significant difference was found between BKM120 only and combination treatments ($p=0.06$), suggesting no overall benefit from the combination.

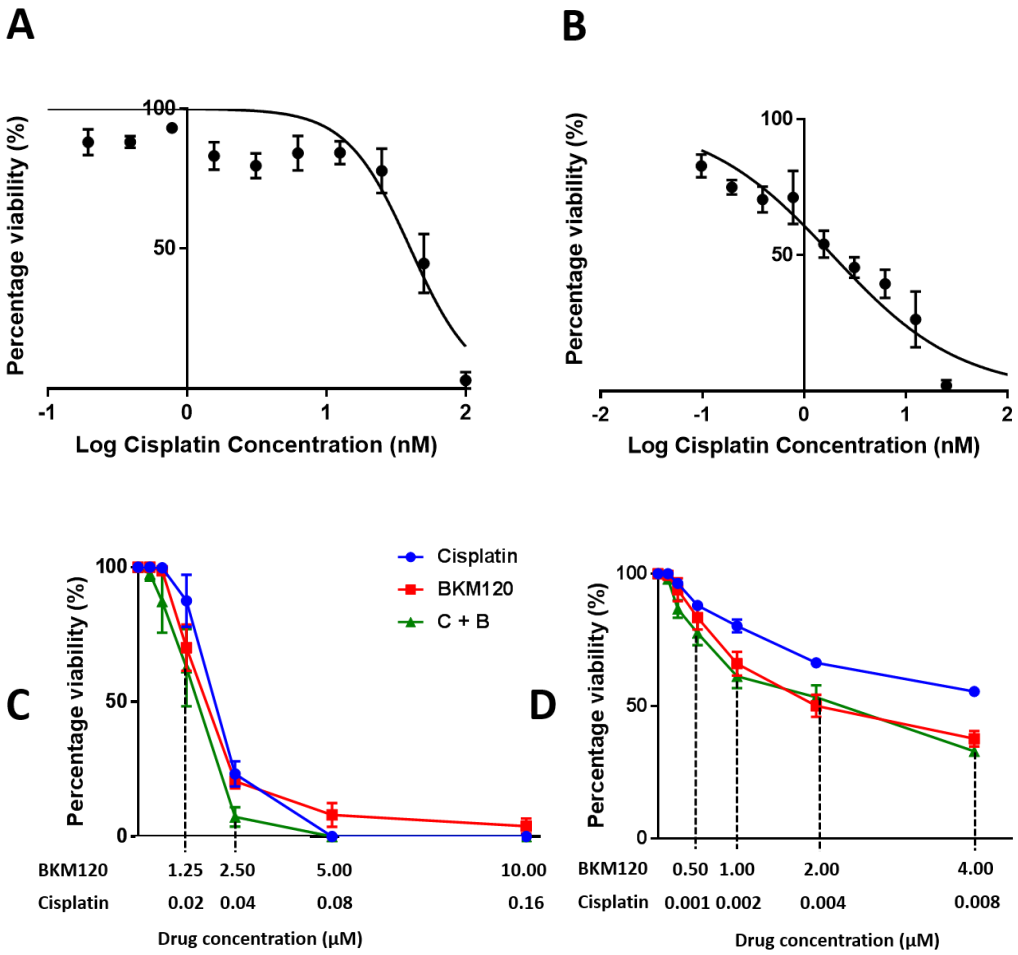


Figure 5-12 IC_{50} values of cisplatin were determined for (A) BXD1425-EPN and (B) EPN12A. (C) BXD-1425EPN and (D) EPN12A cells were treated with combined BKM120/cisplatin (C + B) and BKM120 or cisplatin only for 72 hours followed by a MTT viability assay. Analysis using a two-way (post hoc) ANOVA test showed no significant difference between the combination and single treatment conditions in both BXD-1425EPN and EPN12A cells.

5.2.5.3 Investigating the effects of BKM120 and gemcitabine combination treatment in ependymoma

Gemcitabine (2'-2'-difluorodeoxycytidine, dFdC) principally serves as a nucleoside analogue that gets modified through triphosphorylation (dFdCTP) to effectively mimic cytidine. Its integration into the nascent DNA structure enables addition of another base before halting polymerisation (masked chain termination) (Plunkett, Huang et al. 1995), which increases genomic errors that would trigger cell death in a manner akin to cisplatin. Apart from potential resistance mechanisms arising from activation of DNA repair pathways, it was also proposed that cancers could circumvent the effects of gemcitabine through the establishment as well as stabilisation of stalled replication forks (Karnitz, Flatten et al. 2005, Bryant, Elias et al. 2015). Initiation of DNA replication was also one of the downregulated processes identified from post-

transcriptomic analysis, which in conjunction with loss of DNA repair systems, would putatively confer sensitivity towards gemcitabine.

A 50% reduction in cell viability post-gemcitabine treatment was only observed with EPN12A cells, with a calculated IC_{50} of 136.6 nM (Fig. 5-13A). A two-way ANOVA showed an overall significant difference in cell viability trends between all the treatment conditions performed in these cells (***$p<0.001$) (Fig. 5-13B). Post-hoc tests also confirmed that there was a significant difference between BKM120/gemcitabine co-treatments and both BKM120 (***$p<0.001$) and gemcitabine (***$p<0.001$) only treatments. According to their inhibitory profiles on Fig. 13B, this significant difference was suggestive of the combination treatment being more effective compared to either BKM120 or gemcitabine alone. In order to elucidate the effect of this combination, analysis of the drug interaction using the Chou-Talalay method was performed (Chou 2010). Results indicated that intermediate combined effective doses of BKM120/gemcitabine (0.2875 – 1.15 μM) were synergistic (Table 5-3) as indicated by the combination index (CI) of 0.3 – 0.7 (see section 2.3.6). However, this effect was lost when the cells were treated with either the highest or lowest combined effective drug concentration of BKM120/gemcitabine since the CI was 0.9 – 1.2, implying an additive to slight antagonistic effects. Since co-treating BKM120 with gemcitabine displayed comparable tumour suppressive potencies as increasing the doses of BKM120, it is then put forward that the theapeutic benefits of BKM120/gemcitabine combinations may potentially be achieved if intermediate doses of BKM120 and gemcitabine were considered due to their synergistic interaction. Treatment of other ependymoma cell lines with BKM120 and gemcitabine is necessary to ascertain if such biological effects are consistently maintained.

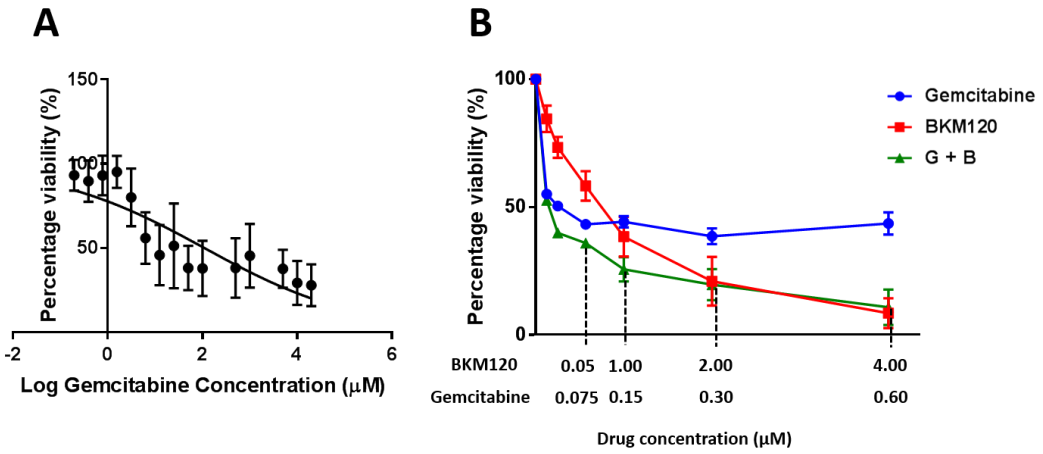


Figure 5-13 (A) EPN12A cells were treated with various gemcitabine concentrations for 72 hours to determine its IC_{50} using non-linear regression analysis. (B) The inhibition curve of the gemcitabine/BKM120 co-treatments (G + B) was compared to that of gemcitabine or BKM120 only treatment, where an overall significant interaction was found between the cell viability trends of various treatment condition. Statistical analysis was performed using a two-way (post-hoc) ANOVA test.

Table 5-3 Chou-Talalay analysis of BKM120/gemcitabine combination treatment in EPN12A cells. Data shows the CI values for the actual experimental doses used in the experiments. (**Key:** **Fa=** the inhibitory effect on cell viability in response to a particular effective drug concentration; **CI=** the interaction and overall effect of the drugs used in a combination; **** =** combined effective doses which produced a synergistic effect).

BKM120 (μM)	Gemcitabine (μM)	Total dose (μM)	Fa	CI
0.125	0.01875	0.1438	0.47	1.5201
0.250	0.03750	0.2875**	0.60	0.3520
0.500	0.07500	0.5750**	0.64	0.5331
1.000	0.15000	1.1500**	0.74	0.6621
2.000	0.30000	2.3000	0.80	0.9884
4.000	0.60000	4.6000	0.89	1.0881

5.3 Discussion

This chapter provided experimental data to validate the findings obtained from the previous transcriptomic analysis of PI3K-inhibited ependymoma cells. Two functional aspects were the prime focus of this work. The first was to elucidate a molecular mechanism that could be attributed to the instigation of cell cycle arrest in ependymoma following BKM120 treatment. The second involved exploring whether downregulation of cellular responses that would confer resistance to conventional chemotherapy following PI3K pathway inhibition would sensitise cells to the effects of common anti-cancer drugs.

This effectively highlights whether implementation of this approach holds a potential treatment benefit in ependymoma.

In this chapter, it was investigated whether the FOXO/Rb/E2F1 signalling axis in response to treatment with BKM120 mediates cell cycle arrest in ependymoma. It was demonstrated that BKM120 treatment only reduced FOXO1 phosphorylation but not FOXO3. However, FOXO1 inhibition did not increase ependymoma cell viability which suggests that there are other mediators of cell cycle arrest that are independent from FOXO1 acitivty. There was also a reduction in phospho-Rb levels following BKM120 treatment but its ability to suppress E2F1 transcription remains undetermined as no significant difference in the E2F-induced luciferase output was observed between drug treated and vehicle treated cells. Currently, more experimental evidence is required to support the role of the FOXO/Rb/E2F1 signalling axis as instigators of cell cycle arrest in ependymoma after inhibiting the PI3K pathway. Finally, combining BKM120 with gemcitabine, but not paclitaxel or cisplatin, showed synergistic effects highlighting a potential benefit for treating these tumours.

5.3.1 The role of FOXOs in ependymoma cell cycle arrest

It was hypothesised that BKM120-mediated inhibition of the PI3K pathway leads to the activation of FOXO proteins in ependymoma, which are known regulators of cell cycle arrest. This project specifically focused on FOXO1 and FOXO3, whose shared high sequence homology (Wang, M., Zhang et al. 2009) has shown a well-documented involvement in cell cycle arrest (Schmidt, Fernandez de Mattos et al. 2002b). Western blot analysis indicated that BKM120 treatment of ependymoma cells only decreased phosphorylation of FOXO1 but not FOXO3, denoting that FOXO1 was more likely to be targeted by PI3K signalling than FOXO3 in ependymoma. If the activation of FOXO1 played a crucial role in promoting ependymoma cell cycle arrest, its inhibition would therefore rescue proliferation and viability post-BKM120 treatment. However, this was not the case as there were similar cell viability trends between the combined BKM120/FOXO1 inhibitor AS1842856 treatment and BKM120 mono-treatments.

FOXO1 is a known suppressor of tumourigenesis including several CNS cancers (Lau, Koty et al. 2009, Srivastava, Yasruel et al. 2009, Tang, Liu et al. 2016). However, results showed that the induction of cell cycle arrest in ependymoma in response to BKM120 may not necessarily depend on the activity of FOXO proteins which implicates alternative mechanisms in this process. For instance, another downstream target of PI3K/AKT signalling is GSK3β. Phosphorylation by AKT inhibits GSK3β from mediating the degradation of β-catenin (see section 1.3.3.2) whose transcriptional targets, which

include *CCND1*, are also involved in cell cycle progression. Another study also demonstrated the involvement of the mTOR targets p70S6 kinase and eIF4E during cell cycle progression, with which an arrest was observed as a result of mTOR signalling loss (Fingar, Richardson et al. 2004). It was also proposed that the C/EBP transcription factors were instigators of cell cycle arrest by maintaining a phosphorylated state, usually through the PI3K pathway in conjunction with the inhibition of PP2A phosphatases (Wang, H., Iakova et al. 2001, Johnson, P. F. 2005). Moreover, it is known that various pathway crosstalks could underlie non-AKT mechanisms of FOXO negative regulation. Kinases such as SGK and PKA can also recognise several consensus peptide sequences in various clusters of phosphorylation sites on FOXO proteins (Tzivion, Dobson et al. 2011) while MAPK has been implicated as a co-factor for FOXO protein regulation (Yang, J. Y., Zong et al. 2008, Roy, Srivastava et al. 2010). In this study, activation of FOXO1 due to inhibition of PI3K/AKT signalling may lead to these kinases serving as a surrogate to re-phosphorylate and consequently inactivate FOXO1. This would essentially rescue the decrease in cell viability that was induced by the treatment of BKM120. Since this was not the case, it further supports the argument that there are separate mechanisms independent from FOXO1 activity that may have been at work in promoting cell cycle arrest in ependymoma.

AS1842856 only inhibits FOXO1 when it is in its dephosphorylated state (Zou, Liu et al. 2014). According to the western blot analysis, AS1842856 could have exerted its effects on FOXO1 after treating ependymoma cells with BKM120 for one hour since FOXO1 was already found to be active under these conditions. However, the effects of AS1842856 were analysed for 72 hours as performed in a standard MTT assay set-up in this project. While BKM120 could inhibit ependymoma cell viability for as long as 72 hours, it is not known whether AS1842856 could reverse the effects of BKM120 and sustain it for such a long period. Studies which employed AS1842856 in their experiments for various purposes involved incubation periods between 72-96 hours (Tan, P., Guan et al. 2015, Buttrick, Wang et al. 2018), suggesting that the drug could be stable long-term. If AS1842856 did not degrade during the duration of the MTT assay then it is put forward that it did not have the capacity to counteract the effects of BKM120-mediated PI3K pathway inhibition. Therefore, it is possible that any potential rescue in viability may have occurred earlier than the 72 hour endpoint and this could have been overlooked.

Moreover, only the roles of FOXO1 and FOXO3 in inducing cell cycle arrest were investigated in this thesis. Other FOXO members including FOXO4 and FOXO6, also possess the phosphorylation motif necessary to be regulated by AKT and are thought to participate in tumour suppression (Schmidt, Fernandez de Mattos et al. 2002c, Jacobs,

van der Heide et al. 2003). Inclusion of these FOXO proteins should therefore be considered in future work.

5.3.2 The involvement of the Rb/E2F1 pathway in ependymoma cell cycle arrest

Post-transcriptomic analysis of BKM120-treated ependymoma cells identified a downregulation of cell cycle related genes that are normally regulated by E2F1. It was hypothesised that PI3K pathway inhibition causes ependymoma cell cycle arrest through the consequent hypophosphorylation of Rb which physically sequesters E2F1 to inhibit its transcriptional activity. The result of the formation of Rb/E2F1 complexes induces cell cycle arrest usually in the G_1/S phase (Martelli, Livingston 1999). Western blot analysis indicated a dose-dependent decrease in phospho-Rb levels, following treatment with BKM120, which is typical in cells undergoing arrest. It was also found that BKM120 treatment of ependymoma cells caused a decrease in total Rb protein levels, which was shown to be an effect when cells become arrested at the G_1/S phase (Liu, Korc 2012, Vijayaraghavan, Karakas et al. 2017). From this, it could be suggested that perhaps during G_1/S arrest in ependymoma following PI3K inhibition, Rb becomes hypophosphorylated where it physically binds to E2F1 to prevent transcription of genes. At the same time, any unbound Rb proteins may have been subjected to degradation following loss of CDK4/6 functioning through an unknown mechanism. However, transfection of luciferase reporter constructs under the influence of an E2F promoter in BXD-1425EPN cells showed no significant difference in reporter activity between the vehicle control and BKM120 treated cells. This implies that BKM120-induced hypophosphorylation of Rb did not reduce the transcriptional output of E2F1, which argues that an alternative mechanism independent of the Rb/E2F1 pathway is involved in inducing ependymoma cell cycle arrest.

In this study, a non-specific E2F reporter promoter was used for the luciferase assays which means that it could also detect the activity from other E2F members. This is particularly relevant with E2F4 and E2F6 which were also identified in the post-microarray analysis as regulators of several cell cycle genes (see section 4.2.4). E2F4 and E2F6 are known repressors of gene expression (Christensen, Cloos et al. 2005, Dimova, Dyson 2005). Interestingly, E2F4 requires binding to hypophosphorylated Rb proteins to form a transcriptional repressor complex whereas E2F6 activity is not affected by Rb proteins as these do not bind to each other (Hsu, Sage 2016). With the inhibition of PI3K signalling, both E2F4 and E2F6 may be recruited to E2F binding sites to suppress gene expression, especially those that are essential for regulating cell cycle and this should consequently reflect as a decrease in luciferase reporter activity. Having shown a

non-significant difference in the luciferase output between vehicle and BKM120 treatment, it indicates that E2F4 and E2F6 may also not be associated with regulating cell cycle progression in ependymoma. This further supports the involvement of other mechanisms that do not constitute the activity of both Rb and E2F in promoting the cytostatic effects of treating with BKM120

It is also suggested that the lack of inhibition of E2F1-mediated transcription in response to BKM120 treatment could be due to the activation of an alternative E2F1 transcriptional program. This was highlighted in several studies (Hallstrom, Mori et al. 2008, Shats, Gatza et al. 2013) where E2F1 upregulates a subset of genes, which are otherwise silenced in the presence of a growth signal particularly through the PI3K pathway. Expression of these genes usually confers an anti-tumourigenic effect which supports the role of E2F1 as a tumour suppressor, in a context-dependent manner (Jacks, Fazeli et al. 1992, Field, Tsai et al. 1996). Therefore, it is possible that E2F1 transcriptional activity could still be present even after inhibiting the PI3K pathway in ependymoma. While the aforementioned mechanisms mainly concerned apoptotic cell death outcomes which are contrary to the findings of this project, this does not necessarily imply that no E2F1 transcription has taken place in ependymoma despite treatment of BKM120. This mechanism could therefore underlie the non-significant reduction in luciferase reporter activity in ependymoma cells even after treatment with BKM120. The limitation in accepting this model is that the transcriptomic data presented no indications of a discrete set of (upregulated) E2F1 genes that would suppress survival and viability. If an alternative E2F1 transcriptional program did exist in the absence of a survival signal, it implies that E2F1 was indeed free instead of being physically bound to Rb under these conditions. Therefore, repression of cell cycle genes may not necessarily be exclusive to the formation of Rb/E2F1 complexes but through various molecular mechanisms that would alter E2F1's common transcriptional patterns (Harbour, Dean 2000, McNair, Xu et al. 2018).

So far, further functional work is required to verify if the formation of the Rb/E2F1 complex is linked to the induction of ependymoma cell cycle arrest. There is evidence that BKM120 resulted in hypophosphorylation of Rb proteins but whether this consequently leads to a downregulation of cell cycle gene expression remains elusive. To prove this mechanism, it is necessary to investigate whether there is physical binding between Rb and E2F1, and if this prevents the latter from binding to promoter sequences which would signify potential loss of transcription. Future work should also expand from an E2F1-based analysis in elucidating the events leading to cell cycle arrest. Further studies to

understand the roles of the E2F4 and E2F6 repressor proteins could be a prospect to characterise the downstream effects of blocking the PI3K pathway in ependymoma.

5.3.3 PI3K pathway inhibition as part of a combination therapy in ependymoma

Given that PI3K signalling contributes towards resistance mechanisms, several cancer studies have focused on elucidating PI3K pathway-associated mechanisms that negate the effects of many chemotherapeutic agents (West, Castillo et al. 2002, Brown, Toker 2015). Based on the microarray analysis, several biological processes which were previously associated with conferring resistance to various pharmacological agents were found to be downregulated in ependymoma following inhibition of the PI3K pathway. These included DNA repair pathways (Sakthivel, Hariharan 2017) and G_2/M related functions such as microtubule treadmilling, spindle formation and kinetochore functioning (Anand, Penrhyn-Lowe et al. 2003, Spankuch, Kurunci-Csacsko et al. 2007, Li, Z., Dai et al. 2016). Based on these results, this project investigated whether inhibition of the PI3K pathway could enhance the tumour suppressive effects of paclitaxel, cisplatin or gemcitabine treatment in ependymoma cells.

5.3.3.1 PI3K pathway inhibition in conjunction with either paclitaxel or cisplatin

It was found that combining BKM120 with either paclitaxel or cisplatin showed no significant difference in cell viability inhibition in both BXD-1425EPN and EPN12A cells compared to either BKM120 or chemotherapeutic drug treatment alone. In effect, the combination treatments produced similar biological responses as when the cells were exposed to single BKM120 or chemotherapeutic drug treatment. Therefore, this suggests that the aforementioned drug combinations produced no further therapeutic enhancement from the single drug conditions.

Some may argue that the inefficiency behind these treatment combinations in ependymoma cells could be related to the potent inhibitory effects of BKM120 in ependymoma. This was generally evident on the MTT assay data presented in which the inhibitory profile shown by the BKM120/chemotherapy combination was congruent to that of BKM120 alone. From this, it is put forward that most of the tumour suppressive effects originated from BKM120 treatment therefore addition of a second chemotherapeutic drug would have been futile. Nevertheless, this does not necessarily dismiss that PI3K pathway inhibition in combination with these drugs is a suitable strategy for treating ependymal tumours. Since it has been discussed previously that BKM120 may have off-target effects

on microtubule dynamics especially at the concentrations tested in these experiments, it is possible that the effective reduction in ependymoma cell viability could have originated from both PI3K pathway inhibition and aberrancies in microtubule polymerisation. If the objective was to investigate whether PI3K pathway inhibition could enhance the therapeutic effects of these chemotherapeutic drugs then BKM120 may not be an appropriate constituent of the tested combination. A different approach would be to substitute BKM120 with an alternative PI3K pathway inhibitor in combination with either paclitaxel or cisplatin. Through this, other deleterious off-targeting that may arise from inhibitor-specific effects is minimised thus clarifying whether inhibition of the PI3K pathway accentuates the effect of paclitaxel and cisplatin. One caveat to this method is that if BKM120 did induce its effects through a separate mechanism that is independent from the canonical PI3K signalling pathway, there are no guarantees that similar effects would be recapitulated using different PI3K pathway inhibitors.

Clinical studies involving administration of paclitaxel or cisplatin in ependymoma patients have mainly shown modest effects with outcomes ranging from partial responses to disease stabilization (Hurwitz, Strauss et al. 2001, Brandes, Cavallo et al. 2005, Lombardi, Pambuku et al. 2013). The inefficient patient responses to these treatments could arguably be attributed to drug resistance whose mechanism is largely unknown. This study's assumption was that if ependymomas did display resistance to these chemotherapeutic drugs, activation of the PI3K pathway might possibly underlie this therapeutic phenotype in tumours as described in other cancers. The MTT assay results showed that single treatment of ependymoma cells with either paclitaxel or cisplatin effectively decreased viability within a clinically relevant, nanomolar range (Fogli, Danesi et al. 2001, Kim, R., Osaki et al. 2001, Rajkumar, Mathew et al. 2016). This data suggests the ependymoma cells used in this study were actually sensitive to single treatments of paclitaxel or cisplatin and co-treatment with BKM120 displayed no further augmentation of tumour suppressive effects. Therefore, the PI3K pathway may not be associated with a potential resistance mechanism to these chemotherapeutic drugs in ependymoma. Targeting the PI3K pathway would then be a separate treatment approach and considering its combination with either paclitaxel or cisplatin is less likely to be advocated as an effective treatment strategy in ependymoma.

Another explanation for the MTT assay results of co-treating BKM120 with either paclitaxel or cisplatin is the potential conflict of effects between the two agents being combined. BKM120 was already shown to inhibit cell cycle in the G_1/S phase therefore co-treating with any other cell cycle inhibitors is deemed redundant if the cells were already arrested. Interestingly, both paclitaxel and cisplatin induce their effects at later

phases of the cell cycle, which consequently leads to an arrest (Mueller, Schittenhelm et al. 2006, Choi, Yoo 2012, Cabrera, Gomez et al. 2015, Velma, Dasari et al. 2016) but this may be negated with an earlier arrest mediated by BKM120. One study has shown that PI3K pathway inhibition can reverse the cell cycle profile of several chemotherapeutic drugs including paclitaxel and cisplatin, so that a G_1/S phase arrest was more evident (Fekete, Santiskulvong et al. 2012). However, the relevance of this model with respect to the combination experiments in this study is yet to be elucidated. It is not known whether an overall arrest at G_1/S phase was produced in response to these BKM120 combination experiments and if this is responsible for preventing the synergy with both paclitaxel and cisplatin. Analysis of cell cycle profiles for all single and combination treatments could have provided a more detailed finding for the results obtained from the MTT assays. Through this, it could be determined if a single treatment of paclitaxel or cisplatin were already inducing a cytotoxic effect in ependymoma and whether more cell death could be produced by co-treating with BKM120.

It is interesting that there was a lack of synergy behind the combination of BKM120 with either paclitaxel or cisplatin in ependymoma considering the vast studies that alluded to the pre-clinical efficiency of these treatments (Xu, Li et al. 2011, Du, Wu et al. 2013, Cai, Tan et al. 2014, Zhang, Y., Bao et al. 2016). Many of these studies have indicated the activation of the PI3K pathway as a significant biomarker for resistance to paclitaxel and cisplatin treatments in cancers. In one clinical study involving patients with metastatic breast cancer, PI3K inhibition with paclitaxel treatments yielded some promising patient outcomes (Sharma, Abramson et al. 2018). Three clinical studies (NCT02439489, NCT02113878, NCT02194049) have also investigated the therapeutic prospect of cisplatin and BKM120 against a broad spectrum of solid malignancies with their results yet to be disclosed. While there is clinical data to suggest that ependymomas may possibly confer resistance to paclitaxel and cisplatin, decreasing the cellular responses which could limit the efficiency of these drugs through PI3K pathway inhibition, resulted in no observable significant therapeutic benefits. At present, the involvement of the PI3K pathway as a resistance mechanism towards paclitaxel and cisplatin in ependymoma remains inconclusive.

5.3.3.2 PI3K pathway inhibition in conjunction with gemcitabine

Drug interaction analysis of the BKM120/gemcitabine co-treatment in EPN12A cells showed a synergistic effect thus suggesting potential therapeutic benefits in ependymoma. This was highlighted on the MTT assay which showed that while gemcitabine alone significantly reduced the viability of EPN12A cells, its inhibitory profile was enhanced when combined with BKM120 as indicated by the significant shift in the

inhibition curve. However, this result was not repeated in BXD-1425EPN cells emphasising the use of further cell lines to determine how widespread this effect would be.

Unlike paclitaxel and cisplatin, these results indicated that the PI3K pathway could have prevented gemcitabine from inducing an optimal tumour suppressive response in ependymoma. One prospective benefit from the BKM120/gemcitabine combination is that these findings have clinical relevance considering that the tested gemcitabine concentrations in these experiments were also within peak plasma ranges (Delauter, Ramanathan et al. 2000, Fogli, Danesi et al. 2001). Indeed several findings have already substantiated the synergistic effects of PI3K pathway inhibition with gemcitabine in various *in vitro* cancer models (Kagawa, Takano et al. 2012, Jung, Yan et al. 2014, Yang, X. L., Lin et al. 2014). A potential mechanism that could explain this drug synergism in ependymoma is the lack of an efficient DNA repair system that could revert the detrimental effects of gemcitabine. According to one study on pancreatic cancer, upregulation of DNA repair genes is responsible for the inefficient responses to gemcitabine (Mathews, Cabarcas et al. 2011). Subsequently, it has been described that increased activity of DNA repair proteins serves as a significant contributing factor towards a chemoresistant phenotype in ependymoma (Ferguson, Zhou et al. 2017). According to the gene expression analysis, inhibition of the PI3K pathway resulted in a downregulation of DNA repair responses in ependymomas. Therefore, eliminating the signalling input from the PI3K pathway would have essentially made the cells more susceptible to the genotoxic effects of gemcitabine as highlighted by the aforementioned studies.

Apart from its genotoxic effect, gemcitabine also serves as an anti-metabolite by inhibiting thymidylate synthase (TYMS) (Honeywell, Ruiz van Haperen et al. 2015) which catalyses the formation of thymidine. TYMS expression was found to be reduced by BKM120 based on the microarray analysis (see appendix 9). It is possible that while BKM120 decreases *TYMS* expression, any residual enzymatic activity would be inhibited by gemcitabine. Therefore, combining PI3K pathway inhibition with gemcitabine would consequently lead to a deregulation in nucleotide levels. This would hinder the creation of nascent DNA molecules, which would stimulate cells to undergo cell death (Juvekar, Hu et al. 2016). However, this model, which could explain the synergy of the BKM120/gemcitabine combination in ependymoma, remains speculative. Nevertheless, it would also be an interesting endeavour to investigate whether PI3K pathway inhibition could enhance the effects of other anti-metabolites in ependymoma. For instance, combination tests could be performed with 5-FU, a known TYMS inhibitor, which is not a

clinically approved treatment for ependymoma but has shown potential in pre-clinical screening (Atkinson, Shelat et al. 2011).

Although, one may also question the extent of the synergistic effects produced by the combined treatment of BKM120 and gemcitabine. Based on the MTT assay, it was shown that treating the cells with around 2 μM BKM120 started to show a similar viability as when it was co-treated with gemcitabine. This suggests that further increases in BKM120 concentration would just be as efficient as when it is combined with gemcitabine thus essentially losing the therapeutic benefits of this combination. Therefore, it is imperative to delineate if a combined treatment of BKM120/gemcitabine is still a better therapeutic approach relative to treating with a higher concentration of BKM120. One possible way to address this is to determine the toxicity that would be produced in each treatment strategy through conducting cell death assays or elucidating the proportion of dead cells by cell cycle analysis.

Despite no reported human-based trials that investigated gemcitabine as a treatment approach for ependymoma, gemcitabine has shown potency in mouse models of supratentorial ependymomas with a particular sensitivity to those that harbour the *RELA* fusion gene (Boulos, Kim et al. 2016). This prospectively supports the benefit of gemcitabine in ependymoma. However, whether its therapeutic success could still be maintained when translated to a more clinical setting is yet to be discerned. Historically, no chemotherapy has been shown to have a significant benefit for ependymoma patients. Therefore, it is possible that administration of gemcitabine as part of ependymoma treatment may also result in sub-optimal responses in recipients. In this study, a potential therapeutic tactic was highlighted in anticipation of a possible resistance towards gemcitabine in ependymoma by incorporating PI3K pathway inhibitors. However, a limitation to this drug combination study is the lack of evidence from other cell lines which could substantiate its therapeutic prospect in ependymoma. Testing this combination would ideally be carried out on additional posterior fossa ependymoma cell lines to establish any consistency in results. By expanding the analysis to supratentorial ependymoma cell lines, evidence could be provided regarding the efficiency of this combination treatment across tumours arising from the different intracranial compartments.

5.3.4 Conclusion

The findings presented in this chapter aimed to elucidate a putative molecular mechanism for the arrest in ependymoma cell cycle in response to BKM120 and evaluate

the therapeutic potential of combining PI3K pathway inhibition with common anti-cancer agents in ependymoma. It was proposed that cell cycle arrest following BKM120 treatment is mediated by FOXO activation and the consequent binding of Rb to E2F1 which downregulates transcription of cell cycle-related genes. This study showed that FOXO1, but not FOXO3, is a direct downstream target of the PI3K pathway but it may not only be the facilitator of cell cycle arrest since its pharmacological inhibition did not cause an increase in cell viability. Suppressing PI3K signalling reduced Rb phosphorylation but no significant effect on E2F-mediated luciferase reporter activity was shown, which highlights the potential involvement of non-Rb/E2F1 mechanisms in inducing ependymoma cell cycle arrest. Further functional studies are necessary to validate whether the FOXO/Rb/E2F1 model is a relevant mechanism towards the induction of cell cycle arrest in ependymoma. Moreover, synergism was observed when BKM120 was combined with gemcitabine, but not paclitaxel or cisplatin, which signified its therapeutic prospect in ependymoma. However, further data is required from other cell lines to conclusively determine whether these drug combinations produce clinical utility in treating ependymoma.

5.4 Summary of chapter findings

- Loss of phosphorylation of FOXO1 but not FOXO3 was observed across all tested ependymoma cell lines after BKM120 treatment, which suggests that its activity is directly regulated by the PI3K pathway in ependymoma.

- Inhibition of FOXO1 with AS1842856 was not enough to rescue cell viability in BKM120-treated cells, implicating the activity of other mechanisms in inducing cell cycle arrest in ependymoma.

- Loss of Rb phosphorylation was also observed in response to BKM120 treatment, but there was also a dose-dependent reduction in total Rb protein levels. Hypophosphorylated Rb in PI3K-inhibited ependymoma cells could be indicative of E2F1 sequestration and loss of transcriptional activity.

- BKM120 treatment showed no significant decrease in the E2F-mediated luciferase reporter activity, which implicates a separate mechanism for promoting cell cycle arrest that is not related to the Rb/E2F1 activity. Additional repeats may be required to determine significance between treatment conditions according to retrospective statistical analysis.

- Combining BKM120 with gemcitabine, but not paclitaxel and cisplatin, showed potential synergistic effects in one ependymoma cell line (EPN12A). Further data on other cell lines is necessary to conclusively define the benefits of this combination in ependymoma.

CHAPTER 6. FINAL DISCUSSION AND FUTURE WORK

This project followed on the work that was introduced by Rogers, Mayne et al. (2013) on investigating the underlying biology of paediatric ependymomas using the PI3K pathway as a molecular basis. In this study, the following research questions were addressed:

1.) How does the PI3K pathway regulate survival in ependymoma?
    - Employment of several ependymoma cell lines to determine whether inhibition of the PI3K pathway resulted in a decrease in cell viability
    - Instigation of functional experiments to elucidate whether the decrease in cell viability was associated with cytotoxic or cytostatic responses to PI3K pathway inhibition
    - Functional elucidation of the PI3K/AKT signalling node, rather than other non-canonical effectors, as the principal driver of the observed cellular responses in ependymoma

2.) What are the downstream targets of the PI3K pathway that may play a role in disease pathogenesis?
    - Analysis of whole transciptomic profile of ependymoma cells to evaluate changes in gene expression post-PI3K pathway inhibition
    - Gene ontology analysis to elucidate molecular processes that were affected by PI3K pathway inhibition
    - Elucidation of a molecular mechanism that would link the PI3K pathway to the regulation of the identified biological functions
    - Isolation of potential PI3K pathway downstream nodes that are of pharmacological interest

3.) Can these proposed PI3K pathway mechanisms be experimentally validated and what are their clinical implications?
    - Perform a series of functional assays to support whether the suggested molecular mechanisms have a regulatory role towards these enriched cellular processes
    - Investigation of treatment combinations between PI3K inhibitor and chemotherapy drugs predicted to work together from transcriptomic data

Overall, the findings in this study have demonstrated that targeting the PI3K pathway in ependymoma using BKM120 led to a decrease in cell viability at

concentrations observed in patient plasma post-treatment, suggesting there is therapeutic potential in targeting the pathway in these tumours. However, BKM120 treatment showed no induction of cell death responses but cell cycle arrest was demonstrated instead, highlighting the cytostatic effect of inhibiting PI3K signalling in ependymoma. It was postulated that the underlying cell cycle arrest mechanism was mediated by FOXO proteins and the formation of the Rb/E2F1 complex but the experimental data so far has not supported this hypothesis. BKM120 treatment of ependymoma cells also resulted in a downregulation of processes that may contribute to tumourigenesis including DNA damage responses and various G_2/M-related functions. Co-treating BKM120 with gemcitabine, but not cisplatin or paclitaxel, indicated an enhanced cellular response to the chemotherapy thus suggesting its utility as an effective treatment combination. Finally, elucidation of the role of AKT as a primary effector of the pathway is yet to be accomplished in order to support the conclusion that these experimental observations in ependymoma were mediated by the activation of the canonical PI3K signalling.

6.1 PI3K pathway inhibition – a therapeutic prospect

Deciphering the molecular biology of paediatric ependymomas enables a better understanding of the enigmatic pathological behaviour of these tumours. The PI3K signalling pathway, whose implication in the progression of many malignancies is well documented, was put forward as a crucial regulator of ependymoma tumourigenesis, having identified its activation in a high percentage of primary tumours (Rogers, Mayne et al. 2013). This was further supported by the identification of its prognostic role in which its activation correlated with a poor progression free survival. It was then highlighted that suppression of the PI3K pathway produces an anti-tumourigenic effect that could then be exploited as a potential therapeutic approach. This specifically addresses the lack of effective treatment modalities in ependymoma which arises from the general resistant nature that these tumours confer towards conventional chemotherapy. In this study, the pan-Class I PI3K enzyme inhibitor BKM120 (Buparlisib) was exploited as the primary tool in inhibiting the PI3K pathway in ependymoma cells. BKM120 is considered as one of the most clinically advanced agents that target the PI3K pathway. It has displayed tumour suppressive effects against various cancer models (Koul, Fu et al. 2012, Speranza, Nowicki et al. 2016, Yang, S., Li et al. 2017) and is currently being assessed in human-based trials either as a monotherapy or part of a combination (Vansteenkiste, Canon et al. 2015, Armstrong, A. J., Halabi et al. 2017, Zhao, H. F., Wang et al. 2017). Its particular ability to penetrate the blood-brain barrier (Maira, Pecchi et al. 2012) also indicates its suitability as a chemotherapeutic candidate for treating CNS tumours, including ependymoma.

BKM120-mediated inhibition of PI3K signalling led to a significant reduction in viability of cell lines derived from both supratentorial and posterior fossa ependymoma at concentrations that are clinically achievable (Bendell, Rodon et al. 2012a). Interestingly, posterior fossa ependymoma cell lines showed a significantly increased sensitivity towards the inhibitory effects of BKM120 relative to the supratentorial cell lines. This is despite the pathway being active in a significantly higher percentage of supratentorial tumours in comparison to tumours from the other CNS regions (Rogers, Mayne et al. 2013). It was put forward that this difference could be associated with the unique molecular profiles that constitute the current ependymoma tumour classification system (Pajtler, Witt et al. 2015). However, the fact that both supratentorial and posterior fossa ependymoma cells were responsive to suppression of PI3K signalling suggests that it holds therapeutic promise across different patient cases.

The clinical implication of this work is further highlighted as one may argue that PI3K pathway inhibition could be employed to treat *C11orf95/RELA* fusion-positive supratentorial as well as posterior fossa group A tumours (PF-EPN-A), which both display a poor patient prognosis. This notion is conveyed on the basis that all the tested supratentorial ependymoma cell lines harboured this fusion gene whereas at least one of the posterior fossa ependymoma cell lines were classified under the PF-EPN-A subgroup. Targeting the PI3K pathway is especially advantageous in younger cohorts should radiotherapy be delayed in favour of chemotherapy. From a clinical point of view, activation of the PI3K pathway could also be used to stratify patients according to their prognosis and potential therapeutic outcome which would help improve disease management.

In this project, treatment of ependymoma cells with BKM120 induced cytostatic rather than cytotoxic effects. An arrest was predominantly found in the G_1/S phase of the cell cycle, which supported previously documented findings of inhibiting the PI3K pathway in other cancers (Fekete, Santiskulvong et al. 2012, Dan, Okamura et al. 2012). This suggests that PI3K pathway inhibition is only suitable for disease stabilisation rather than as a first-line of therapy and its use would be better as part of a treatment combination. Whether there are other PI3K pathway directed agents that are superior over BKM120 at potently inhibiting ependymoma tumourigenesis is yet to be elucidated. Indeed, there are several agents developed that target different nodes of the PI3K pathway, as outlined in section 1.5, which could be used for future investigations. Testing a number of PI3K pathway inhibitors would determine whether the cellular responses observed following BKM120 treatment could be recapitulated thus attributing therapeutic effects which are specific to the PI3K pathway. Arguably, this would even potentially ascertain the most

suitable class of pathway inhibitors that could be used to treat ependymomas. Therefore, this considers the notion of personalised medicine which remains a desirable aim in the current approach towards clinical management of cancers.

6.1.1 The role of canonical PI3K/AKT signalling in ependymoma

Despite BKM120's demonstrable potential as a treatment option against ependymomas due to the clinically relevant range of concentrations used, one limitation associated with this drug is its reported off-target effects on microtubule dynamics (Brachmann, Kleylein-Sohn et al. 2012). This was particularly induced at concentrations above 1 μM, which is an issue considering most of the tested concentrations in this project were above this off-target threshold. Since the project's aim was to elucidate the pathological role of the PI3K pathway in paediatric ependymoma, treatment of cells with BKM120 could be a disadvantage, as the resulting tumour suppressive effects would be confounded by microtubule instability. As suggested in the previous chapters, one way to ascertain BKM120's off-target effects is to assay microtubule treadmilling with the same concentrations used to treat ependymoma cells in this study. Alternatively, it would also be ideal to consider other inhibitors of the pathway which possess minimal off-target effects. In this project, the effects of AKT inhibitors in ependymoma were also investigated.

Several studies have alluded to the pathological relevance of AKT in ependymomas including the involvement of *AKT2* as a novel ependymoma oncogene (Mohankumar, Currle et al. 2015) and *AKT3* whose expression may impact tumourigenesis due to its association with super enhancers (Mack, Pajtler et al. 2018). Targeting AKT then presents an alternative method to BKM120 in inhibiting the PI3K signalling pathway due to its role as a downstream effector that propagates signals to its substrates to support cell survival and viability. It also enables the investigation of whether the biological effects displayed in ependymoma in response to BKM120 treatment were actually mediated by canonical PI3K/AKT signalling. However, treatment of ependymoma cells with either an allosteric (perifosine) or ATP-competitive AKT inhibitor (GDC-0068) did not reduce the cell viability. From this, two possible conclusions were emphasised: either ependymomas confer resistance towards AKT inhibitors or the biological effects observed in ependymoma so far is mediated through the activation of a non-canonical PI3K signalling cascade.

There is a possibility that these cells are intrinsically resistant to the effects of AKT inhibition since immunoblot analysis of pAKT levels post-treatment showed that the drugs were active. Loss of efficiency of AKT inhibitors could be associated with several PI3K

pathway feedback loops that are often stimulated in response to pharmacological treatment, resulting in the reactivation of the cascade. One particular example was demonstrated by Chandarlapaty, Sawai et al. (2011) in which loss of AKT activity promoted an upregulation of RTK expression which would hyperactivate multiple signalling pathways including the PI3K pathway. Clinical evaluation of AKT inhibitors in treating a variety of CNS tumours has insinuated a potential resistance to these agents due to the modest patient outcomes (Becher, Millard et al. 2017) despite displaying pre-clinical efficiency against a broad range of cancers. If ependymoma cells did confer resistance towards AKT inhibitors, then this further indicates the inadequacy of monotherapeutically targeting the PI3K pathway in ependymoma as a treatment option. However, future work may include the elucidation of resistance mechanisms to these inhibitors in order to enhance the cellular sensitivity towards these agents. For instance, concurrent targeting of RTK and AKT could be examined if RTK upregulation was found to be a contributing factor towards inefficacies of AKT inhibitors.

Some may argue that BKM120-mediated inhibition of the PI3K pathway is more effective than AKT inhibitors since abrogating PI3K activity would essentially affect more downstream targets due to its position as the primary regulator in the cascade series. However, this global effect produced by PI3K inhibition in ependymoma raises the question of whether a separate signalling pathway that is unrelated to AKT was deactivated which ultimately results in cell viability reduction. Other known effectors of downstream PI3K signalling which promote cell survival in a non-canonical manner are SGK and BTK kinases (Park, Leong et al. 1999, Qiu, Kung 2000). It is reasoned that if the conventional AKT signalling was not involved in propagating the PI3K cascade downstream then PI3K/AKT axis could not be considered as an alternative therapeutic target in ependymoma. A proposed follow up work could be done which would functionally investigate these candidate non-AKT effectors of PI3K signalling. This would involve analysing their phospho-status in response to BKM120 treatment and if inhibiting these kinases confers tumour suppressive effects in ependymoma.

Enhancement or complete elimination of AKT activity have been suggested as a prospective strategy to elucidate if canonical PI3K signalling is associated with supporting the biological responses shown in ependymoma. Two methods whose optimisations were initiated in this study could be continued in future investigations regarding this aspect of the study:

- siRNA-mediated knockdown of AKT isoforms

- transfection of plasmid constructs which either express a dominant negative AKT that would negate the activity of its wild-type counterpart or a constitutively active AKT that would reduce the effects of upstream inhibition of the pathway

6.1.2 Inhibiting the PI3K pathway in ependymoma: tipping the balance towards cell death

6.1.2.1 The involvement of autophagy

This study has already demonstrated that inhibition of the PI3K pathway through BKM120 treatment in ependymoma did not stimulate cell death responses. Therefore, improving the utility of PI3K pathway suppression in treating ependymomas requires searching for potential drugs that could be combined which would drive these tumours to undergo cell death.

One possibility which could account for the lack of apoptotic cell death in ependymoma following BKM120 treatment is due to a failure to establish the molecular machinery that instigate these processes. The absence of apoptotic responses was particularly highlighted in GBM (Lefranc, Brotchi et al. 2005), however this originates from mutations or alterations in several apoptotic components which were not previously implicated in ependymoma. This study only looked at one apoptotic parameter, cleaved caspase-3, but this did not necessarily demonstrate whether ependymomas harbour a malfunction along the apoptotic pathway. It is then argued that apoptosis may have been blocked downstream of the PI3K pathway following BKM120 treatment through an unknown mechanism. One may infer that autophagy may have interfered with the induction of apoptotic cell death in ependymoma, as functionally demonstrated in other studies (Zhou, Y., Sun et al. 2014, Yang, P., Ling et al. 2018). This study has shown that treatment of ependymoma cells with BKM120 activated autophagy, which could provide the basis to support this hypothesis.

The fact that the evidence obtained throughout the progress of this study has highlighted that no cell death resulted from inhibiting the PI3K pathway suggests that autophagy could not have produced any cytotoxic effects in ependymoma. Instead, a more protective mechanism which encourages ependymoma cell survival may be associated with the activation of autophagy as mentioned above. The MTT assay consisting of BKM120/CQ co-treatments may not have demonstrated this but it would have been essential to take the analysis further. For instance, there was an insignificant difference in the cell viability trend between BKM120 only and BKM120/CQ co-treatment of ependymoma cells. While the single BKM120 treatment resulted in ependymoma cell

cycle arrest, no cell death followed which could be due to the induction of autophagic responses. When autophagy was blocked through CQ co-treatment, cytoprotection was eliminated thus stimulating cell death. This could not have been determined using MTT assay as a sole basis since the overall reduction in viability did not change but the mechanism at which this has taken place instead. Cell death assays or even probing for cleaved caspase-3 proteins of BKM120/CQ-treated cells could be undertaken to give further evidence that would address this hypothesis. Through these, it could be clarified if autophagy could rationally be targeted in conjunction with PI3K pathway inhibition to produce cell death thus proposing its potential for treating ependymoma. If proven to be contributory towards survival, one would argue that inhibiting autophagy could circumvent a putative resistance mechanism to PI3K pathway inhibition in ependymoma.

6.1.2.2 Combination with TRAIL ligands

Tumor necrosis factor-related apoptosis-inducing ligands (TRAIL) belongs to the tumour necrosis factor (TNF) family of ligands which could stimulate apoptotic cell death programme through the activation of the extrinsic pathway (Ashkenazi 2002). TRAIL activates the death receptors DR4 and DR5 which leads to receptor trimerisation and consequent activation of caspase-8 and caspase-10. These initiator caspases, in turn, activate caspase-3 which instigates the cleavage of several key cellular proteins leading to cell death. TRAIL-mediated activation of the extrinsic pathway of apoptosis has been shown to effectively promote cell death in cancers relative to normal cells, which makes it an attractive therapeutic approach for the treatment of several malignancies (Zhang, X. D., Franco et al. 1999). The non-specific effects of TRAIL towards normal cells could be attributed to their expression of decoy receptors, which could also bind TRAIL but not induce apoptosis, while cancers show a deficiency in these receptors (Gura 1997). Pre-clinical studies have shown that inhibition of the PI3K pathway could synergise with TRAIL-mediated apoptosis in cancers such as lung cancer (Kandasamy, Srivastava 2002), leukaemia (Tazzari, Tabellini et al. 2008) and neuroblastoma (Opel, Naumann et al. 2011). Several mechanisms have been suggested to explain this synergy including the enhanced cleavage of the pro-apoptotic protein Bid which instigates the intrinsic apoptotic pathway by increasing the permeability of the outer mitochondrial membrane (see section 1.3.3.7) (Green 2000, Opel, Naumann et al. 2011). Another one is through the downregulation of the NF-κB pathway, in response to PI3K inhibition, whose targets include FLIP and XIAP which negatively regulate apoptosis (Ravi, Bedi 2002, Opel, Naumann et al. 2011). Therefore, combining PI3K inhibition with TRAIL may also have therapeutic benefits in ependymoma in that there is a possibility of inducing a more cytotoxic rather than a cytostatic outcome.

6.2 The PI3K signalling network and identification of other suitable co-targets in treating ependymoma

Employment of microarray technology in this study has generated a global and unbiased analysis of the downstream effects following inhibition of the PI3K pathway. Through the analysis of the whole ependymoma transcriptome, cellular processes within the PI3K signalling network were identified which may account for tumour survival and viability. The data obtained from these analyses has also been instrumental towards identifying potential drug combinations that could synergise with PI3K pathway inhibitors, which were then either investigated in this study or considered as part of future project directions.

6.2.1 The synergy behind gemcitabine and PI3K pathway inhibition in ependymoma

GO analysis of the ependymoma DEGs obtained in the transcriptomic work has identified DNA damage repair as a significant biological enrichment, whose genes were downregulated suggesting loss of such responses post-BKM120 treatment. Previous studies have shown that an augmented DNA repair system conferred resistance to DNA damaging agents including cisplatin and gemcitabine. PI3K signalling was shown to be an underlying molecular contributor to this resistance so that its inhibition enhanced the effects of these drugs in several pre-clinical studies (Wong, Ma et al. 2015, Zhang, Y., Bao et al. 2016). In ependymoma, it was hypothesised that PI3K pathway inhibition could enhance the sensitivity of cells to these conventional chemotherapeutic agents. Interestingly, a significant synergistic effect was only found in this study when BKM120 was combined with gemcitabine. Despite the capacity of both cisplatin and gemcitabine to introduce genomic lesions, their modes of action are different which implies that gemcitabine may have been more superior at synergising with the effects of BKM120-mediated inhibition of the PI3K pathway than cisplatin.

Several mechanisms have been put forward to explain the synergy observed with combining BKM120 and gemcitabine in ependymoma. These include the downregulation of DNA repair proteins which have been contributory to the chemoresistant nature of these tumours (Ferguson, Zhou et al. 2017) and the production of an imbalanced nucleotide reservoir that would hinder the creation of nascent DNA molecules, resulting in cell death (Honeywell, Ruiz van Haperen et al. 2015, Juvekar, Hu et al. 2016). While the effects of gemcitabine in ependymoma showed augmentation by co-treating with BKM120, it must be elicited the extent at which this treatment combination remains clinically relevant before it starts producing effects that are indifferent to BKM120

monotherapy. This was highlighted on the MTT assay where the BKM120/gemcitabine combination seemed to reduce cell viability as effectively as increasing the concentration of BKM120. Therefore, careful consideration must be observed in generalising these findings in all tumour cases especially when the data was also obtained from one cell line. Since these conclusions were drawn from analysis of the posterior fossa ependymoma cell line EPN12A, data from its supratentorial counterparts would be able to validate whether a synergistic effect could also be observed. This would substantiate the prospect of these treatments in managing ependymal tumours that develop from the two anatomically distinct intracranial compartments.

It was investigated in this project whether loss of DNA repair systems following PI3K pathway inhibition in ependymoma would enhance the effects of drugs that confer genotoxicity. So far, cisplatin and gemcitabine, whose mechanisms at producing genomic lesions differ, were tested in combination with BKM120. However, it would be interesting whether alternative genotoxic agents would also synergise with inhibiting PI3K signalling in ependymoma. For instance, the anti-metabolite 5-FU (fluorouracil) which shares a similar mechanism as gemcitabine has been shown to have potent anti-tumourigenic effects in ependymoma in a high-throughput drug screen (Atkinson, Shelat et al. 2011). Whether these have synergistic potential with inhibiting the PI3K pathway in ependymoma is subject to future investigation. Other classes of DNA damaging agents such as alkylating agents and topoisomerase inhibitors could also be considered in follow up studies. An example for each class is temozolomide (TMZ) and etoposide, respectively, which were shown to potently suppress tumourigenesis of *in vitro* cancer models in conjunction with PI3K pathway inhibition (Yu, H. G., Ai et al. 2008, Lai, Yeo et al. 2017, Shi, Guo et al. 2017, Haas, Klinger et al. 2018).

6.2.2 Potential targeting of gene functions in ependymoma that were upregulated following PI3K pathway inhibition

Biological enrichment of a small proportion of upregulated genes on the microarray has identified regulation of the MAPK pathway and reactivation of the PI3K pathway as significant cellular responses to BKM120 treatment. The cross-talk between these two pathways describes the classic compensatory mechanism in cancers (Mendoza, Er et al. 2011) thus often underlying the resistance to treatment with pathway inhibitors. In ependymoma, it is possible that the non-induction of cell death following inhibition of the PI3K pathway was attributed to the activation of the MAPK pathway which would provide the necessary mitogenic signals to support survival and viability. Moreover, the capacity of MAPK pathway to regulate various nodes of PI3K/AKT/mTOR signalling

axis could also diminish the tumour suppressive efficacy of some PI3K pathway directed agents. This is particularly applicable in *C11orf95/RELA* fusion positive supratentorial and PF-EPN-A subgroups where the MAPK signalling pathway was found to be upregulated (Pajtler, Witt et al. 2015). Therefore, combined PI3K/MAPK pathway inhibition in ependymoma could offer an improved approach at suppressing tumourigenesis through the circumvention of the inter-pathway compensation between these two signalling cascades. Indeed, several studies have already demonstrated that co-inhibition of both PI3K and MAPK signalling pathways induced potent anti-tumourigenic effects in various cancers (Lasithiotakis, Sinnberg et al. 2008, Muranen, Selfors et al. 2016, McNeill, Canoutas et al. 2017).

Gene expression analysis also indicated an increase in *PDGFRA* expression following BKM120 treatment which is capable of activating both PI3K and MAPK signalling cascades (MacDonald, T. J., Brown et al. 2001, Chakravarty, Pedraza et al. 2017). This subsequently forms a feedback loop which leads to a decreased sensitivity towards PI3K pathway inhibitors. This finding was demonstrated in a study by Chandarlapaty, Sawai et al. (2011) in which inhibition of the PI3K pathway resulted in FOXO-mediated expression of cell surface RTK, so that simultaneous inhibition of RTK and PI3K signalling yielded a more potent tumour suppressive effect. Based on this finding, it is proposed that inhibition of the PI3K pathway could be carried out in conjunction with PDGFRα inhibitors such as crenolanib and amuvatinib. Further rationale to target PDGFRα is its capability to dimerise and transactivate EGFRs (He, Levitzki et al. 2001, Chakravarty, Pedraza et al. 2017), which were found to be overexpressed in ependymomas consequently leading to saturation of survival signals such as PI3K and MAPK (Gilbertson, Bentley et al. 2002, Moreno, Popov et al. 2013, Sie, den Dunnen et al. 2015). This warrants the use of RTK inhibitors (RTKi) to simultaneously attenuate multiple cell survival pathways and help prevent the reactivation of these pathways through by-passing feedback loops that could be generated following treatment with pathway inhibitors. While several RTKi have already entered clinical evaluation in paediatric CNS tumours, results so far have only shown modest effects (Jakacki, Hamilton et al. 2008, Broniscer, Baker et al. 2009, Pollack, Stewart et al. 2011). Several resistance mechanisms were highlighted including an upregulation of RTK ligands that would compete with RTKi for binding thus diluting its effects (Sie, den Dunnen et al. 2015).

Interestingly, reactivation of PI3K signalling was attributed to the activity of several upregulated microRNAs conferring oncogenic properties including *MIR221*, *MIR222* and *MIR21*. All three microRNAs were shown to target *PTEN* (Pezzolesi, Platzer et al. 2008, Garofalo, Quintavalle et al. 2012) which is the chief negative regulator of the PI3K

pathway thus enhancing signalling output. If these microRNAs dampen the inhibitory effects of PI3K pathway agents, one could therefore utilise these as prospective targets to improve the performance of PI3K pathway inhibitors. At present, there is research into gene therapy-based methods with an aim to normalise expression of microRNAs that favour oncogenesis. Strategies involving small synthetic molecules that bind to microRNAs such as antisense oligonucleotides (ASOs) and long non-coding RNA (lncRNA) have already been investigated as a potential therapeutic tactic in cancers (Ji, Sun et al. 2017). Other methods use decoy transcripts such as miRNA sponges and miR-Mask which competitively bind to certain regions on the microRNA thus preventing its interaction with targets and effectively silencing its function (Garzon, Marcucci et al. 2010).

The prospect of microRNA signatures for diagnostic, prognostic and therapeutic purposes is currently being advocated in a broad range of cancers including paediatric brain tumours (Tantawy, Elzayat et al. 2018). Certainly in ependymoma where much of the underlying biology remains elusive, surveying the fluctuations in microRNA expression may also pinpoint several gains or losses in gene activity that are conducive towards disease pathogenesis (Costa, Bischof et al. 2011, Lourdusamy, Rahman et al. 2015). Since the microarray data has demonstrated that the PI3K pathway also regulated the expression of certain microRNAs, it would be interesting to solely explore the resulting ependymoma microRNA profile post-BKM120 treatment and determine microRNA-mRNA interactions that are of pathological significance in these tumours.

6.2.3 *C11orf95/RELA* fusion gene and the NFκB pathway

It has been shown that about 70% of supratentorial ependymal tumours harbor the *C11orf95/RELA* fusion gene, which arises from chromothropsis on chromosome 11q13.1 (Parker, Mohankumar et al., 2014). A biological consequence of this involves an increased signalling output from the NFκB pathway and upregulation of its downstream target genes. The cross talk between the PI3K and NFκB pathways has been reported in cancers, prompting similar studies to be performed in paediatric ependymomas. Having indicated that a higher percentage of supratentorial ependymomas have activated PI3K pathway in relation to their posterior fossa and spinal counterparts, previous work conducted at CBTRC has aimed to investigate whether the concurrent activation of these signalling cascades influence the pathogenesis of many supratentorial tumours. However, unpublished immunohistochemical data has shown no correlation between RELA (NFκB) protein levels with fusion status, which could suggest that upregulation of downstream processes may not be reliant upon the intracellular quantity of RELA.

Moreover, knockdown of RELA did not have an effect on pAKT levels thus implying that the two pathways in ependymoma are independent of each other. Nevertheless, it cannot be ruled out that increased NFκB signalling does not contribute towards disease progression considering its potential as a chemotherapeutic target to treat many malignancies (Xia, Shen et al., 2014). It could then be hypothesised that simultaneous signalling through both the PI3K and NFκB pathways induces ependymoma tumourigenesis. Future work may therefore include *in vitro* analysis of co-inhibiting PI3K and NFκB signalling predominantly on the supratentorial cell lines which were found to be positive for the *C11orf95/RELA* fusion gene.

6.3 Establishing the molecular mechanisms that promote the responses to PI3K pathway inhibition in ependymoma

To understand the mechanism of action of PI3K pathway inhibitors in ependymoma, it is necessary to elucidate the molecular events that facilitate the responses following treatment. In this study, it was investigated how BKM120-mediated inhibition of the PI3K pathway resulted in cell cycle arrest in ependymoma. The proposed mechanism was through the activation of FOXO proteins following inhibition of the PI3K pathway, consequently leading to the formation of the Rb/E2F1 complex, which decreases E2F1-mediated expression of genes.

So far, it was demonstrated that inhibition of the PI3K pathway leads to the loss of FOXO1 phosphorylation but not FOXO3 which implicates FOXO1 as a direct downstream target of the pathway. Reduction in Rb phosphorylation was also found in response to BKM120 treatment but this did not significantly decrease the E2F-mediated luciferase output. As discussed in the previous chapter, more experimental evidence is required to validate this as a mechanism of cell cycle arrest in ependymoma. This includes investigating the involvement of other FOXO proteins, apart from FOXO1 and FOXO3, which equally manifest tumour suppressive consequences that are negatively regulated by the PI3K pathway. Inclusion of other members of the E2F family of transcription factors in future functional work would also depict a broader perspective on the regulatory mechanism for the expression of genes necessary for cell cycle progression. In particular, E2F4 and E2F6, as identified on the Cytoscape gene interaction map, may play a role in promoting cell cycle arrest due to their function as transcriptional repressors (Christensen, Cloos et al. 2005, Dimova, Dyson 2005).

From a technical perspective, employment of the luciferase reporter assay to quantify the level of E2F-mediated expression in response to PI3K pathway inhibition may require further experimental repeats. This was based on retrospective data analysis which

suggested that the overall data obtained may have been underpowered. This was based on several factors which include the number of repeats performed, the significance threshold set for the analysis ($p<0.05$) and the difference in the reporter gene activity between the drug treated and vehicle treated cells. Moreover, the emphasised limitation to this work was that the luciferase constructs used were not specific to the activity of a particular E2F protein. An alternative method which enables individual analysis of E2F activity would be through electromobility shift assays (EMSAs). This considers the isolation of nuclear fractions from drug treated cells followed by detection of any E2F proteins of interest. Successful E2F binding to probe sequences would manifest a super shift in the migratory profile. This gives evidence of whether or not these proteins have been translocated into the nucleus in response to BKM120 treatment, indicating the activation status of E2F-mediated transcription.

It is also noted that there was no experimental proof to account for the events between FOXO activation and the consequential hypophosphorylation of Rb that would lead to its binding to E2F1. Western blot analysis of cell cycle inhibitors such as members of the Cip/Kip and Ink4 family could be performed to determine if their levels increase post-inhibition of the PI3K pathway. Kinase assays could also be performed to demonstrate whether this subsequently reduces the activity of CDK4/6-cyclin D activity, whose role is predominantly associated with Rb phosphorylation. It is also worth investigating other cell cycle arrest mechanisms that are independent of the proposed FOXO/Rb/E2F axis. For instance, activation of GSK3β downstream of the PI3K pathway may have implications in BKM120-associated cell cycle arrest in ependymoma. GSK3β is a component of the Destruction Complex which directs β-catenin, whose transcriptional targets include *CCND1*, towards proteasomal degradation (Cross, Alessi et al. 1995). The nuclear transcription factor Y (NFY), which was also identified on the GSEA transcription factor analysis (see section 4.2.4), could be evaluated as a downstream PI3K pathway regulator of cell cycle progression. NFY targets several cell cycle genes but its activity is principally associated with G_2/M transition. It was also conveyed that loss of NFY activity is necessary to promote checkpoints in the G_2/M phase especially upon detection of DNA damage (Manni, Mazzaro et al. 2001, Benatti, Basile et al. 2008). It is therefore explained that while a decrease in E2F1 transcription is attributed to G_1/S arrest in ependymoma, suppression of NFY activity could have occurred thus accounting for the reduction of G_2/M-related processes identified in the gene expression data.

6.4 Proposed general future work

6.4.1 The PI3K pathway as a regulator of migration

Examining other cellular processes affected by PI3K pathway inhibition further explains how these agents promote a tumour suppressive effect in ependymoma. This study has so far demonstrated that BKM120 treatment of ependymoma cells did not induce a cytotoxic, albeit a cytostatic effect through cell cycle arrest at G_1/S phase. Another prospect that could be investigated for future work is the involvement of the PI3K pathway in cell migration. Ependymomas, despite recurring locally and only invading adjacent brain parenchyma, can also metastasise to distant locations usually through leptomeningeal dissemination in reported cases (Yuh, Barkovich et al. 2009). Indeed, the PI3K pathway could also regulate cellular functions that stimulate cell motility including cytoskeletal organisation, cell polarisation and formation of focal adhesions (Cain, Ridley 2009). Functional experiments that could be undertaken include migration and wound healing assays. This could then be supported by scrutinising the organisation of the cytoskeletal system to determine any changes that would be indicative of abrogating the overall cellular movement following loss of PI3K signalling.

6.5.1 Data collection at various endpoints

Most of the experiments performed in this study could have benefited from the progressive collection of data using various endpoints. This was particularly highlighted in the preparation of samples for transcriptomic analysis. The gene expression data presented in this study was a result of a 24 hour BKM120 treatment of ependymoma cells. However, initial western blot data showed that inhibition of the PI3K pathway could be achieved following a one-hour incubation with BKM120. It is of interest whether such conditions would generate a different expression profile as this would more likely have isolated early-response genes that are rapidly transcribed due to exposure to external stimuli.

6.5.2 Proteomics

It is believed that gene expression patterns reflect the level of their cellular activity. However, this methodology does not account for post-translational modifications that would modulate the subsequent function of proteins. This is especially important since the project deals with enzymatic cascades whose propagation relies on these post-translational modifications. Western blot analysis enabled the detection of phosphorylation status of various downstream targets of the PI3K pathway but this could be achieved much more efficiently using a more high-throughput approach. A

phosphokinase array is an example which can elucidate a phosphoproteomic profile that could be subjected to bioinformatic analysis in order to pinpoint potential signalling pathways and cellular processes that are affected by PI3K pathway inhibition. Therefore, having both transcriptomic and proteomic data would enable biological processes to be cross-referenced thus enhancing the analysis this study.

Several aspects of this project could have been provided with supporting evidence through this approach particularly in characterising the molecular mechanism that links PI3K inhibition with cell cycle arrest. This approach could also feasibly identify whether there is an upregulation of MAPK signalling pathway, based on the phospho-status of its components, following treatment with BKM120. This would therefore indicate whether there is rationale for co-inhibiting this pathway alongside PI3K signalling, highlighting its potential therapeutic utility.

In this project, phosphoproteomic study was also considered which involved electrophoresis-mediated protein resolution of cellular fractions to compare the resulting profiles from drug treated and vehicle treated ependymoma cells. Putative downstream targets would manifest as protein bands that are expressed differently between the two treatment conditions, which could then be identified using mass spectrometry. The approach also presented an unbiased approach at determining downstream targets that can be put forward for further functional analysis. A pilot study was already undertaken which included optimisation of sample preparations but could not be completed due to time constraints.

6.5.3 Advancement from using 2D ependymoma models

This project mainly depended on cell line work to achieve its aims and objectives. Future prospects include the use of more sophisticated disease models that better represent the tumour microenvironment. Our research group has already instigated the creation of 3D ependymoma models with stark differences in gene expression patterns relative to its 2D counterpart (Ward, Lourdusamy et al. 2014) including loss of cell cycle and mitotic genes, which signified a reduced proliferative profile. The same study also demonstrated the disparity in treatment outcomes, implicating a phenotypic shift that may closely resemble true drug responses. While Ward and colleagues' data was predominantly based on BXD1425-EPN cell work, creating an array of 3D models by optimising the other established ependymoma cell lines would be ideal to determine whether similar tumour behaviours could also be recapitulated. Ultimately, assaying the effects of PI3K pathway inhibition in ependymoma would be investigated in mouse models

as an insight towards the implication of targeting the PI3K pathway when translated in a more clinical setting. If the PI3K signalling cascade presents a significant biological aspect towards disease pathogenesis, it is hypothesised that its inhibition would also prolong survival of ependymoma mouse models despite demonstrable cytostaticity *in vitro.* Early research into characterising ependymoma tumours involved the identification of molecular signatures that are compartment specific (Taylor et al., 2005). Not only did this highlight that ependymomas have separate disease entities but it explained the fundamental aspects of generating a sophisticated disease model that would advance understanding in future studies. Indeed, success has been realised by Johnson and colleagues in which implantation of modified NSCs faithfully captured both transcriptomic and histologic features of supratentorial tumours. Mohankummar and colleagues also exploited the use of mouse models to experimentally pinpoint novel oncogenes and tumour suppressor genes that could drive the development of ependymomas. Their work further characterised the underlying biology of these enigmatic tumours, providing the convenience of putative targets that can be seen of pathogenic significance. With expertise slowly being attained in utilising these models, transition of drug screening from *in vitro* to a more *in vivo* context becomes more likely in order to assess potent chemotherapeutic agents that also deliver little adverse effects; an objective that is yet to be realised into finding an effective ependymoma treatment (Atkinson et al., 2010). It is this very same approach that needs to be undertaken to certainly confirm the efficacy of inhibiting the PI3K pathway as part of treatment regimes in ependymoma. The permeability of the BBB towards BKM120 would feasibly address this, following prospective tests on ependymoma mouse models thus supporting existing preclinical data and assessing its likelihood for further clinical use.

6.5.4 Final conclusion

The PI3K pathway regulates survival and viability of paediatric ependymomas and targeting it presents an attractive therapeutic approach for treating a high percentage of diagnosed cases. In this study, treatment of ependymoma cells with the pan-Class I PI3K inhibitor BKM120 reduced cell viability within a clinically relevant concentration range which emphasises its clinical potential in treating these tumours. However, BKM120 only produced a cytostatic response in ependymoma, suggesting that PI3K pathway inhibitors would not be effective as a monotherapy and should be considered as part of a combination treatment instead. So far, the mechanism for inducing ependymoma cell cycle arrest following BKM120 is yet to be determined. Preliminary findings have instigated the role of the Rb/E2F1 complex in blocking cell cycle progression, but whether this is associated with FOXO1 activation remains inconclusive. Suppression of the PI3K

pathway in ependymoma also resulted in a downregulation of several cellular functions which could be associated with disease pathogenesis including DNA repair responses and G_2/M-related processes. Analysis of gene expression data has identified a potential synergistic drug combination of BKM120 and gemcitabine but further functional work is required from other cell lines to support these conclusions. Future therapeutic avenues that could be investigated based on the transcriptomic analysis include simultaneous targeting of the PI3K and MAPK pathways, co-treatment with RTK/PI3K pathway inhibitors and manipulation of relevant microRNA expression. Finally, it is also crucial to delineate whether these ependymoma responses are actually mediated by canonical PI3K/AKT signalling to support both its role in disease pathogenesis and a prospective therapeutic target to treat these tumours.

BIBLIOGRAPHY

ADDIE, M., BALLARD, P., BUTTAR, D., CRAFTER, C., CURRIE, G., DAVIES, B.R., DEBRECZENI, J., DRY, H., DUDLEY, P., GREENWOOD, R., JOHNSON, P.D., KETTLE, J.G., LANE, C., LAMONT, G., LEACH, A., LUKE, R.W., MORRIS, J., OGILVIE, D., PAGE, K., PASS, M., PEARSON, S. and RUSTON, L., 2013. Discovery of 4-amino-N-[(1S)-1-(4-chlorophenyl)-3-hydroxypropyl]-1-(7H-pyrrolo[2,3-d]pyrimidin -4-yl)piperidine-4-carboxamide (AZD5363), an orally bioavailable, potent inhibitor of Akt kinases. *Journal of medicinal chemistry,* **56**(5), pp. 2059-2073.

ADELMAN, C.A., LOLO, R.L., BIRKBAK, N.J., MURINA, O., MATSUZAKI, K., HOREJSI, Z., PARMAR, K., BOREL, V., SKEHEL, J.M., STAMP, G., D'ANDREA, A., SARTORI, A.A., SWANTON, C. and BOULTON, S.J., 2013. HELQ promotes RAD51 paralogue-dependent repair to avert germ cell loss and tumorigenesis. *Nature,* **502**(7471), pp. 381-384.

ADRAIN, C., CREAGH, E.M. and MARTIN, S.J., 2001. Apoptosis-associated release of Smac/DIABLO from mitochondria requires active caspases and is blocked by Bcl-2. *The EMBO journal,* **20**(23), pp. 6627-6636.

AGLIANO, A., BALARAJAH, G., CIOBOTA, D.M., SIDHU, J., CLARKE, P.A., JONES, C., WORKMAN, P., LEACH, M.O. and AL-SAFFAR, N.M.S., 2017. Pediatric and adult glioblastoma radiosensitization induced by PI3K/mTOR inhibition causes early metabolic alterations detected by nuclear magnetic resonance spectroscopy. *Oncotarget,* **8**(29), pp. 47969-47983.

AHRONOWITZ, I., XIN, W., KIELY, R., SIMS, K., MACCOLLIN, M. and NUNES, F.P., 2007. Mutational spectrum of the NF2 gene: a meta-analysis of 12 years of research and diagnostic laboratory findings. *Human mutation,* **28**(1), pp. 1-12.

ALERS, S., LOFFLER, A.S., WESSELBORG, S. and STORK, B., 2012. The incredible ULKs. *Cell communication and signaling : CCS,* **10**(1), pp. 7-811X-10-7.

ANAND, S., PENRHYN-LOWE, S. and VENKITARAMAN, A.R., 2003. AURORA-A amplification overrides the mitotic spindle assembly checkpoint, inducing resistance to Taxol. *Cancer cell,* **3**(1), pp. 51-62.

ANDERSON, J.L., PARK, A., AKIYAMA, R., TAP, W.D., DENNY, C.T. and FEDERMAN, N., 2015. Evaluation of In Vitro Activity of the Class I PI3K Inhibitor Buparlisib (BKM120) in Pediatric Bone and Soft Tissue Sarcomas. *PloS one,* **10**(9), pp. e0133610.

ANGLIKER, N. and RUEGG, M.A., 2013. In vivo evidence for mTORC2-mediated actin cytoskeleton rearrangement in neurons. *Bioarchitecture,* **3**(4), pp. 113-118.

ARAKI, Y., KU, W.C., AKIOKA, M., MAY, A.I., HAYASHI, Y., ARISAKA, F., ISHIHAMA, Y. and OHSUMI, Y., 2013. Atg38 is required for autophagy-specific phosphatidylinositol 3-kinase complex integrity. *The Journal of cell biology,* **203**(2), pp. 299-313.

ARBOLEDA, M.J., LYONS, J.F., KABBINAVAR, F.F., BRAY, M.R., SNOW, B.E., AYALA, R., DANINO, M., KARLAN, B.Y. and SLAMON, D.J., 2003. Overexpression of AKT2/protein kinase

Bbeta leads to up-regulation of beta1 integrins, increased invasion, and metastasis of human breast and ovarian cancer cells. *Cancer research,* **63**(1), pp. 196-206.

ARCARO, A., DOEPFNER, K.T., BOLLER, D., GUERREIRO, A.S., SHALABY, T., JACKSON, S.P., SCHOENWAELDER, S.M., DELATTRE, O., GROTZER, M.A. and FISCHER, B., 2007. Novel role for insulin as an autocrine growth factor for malignant brain tumour cells. *The Biochemical journal,* **406**(1), pp. 57-66.

ARCARO, A., ZVELEBIL, M.J., WALLASCH, C., ULLRICH, A., WATERFIELD, M.D. and DOMIN, J., 2000. Class II phosphoinositide 3-kinases are downstream targets of activated polypeptide growth factor receptors. *Molecular and cellular biology,* **20**(11), pp. 3817-3830.

ARMSTRONG, A.J., HALABI, S., HEALY, P., ALUMKAL, J.J., WINTERS, C., KEPHART, J., BITTING, R.L., HOBBS, C., SOLEAU, C.F., BEER, T.M., SLOTTKE, R., MUNDY, K., YU, E.Y. and GEORGE, D.J., 2017. Phase II trial of the PI3 kinase inhibitor buparlisib (BKM-120) with or without enzalutamide in men with metastatic castration resistant prostate cancer. *European journal of cancer (Oxford, England : 1990),* **81**, pp. 228-236.

ARMSTRONG, T.S., VERA-BOLANOS, E. and GILBERT, M.R., 2011. Clinical course of adult patients with ependymoma: results of the Adult Ependymoma Outcomes Project. *Cancer,* **117**(22), pp. 5133-5141.

ASHKENAZI, A., 2002. Targeting death and decoy receptors of the tumour-necrosis factor superfamily. *Nature reviews.Cancer,* **2**(6), pp. 420-430.

ATKINSON, J.M., SHELAT, A.A., CARCABOSO, A.M., KRANENBURG, T.A., ARNOLD, L.A., BOULOS, N., WRIGHT, K., JOHNSON, R.A., POPPLETON, H., MOHANKUMAR, K.M., FEAU, C., PHOENIX, T., GIBSON, P., ZHU, L., TONG, Y., EDEN, C., ELLISON, D.W., PRIEBE, W., KOUL, D., YUNG, W.K., GAJJAR, A., STEWART, C.F., GUY, R.K. and GILBERTSON, R.J., 2011. An integrated in vitro and in vivo high-throughput screen identifies treatment leads for ependymoma. *Cancer cell,* **20**(3), pp. 384-399.

BACKER, J.M., 2008. The regulation and function of Class III PI3Ks: novel roles for Vps34. *The Biochemical journal,* **410**(1), pp. 1-17.

BAHRAMI, S. and DRABLOS, F., 2016. Gene regulation in the immediate-early response process. *Advances in biological regulation,* **62**, pp. 37-49.

BAI, D., UENO, L. and VOGT, P.K., 2009. Akt-mediated regulation of NFkappaB and the essentialness of NFkappaB for the oncogenicity of PI3K and Akt. *International journal of cancer,* **125**(12), pp. 2863-2870.

BALL, K.L., LAIN, S., FAHRAEUS, R., SMYTHE, C. and LANE, D.P., 1997. Cell-cycle arrest and inhibition of Cdk4 activity by small peptides based on the carboxy-terminal domain of p21WAF1. *Current biology : CB,* **7**(1), pp. 71-80.

BANERJI, U., DEAN, E.J., PEREZ-FIDALGO, J.A., BATIST, G., BEDARD, P.L., YOU, B., WESTIN, S.N., KABOS, P., GARRETT, M.D., TALL, M., AMBROSE, H., BARRETT, J.C., CARR, T.H., CHEUNG, S.Y.A., CORCORAN, C., CULLBERG, M., DAVIES, B.R., DE BRUIN, E.C., ELVIN, P., FOXLEY, A., LAWRENCE, P., LINDEMANN, J.P.O., MAUDSLEY, R., PASS, M., ROWLANDS, V., RUGMAN, P., SCHIAVON, G., YATES, J. and SCHELLENS, J.H.M., 2018. A Phase I Open-Label

Study to Identify a Dosing Regimen of the Pan-AKT Inhibitor AZD5363 for Evaluation in Solid Tumors and in PIK3CA-Mutated Breast and Gynecologic Cancers. *Clinical cancer research : an official journal of the American Association for Cancer Research,* **24**(9), pp. 2050-2059.

BAR-SHAVIT, R., MAOZ, M., KANCHARLA, A., NAG, J.K., AGRANOVICH, D., GRISARU-GRANOVSKY, S. and UZIELY, B., 2016. G Protein-Coupled Receptors in Cancer. *International journal of molecular sciences,* **17**(8), pp. 10.3390/ijms17081320.

BARTALUCCI, N., TOZZI, L., BOGANI, C., MARTINELLI, S., ROTUNNO, G., VILLEVAL, J.L. and VANNUCCHI, A.M., 2013. Co-targeting the PI3K/mTOR and JAK2 signalling pathways produces synergistic activity against myeloproliferative neoplasms. *Journal of Cellular and Molecular Medicine,* **17**(11), pp. 1385-1396.

BAYLISS, J., MUKHERJEE, P., LU, C., JAIN, S.U., CHUNG, C., MARTINEZ, D., SABARI, B., MARGOL, A.S., PANWALKAR, P., PAROLIA, A., PEKMEZCI, M., MCEACHIN, R.C., CIESLIK, M., TAMRAZI, B., GARCIA, B.A., LA ROCCA, G., SANTI, M., LEWIS, P.W., HAWKINS, C., MELNICK, A., DAVID ALLIS, C., THOMPSON, C.B., CHINNAIYAN, A.M., JUDKINS, A.R. and VENNETI, S., 2016. Lowered H3K27me3 and DNA hypomethylation define poorly prognostic pediatric posterior fossa ependymomas. *Science translational medicine,* **8**(366), pp. 366ra161.

BECHER, O.J., MILLARD, N.E., MODAK, S., KUSHNER, B.H., HAQUE, S., SPASOJEVIC, I., TRIPPETT, T.M., GILHEENEY, S.W., KHAKOO, Y., LYDEN, D.C., DE BRAGANCA, K.C., KOLESAR, J.M., HUSE, J.T., KRAMER, K., CHEUNG, N.V. and DUNKEL, I.J., 2017. A phase I study of single-agent perifosine for recurrent or refractory pediatric CNS and solid tumors. *PloS one,* **12**(6), pp. e0178593.

BENATTI, P., BASILE, V., MERICO, D., FANTONI, L.I., TAGLIAFICO, E. and IMBRIANO, C., 2008. A balance between NF-Y and p53 governs the pro- and anti-apoptotic transcriptional response. *Nucleic acids research,* **36**(5), pp. 1415-1428.

BENDELL, J.C., NEMUNAITIS, J., VUKELJA, S.J., HAGENSTAD, C., CAMPOS, L.T., HERMANN, R.C., SPORTELLI, P., GARDNER, L. and RICHARDS, D.A., 2011. Randomized placebo-controlled phase II trial of perifosine plus capecitabine as second- or third-line therapy in patients with metastatic colorectal cancer. *Journal of clinical oncology : official journal of the American Society of Clinical Oncology,* **29**(33), pp. 4394-4400.

BENDELL, J.C., RODON, J., BURRIS, H.A., DE JONGE, M., VERWEIJ, J., BIRLE, D., DEMANSE, D., DE BUCK, S.S., RU, Q.C., PETERS, M., GOLDBRUNNER, M. and BASELGA, J., 2012a. Phase I, dose-escalation study of BKM120, an oral pan-Class I PI3K inhibitor, in patients with advanced solid tumors. *Journal of clinical oncology : official journal of the American Society of Clinical Oncology,* **30**(3), pp. 282-290.

BHAGWAT, S.V., GOKHALE, P.C., CREW, A.P., COOKE, A., YAO, Y., MANTIS, C., KAHLER, J., WORKMAN, J., BITTNER, M., DUDKIN, L., EPSTEIN, D.M., GIBSON, N.W., WILD, R., ARNOLD, L.D., HOUGHTON, P.J. and PACHTER, J.A., 2011. Preclinical characterization of OSI-027, a potent and selective inhibitor of mTORC1 and mTORC2: distinct from rapamycin. *Molecular cancer therapeutics,* **10**(8), pp. 1394-1406.

BI, L., OKABE, I., BERNARD, D.J. and NUSSBAUM, R.L., 2002. Early embryonic lethality in mice deficient in the p110beta catalytic subunit of PI 3-kinase. *Mammalian genome : official journal of the International Mammalian Genome Society,* **13**(3), pp. 169-172.

BIRCH, J.M. and MARSDEN, H.B., 1987. A classification scheme for childhood cancer. *International journal of cancer,* **40**(5), pp. 620-624.

BLAKE, J.F., XU, R., BENCSIK, J.R., XIAO, D., KALLAN, N.C., SCHLACHTER, S., MITCHELL, I.S., SPENCER, K.L., BANKA, A.L., WALLACE, E.M., GLOOR, S.L., MARTINSON, M., WOESSNER, R.D., VIGERS, G.P., BRANDHUBER, B.J., LIANG, J., SAFINA, B.S., LI, J., ZHANG, B., CHABOT, C., DO, S., LEE, L., OEH, J., SAMPATH, D., LEE, B.B., LIN, K., LIEDERER, B.M. and SKELTON, N.J., 2012. Discovery and preclinical pharmacology of a selective ATP-competitive Akt inhibitor (GDC-0068) for the treatment of human tumors. *Journal of medicinal chemistry,* **55**(18), pp. 8110-8127.

BOUFFET, E., PERILONGO, G., CANETE, A. and MASSIMINO, M., 1998. Intracranial ependymomas in children: a critical review of prognostic factors and a plea for cooperation. *Medical and pediatric oncology,* **30**(6), pp. 319-29; discussion 329-31.

BOULOS, N., KIM, J., PATAY, Z., BUTCH, E.R., AYAZ, M., SNYDER, S.E., CALABRESE, C., GILBERTSON, R.J. and WRIGHT, K.D. 2016. Differential responses of murine models of supratentorial ependymoma to gemcitabine as measured by MRI and PET-CT. *Neuro-Oncology.* 18(Suppl 3): iii139.

BOZULIC, L., SURUCU, B., HYNX, D. and HEMMINGS, B.A., 2008. PKBalpha/Akt1 acts downstream of DNA-PK in the DNA double-strand break response and promotes survival. *Molecular cell,* **30**(2), pp. 203-213.

BRACHMANN, S.M., HOFMANN, I., SCHNELL, C., FRITSCH, C., WEE, S., LANE, H., WANG, S., GARCIA-ECHEVERRIA, C. and MAIRA, S.M., 2009. Specific apoptosis induction by the dual PI3K/mTor inhibitor NVP-BEZ235 in HER2 amplified and PIK3CA mutant breast cancer cells. *Proceedings of the National Academy of Sciences of the United States of America,* **106**(52), pp. 22299-22304.

BRACHMANN, S.M., KLEYLEIN-SOHN, J., GAULIS, S., KAUFFMANN, A., BLOMMERS, M.J., KAZIC-LEGUEUX, M., LABORDE, L., HATTENBERGER, M., STAUFFER, F., VAXELAIRE, J., ROMANET, V., HENRY, C., MURAKAMI, M., GUTHY, D.A., STERKER, D., BERGLING, S., WILSON, C., BRUMMENDORF, T., FRITSCH, C., GARCIA-ECHEVERRIA, C., SELLERS, W.R., HOFMANN, F. and MAIRA, S.M., 2012. Characterization of the mechanism of action of the pan class I PI3K inhibitor NVP-BKM120 across a broad range of concentrations. *Molecular cancer therapeutics,* **11**(8), pp. 1747-1757.

BRADHAM, C. and MCCLAY, D.R., 2006. p38 MAPK in development and cancer. *Cell cycle (Georgetown, Tex.),* **5**(8), pp. 824-828.

BRANDES, A.A., CAVALLO, G., RENI, M., TOSONI, A., NICOLARDI, L., SCOPECE, L., FRANCESCHI, E., SOTTI, G., TALACCHI, A., TURAZZI, S. and ERMANI, M., 2005. A multicenter retrospective study of chemotherapy for recurrent intracranial ependymal tumors in adults by the Gruppo Italiano Cooperativo di Neuro-Oncologia. *Cancer,* **104**(1), pp. 143-148.

BRENNAN, C.W., VERHAAK, R.G., MCKENNA, A., CAMPOS, B., NOUSHMEHR, H., SALAMA, S.R., ZHENG, S., CHAKRAVARTY, D., SANBORN, J.Z., BERMAN, S.H., BEROUKHIM, R., BERNARD, B., WU, C.J., GENOVESE, G., SHMULEVICH, I., BARNHOLTZ-SLOAN, J., ZOU, L., VEGESNA, R., SHUKLA, S.A., CIRIELLO, G., YUNG, W.K., ZHANG, W., SOUGNEZ, C., MIKKELSEN, T., ALDAPE, K., BIGNER, D.D., VAN MEIR, E.G., PRADOS, M., SLOAN, A., BLACK,

K.L., ESCHBACHER, J., FINOCCHIARO, G., FRIEDMAN, W., ANDREWS, D.W., GUHA, A., IACOCCA, M., O'NEILL, B.P., FOLTZ, G., MYERS, J., WEISENBERGER, D.J., PENNY, R., KUCHERLAPATI, R., PEROU, C.M., HAYES, D.N., GIBBS, R., MARRA, M., MILLS, G.B., LANDER, E., SPELLMAN, P., WILSON, R., SANDER, C., WEINSTEIN, J., MEYERSON, M., GABRIEL, S., LAIRD, P.W., HAUSSLER, D., GETZ, G., CHIN, L. and TCGA RESEARCH NETWORK, 2013. The somatic genomic landscape of glioblastoma. *Cell,* **155**(2), pp. 462-477.

BRITSCHGI, A., ANDRAOS, R., BRINKHAUS, H., KLEBBA, I., ROMANET, V., MULLER, U., MURAKAMI, M., RADIMERSKI, T. and BENTIRES-ALJ, M., 2012. JAK2/STAT5 inhibition circumvents resistance to PI3K/mTOR blockade: a rationale for cotargeting these pathways in metastatic breast cancer. *Cancer cell,* **22**(6), pp. 796-811.

BRONISCER, A., BAKER, S.J., STEWART, C.F., MERCHANT, T.E., LANINGHAM, F.H., SCHAIQUEVICH, P., KOCAK, M., MORRIS, E.B., ENDERSBY, R., ELLISON, D.W. and GAJJAR, A., 2009. Phase I and pharmacokinetic studies of erlotinib administered concurrently with radiotherapy for children, adolescents, and young adults with high-grade glioma. *Clinical cancer research : an official journal of the American Association for Cancer Research,* **15**(2), pp. 701-707.

BROWN, K.K. and TOKER, A., 2015. The phosphoinositide 3-kinase pathway and therapy resistance in cancer. *F1000prime reports,* **7**, pp. 13-13. eCollection 2015.

BRUNET, A., PARK, J., TRAN, H., HU, L.S., HEMMINGS, B.A. and GREENBERG, M.E., 2001. Protein kinase SGK mediates survival signals by phosphorylating the forkhead transcription factor FKHRL1 (FOXO3a). *Molecular and cellular biology,* **21**(3), pp. 952-965.

BRYANT, V.L., ELIAS, R.M., MCCARTHY, S.M., YEATMAN, T.J. and ALEXANDROW, M.G., 2015. Suppression of Reserve MCM Complexes Chemosensitizes to Gemcitabine and 5-Fluorouracil. *Molecular cancer research : MCR,* **13**(9), pp. 1296-1305.

BUDAY, L., EGAN, S.E., RODRIGUEZ VICIANA, P., CANTRELL, D.A. and DOWNWARD, J., 1994. A complex of Grb2 adaptor protein, Sos exchange factor, and a 36-kDa membrane-bound tyrosine phosphoprotein is implicated in ras activation in T cells. *The Journal of biological chemistry,* **269**(12), pp. 9019-9023.

BUTTRICK, T.S., WANG, W., YUNG, C., TRIEU, K.G., PATEL, K., KHOURY, S.J., AI, X. and ELYAMAN, W., 2018. Foxo1 Promotes Th9 Cell Differentiation and Airway Allergy. *Scientific reports,* **8**(1), pp. 818-018-19315-z.

CABRERA, M., GOMEZ, N., REMES LENICOV, F., ECHEVERRIA, E., SHAYO, C., MOGLIONI, A., FERNANDEZ, N. and DAVIO, C., 2015. G2/M Cell Cycle Arrest and Tumor Selective Apoptosis of Acute Leukemia Cells by a Promising Benzophenone Thiosemicarbazone Compound. *PloS one,* **10**(9), pp. e0136878.

CAGE, T.A., CHANTHERY, Y., CHESLER, L., GRIMMER, M., KNIGHT, Z., SHOKAT, K., WEISS, W.A. and GUSTAFSON, W.C., 2015. Downregulation of MYCN through PI3K Inhibition in Mouse Models of Pediatric Neural Cancer. *Frontiers in oncology,* **5**, pp. 111.

CAGE, T.A., CLARK, A.J., ARANDA, D., GUPTA, N., SUN, P.P., PARSA, A.T. and AUGUSTE, K.I., 2013. A systematic review of treatment outcomes in pediatric patients with intracranial ependymomas. *Journal of neurosurgery.Pediatrics,* **11**(6), pp. 673-681.

CAI, Y., TAN, X., LIU, J., SHEN, Y., WU, D., REN, M., HUANG, P. and YU, D., 2014. Inhibition of PI3K/Akt/mTOR signaling pathway enhances the sensitivity of the SKOV3/DDP ovarian cancer cell line to cisplatin in vitro. *Chinese journal of cancer research = Chung-kuo yen cheng yen chiu,* **26**(5), pp. 564-572.

CAIN, R.J. and RIDLEY, A.J., 2009. Phosphoinositide 3-kinases in cell migration. *Biology of the cell,* **101**(1), pp. 13-29.

CALNAN, D.R. and BRUNET, A., 2008. The FoxO code. *Oncogene,* **27**(16), pp. 2276-2288.

CALZOLARI, F. and MALATESTA, P., 2010. Recent insights into PDGF-induced gliomagenesis. *Brain pathology (Zurich, Switzerland),* **20**(3), pp. 527-538.

CANTLEY, L.C., 2002. The phosphoinositide 3-kinase pathway. *Science (New York, N.Y.),* **296**(5573), pp. 1655-1657.

CARRACEDO, A., MA, L., TERUYA-FELDSTEIN, J., ROJO, F., SALMENA, L., ALIMONTI, A., EGIA, A., SASAKI, A.T., THOMAS, G., KOZMA, S.C., PAPA, A., NARDELLA, C., CANTLEY, L.C., BASELGA, J. and PANDOLFI, P.P., 2008. Inhibition of mTORC1 leads to MAPK pathway activation through a PI3K-dependent feedback loop in human cancer. *The Journal of clinical investigation,* **118**(9), pp. 3065-3074.

CARTER, M., NICHOLSON, J., ROSS, F., CROLLA, J., ALLIBONE, R., BALAJI, V., PERRY, R., WALKER, D., GILBERTSON, R. and ELLISON, D.W., 2002. Genetic abnormalities detected in ependymomas by comparative genomic hybridisation. *British journal of cancer,* **86**(6), pp. 929-939.

CARVER, B.S., CHAPINSKI, C., WONGVIPAT, J., HIERONYMUS, H., CHEN, Y., CHANDARLAPATY, S., ARORA, V.K., LE, C., KOUTCHER, J., SCHER, H., SCARDINO, P.T., ROSEN, N. and SAWYERS, C.L., 2011. Reciprocal feedback regulation of PI3K and androgen receptor signaling in PTEN-deficient prostate cancer. *Cancer cell,* **19**(5), pp. 575-586.

CASTELLANO, E. and DOWNWARD, J., 2011. RAS Interaction with PI3K: More Than Just Another Effector Pathway. *Genes & cancer,* **2**(3), pp. 261-274.

CASTELLANO, E., SHERIDAN, C., THIN, M.Z., NYE, E., SPENCER-DENE, B., DIEFENBACHER, M.E., MOORE, C., KUMAR, M.S., MURILLO, M.M., GRONROOS, E., LASSAILLY, F., STAMP, G. and DOWNWARD, J., 2013. Requirement for interaction of PI3-kinase p110alpha with RAS in lung tumor maintenance. *Cancer cell,* **24**(5), pp. 617-630.

CAVDAR KOC, E., BURKHART, W., BLACKBURN, K., MOSELEY, A. and SPREMULLI, L.L., 2001. The small subunit of the mammalian mitochondrial ribosome. Identification of the full complement of ribosomal proteins present. *The Journal of biological chemistry,* **276**(22), pp. 19363-19374.

CHAKRAVARTY, D., PEDRAZA, A.M., COTARI, J., LIU, A.H., PUNKO, D., KOKROO, A., HUSE, J.T., ALTAN-BONNET, G. and BRENNAN, C.W., 2017. EGFR and PDGFRA co-expression and heterodimerization in glioblastoma tumor sphere lines. *Scientific reports,* **7**(1), pp. 9043-017-08940-9.

CHAMBERLAIN, M.C., 2003. Ependymomas. *Current neurology and neuroscience reports,* **3**(3), pp. 193-199.

CHANDARLAPATY, S., SAWAI, A., SCALTRITI, M., RODRIK-OUTMEZGUINE, V., GRBOVIC-HUEZO, O., SERRA, V., MAJUMDER, P.K., BASELGA, J. and ROSEN, N., 2011. AKT inhibition relieves feedback suppression of receptor tyrosine kinase expression and activity. *Cancer cell,* **19**(1), pp. 58-71.

CHEN, C.M., SMITH, D.M., PETERS, M.A., SAMSON, M.E., ZITZ, J., TABIN, C.J. and CEPKO, C.L., 1999. Production and design of more effective avian replication-incompetent retroviral vectors. *Developmental biology,* **214**(2), pp. 370-384.

CHEN, J., 2016. The Cell-Cycle Arrest and Apoptotic Functions of p53 in Tumor Initiation and Progression. *Cold Spring Harbor perspectives in medicine,* **6**(3), pp. a026104.

CHEUNG, L.W., HENNESSY, B.T., LI, J., YU, S., MYERS, A.P., DJORDJEVIC, B., LU, Y., STEMKE-HALE, K., DYER, M.D., ZHANG, F., JU, Z., CANTLEY, L.C., SCHERER, S.E., LIANG, H., LU, K.H., BROADDUS, R.R. and MILLS, G.B., 2011. High frequency of PIK3R1 and PIK3R2 mutations in endometrial cancer elucidates a novel mechanism for regulation of PTEN protein stability. *Cancer discovery,* **1**(2), pp. 170-185.

CHEUNG, L.W. and MILLS, G.B., 2016. Targeting therapeutic liabilities engendered by PIK3R1 mutations for cancer treatment. *Pharmacogenomics,* **17**(3), pp. 297-307.

CHEUNG, M., SHARMA, A., MADHUNAPANTULA, S.V. and ROBERTSON, G.P., 2008. Akt3 and mutant V600E B-Raf cooperate to promote early melanoma development. *Cancer research,* **68**(9), pp. 3429-3439.

CHILDREN WITH CANCER UK, 2018. Childhood cancer facts and figures. [WWW] URL https://www.childrenwithcancer.org.uk/childhood-cancer-info/childhood-cancer-facts-figures/ (accessed 05.07.18).

CHIRNOMAS, D., TANIGUCHI, T., DE LA VEGA, M., VAIDYA, A.P., VASSERMAN, M., HARTMAN, A.R., KENNEDY, R., FOSTER, R., MAHONEY, J., SEIDEN, M.V. and D'ANDREA, A.D., 2006. Chemosensitization to cisplatin by inhibitors of the Fanconi anemia/BRCA pathway. *Molecular cancer therapeutics,* **5**(4), pp. 952-961.

CHO, H., MU, J., KIM, J.K., THORVALDSEN, J.L., CHU, Q., CRENSHAW, E.B.,3rd, KAESTNER, K.H., BARTOLOMEI, M.S., SHULMAN, G.I. and BIRNBAUM, M.J., 2001. Insulin resistance and a diabetes mellitus-like syndrome in mice lacking the protein kinase Akt2 (PKB beta). *Science (New York, N.Y.),* **292**(5522), pp. 1728-1731.

CHOI, Y.H. and YOO, Y.H., 2012. Taxol-induced growth arrest and apoptosis is associated with the upregulation of the Cdk inhibitor, p21WAF1/CIP1, in human breast cancer cells. *Oncology reports,* **28**(6), pp. 2163-2169.

CHOU, T.C., 2010. Drug combination studies and their synergy quantification using the Chou-Talalay method. *Cancer research,* **70**(2), pp. 440-446.

CHRISTENSEN, J., CLOOS, P., TOFTEGAARD, U., KLINKENBERG, D., BRACKEN, A.P., TRINH, E., HEERAN, M., DI STEFANO, L. and HELIN, K., 2005. Characterization of E2F8, a novel E2F-like

cell-cycle regulated repressor of E2F-activated transcription. *Nucleic acids research,* **33**(17), pp. 5458-5470.

CIRSTEA, D., HIDESHIMA, T., RODIG, S., SANTO, L., POZZI, S., VALLET, S., IKEDA, H., PERRONE, G., GORGUN, G., PATEL, K., DESAI, N., SPORTELLI, P., KAPOOR, S., VALI, S., MUKHERJEE, S., MUNSHI, N.C., ANDERSON, K.C. and RAJE, N., 2010. Dual inhibition of akt/mammalian target of rapamycin pathway by nanoparticle albumin-bound-rapamycin and perifosine induces antitumor activity in multiple myeloma. *Molecular cancer therapeutics,* **9**(4), pp. 963-975.

CIVALLERO, M., COSENZA, M., POZZI, S., BARI, A., FERRI, P. and SACCHI, S., 2015. Activity of BKM120 and BEZ235 against Lymphoma Cells. *BioMed research international,* **2015**, pp. 870918.

CIZKOVA, M., VACHER, S., MESEURE, D., TRASSARD, M., SUSINI, A., MLCUCHOVA, D., CALLENS, C., ROULEAU, E., SPYRATOS, F., LIDEREAU, R. and BIECHE, I., 2013. PIK3R1 underexpression is an independent prognostic marker in breast cancer. *BMC cancer,* **13**, pp. 545-2407-13-545.

CLAYTON, E.L., MINOGUE, S. and WAUGH, M.G., 2013. Mammalian phosphatidylinositol 4-kinases as modulators of membrane trafficking and lipid signaling networks. *Progress in lipid research,* **52**(3), pp. 294-304.

CLEARY, J.M. and SHAPIRO, G.I., 2010. Development of phosphoinositide-3 kinase pathway inhibitors for advanced cancer. *Current oncology reports,* **12**(2), pp. 87-94.

COHEN-KAPLAN, V., CIECHANOVER, A. and LIVNEH, I., 2016. P62 at the Crossroad of the Ubiquitin-Proteasome System and Autophagy. *Oncotarget,* **7**(51), pp. 83833-83834.

COLLADO, M., MEDEMA, R.H., GARCIA-CAO, I., DUBUISSON, M.L., BARRADAS, M., GLASSFORD, J., RIVAS, C., BURGERING, B.M., SERRANO, M. and LAM, E.W., 2000. Inhibition of the phosphoinositide 3-kinase pathway induces a senescence-like arrest mediated by p27Kip1. *The Journal of biological chemistry,* **275**(29), pp. 21960-21968.

CONOVER, J.C., DOETSCH, F., GARCIA-VERDUGO, J.M., GALE, N.W., YANCOPOULOS, G.D. and ALVAREZ-BUYLLA, A., 2000. Disruption of Eph/ephrin signaling affects migration and proliferation in the adult subventricular zone. *Nature neuroscience,* **3**(11), pp. 1091-1097.

COSTA, F.F., BISCHOF, J.M., VANIN, E.F., LULLA, R.R., WANG, M., SREDNI, S.T., RAJARAM, V., BONALDO MDE, F., WANG, D., GOLDMAN, S., TOMITA, T. and SOARES, M.B., 2011. Identification of microRNAs as potential prognostic markers in ependymoma. *PloS one,* **6**(10), pp. e25114.

CRABB, S.J., BIRTLE, A.J., MARTIN, K., DOWNS, N., RATCLIFFE, I., MAISHMAN, T., ELLIS, M., GRIFFITHS, G., THOMPSON, S., KSIAZEK, L., KHOO, V. and JONES, R.J., 2017. ProCAID: a phase I clinical trial to combine the AKT inhibitor AZD5363 with docetaxel and prednisolone chemotherapy for metastatic castration resistant prostate cancer. *Investigational new drugs,* **35**(5), pp. 599-607.

CROSS, D.A., ALESSI, D.R., COHEN, P., ANDJELKOVICH, M. and HEMMINGS, B.A., 1995. Inhibition of glycogen synthase kinase-3 by insulin mediated by protein kinase B. *Nature,* **378**(6559), pp. 785-789.

CUI, W., CAI, Y., WANG, W., LIU, Z., WEI, P., BI, R., CHEN, W., SUN, M. and ZHOU, X., 2014. Frequent copy number variations of PI3K/AKT pathway and aberrant protein expressions of PI3K subunits are associated with inferior survival in diffuse large B cell lymphoma. *Journal of translational medicine,* **12**, pp. 10-5876-12-10.

CUNNINGHAM, J.T., RODGERS, J.T., ARLOW, D.H., VAZQUEZ, F., MOOTHA, V.K. and PUIGSERVER, P., 2007. mTOR controls mitochondrial oxidative function through a YY1-PGC-1alpha transcriptional complex. *Nature,* **450**(7170), pp. 736-740.

DAN, S., OKAMURA, M., MUKAI, Y., YOSHIMI, H., INOUE, Y., HANYU, A., SAKAUE-SAWANO, A., IMAMURA, T., MIYAWAKI, A. and YAMORI, T., 2012. ZSTK474, a specific phosphatidylinositol 3-kinase inhibitor, induces G1 arrest of the cell cycle in vivo. *European journal of cancer (Oxford, England : 1990),* **48**(6), pp. 936-943.

DANIELSEN, S.A., EIDE, P.W., NESBAKKEN, A., GUREN, T., LEITHE, E. and LOTHE, R.A., 2015. Portrait of the PI3K/AKT pathway in colorectal cancer. *Biochimica et biophysica acta,* **1855**(1), pp. 104-121.

DASEN, J.S., LIU, J.P. and JESSELL, T.M., 2003. Motor neuron columnar fate imposed by sequential phases of Hox-c activity. *Nature,* **425**(6961), pp. 926-933.

DATTA, S.R., DUDEK, H., TAO, X., MASTERS, S., FU, H., GOTOH, Y. and GREENBERG, M.E., 1997. Akt phosphorylation of BAD couples survival signals to the cell-intrinsic death machinery. *Cell,* **91**(2), pp. 231-241.

DELAUTER, B.J., RAMANATHAN, R.K., EGORIN, M.J., STOVER, L.L., ZUHOWSKI, E.G., PLUNKETT, W. and ZAMBONI, W.C., 2000. Pharmacokinetics of gemcitabine and 2',2'-difluorodeoxyuridine in a patient with ascites. *Pharmacotherapy,* **20**(10), pp. 1204-1207.

DHILLON, A.S., HAGAN, S., RATH, O. and KOLCH, W., 2007. MAP kinase signalling pathways in cancer. *Oncogene,* **26**(22), pp. 3279-3290.

DIAZ, A.K. and BAKER, S.J., 2014. The genetic signatures of pediatric high-grade glioma: no longer a one-act play. *Seminars in radiation oncology,* **24**(4), pp. 240-247.

DIMOVA, D.K. and DYSON, N.J., 2005. The E2F transcriptional network: old acquaintances with new faces. *Oncogene,* **24**(17), pp. 2810-2826.

DOLLY, S.O., WAGNER, A.J., BENDELL, J.C., KINDLER, H.L., KRUG, L.M., SEIWERT, T.Y., ZAUDERER, M.G., LOLKEMA, M.P., APT, D., YEH, R.F., FREDRICKSON, J.O., SPOERKE, J.M., KOEPPEN, H., WARE, J.A., LAUCHLE, J.O., BURRIS, H.A.,3rd and DE BONO, J.S., 2016. Phase I Study of Apitolisib (GDC-0980), Dual Phosphatidylinositol-3-Kinase and Mammalian Target of Rapamycin Kinase Inhibitor, in Patients with Advanced Solid Tumors. *Clinical cancer research : an official journal of the American Association for Cancer Research,* **22**(12), pp. 2874-2884.

DU, F., WU, X., LIU, Y., WANG, T., QI, X., MAO, Y., JIANG, L., ZHU, Y., CHEN, Y., ZHU, R., HAN, X., JIN, J., MA, X. and HUA, D., 2013. Acquisition of paclitaxel resistance via PI3Kdependent epithelialmesenchymal transition in A2780 human ovarian cancer cells. *Oncology reports,* **30**(3), pp. 1113-1118.

DYER, S., PREBBLE, E., DAVISON, V., DAVIES, P., RAMANI, P., ELLISON, D. and GRUNDY, R., 2002. Genomic imbalances in pediatric intracranial ependymomas define clinically relevant groups. *The American journal of pathology,* **161**(6), pp. 2133-2141.

EASTMAN, A., 1990. Activation of programmed cell death by anticancer agents: cisplatin as a model system. *Cancer cells (Cold Spring Harbor, N.Y.: 1989),* **2**(8-9), pp. 275-280.

EATON, B.R. and YOCK, T., 2014. The use of proton therapy in the treatment of benign or low-grade pediatric brain tumors. *Cancer journal (Sudbury, Mass.),* **20**(6), pp. 403-408.

EDEN, E., NAVON, R., STEINFELD, I., LIPSON, D. and YAKHINI, Z., 2009a. GOrilla: a tool for discovery and visualization of enriched GO terms in ranked gene lists. *BMC bioinformatics,* **10**, pp. 48-2105-10-48.

ELIS, W., TRIANTAFELLOW, E., WOLTERS, N.M., SIAN, K.R., CAPONIGRO, G., BORAWSKI, J., GAITHER, L.A., MURPHY, L.O., FINAN, P.M. and MACKEIGAN, J.P., 2008. Down-regulation of class II phosphoinositide 3-kinase alpha expression below a critical threshold induces apoptotic cell death. *Molecular cancer research : MCR,* **6**(4), pp. 614-623.

ELKABETS, M., VORA, S., JURIC, D., MORSE, N., MINO-KENUDSON, M., MURANEN, T., TAO, J., CAMPOS, A.B., RODON, J., IBRAHIM, Y.H., SERRA, V., RODRIK-OUTMEZGUINE, V., HAZRA, S., SINGH, S., KIM, P., QUADT, C., LIU, M., HUANG, A., ROSEN, N., ENGELMAN, J.A., SCALTRITI, M. and BASELGA, J., 2013. mTORC1 inhibition is required for sensitivity to PI3K p110alpha inhibitors in PIK3CA-mutant breast cancer. *Science translational medicine,* **5**(196), pp. 196ra99.

ELLISON, D.W., KOCAK, M., FIGARELLA-BRANGER, D., FELICE, G., CATHERINE, G., PIETSCH, T., FRAPPAZ, D., MASSIMINO, M., GRILL, J., BOYETT, J.M. and GRUNDY, R.G., 2011. Histopathological grading of pediatric ependymoma: reproducibility and clinical relevance in European trial cohorts. *Journal of negative results in biomedicine,* **10**, pp. 7-5751-10-7.

ENGELMAN, J.A., LUO, J. and CANTLEY, L.C., 2006. The evolution of phosphatidylinositol 3-kinases as regulators of growth and metabolism. *Nature reviews.Genetics,* **7**(8), pp. 606-619.

ENOS, M.E., BANCOS, S.A., BUSHNELL, T. and CRISPE, I.N., 2008. E2F4 modulates differentiation and gene expression in hematopoietic progenitor cells during commitment to the lymphoid lineage. *Journal of immunology (Baltimore, Md.: 1950),* **180**(6), pp. 3699-3707.

FAURY, D., NANTEL, A., DUNN, S.E., GUIOT, M.C., HAQUE, T., HAUSER, P., GARAMI, M., BOGNAR, L., HANZELY, Z., LIBERSKI, P.P., LOPEZ-AGUILAR, E., VALERA, E.T., TONE, L.G., CARRET, A.S., DEL MAESTRO, R.F., GLEAVE, M., MONTES, J.L., PIETSCH, T., ALBRECHT, S. and JABADO, N., 2007. Molecular profiling identifies prognostic subgroups of pediatric glioblastoma and shows increased YB-1 expression in tumors. *Journal of clinical oncology : official journal of the American Society of Clinical Oncology,* **25**(10), pp. 1196-1208.

FAUSTO, N., 2000. Liver regeneration. *Journal of hepatology,* **32**(1 Suppl), pp. 19-31.

FEKETE, M., SANTISKULVONG, C., ENG, C. and DORIGO, O., 2012. Effect of PI3K/Akt pathway inhibition-mediated G1 arrest on chemosensitization in ovarian cancer cells. *Anticancer Research,* **32**(2), pp. 445-452.

FELDMAN, M.E., APSEL, B., UOTILA, A., LOEWITH, R., KNIGHT, Z.A., RUGGERO, D. and SHOKAT, K.M., 2009. Active-site inhibitors of mTOR target rapamycin-resistant outputs of mTORC1 and mTORC2. *PLoS biology,* **7**(2), pp. e38.

FERGUSON, S.D., ZHOU, S., XIU, J., HASHIMOTO, Y., SANAI, N., KIM, L., KESARI, S., DE GROOT, J., SPETZLER, D. and HEIMBERGER, A.B., 2017. Ependymomas overexpress chemoresistance and DNA repair-related proteins. *Oncotarget,* **9**(8), pp. 7822-7831.

FERNANDEZ DE MATTOS, S., ESSAFI, A., SOEIRO, I., PIETERSEN, A.M., BIRKENKAMP, K.U., EDWARDS, C.S., MARTINO, A., NELSON, B.H., FRANCIS, J.M., JONES, M.C., BROSENS, J.J., COFFER, P.J. and LAM, E.W., 2004. FoxO3a and BCR-ABL regulate cyclin D2 transcription through a STAT5/BCL6-dependent mechanism. *Molecular and cellular biology,* **24**(22), pp. 10058-10071.

FIELD, S.J., TSAI, F.Y., KUO, F., ZUBIAGA, A.M., KAELIN, W.G.,Jr, LIVINGSTON, D.M., ORKIN, S.H. and GREENBERG, M.E., 1996. E2F-1 functions in mice to promote apoptosis and suppress proliferation. *Cell,* **85**(4), pp. 549-561.

FIGARELLA-BRANGER, D., CIVATTE, M., BOUVIER-LABIT, C., GOUVERNET, J., GAMBARELLI, D., GENTET, J.C., LENA, G., CHOUX, M. and PELLISSIER, J.F., 2000. Prognostic factors in intracranial ependymomas in children. *Journal of neurosurgery,* **93**(4), pp. 605-613.

FINGAR, D.C., RICHARDSON, C.J., TEE, A.R., CHEATHAM, L., TSOU, C. and BLENIS, J., 2004. mTOR controls cell cycle progression through its cell growth effectors S6K1 and 4E-BP1/eukaryotic translation initiation factor 4E. *Molecular and cellular biology,* **24**(1), pp. 200-216.

FISKUS, W., VERSTOVSEK, S., MANSHOURI, T., SMITH, J.E., PETH, K., ABHYANKAR, S., MCGUIRK, J. and BHALLA, K.N., 2013. Dual PI3K/AKT/mTOR inhibitor BEZ235 synergistically enhances the activity of JAK2 inhibitor against cultured and primary human myeloproliferative neoplasm cells. *Molecular cancer therapeutics,* **12**(5), pp. 577-588.

FOGLI, S., DANESI, R., DE BRAUD, F., DE PAS, T., CURIGLIANO, G., GIOVANNETTI, G. and DEL TACCA, M., 2001. Drug distribution and pharmacokinetic/pharmacodynamic relationship of paclitaxel and gemcitabine in patients with non-small-cell lung cancer. *Annals of oncology : official journal of the European Society for Medical Oncology,* **12**(11), pp. 1553-1559.

FOSTER, K.A., JANE, E.P., PREMKUMAR, D.R., MORALES, A. and POLLACK, I.F., 2015. NVP-BKM120 potentiates apoptosis in tumor necrosis factor-related apoptosis-inducing ligand-resistant glioma cell lines via upregulation of Noxa and death receptor 5. *International journal of oncology,* **47**(2), pp. 506-516.

FOULADI, M., STEWART, C.F., BLANEY, S.M., ONAR-THOMAS, A., SCHAIQUEVICH, P., PACKER, R.J., GOLDMAN, S., GEYER, J.R., GAJJAR, A., KUN, L.E., BOYETT, J.M. and GILBERTSON, R.J., 2013. A molecular biology and phase II trial of lapatinib in children with

refractory CNS malignancies: a pediatric brain tumor consortium study. *Journal of neuro-oncology,* **114**(2), pp. 173-179.

FRANZ, D.N., BELOUSOVA, E., SPARAGANA, S., BEBIN, E.M., FROST, M., KUPERMAN, R., WITT, O., KOHRMAN, M.H., FLAMINI, J.R., WU, J.Y., CURATOLO, P., DE VRIES, P.J., BERKOWITZ, N., ANAK, O., NIOLAT, J. and JOZWIAK, S., 2014. Everolimus for subependymal giant cell astrocytoma in patients with tuberous sclerosis complex: 2-year open-label extension of the randomised EXIST-1 study. *The Lancet.Oncology,* **15**(13), pp. 1513-1520.

FRASSON, C., RAMPAZZO, E., ACCORDI, B., BEGGIO, G., PISTOLLATO, F., BASSO, G. and PERSANO, L., 2015. Inhibition of PI3K Signalling Selectively Affects Medulloblastoma Cancer Stem Cells. *BioMed research international,* **2015**, pp. 973912.

FRESNO VARA, J.A., CASADO, E., DE CASTRO, J., CEJAS, P., BELDA-INIESTA, C. and GONZALEZ-BARON, M., 2004. PI3K/Akt signalling pathway and cancer. *Cancer treatment reviews,* **30**(2), pp. 193-204.

FRITSCH, C., HUANG, A., CHATENAY-RIVAUDAY, C., SCHNELL, C., REDDY, A., LIU, M., KAUFFMANN, A., GUTHY, D., ERDMANN, D., DE POVER, A., FURET, P., GAO, H., FERRETTI, S., WANG, Y., TRAPPE, J., BRACHMANN, S.M., MAIRA, S.M., WILSON, C., BOEHM, M., GARCIA-ECHEVERRIA, C., CHENE, P., WIESMANN, M., COZENS, R., LEHAR, J., SCHLEGEL, R., CARAVATTI, G., HOFMANN, F. and SELLERS, W.R., 2014. Characterization of the novel and specific PI3Kalpha inhibitor NVP-BYL719 and development of the patient stratification strategy for clinical trials. *Molecular cancer therapeutics,* **13**(5), pp. 1117-1129.

FRITSCH, R., DE KRIJGER, I., FRITSCH, K., GEORGE, R., REASON, B., KUMAR, M.S., DIEFENBACHER, M., STAMP, G. and DOWNWARD, J., 2013. RAS and RHO families of GTPases directly regulate distinct phosphoinositide 3-kinase isoforms. *Cell,* **153**(5), pp. 1050-1063.

FRUMAN, D.A., CHIU, H., HOPKINS, B.D., BAGRODIA, S., CANTLEY, L.C. and ABRAHAM, R.T., 2017. The PI3K Pathway in Human Disease. *Cell,* **170**(4), pp. 605-635.

FRUMAN, D.A. and ROMMEL, C., 2014. PI3K and cancer: lessons, challenges and opportunities. *Nature reviews.Drug discovery,* **13**(2), pp. 140-156.

FU, L., KIM, Y.A., WANG, X., WU, X., YUE, P., LONIAL, S., KHURI, F.R. and SUN, S.Y., 2009. Perifosine inhibits mammalian target of rapamycin signaling through facilitating degradation of major components in the mTOR axis and induces autophagy. *Cancer research,* **69**(23), pp. 8967-8976.

GADGIL, N., HANSEN, D., BARRY, J., CHANG, R. and LAM, S., 2016. Posterior fossa syndrome in children following tumor resection: Knowledge update. *Surgical neurology international,* **7**(Suppl 6), pp. S179-83.

GALLIA, G.L., RAND, V., SIU, I.M., EBERHART, C.G., JAMES, C.D., MARIE, S.K., OBA-SHINJO, S.M., CARLOTTI, C.G., CABALLERO, O.L., SIMPSON, A.J., BROCK, M.V., MASSION, P.P., CARSON BS, S. and RIGGINS, G.J., 2006. PIK3CA gene mutations in pediatric and adult glioblastoma multiforme. *Molecular cancer research : MCR,* **4**(10), pp. 709-714.

GAO, C., CAO, W., BAO, L., ZUO, W., XIE, G., CAI, T., FU, W., ZHANG, J., WU, W., ZHANG, X. and CHEN, Y.G., 2010. Autophagy negatively regulates Wnt signalling by promoting Dishevelled degradation. *Nature cell biology,* **12**(8), pp. 781-790.

GARCIA, Z., KUMAR, A., MARQUES, M., CORTES, I. and CARRERA, A.C., 2006. Phosphoinositide 3-kinase controls early and late events in mammalian cell division. *The EMBO journal,* **25**(4), pp. 655-661.

GARCIN, C.L. and HABIB, S.J., 2017. A Comparative Perspective on Wnt/beta-Catenin Signalling in Cell Fate Determination. *Results and problems in cell differentiation,* **61**, pp. 323-350.

GARLICH, J.R., DE, P., DEY, N., SU, J.D., PENG, X., MILLER, A., MURALI, R., LU, Y., MILLS, G.B., KUNDRA, V., SHU, H.K., PENG, Q. and DURDEN, D.L., 2008. A vascular targeted pan phosphoinositide 3-kinase inhibitor prodrug, SF1126, with antitumor and antiangiogenic activity. *Cancer research,* **68**(1), pp. 206-215.

GAROFALO, M., QUINTAVALLE, C., ROMANO, G., CROCE, C.M. and CONDORELLI, G., 2012. miR221/222 in cancer: their role in tumor progression and response to therapy. *Current Molecular Medicine,* **12**(1), pp. 27-33.

GARRETT, J.T., CHAKRABARTY, A. and ARTEAGA, C.L., 2011. Will PI3K pathway inhibitors be effective as single agents in patients with cancer? *Oncotarget,* **2**(12), pp. 1314-1321.

GARZON, R., MARCUCCI, G. and CROCE, C.M., 2010. Targeting microRNAs in cancer: rationale, strategies and challenges. *Nature reviews.Drug discovery,* **9**(10), pp. 775-789.

GEORGAKIS, G.V., LI, Y., RASSIDAKIS, G.Z., MEDEIROS, L.J., MILLS, G.B. and YOUNES, A., 2006. Inhibition of the phosphatidylinositol-3 kinase/Akt promotes G1 cell cycle arrest and apoptosis in Hodgkin lymphoma. *British journal of haematology,* **132**(4), pp. 503-511.

GHOBRIAL, I.M., ROCCARO, A., HONG, F., WELLER, E., RUBIN, N., LEDUC, R., ROURKE, M., CHUMA, S., SACCO, A., JIA, X., AZAB, F., AZAB, A.K., RODIG, S., WARREN, D., HARRIS, B., VARTICOVSKI, L., SPORTELLI, P., LELEU, X., ANDERSON, K.C. and RICHARDSON, P.G., 2010. Clinical and translational studies of a phase II trial of the novel oral Akt inhibitor perifosine in relapsed or relapsed/refractory Waldenstrom's macroglobulinemia. *Clinical cancer research : an official journal of the American Association for Cancer Research,* **16**(3), pp. 1033-1041.

GILBERTSON, R.J., BENTLEY, L., HERNAN, R., JUNTTILA, T.T., FRANK, A.J., HAAPASALO, H., CONNELLY, M., WETMORE, C., CURRAN, T., ELENIUS, K. and ELLISON, D.W., 2002. ERBB receptor signaling promotes ependymoma cell proliferation and represents a potential novel therapeutic target for this disease. *Clinical cancer research : an official journal of the American Association for Cancer Research,* **8**(10), pp. 3054-3064.

GILLS, J.J. and DENNIS, P.A., 2009. Perifosine: update on a novel Akt inhibitor. *Current oncology reports,* **11**(2), pp. 102-110.

GODFRAIND, C., KACZMARSKA, J.M., KOCAK, M., DALTON, J., WRIGHT, K.D., SANFORD, R.A., BOOP, F.A., GAJJAR, A., MERCHANT, T.E. and ELLISON, D.W., 2012. Distinct disease-risk

groups in pediatric supratentorial and posterior fossa ependymomas. *Acta Neuropathologica,* **124**(2), pp. 247-257.

GOEL, R., PHILLIPS-MASON, P.J., RABEN, D.M. and BALDASSARE, J.J., 2002. alpha-Thrombin induces rapid and sustained Akt phosphorylation by beta-arrestin1-dependent and -independent mechanisms, and only the sustained Akt phosphorylation is essential for G1 phase progression. *The Journal of biological chemistry,* **277**(21), pp. 18640-18648.

GONG, C., LIAO, H., WANG, J., LIN, Y., QI, J., QIN, L., TIAN, L.Q. and GUO, F.J., 2012. LY294002 induces G0/G1 cell cycle arrest and apoptosis of cancer stem-like cells from human osteosarcoma via down-regulation of PI3K activity. *Asian Pacific journal of cancer prevention : APJCP,* **13**(7), pp. 3103-3107.

GONZALEZ-GARCIA, A. and CARRERA, A.C., 2012. P85beta Increases Phosphoinositide 3-Kinase Activity and Accelerates Tumor Progression. *Cell cycle (Georgetown, Tex.),* **11**(19), pp. 3523-3524.

GRAUPERA, M., GUILLERMET-GUIBERT, J., FOUKAS, L.C., PHNG, L.K., CAIN, R.J., SALPEKAR, A., PEARCE, W., MEEK, S., MILLAN, J., CUTILLAS, P.R., SMITH, A.J., RIDLEY, A.J., RUHRBERG, C., GERHARDT, H. and VANHAESEBROECK, B., 2008. Angiogenesis selectively requires the p110alpha isoform of PI3K to control endothelial cell migration. *Nature,* **453**(7195), pp. 662-666.

GREEN, D.R., 2000. Apoptotic pathways: paper wraps stone blunts scissors. *Cell,* **102**(1), pp. 1-4.

GREENBERGER, B.A., PULSIFER, M.B., EBB, D.H., MACDONALD, S.M., JONES, R.M., BUTLER, W.E., HUANG, M.S., MARCUS, K.J., OBERG, J.A., TARBELL, N.J. and YOCK, T.I., 2014. Clinical outcomes and late endocrine, neurocognitive, and visual profiles of proton radiation for pediatric low-grade gliomas. *International journal of radiation oncology, biology, physics,* **89**(5), pp. 1060-1068.

GREER, E.L. and BRUNET, A., 2005. FOXO transcription factors at the interface between longevity and tumor suppression. *Oncogene,* **24**(50), pp. 7410-7425.

GRILL, J., LE DELEY, M.C., GAMBARELLI, D., RAQUIN, M.A., COUANET, D., PIERRE-KAHN, A., HABRAND, J.L., DOZ, F., FRAPPAZ, D., GENTET, J.C., EDAN, C., CHASTAGNER, P., KALIFA, C. and FRENCH SOCIETY OF PEDIATRIC ONCOLOGY, 2001. Postoperative chemotherapy without irradiation for ependymoma in children under 5 years of age: a multicenter trial of the French Society of Pediatric Oncology. *Journal of clinical oncology : official journal of the American Society of Clinical Oncology,* **19**(5), pp. 1288-1296.

GRILL, J., PUGET, S., ANDREIUOLO, F., PHILIPPE, C., MACCONAILL, L. and KIERAN, M.W., 2012. Critical oncogenic mutations in newly diagnosed pediatric diffuse intrinsic pontine glioma. *Pediatric blood & cancer,* **58**(4), pp. 489-491.

GRILL, J., RENAUX, V.K., BULTEAU, C., VIGUIER, D., LEVY-PIEBOIS, C., SAINTE-ROSE, C., DELLATOLAS, G., RAQUIN, M.A., JAMBAQUE, I. and KALIFA, C., 1999. Long-term intellectual outcome in children with posterior fossa tumors according to radiation doses and volumes. *International journal of radiation oncology, biology, physics,* **45**(1), pp. 137-145.

GRITSMAN, K., YUZUGULLU, H., VON, T., YAN, H., CLAYTON, L., FRITSCH, C., MAIRA, S.M., HOLLINGWORTH, G., CHOI, C., KHANDAN, T., PAKTINAT, M., OKABE, R.O., ROBERTS, T.M. and ZHAO, J.J., 2014. Hematopoiesis and RAS-driven myeloid leukemia differentially require PI3K isoform p110alpha. *The Journal of clinical investigation,* **124**(4), pp. 1794-1809.

GROOTHUIS, D.R., 2000. The blood-brain and blood-tumor barriers: a review of strategies for increasing drug delivery. *Neuro-oncology,* **2**(1), pp. 45-59.

GRUNDY, R.G., WILNE, S.A., WESTON, C.L., ROBINSON, K., LASHFORD, L.S., IRONSIDE, J., COX, T., CHONG, W.K., CAMPBELL, R.H., BAILEY, C.C., GATTAMANENI, R., PICTON, S., THORPE, N., MALLUCCI, C., ENGLISH, M.W., PUNT, J.A., WALKER, D.A., ELLISON, D.W., MACHIN, D. and CHILDREN'S CANCER AND LEUKAEMIA GROUP (FORMERLY UKCCSG) BRAIN TUMOUR COMMITTEE, 2007. Primary postoperative chemotherapy without radiotherapy for intracranial ependymoma in children: the UKCCSG/SIOP prospective study. *The Lancet.Oncology,* **8**(8), pp. 696-705.

GUAL, P., BARON, V., LEQUOY, V. and VAN OBBERGHEN, E., 1998. Interaction of Janus kinases JAK-1 and JAK-2 with the insulin receptor and the insulin-like growth factor-1 receptor. *Endocrinology,* **139**(3), pp. 884-893.

GUERREIRO, A.S., FATTET, S., KULESZA, D.W., ATAMER, A., ELSING, A.N., SHALABY, T., JACKSON, S.P., SCHOENWAELDER, S.M., GROTZER, M.A., DELATTRE, O. and ARCARO, A., 2011. A sensitized RNA interference screen identifies a novel role for the PI3K p110gamma isoform in medulloblastoma cell proliferation and chemoresistance. *Molecular cancer research : MCR,* **9**(7), pp. 925-935.

GUILLAMO, J.S., CREANGE, A., KALIFA, C., GRILL, J., RODRIGUEZ, D., DOZ, F., BARBAROT, S., ZERAH, M., SANSON, M., BASTUJI-GARIN, S., WOLKENSTEIN, P. and RESEAU NF FRANCE, 2003. Prognostic factors of CNS tumours in Neurofibromatosis 1 (NF1): a retrospective study of 104 patients. *Brain : a journal of neurology,* **126**(Pt 1), pp. 152-160.

GUILLAUME, D.J., JOHNSON, M.A., LI, X.J. and ZHANG, S.C., 2006. Human embryonic stem cell-derived neural precursors develop into neurons and integrate into the host brain. *Journal of neuroscience research,* **84**(6), pp. 1165-1176.

GURA, T., 1997. How TRAIL kills cancer cells, but not normal cells. *Science (New York, N.Y.),* **277**(5327), pp. 768.

GUTTRIDGE, D.C., ALBANESE, C., REUTHER, J.Y., PESTELL, R.G. and BALDWIN, A.S.,Jr, 1999. NF-kappaB controls cell growth and differentiation through transcriptional regulation of cyclin D1. *Molecular and cellular biology,* **19**(8), pp. 5785-5799.

HAAS, B., KLINGER, V., KEKSEL, C., BONIGUT, V., KIEFER, D., CASPERS, J., WALTHER, J., WOS-MAGANGA, M., WEICKHARDT, S., ROHN, G., TIMMER, M., FROTSCHL, R. and ECKSTEIN, N., 2018. Inhibition of the PI3K but not the MEK/ERK pathway sensitizes human glioma cells to alkylating drugs. *Cancer cell international,* **18**, pp. 69-018-0565-4. eCollection 2018.

HALLSTROM, T.C., MORI, S. and NEVINS, J.R., 2008. An E2F1-dependent gene expression program that determines the balance between proliferation and cell death. *Cancer cell,* **13**(1), pp. 11-22.

HANAFUSA, H., TORII, S., YASUNAGA, T. and NISHIDA, E., 2002. Sprouty1 and Sprouty2 provide a control mechanism for the Ras/MAPK signalling pathway. *Nature cell biology,* **4**(11), pp. 850-858.

HARBOUR, J.W. and DEAN, D.C., 2000. The Rb/E2F pathway: expanding roles and emerging paradigms. *Genes & development,* **14**(19), pp. 2393-2409.

HARDIE, D.G., 2007. AMP-activated/SNF1 protein kinases: conserved guardians of cellular energy. *Nature reviews.Molecular cell biology,* **8**(10), pp. 774-785.

HARESH, K.P., GANDHI, A.K., MALLICK, S., BENSON, R., GUPTA, S., SHARMA, D.N., JULKA, P.K. and RATH, G.K., 2017. Prognostic Factors and Survival Outcomes of Intracranial Ependymoma Treated with Multimodality Approach. *Indian journal of medical and paediatric oncology : official journal of Indian Society of Medical & Paediatric Oncology,* **38**(4), pp. 420-426.

HARTMANN, W., DIGON-SONTGERATH, B., KOCH, A., WAHA, A., ENDL, E., DANI, I., DENKHAUS, D., GOODYER, C.G., SORENSEN, N., WIESTLER, O.D. and PIETSCH, T., 2006. Phosphatidylinositol 3'-kinase/AKT signaling is activated in medulloblastoma cell proliferation and is associated with reduced expression of PTEN. *Clinical cancer research : an official journal of the American Association for Cancer Research,* **12**(10), pp. 3019-3027.

HAY, N., 2011. Interplay between FOXO, TOR, and Akt. *Biochimica et biophysica acta,* **1813**(11), pp. 1965-1970.

HE, H., LEVITZKI, A., ZHU, H.J., WALKER, F., BURGESS, A. and MARUTA, H., 2001. Platelet-derived growth factor requires epidermal growth factor receptor to activate p21-activated kinase family kinases. *The Journal of biological chemistry,* **276**(29), pp. 26741-26744.

HEFFRON, T.P., NDUBAKU, C.O., SALPHATI, L., ALICKE, B., CHEONG, J., DROBNICK, J., EDGAR, K., GOULD, S.E., LEE, L.B., LESNICK, J.D., LEWIS, C., NONOMIYA, J., PANG, J., PLISE, E.G., SIDERIS, S., WALLIN, J., WANG, L., ZHANG, X. and OLIVERO, A.G., 2016. Discovery of Clinical Development Candidate GDC-0084, a Brain Penetrant Inhibitor of PI3K and mTOR. *ACS medicinal chemistry letters,* **7**(4), pp. 351-356.

HERON-MILHAVET, L., FRANCKHAUSER, C., RANA, V., BERTHENET, C., FISHER, D., HEMMINGS, B.A., FERNANDEZ, A. and LAMB, N.J., 2006. Only Akt1 is required for proliferation, while Akt2 promotes cell cycle exit through p21 binding. *Molecular and cellular biology,* **26**(22), pp. 8267-8280.

HOBBS, G.A., DER, C.J. and ROSSMAN, K.L., 2016. RAS isoforms and mutations in cancer at a glance. *Journal of cell science,* **129**(7), pp. 1287-1292.

HOELLENRIEGEL, J., MEADOWS, S.A., SIVINA, M., WIERDA, W.G., KANTARJIAN, H., KEATING, M.J., GIESE, N., O'BRIEN, S., YU, A., MILLER, L.L., LANNUTTI, B.J. and BURGER, J.A., 2011. The phosphoinositide 3'-kinase delta inhibitor, CAL-101, inhibits B-cell receptor signaling and chemokine networks in chronic lymphocytic leukemia. *Blood,* **118**(13), pp. 3603-3612.

HOFFMAN, L.M., DONSON, A.M., NAKACHI, I., GRIESINGER, A.M., BIRKS, D.K., AMANI, V., HEMENWAY, M.S., LIU, A.K., WANG, M., HANKINSON, T.C., HANDLER, M.H. and FOREMAN, N.K., 2014. Molecular sub-group-specific immunophenotypic changes are associated with

outcome in recurrent posterior fossa ependymoma. *Acta Neuropathologica,* **127**(5), pp. 731-745.

HOLAND, K., SALM, F. and ARCARO, A., 2011. The phosphoinositide 3-kinase signaling pathway as a therapeutic target in grade IV brain tumors. *Current cancer drug targets,* **11**(8), pp. 894-918.

HOMEWOOD, C.A., WARHURST, D.C., PETERS, W. and BAGGALEY, V.C., 1972. Lysosomes, pH and the anti-malarial action of chloroquine. *Nature,* **235**(5332), pp. 50-52.

HONEYWELL, R.J., RUIZ VAN HAPEREN, V.W., VEERMAN, G., SMID, K. and PETERS, G.J., 2015. Inhibition of thymidylate synthase by 2',2'-difluoro-2'-deoxycytidine (Gemcitabine) and its metabolite 2',2'-difluoro-2'-deoxyuridine. *The international journal of biochemistry & cell biology,* **60**, pp. 73-81.

HONG, D.S., BOWLES, D.W., FALCHOOK, G.S., MESSERSMITH, W.A., GEORGE, G.C., O'BRYANT, C.L., VO, A.C., KLUCHER, K., HERBST, R.S., ECKHARDT, S.G., PETERSON, S., HAUSMAN, D.F., KURZROCK, R. and JIMENO, A., 2012. A multicenter phase I trial of PX-866, an oral irreversible phosphatidylinositol 3-kinase inhibitor, in patients with advanced solid tumors. *Clinical cancer research : an official journal of the American Association for Cancer Research,* **18**(15), pp. 4173-4182.

HOWELL, J.J. and MANNING, B.D., 2011. mTOR couples cellular nutrient sensing to organismal metabolic homeostasis. *Trends in endocrinology and metabolism: TEM,* **22**(3), pp. 94-102.

HSU, J. and SAGE, J., 2016. Novel functions for the transcription factor E2F4 in development and disease. *Cell cycle (Georgetown, Tex.),* **15**(23), pp. 3183-3190.

HU, R., WANG, E., PENG, G., DAI, H. and LIN, S.Y., 2013. Zinc finger protein 668 interacts with Tip60 to promote H2AX acetylation after DNA damage. *Cell cycle (Georgetown, Tex.),* **12**(13), pp. 2033-2041.

HU, Y., GUO, R., WEI, J., ZHOU, Y., JI, W., LIU, J., ZHI, X. and ZHANG, J., 2015. Effects of PI3K inhibitor NVP-BKM120 on overcoming drug resistance and eliminating cancer stem cells in human breast cancer cells. *Cell death & disease,* **6**, pp. e2020.

HUANG DA, W., SHERMAN, B.T. and LEMPICKI, R.A., 2009. Systematic and integrative analysis of large gene lists using DAVID bioinformatics resources. *Nature protocols,* **4**(1), pp. 44-57.

HUANG, H., REGAN, K.M., LOU, Z., CHEN, J. and TINDALL, D.J., 2006. CDK2-dependent phosphorylation of FOXO1 as an apoptotic response to DNA damage. *Science (New York, N.Y.),* **314**(5797), pp. 294-297.

HUANG, H. and TINDALL, D.J., 2011. Regulation of FOXO protein stability via ubiquitination and proteasome degradation. *Biochimica et biophysica acta,* **1813**(11), pp. 1961-1964.

HUANG, H. and TINDALL, D.J., 2007. Dynamic FoxO transcription factors. *Journal of cell science,* **120**(Pt 15), pp. 2479-2487.

HUDES, G.R., BERKENBLIT, A., FEINGOLD, J., ATKINS, M.B., RINI, B.I. and DUTCHER, J., 2009. Clinical trial experience with temsirolimus in patients with advanced renal cell carcinoma. *Seminars in oncology,* **36 Suppl 3**, pp. S26-36.

HURWITZ, C.A., STRAUSS, L.C., KEPNER, J., KRETSCHMAR, C., HARRIS, M.B., FRIEDMAN, H., KUN, L. and KADOTA, R., 2001. Paclitaxel for the treatment of progressive or recurrent childhood brain tumors: a pediatric oncology phase II study. *Journal of pediatric hematology/oncology,* **23**(5), pp. 277-281.

HUSSEIN, D., PUNJARUK, W., STORER, L.C., SHAW, L., OTHMAN, R., PEET, A., MILLER, S., BANDOPADHYAY, G., HEATH, R., KUMARI, R., BOWMAN, K.J., BRAKER, P., RAHMAN, R., JONES, G.D., WATSON, S., LOWE, J., KERR, I.D., GRUNDY, R.G. and COYLE, B., 2011. Pediatric brain tumor cancer stem cells: cell cycle dynamics, DNA repair, and etoposide extrusion. *Neuro-oncology,* **13**(1), pp. 70-83.

HUTTER, S., BOLIN, S., WEISHAUPT, H. and SWARTLING, F.J., 2017. Modeling and Targeting MYC Genes in Childhood Brain Tumors. *Genes,* **8**(4), pp. 10.3390/genes8040107.

HYMAN, D.M., SMYTH, L.M., DONOGHUE, M.T.A., WESTIN, S.N., BEDARD, P.L., DEAN, E.J., BANDO, H., EL-KHOUEIRY, A.B., PEREZ-FIDALGO, J.A., MITA, A., SCHELLENS, J.H.M., CHANG, M.T., REICHEL, J.B., BOUVIER, N., SELCUKLU, S.D., SOUMERAI, T.E., TORRISI, J., ERINJERI, J.P., AMBROSE, H., BARRETT, J.C., DOUGHERTY, B., FOXLEY, A., LINDEMANN, J.P.O., MCEWEN, R., PASS, M., SCHIAVON, G., BERGER, M.F., CHANDARLAPATY, S., SOLIT, D.B., BANERJI, U., BASELGA, J. and TAYLOR, B.S., 2017. AKT Inhibition in Solid Tumors With AKT1 Mutations. *Journal of clinical oncology : official journal of the American Society of Clinical Oncology,* **35**(20), pp. 2251-2259.

INOKI, K., LI, Y., XU, T. and GUAN, K.L., 2003. Rheb GTPase is a direct target of TSC2 GAP activity and regulates mTOR signaling. *Genes & development,* **17**(15), pp. 1829-1834.

IRIE, H.Y., PEARLINE, R.V., GRUENEBERG, D., HSIA, M., RAVICHANDRAN, P., KOTHARI, N., NATESAN, S. and BRUGGE, J.S., 2005. Distinct roles of Akt1 and Akt2 in regulating cell migration and epithelial-mesenchymal transition. *The Journal of cell biology,* **171**(6), pp. 1023-1034.

ISAKOFF, S.J., ENGELMAN, J.A., IRIE, H.Y., LUO, J., BRACHMANN, S.M., PEARLINE, R.V., CANTLEY, L.C. and BRUGGE, J.S., 2005. Breast cancer-associated PIK3CA mutations are oncogenic in mammary epithelial cells. *Cancer research,* **65**(23), pp. 10992-11000.

ISHIKAWA, C., SENBA, M. and MORI, N., 2018. Effects of NVP-BEZ235, a dual phosphatidylinositol 3-kinase/mammalian target of rapamycin inhibitor, on HTLV-1-infected T-cell lines. *Oncology letters,* **15**(4), pp. 5311-5317.

JABER, N. and ZONG, W.X., 2013. Class III PI3K Vps34: essential roles in autophagy, endocytosis, and heart and liver function. *Annals of the New York Academy of Sciences,* **1280**, pp. 48-51.

JACINTO, E., LOEWITH, R., SCHMIDT, A., LIN, S., RUEGG, M.A., HALL, A. and HALL, M.N., 2004. Mammalian TOR complex 2 controls the actin cytoskeleton and is rapamycin insensitive. *Nature cell biology,* **6**(11), pp. 1122-1128.

JACKS, T., FAZELI, A., SCHMITT, E.M., BRONSON, R.T., GOODELL, M.A. and WEINBERG, R.A., 1992. Effects of an Rb mutation in the mouse. *Nature,* **359**(6393), pp. 295-300.

JACKSON, E.L., GARCIA-VERDUGO, J.M., GIL-PEROTIN, S., ROY, M., QUINONES-HINOJOSA, A., VANDENBERG, S. and ALVAREZ-BUYLLA, A., 2006. PDGFR alpha-positive B cells are neural stem cells in the adult SVZ that form glioma-like growths in response to increased PDGF signaling. *Neuron,* **51**(2), pp. 187-199.

JACOBS, F.M., VAN DER HEIDE, L.P., WIJCHERS, P.J., BURBACH, J.P., HOEKMAN, M.F. and SMIDT, M.P., 2003. FoxO6, a novel member of the FoxO class of transcription factors with distinct shuttling dynamics. *The Journal of biological chemistry,* **278**(38), pp. 35959-35967.

JAISWAL, B.S., JANAKIRAMAN, V., KLJAVIN, N.M., CHAUDHURI, S., STERN, H.M., WANG, W., KAN, Z., DBOUK, H.A., PETERS, B.A., WARING, P., DELA VEGA, T., KENSKI, D.M., BOWMAN, K.K., LORENZO, M., LI, H., WU, J., MODRUSAN, Z., STINSON, J., EBY, M., YUE, P., KAMINKER, J.S., DE SAUVAGE, F.J., BACKER, J.M. and SESHAGIRI, S., 2009. Somatic mutations in p85alpha promote tumorigenesis through class IA PI3K activation. *Cancer cell,* **16**(6), pp. 463-474.

JAKACKI, R.I., HAMILTON, M., GILBERTSON, R.J., BLANEY, S.M., TERSAK, J., KRAILO, M.D., INGLE, A.M., VOSS, S.D., DANCEY, J.E. and ADAMSON, P.C., 2008. Pediatric phase I and pharmacokinetic study of erlotinib followed by the combination of erlotinib and temozolomide: a Children's Oncology Group Phase I Consortium Study. *Journal of clinical oncology : official journal of the American Society of Clinical Oncology,* **26**(30), pp. 4921-4927.

JANKU, F., 2017. Phosphoinositide 3-kinase (PI3K) pathway inhibitors in solid tumors: From laboratory to patients. *Cancer treatment reviews,* **59**, pp. 93-101.

JI, W., SUN, B. and SU, C., 2017. Targeting MicroRNAs in Cancer Gene Therapy. *Genes,* **8**(1), pp. 10.3390/genes8010021.

JIA, S., LIU, Z., ZHANG, S., LIU, P., ZHANG, L., LEE, S.H., ZHANG, J., SIGNORETTI, S., LODA, M., ROBERTS, T.M. and ZHAO, J.J., 2008. Essential roles of PI(3)K-p110beta in cell growth, metabolism and tumorigenesis. *Nature,* **454**(7205), pp. 776-779.

JIANG, H., COLEMAN, J., MISKIMINS, R. and MISKIMINS, W.K., 2003. Expression of constitutively active 4EBP-1 enhances p27Kip1 expression and inhibits proliferation of MCF7 breast cancer cells. *Cancer cell international,* **3**(1), pp. 2.

JOHANSSON, G., ANDERSSON, U. and MELIN, B., 2016. Recent developments in brain tumor predisposing syndromes. *Acta Oncologica (Stockholm, Sweden),* **55**(4), pp. 401-411.

JOHNSON, P.F., 2005. Molecular stop signs: regulation of cell-cycle arrest by C/EBP transcription factors. *Journal of cell science,* **118**(Pt 12), pp. 2545-2555.

JOHNSON, R.A., WRIGHT, K.D., POPPLETON, H., MOHANKUMAR, K.M., FINKELSTEIN, D., POUNDS, S.B., RAND, V., LEARY, S.E., WHITE, E., EDEN, C., HOGG, T., NORTHCOTT, P., MACK, S., NEALE, G., WANG, Y.D., COYLE, B., ATKINSON, J., DEWIRE, M., KRANENBURG, T.A., GILLESPIE, Y., ALLEN, J.C., MERCHANT, T., BOOP, F.A., SANFORD, R.A., GAJJAR, A., ELLISON, D.W., TAYLOR, M.D., GRUNDY, R.G. and GILBERTSON, R.J., 2010. Cross-species

genomics matches driver mutations and cell compartments to model ependymoma. *Nature,* **466**(7306), pp. 632-636.

JUNG, K.H., YAN, H.H., FANG, Z., SON, M.K., LEE, H., HONG, S. and HONG, S.S., 2014. HS-104, a PI3K inhibitor, enhances the anticancer efficacy of gemcitabine in pancreatic cancer. *International journal of oncology,* **45**(1), pp. 311-321.

JUVEKAR, A., HU, H., YADEGARYNIA, S., LYSSIOTIS, C.A., ULLAS, S., LIEN, E.C., BELLINGER, G., SON, J., HOK, R.C., SETH, P., DALY, M.B., KIM, B., SCULLY, R., ASARA, J.M., CANTLEY, L.C. and WULF, G.M., 2016. Phosphoinositide 3-kinase inhibitors induce DNA damage through nucleoside depletion. *Proceedings of the National Academy of Sciences of the United States of America,* **113**(30), pp. E4338-47.

KADOCH, C., HARGREAVES, D.C., HODGES, C., ELIAS, L., HO, L., RANISH, J. and CRABTREE, G.R., 2013. Proteomic and bioinformatic analysis of mammalian SWI/SNF complexes identifies extensive roles in human malignancy. *Nature genetics,* **45**(6), pp. 592-601.

KAGAWA, S., TAKANO, S., YOSHITOMI, H., KIMURA, F., SATOH, M., SHIMIZU, H., YOSHIDOME, H., OHTSUKA, M., KATO, A., FURUKAWA, K., MATSUSHITA, K., NOMURA, F. and MIYAZAKI, M., 2012. Akt/mTOR signaling pathway is crucial for gemcitabine resistance induced by Annexin II in pancreatic cancer cells. *The Journal of surgical research,* **178**(2), pp. 758-767.

KANDASAMY, K. and SRIVASTAVA, R.K., 2002. Role of the phosphatidylinositol 3'-kinase/PTEN/Akt kinase pathway in tumor necrosis factor-related apoptosis-inducing ligand-induced apoptosis in non-small cell lung cancer cells. *Cancer research,* **62**(17), pp. 4929-4937.

KANDEL, E.S., SKEEN, J., MAJEWSKI, N., DI CRISTOFANO, A., PANDOLFI, P.P., FELICIANO, C.S., GARTEL, A. and HAY, N., 2002. Activation of Akt/protein kinase B overcomes a G(2)/m cell cycle checkpoint induced by DNA damage. *Molecular and cellular biology,* **22**(22), pp. 7831-7841.

KANG, S., BADER, A.G. and VOGT, P.K., 2005. Phosphatidylinositol 3-kinase mutations identified in human cancer are oncogenic. *Proceedings of the National Academy of Sciences of the United States of America,* **102**(3), pp. 802-807.

KANG, S., DENLEY, A., VANHAESEBROECK, B. and VOGT, P.K., 2006. Oncogenic transformation induced by the p110beta, -gamma, and -delta isoforms of class I phosphoinositide 3-kinase. *Proceedings of the National Academy of Sciences of the United States of America,* **103**(5), pp. 1289-1294.

KARAKAS, B., BACHMAN, K.E. and PARK, B.H., 2006. Mutation of the PIK3CA oncogene in human cancers. *British journal of cancer,* **94**(4), pp. 455-459.

KARNITZ, L.M., FLATTEN, K.S., WAGNER, J.M., LOEGERING, D., HACKBARTH, J.S., ARLANDER, S.J., VROMAN, B.T., THOMAS, M.B., BAEK, Y.U., HOPKINS, K.M., LIEBERMAN, H.B., CHEN, J., CLIBY, W.A. and KAUFMANN, S.H., 2005. Gemcitabine-induced activation of checkpoint signaling pathways that affect tumor cell survival. *Molecular pharmacology,* **68**(6), pp. 1636-1644.

KATAYAMA, K., NAKAMURA, A., SUGIMOTO, Y., TSURUO, T. and FUJITA, N., 2008. FOXO transcription factor-dependent p15(INK4b) and p19(INK4d) expression. *Oncogene,* **27**(12), pp. 1677-1686.

KAYSER, M.S., NOLT, M.J. and DALVA, M.B., 2008. EphB receptors couple dendritic filopodia motility to synapse formation. *Neuron,* **59**(1), pp. 56-69.

KIHARA, A., NODA, T., ISHIHARA, N. and OHSUMI, Y., 2001. Two distinct Vps34 phosphatidylinositol 3-kinase complexes function in autophagy and carboxypeptidase Y sorting in Saccharomyces cerevisiae. *The Journal of cell biology,* **152**(3), pp. 519-530.

KIKUCHI, S., NAGAI, T., KUNITAMA, M., KIRITO, K., OZAWA, K. and KOMATSU, N., 2007. Active FKHRL1 overcomes imatinib resistance in chronic myelogenous leukemia-derived cell lines via the production of tumor necrosis factor-related apoptosis-inducing ligand. *Cancer science,* **98**(12), pp. 1949-1958.

KILDAY, J.P., RAHMAN, R., DYER, S., RIDLEY, L., LOWE, J., COYLE, B. and GRUNDY, R., 2009. Pediatric ependymoma: biological perspectives. *Molecular cancer research : MCR,* **7**(6), pp. 765-786.

KIM, J.E. and CHEN, J., 2004. Regulation of Peroxisome Proliferator-Activated Receptor-Gamma Activity by Mammalian Target of Rapamycin and Amino Acids in Adipogenesis. *Diabetes,* **53**(11), pp. 2748-2756.

KIM, R., OSAKI, A. and TOGE, T., 2001. Pharmacokinetic and biochemical analysis in the treatment of weekly paclitaxel in relapsed breast cancer. *Oncology reports,* **8**(5), pp. 1171-1176.

KIM, S.J., LEE, H.W., BAEK, J.H., CHO, Y.H., KANG, H.G., JEONG, J.S., SONG, J., PARK, H.S. and CHUN, K.H., 2016. Activation of nuclear PTEN by inhibition of Notch signaling induces G2/M cell cycle arrest in gastric cancer. *Oncogene,* **35**(2), pp. 251-260.

KIND, M., KLUKOWSKA-ROTZLER, J., BEREZOWSKA, S., ARCARO, A. and CHARLES, R.P., 2017. Questioning the role of selected somatic PIK3C2B mutations in squamous non-small cell lung cancer oncogenesis. *PloS one,* **12**(10), pp. e0187308.

KIRSCH, D.G. and TARBELL, N.J., 2004. New technologies in radiation therapy for pediatric brain tumors: the rationale for proton radiation therapy. *Pediatric blood & cancer,* **42**(5), pp. 461-464.

KITAGAWA, M., 2016. Notch signalling in the nucleus: roles of Mastermind-like (MAML) transcriptional coactivators. *Journal of Biochemistry,* **159**(3), pp. 287-294.

KNOBBE, C.B. and REIFENBERGER, G., 2003. Genetic alterations and aberrant expression of genes related to the phosphatidyl-inositol-3'-kinase/protein kinase B (Akt) signal transduction pathway in glioblastomas. *Brain pathology (Zurich, Switzerland),* **13**(4), pp. 507-518.

KOLASA, I.K., REMBISZEWSKA, A., FELISIAK, A., ZIOLKOWSKA-SETA, I., MURAWSKA, M., MOES, J., TIMOREK, A., DANSONKA-MIESZKOWSKA, A. and KUPRYJANCZYK, J., 2009. PIK3CA

amplification associates with resistance to chemotherapy in ovarian cancer patients. *Cancer biology & therapy,* **8**(1), pp. 21-26.

KOOS, B., BENDER, S., WITT, H., MERTSCH, S., FELSBERG, J., BESCHORNER, R., KORSHUNOV, A., RIESMEIER, B., PFISTER, S., PAULUS, W. and HASSELBLATT, M., 2011. The transcription factor evi-1 is overexpressed, promotes proliferation, and is prognostically unfavorable in infratentorial ependymomas. *Clinical cancer research : an official journal of the American Association for Cancer Research,* **17**(11), pp. 3631-3637.

KOPS, G.J., MEDEMA, R.H., GLASSFORD, J., ESSERS, M.A., DIJKERS, P.F., COFFER, P.J., LAM, E.W. and BURGERING, B.M., 2002. Control of cell cycle exit and entry by protein kinase B-regulated forkhead transcription factors. *Molecular and cellular biology,* **22**(7), pp. 2025-2036.

KORSHUNOV, A., GOLANOV, A. and TIMIRGAZ, V., 2002. Immunohistochemical markers for prognosis of ependymal neoplasms. *Journal of neuro-oncology,* **58**(3), pp. 255-270.

KORSHUNOV, A., GOLANOV, A. and TIMIRGAZ, V., 2000. Immunohistochemical markers for intracranial ependymoma recurrence. An analysis of 88 cases. *Journal of the neurological sciences,* **177**(1), pp. 72-82.

KOSEOGLU, S., LU, Z., KUMAR, C., KIRSCHMEIER, P. and ZOU, J., 2007. AKT1, AKT2 and AKT3-dependent cell survival is cell line-specific and knockdown of all three isoforms selectively induces apoptosis in 20 human tumor cell lines. *Cancer biology & therapy,* **6**(5), pp. 755-762.

KOUL, D., FU, J., SHEN, R., LAFORTUNE, T.A., WANG, S., TIAO, N., KIM, Y.W., LIU, J.L., RAMNARIAN, D., YUAN, Y., GARCIA-ECHEVRRIA, C., MAIRA, S.M. and YUNG, W.K., 2012. Antitumor activity of NVP-BKM120--a selective pan class I PI3 kinase inhibitor showed differential forms of cell death based on p53 status of glioma cells. *Clinical cancer research : an official journal of the American Association for Cancer Research,* **18**(1), pp. 184-195.

KOUL, D., SHEN, R., KIM, Y.W., KONDO, Y., LU, Y., BANKSON, J., RONEN, S.M., KIRKPATRICK, D.L., POWIS, G. and YUNG, W.K., 2010. Cellular and in vivo activity of a novel PI3K inhibitor, PX-866, against human glioblastoma. *Neuro-oncology,* **12**(6), pp. 559-569.

KROEMER, G. and LEVINE, B., 2008. Autophagic cell death: the story of a misnomer. *Nature reviews.Molecular cell biology,* **9**(12), pp. 1004-1010.

KUMAR, A. and CARRERA, A.C., 2007. New functions for PI3K in the control of cell division. *Cell cycle (Georgetown, Tex.),* **6**(14), pp. 1696-1698.

KWIATKOWSKI, D.J. and MANNING, B.D., 2005. Tuberous sclerosis: a GAP at the crossroads of multiple signaling pathways. *Human molecular genetics,* **14 Spec No. 2**, pp. R251-8.

LAI, Z.Y., YEO, H.Y., CHEN, Y.T., CHANG, K.M., CHEN, T.C., CHUANG, Y.J. and CHANG, S.J., 2017. PI3K inhibitor enhances the cytotoxic response to etoposide and cisplatin in a newly established neuroendocrine cervical carcinoma cell line. *Oncotarget,* **8**(28), pp. 45323-45334.

LAL, M.A., BAE, D., CAMILLI, T.C., PATIERNO, S.R. and CERYAK, S., 2009. AKT1 mediates bypass of the G1/S checkpoint after genotoxic stress in normal human cells. *Cell cycle (Georgetown, Tex.),* **8**(10), pp. 1589-1602.

LANG, F., STRUTZ-SEEBOHM, N., SEEBOHM, G. and LANG, U.E., 2010. Significance of SGK1 in the regulation of neuronal function. *The Journal of physiology,* **588**(Pt 18), pp. 3349-3354.

LASITHIOTAKIS, K.G., SINNBERG, T.W., SCHITTEK, B., FLAHERTY, K.T., KULMS, D., MACZEY, E., GARBE, C. and MEIER, F.E., 2008. Combined inhibition of MAPK and mTOR signaling inhibits growth, induces cell death, and abrogates invasive growth of melanoma cells. *The Journal of investigative dermatology,* **128**(8), pp. 2013-2023.

LAU, C.J., KOTY, Z. and NALBANTOGLU, J., 2009. Differential response of glioma cells to FOXO1-directed therapy. *Cancer research,* **69**(13), pp. 5433-5440.

LEENDERS, A.G., LOPES DA SILVA, F.H., GHIJSEN, W.E. and VERHAGE, M., 2001. Rab3a is involved in transport of synaptic vesicles to the active zone in mouse brain nerve terminals. *Molecular biology of the cell,* **12**(10), pp. 3095-3102.

LEFRANC, F., BROTCHI, J. and KISS, R., 2005. Possible future issues in the treatment of glioblastomas: special emphasis on cell migration and the resistance of migrating glioblastoma cells to apoptosis. *Journal of clinical oncology : official journal of the American Society of Clinical Oncology,* **23**(10), pp. 2411-2422.

LEHMAN, N.L., 2008. Central nervous system tumors with ependymal features: a broadened spectrum of primarily ependymal differentiation? *Journal of neuropathology and experimental neurology,* **67**(3), pp. 177-188.

LI, J.M., HU, P.P., SHEN, X., YU, Y. and WANG, X.F., 1997. E2F4-RB and E2F4-p107 complexes suppress gene expression by transforming growth factor beta through E2F binding sites. *Proceedings of the National Academy of Sciences of the United States of America,* **94**(10), pp. 4948-4953.

LI, S., HUANG, S. and PENG, S.B., 2005. Overexpression of G protein-coupled receptors in cancer cells: involvement in tumor progression. *International journal of oncology,* **27**(5), pp. 1329-1339.

LI, Z., DAI, K., WANG, C., SONG, Y., GU, F., LIU, F. and FU, L., 2016. Expression of Polo-Like Kinase 4(PLK4) in Breast Cancer and Its Response to Taxane-Based Neoadjuvant Chemotherapy. *Journal of Cancer,* **7**(9), pp. 1125-1132.

LIN, J., SAMPATH, D., NANNINI, M.A., LEE, B.B., DEGTYAREV, M., OEH, J., SAVAGE, H., GUAN, Z., HONG, R., KASSEES, R., LEE, L.B., RISOM, T., GROSS, S., LIEDERER, B.M., KOEPPEN, H., SKELTON, N.J., WALLIN, J.J., BELVIN, M., PUNNOOSE, E., FRIEDMAN, L.S. and LIN, K., 2013. Targeting activated Akt with GDC-0068, a novel selective Akt inhibitor that is efficacious in multiple tumor models. *Clinical cancer research : an official journal of the American Association for Cancer Research,* **19**(7), pp. 1760-1772.

LIN, Y., YANG, Z., XU, A., DONG, P., HUANG, Y., LIU, H., LI, F., WANG, H., XU, Q., WANG, Y., SUN, D., ZOU, Y., ZOU, X., WANG, Y., ZHANG, D., LIU, H., WU, X., ZHANG, M., FU, Y., CAI, Z.,

LIU, C. and WU, S., 2015. PIK3R1 negatively regulates the epithelial-mesenchymal transition and stem-like phenotype of renal cancer cells through the AKT/GSK3beta/CTNNB1 signaling pathway. *Scientific reports,* **5**, pp. 8997.

LISABETH, E.M., FALIVELLI, G. and PASQUALE, E.B., 2013. Eph receptor signaling and ephrins. *Cold Spring Harbor perspectives in biology,* **5**(9), pp. 10.1101/cshperspect.a009159.

LIU, F. and KORC, M., 2012. Cdk4/6 inhibition induces epithelial-mesenchymal transition and enhances invasiveness in pancreatic cancer cells. *Molecular cancer therapeutics,* **11**(10), pp. 2138-2148.

LOMBARDI, G., PAMBUKU, A., BELLU, L., DELLA PUPPA, A., RUMANO, L., GARDIMAN, M.P., POMERRI, F. and ZAGONEL, V., 2013. Cisplatin and temozolomide combination in the treatment of supratentorial anaplastic ependymoma. *Chemotherapy,* **59**(3), pp. 176-180.

LONETTI, A., ANTUNES, I.L., CHIARINI, F., ORSINI, E., BUONTEMPO, F., RICCI, F., TAZZARI, P.L., PAGLIARO, P., MELCHIONDA, F., PESSION, A., BERTAINA, A., LOCATELLI, F., MCCUBREY, J.A., BARATA, J.T. and MARTELLI, A.M., 2014. Activity of the pan-class I phosphoinositide 3-kinase inhibitor NVP-BKM120 in T-cell acute lymphoblastic leukemia. *Leukemia,* **28**(6), pp. 1196-1206.

LONG, B.H. and FAIRCHILD, C.R., 1994. Paclitaxel inhibits progression of mitotic cells to G1 phase by interference with spindle formation without affecting other microtubule functions during anaphase and telephase. *Cancer research,* **54**(16), pp. 4355-4361.

LONG, J., ZHU, J.Y., LIU, Y.B., FU, K., TIAN, Y., LI, P.Y., YANG, W.Q., YANG, S.Y., YIN, J.Y., YIN, G. and ZHANG, Y., 2018. Helicase POLQ-like (HELQ) as a novel indicator of platinum-based chemoresistance for epithelial ovarian cancer. *Gynecologic oncology,* **149**(2), pp. 341-349.

LOUIS, D.N., PERRY, A., REIFENBERGER, G., VON DEIMLING, A., FIGARELLA-BRANGER, D., CAVENEE, W.K., OHGAKI, H., WIESTLER, O.D., KLEIHUES, P. and ELLISON, D.W., 2016. The 2016 World Health Organization Classification of Tumors of the Central Nervous System: a summary. *Acta Neuropathologica,* **131**(6), pp. 803-820.

LOURDUSAMY, A., RAHMAN, R., SMITH, S. and GRUNDY, R., 2015. microRNA network analysis identifies miR-29 cluster as key regulator of LAMA2 in ependymoma. *Acta neuropathologica communications,* **3**, pp. 26-015-0206-2.

LU, W., FU, Z., WANG, H., FENG, J., WEI, J. and GUO, J., 2014. Peroxiredoxin 2 is upregulated in colorectal cancer and contributes to colorectal cancer cells' survival by protecting cells from oxidative stress. *Molecular and cellular biochemistry,* **387**(1-2), pp. 261-270.

LUK, S.K., PIEKORZ, R.P., NURNBERG, B. and TONY TO, S.S., 2012. The catalytic phosphoinositol 3-kinase isoform p110delta is required for glioma cell migration and invasion. *European journal of cancer (Oxford, England : 1990),* **48**(1), pp. 149-157.

LY, L.L., YOSHIDA, H. and YAMAGUCHI, M., 2013. Nuclear transcription factor Y and its roles in cellular processes related to human disease. *American journal of cancer research,* **3**(4), pp. 339-346.

LYNCH, J.T., MCEWEN, R., CRAFTER, C., MCDERMOTT, U., GARNETT, M.J., BARRY, S.T. and DAVIES, B.R., 2016. Identification of differential PI3K pathway target dependencies in T-cell acute lymphoblastic leukemia through a large cancer cell panel screen. *Oncotarget,* **7**(16), pp. 22128-22139.

MA, J., XUE, Y., LIU, W., YUE, C., BI, F., XU, J., ZHANG, J., LI, Y., ZHONG, C. and CHEN, Y., 2013. Role of activated Rac1/Cdc42 in mediating endothelial cell proliferation and tumor angiogenesis in breast cancer. *PloS one,* **8**(6), pp. e66275.

MA, Z., ZHU, L., LUO, X., ZHAI, S., LI, P. and WANG, X., 2012. Perifosine enhances mTORC1-targeted cancer therapy by activation of GSK3beta in NSCLC cells. *Cancer biology & therapy,* **13**(11), pp. 1009-1017.

MACDONALD, S.M., SETHI, R., LAVALLY, B., YEAP, B.Y., MARCUS, K.J., CARUSO, P., PULSIFER, M., HUANG, M., EBB, D., TARBELL, N.J. and YOCK, T.I., 2013. Proton radiotherapy for pediatric central nervous system ependymoma: clinical outcomes for 70 patients. *Neuro-oncology,* **15**(11), pp. 1552-1559.

MACDONALD, T.J., BROWN, K.M., LAFLEUR, B., PETERSON, K., LAWLOR, C., CHEN, Y., PACKER, R.J., COGEN, P. and STEPHAN, D.A., 2001. Expression profiling of medulloblastoma: PDGFRA and the RAS/MAPK pathway as therapeutic targets for metastatic disease. *Nature genetics,* **29**(2), pp. 143-152.

MACK, S.C., PAJTLER, K.W., CHAVEZ, L., OKONECHNIKOV, K., BERTRAND, K.C., WANG, X., ERKEK, S., FEDERATION, A., SONG, A., LEE, C., WANG, X., MCDONALD, L., MORROW, J.J., SAIAKHOVA, A., SIN-CHAN, P., WU, Q., MICHAELRAJ, K.A., MILLER, T.E., HUBERT, C.G., RYZHOVA, M., GARZIA, L., DONOVAN, L., DOMBROWSKI, S., FACTOR, D.C., LUU, B., VALENTIM, C.L.L., GIMPLE, R.C., MORTON, A., KIM, L., PRAGER, B.C., LEE, J.J.Y., WU, X., ZUCCARO, J., THOMPSON, Y., HOLGADO, B.L., REIMAND, J., KE, S.Q., TROPPER, A., LAI, S., VIJAYARAJAH, S., DOAN, S., MAHADEV, V., MINAN, A.F., GROBNER, S.N., LIENHARD, M., ZAPATKA, M., HUANG, Z., ALDAPE, K.D., CARCABOSO, A.M., HOUGHTON, P.J., KEIR, S.T., MILDE, T., WITT, H., LI, Y., LI, C.J., BIAN, X.W., JONES, D.T.W., SCOTT, I., SINGH, S.K., HUANG, A., DIRKS, P.B., BOUFFET, E., BRADNER, J.E., RAMASWAMY, V., JABADO, N., RUTKA, J.T., NORTHCOTT, P.A., LUPIEN, M., LICHTER, P., KORSHUNOV, A., SCACHERI, P.C., PFISTER, S.M., KOOL, M., TAYLOR, M.D. and RICH, J.N., 2018. Therapeutic targeting of ependymoma as informed by oncogenic enhancer profiling. *Nature,* **553**(7686), pp. 101-105.

MACK, S.C., WITT, H., PIRO, R.M., GU, L., ZUYDERDUYN, S., STUTZ, A.M., WANG, X., GALLO, M., GARZIA, L., ZAYNE, K., ZHANG, X., RAMASWAMY, V., JAGER, N., JONES, D.T., SILL, M., PUGH, T.J., RYZHOVA, M., WANI, K.M., SHIH, D.J., HEAD, R., REMKE, M., BAILEY, S.D., ZICHNER, T., FARIA, C.C., BARSZCZYK, M., STARK, S., SEKER-CIN, H., HUTTER, S., JOHANN, P., BENDER, S., HOVESTADT, V., TZARIDIS, T., DUBUC, A.M., NORTHCOTT, P.A., PEACOCK, J., BERTRAND, K.C., AGNIHOTRI, S., CAVALLI, F.M., CLARKE, I., NETHERY-BROKX, K., CREASY, C.L., VERMA, S.K., KOSTER, J., WU, X., YAO, Y., MILDE, T., SIN-CHAN, P., ZUCCARO, J., LAU, L., PEREIRA, S., CASTELO-BRANCO, P., HIRST, M., MARRA, M.A., ROBERTS, S.S., FULTS, D., MASSIMI, L., CHO, Y.J., VAN METER, T., GRAJKOWSKA, W., LACH, B., KULOZIK, A.E., VON DEIMLING, A., WITT, O., SCHERER, S.W., FAN, X., MURASZKO, K.M., KOOL, M., POMEROY, S.L., GUPTA, N., PHILLIPS, J., HUANG, A., TABORI, U., HAWKINS, C., MALKIN, D., KONGKHAM, P.N., WEISS, W.A., JABADO, N., RUTKA, J.T., BOUFFET, E., KORBEL, J.O., LUPIEN, M., ALDAPE, K.D., BADER, G.D., EILS, R., LICHTER, P., DIRKS, P.B., PFISTER, S.M.,

KORSHUNOV, A. and TAYLOR, M.D., 2014. Epigenomic alterations define lethal CIMP-positive ependymomas of infancy. *Nature,* **506**(7489), pp. 445-450.

MAGEE, P., SHI, L. and GAROFALO, M., 2015. Role of microRNAs in chemoresistance. *Annals of translational medicine,* **3**(21), pp. 332-5839.2015.11.32.

MAHADEVAN, D., CHIOREAN, E.G., HARRIS, W.B., VON HOFF, D.D., STEJSKAL-BARNETT, A., QI, W., ANTHONY, S.P., YOUNGER, A.E., RENSVOLD, D.M., CORDOVA, F., SHELTON, C.F., BECKER, M.D., GARLICH, J.R., DURDEN, D.L. and RAMANATHAN, R.K., 2012. Phase I pharmacokinetic and pharmacodynamic study of the pan-PI3K/mTORC vascular targeted pro-drug SF1126 in patients with advanced solid tumours and B-cell malignancies. *European journal of cancer (Oxford, England : 1990),* **48**(18), pp. 3319-3327.

MAIRA, S.M., PECCHI, S., HUANG, A., BURGER, M., KNAPP, M., STERKER, D., SCHNELL, C., GUTHY, D., NAGEL, T., WIESMANN, M., BRACHMANN, S., FRITSCH, C., DORSCH, M., CHENE, P., SHOEMAKER, K., DE POVER, A., MENEZES, D., MARTINY-BARON, G., FABBRO, D., WILSON, C.J., SCHLEGEL, R., HOFMANN, F., GARCIA-ECHEVERRIA, C., SELLERS, W.R. and VOLIVA, C.F., 2012. Identification and characterization of NVP-BKM120, an orally available pan-class I PI3-kinase inhibitor. *Molecular cancer therapeutics,* **11**(2), pp. 317-328.

MANNI, I., MAZZARO, G., GURTNER, A., MANTOVANI, R., HAUGWITZ, U., KRAUSE, K., ENGELAND, K., SACCHI, A., SODDU, S. and PIAGGIO, G., 2001. NF-Y mediates the transcriptional inhibition of the cyclin B1, cyclin B2, and cdc25C promoters upon induced G2 arrest. *The Journal of biological chemistry,* **276**(8), pp. 5570-5576.

MANNING, B.D. and CANTLEY, L.C., 2007. AKT/PKB signaling: navigating downstream. *Cell,* **129**(7), pp. 1261-1274.

MANNING, B.D. and TOKER, A., 2017. AKT/PKB Signaling: Navigating the Network. *Cell,* **169**(3), pp. 381-405.

MANTAMADIOTIS, T., 2017. Towards Targeting PI3K-Dependent Regulation of Gene Expression in Brain Cancer. *Cancers,* **9**(6), pp. 10.3390/cancers9060060.

MARINOFF, A.E., MA, C., GUO, D., SNUDERL, M., WRIGHT, K.D., MANLEY, P.E., AL-SAYEGH, H., SINAI, C.E., ULLRICH, N.J., MARCUS, K., HAAS-KOGAN, D., GOUMNEROVA, L., LONDON, W.B., KIERAN, M.W., CHI, S.N., FANGUSARO, J. and BANDOPADHAYAY, P., 2017. Rethinking childhood ependymoma: a retrospective, multi-center analysis reveals poor long-term overall survival. *Journal of neuro-oncology,* **135**(1), pp. 201-211.

MARONE, R., CMILJANOVIC, V., GIESE, B. and WYMANN, M.P., 2008. Targeting phosphoinositide 3-kinase: moving towards therapy. *Biochimica et biophysica acta,* **1784**(1), pp. 159-185.

MARTELLI, F. and LIVINGSTON, D.M., 1999. Regulation of endogenous E2F1 stability by the retinoblastoma family proteins. *Proceedings of the National Academy of Sciences of the United States of America,* **96**(6), pp. 2858-2863.

MASSACESI, C., DI TOMASO, E., URBAN, P., GERMA, C., QUADT, C., TRANDAFIR, L., AIMONE, P., FRETAULT, N., DHARAN, B., TAVORATH, R. and HIRAWAT, S., 2016. PI3K inhibitors as

new cancer therapeutics: implications for clinical trial design. *OncoTargets and therapy,* **9**, pp. 203-210.

MATHEWS, L.A., CABARCAS, S.M., HURT, E.M., ZHANG, X., JAFFEE, E.M. and FARRAR, W.L., 2011. Increased expression of DNA repair genes in invasive human pancreatic cancer cells. *Pancreas,* **40**(5), pp. 730-739.

MATSUZAKI, H., DAITOKU, H., HATTA, M., TANAKA, K. and FUKAMIZU, A., 2003. Insulin-induced phosphorylation of FKHR (Foxo1) targets to proteasomal degradation. *Proceedings of the National Academy of Sciences of the United States of America,* **100**(20), pp. 11285-11290.

MAYER, I.A., ABRAMSON, V.G., FORMISANO, L., BALKO, J.M., ESTRADA, M.V., SANDERS, M.E., JURIC, D., SOLIT, D., BERGER, M.F., WON, H.H., LI, Y., CANTLEY, L.C., WINER, E. and ARTEAGA, C.L., 2017. A Phase Ib Study of Alpelisib (BYL719), a PI3Kalpha-Specific Inhibitor, with Letrozole in ER+/HER2- Metastatic Breast Cancer. *Clinical cancer research : an official journal of the American Association for Cancer Research,* **23**(1), pp. 26-34.

MAYO, L.D. and DONNER, D.B., 2001. A phosphatidylinositol 3-kinase/Akt pathway promotes translocation of Mdm2 from the cytoplasm to the nucleus. *Proceedings of the National Academy of Sciences of the United States of America,* **98**(20), pp. 11598-11603.

MCKENDRICK, L., MORLEY, S.J., PAIN, V.M., JAGUS, R. and JOSHI, B., 2001. Phosphorylation of eukaryotic initiation factor 4E (eIF4E) at Ser209 is not required for protein synthesis in vitro and in vivo. *European journal of biochemistry / FEBS,* **268**(20), pp. 5375-5385.

MCLENDON, R.E., LIPP, E., SATTERFIELD, D., EHINGER, M., AUSTIN, A., FLEMING, D., PERKINSON, K., LEFAIVRE, M., ZAGZAG, D., WIENER, B., GURURANGAN, S., FUCHS, H., FRIEDMAN, H.S., HERNDON, J.E.,2nd and HEALY, P., 2015. Prognostic marker analysis in pediatric intracranial ependymomas. *Journal of neuro-oncology,* **122**(2), pp. 255-261.

MCNAIR, C., XU, K., MANDIGO, A.C., BENELLI, M., LEIBY, B., RODRIGUES, D., LINDBERG, J., GRONBERG, H., CRESPO, M., DE LAERE, B., DIRIX, L., VISAKORPI, T., LI, F., FENG, F.Y., DE BONO, J., DEMICHELIS, F., RUBIN, M.A., BROWN, M. and KNUDSEN, K.E., 2018. Differential impact of RB status on E2F1 reprogramming in human cancer. *The Journal of clinical investigation,* **128**(1), pp. 341-358.

MCNEILL, R.S., CANOUTAS, D.A., STUHLMILLER, T.J., DHRUV, H.D., IRVIN, D.M., BASH, R.E., ANGUS, S.P., HERRING, L.E., SIMON, J.M., SKINNER, K.R., LIMAS, J.C., CHEN, X., SCHMID, R.S., SIEGEL, M.B., VAN SWEARINGEN, A.E.D., HADLER, M.J., SULMAN, E.P., SARKARIA, J.N., ANDERS, C.K., GRAVES, L.M., BERENS, M.E., JOHNSON, G.L. and MILLER, C.R., 2017. Combination therapy with potent PI3K and MAPK inhibitors overcomes adaptive kinome resistance to single agents in preclinical models of glioblastoma. *Neuro-oncology,* **19**(11), pp. 1469-1480.

MEBRATU, Y. and TESFAIGZI, Y., 2009. How ERK1/2 activation controls cell proliferation and cell death: Is subcellular localization the answer? *Cell cycle (Georgetown, Tex.),* **8**(8), pp. 1168-1175.

MEDEMA, R.H., KOPS, G.J., BOS, J.L. and BURGERING, B.M., 2000. AFX-like Forkhead transcription factors mediate cell-cycle regulation by Ras and PKB through p27kip1. *Nature,* **404**(6779), pp. 782-787.

MENDOZA, M.C., ER, E.E. and BLENIS, J., 2011. The Ras-ERK and PI3K-mTOR pathways: cross-talk and compensation. *Trends in biochemical sciences,* **36**(6), pp. 320-328.

MERCHANT, T.E., LI, C., XIONG, X., KUN, L.E., BOOP, F.A. and SANFORD, R.A., 2009. Conformal radiotherapy after surgery for paediatric ependymoma: a prospective study. *The Lancet.Oncology,* **10**(3), pp. 258-266.

MERCHANT, T.E., MULHERN, R.K., KRASIN, M.J., KUN, L.E., WILLIAMS, T., LI, C., XIONG, X., KHAN, R.B., LUSTIG, R.H., BOOP, F.A. and SANFORD, R.A., 2004. Preliminary results from a phase II trial of conformal radiation therapy and evaluation of radiation-related CNS effects for pediatric patients with localized ependymoma. *Journal of clinical oncology : official journal of the American Society of Clinical Oncology,* **22**(15), pp. 3156-3162.

MESSAHEL, B., ASHLEY, S., SARAN, F., ELLISON, D., IRONSIDE, J., PHIPPS, K., COX, T., CHONG, W.K., ROBINSON, K., PICTON, S., PINKERTON, C.R., MALLUCCI, C., MACARTHUR, D., JASPAN, T., MICHALSKI, A., GRUNDY, R.G. and CHILDREN'S CANCER LEUKAEMIA GROUP BRAIN TUMOUR COMMITTEE, 2009. Relapsed intracranial ependymoma in children in the UK: patterns of relapse, survival and therapeutic outcome. *European journal of cancer (Oxford, England : 1990),* **45**(10), pp. 1815-1823.

MESTER, J. and ENG, C., 2012. Estimate of de novo mutation frequency in probands with PTEN hamartoma tumor syndrome. *Genetics in medicine : official journal of the American College of Medical Genetics,* **14**(9), pp. 819-822.

MEUILLET, E.J., 2011. Novel inhibitors of AKT: assessment of a different approach targeting the pleckstrin homology domain. *Current medicinal chemistry,* **18**(18), pp. 2727-2742.

MICHELS, J., VITALE, I., SENOVILLA, L., ENOT, D.P., GARCIA, P., LISSA, D., OLAUSSEN, K.A., BRENNER, C., SORIA, J.C., CASTEDO, M. and KROEMER, G., 2013. Synergistic interaction between cisplatin and PARP inhibitors in non-small cell lung cancer. *Cell cycle (Georgetown, Tex.),* **12**(6), pp. 877-883.

MIKOSZ, C.A., BRICKLEY, D.R., SHARKEY, M.S., MORAN, T.W. and CONZEN, S.D., 2001. Glucocorticoid receptor-mediated protection from apoptosis is associated with induction of the serine/threonine survival kinase gene, sgk-1. *The Journal of biological chemistry,* **276**(20), pp. 16649-16654.

MILDE, T., KLEBER, S., KORSHUNOV, A., WITT, H., HIELSCHER, T., KOCH, P., KOPP, H.G., JUGOLD, M., DEUBZER, H.E., OEHME, I., LODRINI, M., GRONE, H.J., BENNER, A., BRUSTLE, O., GILBERTSON, R.J., VON DEIMLING, A., KULOZIK, A.E., PFISTER, S.M., MARTIN-VILLALBA, A. and WITT, O., 2011. A novel human high-risk ependymoma stem cell model reveals the differentiation-inducing potential of the histone deacetylase inhibitor Vorinostat. *Acta Neuropathologica,* **122**(5), pp. 637-650.

MILLER, T.W., REXER, B.N., GARRETT, J.T. and ARTEAGA, C.L., 2011. Mutations in the phosphatidylinositol 3-kinase pathway: role in tumor progression and therapeutic implications in breast cancer. *Breast cancer research : BCR,* **13**(6), pp. 224.

MILLIS, S.Z., IKEDA, S., REDDY, S., GATALICA, Z. and KURZROCK, R., 2016. Landscape of Phosphatidylinositol-3-Kinase Pathway Alterations Across 19784 Diverse Solid Tumors. *JAMA oncology,* **2**(12), pp. 1565-1573.

MINOGUE, S., WAUGH, M.G., DE MATTEIS, M.A., STEPHENS, D.J., BERDITCHEVSKI, F. and HSUAN, J.J., 2006. Phosphatidylinositol 4-kinase is required for endosomal trafficking and degradation of the EGF receptor. *Journal of cell science,* **119**(Pt 3), pp. 571-581.

MODENA, P., LUALDI, E., FACCHINETTI, F., VELTMAN, J., REID, J.F., MINARDI, S., JANSSEN, I., GIANGASPERO, F., FORNI, M., FINOCCHIARO, G., GENITORI, L., GIORDANO, F., RICCARDI, R., SCHOENMAKERS, E.F., MASSIMINO, M. and SOZZI, G., 2006. Identification of tumor-specific molecular signatures in intracranial ependymoma and association with clinical characteristics. *Journal of clinical oncology : official journal of the American Society of Clinical Oncology,* **24**(33), pp. 5223-5233.

MODUR, V., NAGARAJAN, R., EVERS, B.M. and MILBRANDT, J., 2002. FOXO proteins regulate tumor necrosis factor-related apoptosis inducing ligand expression. Implications for PTEN mutation in prostate cancer. *The Journal of biological chemistry,* **277**(49), pp. 47928-47937.

MOHAN, N., SHEN, Y., DOKMANOVIC, M., ENDO, Y., HIRSCH, D.S. and WU, W.J., 2016. VPS34 regulates TSC1/TSC2 heterodimer to mediate RheB and mTORC1/S6K1 activation and cellular transformation. *Oncotarget,* **7**(32), pp. 52239-52254.

MOHANKUMAR, K.M., CURRLE, D.S., WHITE, E., BOULOS, N., DAPPER, J., EDEN, C., NIMMERVOLL, B., THIRUVENKATAM, R., CONNELLY, M., KRANENBURG, T.A., NEALE, G., OLSEN, S., WANG, Y.D., FINKELSTEIN, D., WRIGHT, K., GUPTA, K., ELLISON, D.W., THOMAS, A.O. and GILBERTSON, R.J., 2015. An in vivo screen identifies ependymoma oncogenes and tumor-suppressor genes. *Nature genetics,* **47**(8), pp. 878-887.

MOLINA-CERRILLO, J., ALONSO-GORDOA, T., GAJATE, P. and GRANDE, E., 2017. Bruton's tyrosine kinase (BTK) as a promising target in solid tumors. *Cancer treatment reviews,* **58**, pp. 41-50.

MONIZ, L.S. and STAMBOLIC, V., 2011. Nek10 mediates G2/M cell cycle arrest and MEK autoactivation in response to UV irradiation. *Molecular and cellular biology,* **31**(1), pp. 30-42.

MOORE, H.C., 2014. An overview of chemotherapy-related cognitive dysfunction, or 'chemobrain'. *Oncology (Williston Park, N.Y.),* **28**(9), pp. 797-804.

MORENO, L., POPOV, S., JURY, A., AL SARRAJ, S., JONES, C. and ZACHAROULIS, S., 2013. Role of platelet derived growth factor receptor (PDGFR) over-expression and angiogenesis in ependymoma. *Journal of neuro-oncology,* **111**(2), pp. 169-176.

MOTZER, R.J., ESCUDIER, B., OUDARD, S., HUTSON, T.E., PORTA, C., BRACARDA, S., GRUNWALD, V., THOMPSON, J.A., FIGLIN, R.A., HOLLAENDER, N., KAY, A., RAVAUD, A. and RECORD-1 STUDY GROUP, 2010. Phase 3 trial of everolimus for metastatic renal cell carcinoma : final results and analysis of prognostic factors. *Cancer,* **116**(18), pp. 4256-4265.

MUELLER, S., SCHITTENHELM, M., HONECKER, F., MALENKE, E., LAUBER, K., WESSELBORG, S., HARTMANN, J.T., BOKEMEYER, C. and MAYER, F., 2006. Cell-cycle progression and response of germ cell tumors to cisplatin in vitro. *International journal of oncology,* **29**(2), pp. 471-479.

MULHERN, R.K., HANCOCK, J., FAIRCLOUGH, D. and KUN, L., 1992. Neuropsychological status of children treated for brain tumors: a critical review and integrative analysis. *Medical and pediatric oncology,* **20**(3), pp. 181-191.

MURANEN, T., SELFORS, L.M., HWANG, J., GALLEGOS, L.L., COLOFF, J.L., THOREEN, C.C., KANG, S.A., SABATINI, D.M., MILLS, G.B. and BRUGGE, J.S., 2016. ERK and p38 MAPK Activities Determine Sensitivity to PI3K/mTOR Inhibition via Regulation of MYC and YAP. *Cancer research,* **76**(24), pp. 7168-7180.

MURGA, C., LAGUINGE, L., WETZKER, R., CUADRADO, A. and GUTKIND, J.S., 1998. Activation of Akt/protein kinase B by G protein-coupled receptors. A role for alpha and beta gamma subunits of heterotrimeric G proteins acting through phosphatidylinositol-3-OH kinasegamma. *The Journal of biological chemistry,* **273**(30), pp. 19080-19085.

NAGASHIMA, T., SHIGEMATSU, N., MARUKI, R., URANO, Y., TANAKA, H., SHIMAYA, A., SHIMOKAWA, T. and SHIBASAKI, M., 2010. Discovery of novel forkhead box O1 inhibitors for treating type 2 diabetes: improvement of fasting glycemia in diabetic db/db mice. *Molecular pharmacology,* **78**(5), pp. 961-970.

NEIL, J., SHANNON, C., MOHAN, A., LAURENT, D., MURALI, R. and JHANWAR-UNIYAL, M., 2016. ATP-site binding inhibitor effectively targets mTORC1 and mTORC2 complexes in glioblastoma. *International journal of oncology,* **48**(3), pp. 1045-1052.

NEJAT, F., EL KHASHAB, M. and RUTKA, J.T., 2008. Initial management of childhood brain tumors: neurosurgical considerations. *Journal of child neurology,* **23**(10), pp. 1136-1148.

NI, J., LIU, Q., XIE, S., CARLSON, C., VON, T., VOGEL, K., RIDDLE, S., BENES, C., ECK, M., ROBERTS, T., GRAY, N. and ZHAO, J., 2012. Functional characterization of an isoform-selective inhibitor of PI3K-p110beta as a potential anticancer agent. *Cancer discovery,* **2**(5), pp. 425-433.

NITULESCU, G.M., MARGINA, D., JUZENAS, P., PENG, Q., OLARU, O.T., SALOUSTROS, E., FENGA, C., SPANDIDOS, D.A., LIBRA, M. and TSATSAKIS, A.M., 2016. Akt inhibitors in cancer treatment: The long journey from drug discovery to clinical use (Review). *International journal of oncology,* **48**(3), pp. 869-885.

NOISA, P., LUND, C., KANDURI, K., LUND, R., LAHDESMAKI, H., LAHESMAA, R., LUNDIN, K., CHOKECHUWATTANALERT, H., OTONKOSKI, T., TUURI, T. and RAIVIO, T., 2014. Notch signaling regulates the differentiation of neural crest from human pluripotent stem cells. *Journal of cell science,* **127**(Pt 9), pp. 2083-2094.

NOLTING, S., RENTSCH, J., FREITAG, H., DETJEN, K., BRIEST, F., MOBS, M., WEISSMANN, V., SIEGMUND, B., AUERNHAMMER, C.J., ARISTIZABAL PRADA, E.T., LAUSEKER, M., GROSSMAN, A., EXNER, S., FISCHER, C., GROTZINGER, C., SCHRADER, J., GRABOWSKI, P. and GERMAN NET-Z STUDY GROUP, 2017. The selective PI3Kalpha inhibitor BYL719 as a novel

therapeutic option for neuroendocrine tumors: Results from multiple cell line models. *PloS one,* **12**(8), pp. e0182852.

NORTHCOTT, P.A., SHIH, D.J., PEACOCK, J., GARZIA, L., MORRISSY, A.S., ZICHNER, T., STUTZ, A.M., KORSHUNOV, A., REIMAND, J., SCHUMACHER, S.E., BEROUKHIM, R., ELLISON, D.W., MARSHALL, C.R., LIONEL, A.C., MACK, S., DUBUC, A., YAO, Y., RAMASWAMY, V., LUU, B., ROLIDER, A., CAVALLI, F.M., WANG, X., REMKE, M., WU, X., CHIU, R.Y., CHU, A., CHUAH, E., CORBETT, R.D., HOAD, G.R., JACKMAN, S.D., LI, Y., LO, A., MUNGALL, K.L., NIP, K.M., QIAN, J.Q., RAYMOND, A.G., THIESSEN, N.T., VARHOL, R.J., BIROL, I., MOORE, R.A., MUNGALL, A.J., HOLT, R., KAWAUCHI, D., ROUSSEL, M.F., KOOL, M., JONES, D.T., WITT, H., FERNANDEZ-L, A., KENNEY, A.M., WECHSLER-REYA, R.J., DIRKS, P., AVIV, T., GRAJKOWSKA, W.A., PEREK-POLNIK, M., HABERLER, C.C., DELATTRE, O., REYNAUD, S.S., DOZ, F.F., PERNET-FATTET, S.S., CHO, B.K., KIM, S.K., WANG, K.C., SCHEURLEN, W., EBERHART, C.G., FEVRE-MONTANGE, M., JOUVET, A., POLLACK, I.F., FAN, X., MURASZKO, K.M., GILLESPIE, G.Y., DI ROCCO, C., MASSIMI, L., MICHIELS, E.M., KLOOSTERHOF, N.K., FRENCH, P.J., KROS, J.M., OLSON, J.M., ELLENBOGEN, R.G., ZITTERBART, K., KREN, L., THOMPSON, R.C., COOPER, M.K., LACH, B., MCLENDON, R.E., BIGNER, D.D., FONTEBASSO, A., ALBRECHT, S., JABADO, N., LINDSEY, J.C., BAILEY, S., GUPTA, N., WEISS, W.A., BOGNAR, L., KLEKNER, A., VAN METER, T.E., KUMABE, T., TOMINAGA, T., ELBABAA, S.K., LEONARD, J.R., RUBIN, J.B., LIAU, L.M., VAN MEIR, E.G., FOULADI, M., NAKAMURA, H., CINALLI, G., GARAMI, M., HAUSER, P., SAAD, A.G., IOLASCON, A., JUNG, S., CARLOTTI, C.G., VIBHAKAR, R., RA, Y.S., ROBINSON, S., ZOLLO, M., FARIA, C.C., CHAN, J.A., LEVY, M.L., SORENSEN, P.H., MEYERSON, M., POMEROY, S.L., CHO, Y.J., BADER, G.D., TABORI, U., HAWKINS, C.E., BOUFFET, E., SCHERER, S.W., RUTKA, J.T., MALKIN, D., CLIFFORD, S.C., JONES, S.J., KORBEL, J.O., PFISTER, S.M., MARRA, M.A. and TAYLOR, M.D., 2012. Subgroup-specific structural variation across 1,000 medulloblastoma genomes. *Nature,* **488**(7409), pp. 49-56.

O'DONNELL, A., ODROWAZ, Z. and SHARROCKS, A.D., 2012. Immediate-early gene activation by the MAPK pathways: what do and don't we know? *Biochemical Society transactions,* **40**(1), pp. 58-66.

OBERLEY, M.J., INMAN, D.R. and FARNHAM, P.J., 2003. E2F6 negatively regulates BRCA1 in human cancer cells without methylation of histone H3 on lysine 9. *The Journal of biological chemistry,* **278**(43), pp. 42466-42476.

OECKINGHAUS, A. and GHOSH, S., 2009. The NF-kappaB family of transcription factors and its regulation. *Cold Spring Harbor perspectives in biology,* **1**(4), pp. a000034.

OGAWA, H., ISHIGURO, K., GAUBATZ, S., LIVINGSTON, D.M. and NAKATANI, Y., 2002. A complex with chromatin modifiers that occupies E2F- and Myc-responsive genes in G0 cells. *Science (New York, N.Y.),* **296**(5570), pp. 1132-1136.

OKKENHAUG, K., BILANCIO, A., FARJOT, G., PRIDDLE, H., SANCHO, S., PESKETT, E., PEARCE, W., MEEK, S.E., SALPEKAR, A., WATERFIELD, M.D., SMITH, A.J. and VANHAESEBROECK, B., 2002. Impaired B and T cell antigen receptor signaling in p110delta PI 3-kinase mutant mice. *Science (New York, N.Y.),* **297**(5583), pp. 1031-1034.

OKKENHAUG, K. and VANHAESEBROECK, B., 2003. PI3K in lymphocyte development, differentiation and activation. *Nature reviews.Immunology,* **3**(4), pp. 317-330.

OKUDELA, K., SUZUKI, M., KAGEYAMA, S., BUNAI, T., NAGURA, K., IGARASHI, H., TAKAMOCHI, K., SUZUKI, K., YAMADA, T., NIWA, H., OHASHI, R., OGAWA, H., MORI, H., KITAMURA, H., KANEKO, T., TSUNEYOSHI, T. and SUGIMURA, H., 2007. PIK3CA mutation and amplification in human lung cancer. *Pathology international,* **57**(10), pp. 664-671.

OPEL, D., NAUMANN, I., SCHNEIDER, M., BERTELE, D., DEBATIN, K.M. and FULDA, S., 2011. Targeting aberrant PI3K/Akt activation by PI103 restores sensitivity to TRAIL-induced apoptosis in neuroblastoma. *Clinical cancer research : an official journal of the American Association for Cancer Research,* **17**(10), pp. 3233-3247.

OSTROM, Q.T., GITTLEMAN, H., FULOP, J., LIU, M., BLANDA, R., KROMER, C., WOLINSKY, Y., KRUCHKO, C. and BARNHOLTZ-SLOAN, J.S., 2015. CBTRUS Statistical Report: Primary Brain and Central Nervous System Tumors Diagnosed in the United States in 2008-2012. *Neuro-oncology,* **17 Suppl 4**, pp. iv1-iv62.

OZAWA, T., BRENNAN, C.W., WANG, L., SQUATRITO, M., SASAYAMA, T., NAKADA, M., HUSE, J.T., PEDRAZA, A., UTSUKI, S., YASUI, Y., TANDON, A., FOMCHENKO, E.I., OKA, H., LEVINE, R.L., FUJII, K., LADANYI, M. and HOLLAND, E.C., 2010. PDGFRA gene rearrangements are frequent genetic events in PDGFRA-amplified glioblastomas. *Genes & development,* **24**(19), pp. 2205-2218.

PACKER, R.J., GOLDWEIN, J., NICHOLSON, H.S., VEZINA, L.G., ALLEN, J.C., RIS, M.D., MURASZKO, K., RORKE, L.B., WARA, W.M., COHEN, B.H. and BOYETT, J.M., 1999. Treatment of children with medulloblastomas with reduced-dose craniospinal radiation therapy and adjuvant chemotherapy: A Children's Cancer Group Study. *Journal of clinical oncology : official journal of the American Society of Clinical Oncology,* **17**(7), pp. 2127-2136.

PACKER, R.J., SUTTON, L.N., ELTERMAN, R., LANGE, B., GOLDWEIN, J., NICHOLSON, H.S., MULNE, L., BOYETT, J., D'ANGIO, G. and WECHSLER-JENTZSCH, K., 1994. Outcome for children with medulloblastoma treated with radiation and cisplatin, CCNU, and vincristine chemotherapy. *Journal of neurosurgery,* **81**(5), pp. 690-698.

PAI, S.G., CARNEIRO, B.A., MOTA, J.M., COSTA, R., LEITE, C.A., BARROSO-SOUSA, R., KAPLAN, J.B., CHAE, Y.K. and GILES, F.J., 2017. Wnt/beta-catenin pathway: modulating anticancer immune response. *Journal of hematology & oncology,* **10**(1), pp. 101-017-0471-6.

PAJTLER, K.W., WEN, J., SILL, M., LIN, T., ORISME, W., TANG, B., HUBNER, J.M., RAMASWAMY, V., JIA, S., DALTON, J.D., HAUPFEAR, K., ROGERS, H.A., PUNCHIHEWA, C., LEE, R., EASTON, J., WU, G., RITZMANN, T.A., CHAPMAN, R., CHAVEZ, L., BOOP, F.A., KLIMO, P., SABIN, N.D., OGG, R., MACK, S.C., FREIBAUM, B.D., KIM, H.J., WITT, H., JONES, D.T.W., VO, B., GAJJAR, A., POUNDS, S., ONAR-THOMAS, A., ROUSSEL, M.F., ZHANG, J., TAYLOR, J.P., MERCHANT, T.E., GRUNDY, R., TATEVOSSIAN, R.G., TAYLOR, M.D., PFISTER, S.M., KORSHUNOV, A., KOOL, M. and ELLISON, D.W., 2018. Molecular heterogeneity and CXorf67 alterations in posterior fossa group A (PFA) ependymomas. *Acta Neuropathologica,* **136**(2), pp. 211-226.

PAJTLER, K.W., WITT, H., SILL, M., JONES, D.T., HOVESTADT, V., KRATOCHWIL, F., WANI, K., TATEVOSSIAN, R., PUNCHIHEWA, C., JOHANN, P., REIMAND, J., WARNATZ, H.J., RYZHOVA, M., MACK, S., RAMASWAMY, V., CAPPER, D., SCHWEIZER, L., SIEBER, L., WITTMANN, A., HUANG, Z., VAN SLUIS, P., VOLCKMANN, R., KOSTER, J., VERSTEEG, R., FULTS, D.,

TOLEDANO, H., AVIGAD, S., HOFFMAN, L.M., DONSON, A.M., FOREMAN, N., HEWER, E., ZITTERBART, K., GILBERT, M., ARMSTRONG, T.S., GUPTA, N., ALLEN, J.C., KARAJANNIS, M.A., ZAGZAG, D., HASSELBLATT, M., KULOZIK, A.E., WITT, O., COLLINS, V.P., VON HOFF, K., RUTKOWSKI, S., PIETSCH, T., BADER, G., YASPO, M.L., VON DEIMLING, A., LICHTER, P., TAYLOR, M.D., GILBERTSON, R., ELLISON, D.W., ALDAPE, K., KORSHUNOV, A., KOOL, M. and PFISTER, S.M., 2015. Molecular Classification of Ependymal Tumors across All CNS Compartments, Histopathological Grades, and Age Groups. *Cancer cell,* **27**(5), pp. 728-743.

PALMA, L., CELLI, P., MARIOTTINI, A., ZALAFFI, A. and SCHETTINI, G., 2000. The importance of surgery in supratentorial ependymomas. Long-term survival in a series of 23 cases. *Child's nervous system : ChNS : official journal of the International Society for Pediatric Neurosurgery,* **16**(3), pp. 170-175.

PARK, J., LEONG, M.L., BUSE, P., MAIYAR, A.C., FIRESTONE, G.L. and HEMMINGS, B.A., 1999. Serum and glucocorticoid-inducible kinase (SGK) is a target of the PI 3-kinase-stimulated signaling pathway. *The EMBO journal,* **18**(11), pp. 3024-3033.

PARKER, M., MOHANKUMAR, K.M., PUNCHIHEWA, C., WEINLICH, R., DALTON, J.D., LI, Y., LEE, R., TATEVOSSIAN, R.G., PHOENIX, T.N., THIRUVENKATAM, R., WHITE, E., TANG, B., ORISME, W., GUPTA, K., RUSCH, M., CHEN, X., LI, Y., NAGAHAWHATTE, P., HEDLUND, E., FINKELSTEIN, D., WU, G., SHURTLEFF, S., EASTON, J., BOGGS, K., YERGEAU, D., VADODARIA, B., MULDER, H.L., BECKSFORT, J., GUPTA, P., HUETHER, R., MA, J., SONG, G., GAJJAR, A., MERCHANT, T., BOOP, F., SMITH, A.A., DING, L., LU, C., OCHOA, K., ZHAO, D., FULTON, R.S., FULTON, L.L., MARDIS, E.R., WILSON, R.K., DOWNING, J.R., GREEN, D.R., ZHANG, J., ELLISON, D.W. and GILBERTSON, R.J., 2014. C11orf95-RELA fusions drive oncogenic NF-kappaB signalling in ependymoma. *Nature,* **506**(7489), pp. 451-455.

PARKIN, D.M., PISANI, P. and FERLAY, J., 1999. Global cancer statistics. *CA: a cancer journal for clinicians,* **49**(1), pp. 33-64, 1.

PARSONS, D.W., LI, M., ZHANG, X., JONES, S., LEARY, R.J., LIN, J.C., BOCA, S.M., CARTER, H., SAMAYOA, J., BETTEGOWDA, C., GALLIA, G.L., JALLO, G.I., BINDER, Z.A., NIKOLSKY, Y., HARTIGAN, J., SMITH, D.R., GERHARD, D.S., FULTS, D.W., VANDENBERG, S., BERGER, M.S., MARIE, S.K., SHINJO, S.M., CLARA, C., PHILLIPS, P.C., MINTURN, J.E., BIEGEL, J.A., JUDKINS, A.R., RESNICK, A.C., STORM, P.B., CURRAN, T., HE, Y., RASHEED, B.A., FRIEDMAN, H.S., KEIR, S.T., MCLENDON, R., NORTHCOTT, P.A., TAYLOR, M.D., BURGER, P.C., RIGGINS, G.J., KARCHIN, R., PARMIGIANI, G., BIGNER, D.D., YAN, H., PAPADOPOULOS, N., VOGELSTEIN, B., KINZLER, K.W. and VELCULESCU, V.E., 2011. The genetic landscape of the childhood cancer medulloblastoma. *Science (New York, N.Y.),* **331**(6016), pp. 435-439.

PATTON, D.T., GARDEN, O.A., PEARCE, W.P., CLOUGH, L.E., MONK, C.R., LEUNG, E., ROWAN, W.C., SANCHO, S., WALKER, L.S., VANHAESEBROECK, B. and OKKENHAUG, K., 2006. Cutting edge: the phosphoinositide 3-kinase p110 delta is critical for the function of CD4+CD25+Foxp3+ regulatory T cells. *Journal of immunology (Baltimore, Md.: 1950),* **177**(10), pp. 6598-6602.

PAUGH, B.S., QU, C., JONES, C., LIU, Z., ADAMOWICZ-BRICE, M., ZHANG, J., BAX, D.A., COYLE, B., BARROW, J., HARGRAVE, D., LOWE, J., GAJJAR, A., ZHAO, W., BRONISCER, A., ELLISON, D.W., GRUNDY, R.G. and BAKER, S.J., 2010. Integrated molecular genetic profiling of pediatric high-grade gliomas reveals key differences with the adult disease. *Journal of*

clinical oncology : official journal of the American Society of Clinical Oncology, **28**(18), pp. 3061-3068.

PENG, X.D., XU, P.Z., CHEN, M.L., HAHN-WINDGASSEN, A., SKEEN, J., JACOBS, J., SUNDARARAJAN, D., CHEN, W.S., CRAWFORD, S.E., COLEMAN, K.G. and HAY, N., 2003. Dwarfism, impaired skin development, skeletal muscle atrophy, delayed bone development, and impeded adipogenesis in mice lacking Akt1 and Akt2. *Genes & development,* **17**(11), pp. 1352-1365.

PEREIRA, J.K., MACHADO-NETO, J.A., LOPES, M.R., MORINI, B.C., TRAINA, F., COSTA, F.F., SAAD, S.T. and FAVARO, P., 2015. Molecular effects of the phosphatidylinositol-3-kinase inhibitor NVP-BKM120 on T and B-cell acute lymphoblastic leukaemia. *European journal of cancer (Oxford, England : 1990),* **51**(14), pp. 2076-2085.

PERSENGIEV, S.P., KONDOVA, I.I. and KILPATRICK, D.L., 1999. E2F4 actively promotes the initiation and maintenance of nerve growth factor-induced cell differentiation. *Molecular and cellular biology,* **19**(9), pp. 6048-6056.

PETERSON, T.R., LAPLANTE, M., THOREEN, C.C., SANCAK, Y., KANG, S.A., KUEHL, W.M., GRAY, N.S. and SABATINI, D.M., 2009. DEPTOR is an mTOR inhibitor frequently overexpressed in multiple myeloma cells and required for their survival. *Cell,* **137**(5), pp. 873-886.

PEYRE, M., COMMO, F., DANTAS-BARBOSA, C., ANDREIUOLO, F., PUGET, S., LACROIX, L., DRUSCH, F., SCOTT, V., VARLET, P., MAUGUEN, A., DESSEN, P., LAZAR, V., VASSAL, G. and GRILL, J., 2010. Portrait of ependymoma recurrence in children: biomarkers of tumor progression identified by dual-color microarray-based gene expression analysis. *PloS one,* **5**(9), pp. e12932.

PEYTON, J.D., AHNERT, J.R., BURRIS, H., BRITTEN, C., CHEN, L.C., TABERNERO, J., DUVAL, V., ROUYRRE, N., SILVA, A.P., QUADT, C. and BASELGA, J., 2011. A dose-escalation study with the novel formulation of the oral pan-class I PI3K inhibitor BEZ235, solid dispersion system (SDS) sachet, in patients with advanced solid tumors. *Journal of clinical oncology.* 29.15(Suppl.3066).

PEZZOLESI, M.G., PLATZER, P., WAITE, K.A. and ENG, C., 2008. Differential expression of PTEN-targeting microRNAs miR-19a and miR-21 in Cowden syndrome. *American Journal of Human Genetics,* **82**(5), pp. 1141-1149.

PINES, J. and HUNTER, T., 1992. Cyclins A and B1 in the human cell cycle. *Ciba Foundation symposium,* **170**, pp. 187-96; discussion 196-204.

PITTER, K.L., GALBAN, C.J., GALBAN, S., TEHRANI, O.S., LI, F., CHARLES, N., BRADBURY, M.S., BECHER, O.J., CHENEVERT, T.L., REHEMTULLA, A., ROSS, B.D., HOLLAND, E.C. and HAMBARDZUMYAN, D., 2011. Perifosine and CCI 779 co-operate to induce cell death and decrease proliferation in PTEN-intact and PTEN-deficient PDGF-driven murine glioblastoma. *PloS one,* **6**(1), pp. e14545.

PIVA, R., BELARDO, G. and SANTORO, M.G., 2006. NF-kappaB: a stress-regulated switch for cell survival. *Antioxidants & redox signaling,* **8**(3-4), pp. 478-486.

PLUNKETT, W., HUANG, P., XU, Y.Z., HEINEMANN, V., GRUNEWALD, R. and GANDHI, V., 1995. Gemcitabine: metabolism, mechanisms of action, and self-potentiation. *Seminars in oncology,* **22**(4 Suppl 11), pp. 3-10.

POLLACK, I.F., HAMILTON, R.L., BURGER, P.C., BRAT, D.J., ROSENBLUM, M.K., MURDOCH, G.H., NIKIFOROVA, M.N., HOLMES, E.J., ZHOU, T., COHEN, K.J., JAKACKI, R.I. and CHILDREN'S ONCOLOGY GROUP, 2010. Akt activation is a common event in pediatric malignant gliomas and a potential adverse prognostic marker: a report from the Children's Oncology Group. *Journal of neuro-oncology,* **99**(2), pp. 155-163.

POLLACK, I.F., HAMILTON, R.L., JAMES, C.D., FINKELSTEIN, S.D., BURNHAM, J., YATES, A.J., HOLMES, E.J., ZHOU, T., FINLAY, J.L. and CHILDREN'S ONCOLOGY GROUP, 2006. Rarity of PTEN deletions and EGFR amplification in malignant gliomas of childhood: results from the Children's Cancer Group 945 cohort. *Journal of neurosurgery,* **105**(5 Suppl), pp. 418-424.

POLLACK, I.F., POLINKO, P., ALBRIGHT, A.L., TOWBIN, R. and FITZ, C., 1995. Mutism and pseudobulbar symptoms after resection of posterior fossa tumors in children: incidence and pathophysiology. *Neurosurgery,* **37**(5), pp. 885-893.

POLLACK, I.F., STEWART, C.F., KOCAK, M., POUSSAINT, T.Y., BRONISCER, A., BANERJEE, A., DOUGLAS, J.G., KUN, L.E., BOYETT, J.M. and GEYER, J.R., 2011. A phase II study of gefitinib and irradiation in children with newly diagnosed brainstem gliomas: a report from the Pediatric Brain Tumor Consortium. *Neuro-oncology,* **13**(3), pp. 290-297.

POLOSUKHINA, D., LOVE, H.D., CORREA, H., SU, Z., DAHLMAN, K.B., PAO, W., MOSES, H.L., ARTEAGA, C.L., LOVVORN, H.N.,3rd, ZENT, R. and CLARK, P.E., 2017. Functional KRAS mutations and a potential role for PI3K/AKT activation in Wilms tumors. *Molecular oncology,* **11**(4), pp. 405-421.

PORSTMANN, T., SANTOS, C.R., GRIFFITHS, B., CULLY, M., WU, M., LEEVERS, S., GRIFFITHS, J.R., CHUNG, Y.L. and SCHULZE, A., 2008. SREBP activity is regulated by mTORC1 and contributes to Akt-dependent cell growth. *Cell metabolism,* **8**(3), pp. 224-236.

PREUSSER, M., WOLFSBERGER, S., CZECH, T., SLAVC, I., BUDKA, H. and HAINFELLNER, J.A., 2005. Survivin expression in intracranial ependymomas and its correlation with tumor cell proliferation and patient outcome. *American Journal of Clinical Pathology,* **124**(4), pp. 543-549.

PUGH, T.J., MOROZOVA, O., ATTIYEH, E.F., ASGHARZADEH, S., WEI, J.S., AUCLAIR, D., CARTER, S.L., CIBULSKIS, K., HANNA, M., KIEZUN, A., KIM, J., LAWRENCE, M.S., LICHENSTEIN, L., MCKENNA, A., PEDAMALLU, C.S., RAMOS, A.H., SHEFLER, E., SIVACHENKO, A., SOUGNEZ, C., STEWART, C., ALLY, A., BIROL, I., CHIU, R., CORBETT, R.D., HIRST, M., JACKMAN, S.D., KAMOH, B., KHODABAKSHI, A.H., KRZYWINSKI, M., LO, A., MOORE, R.A., MUNGALL, K.L., QIAN, J., TAM, A., THIESSEN, N., ZHAO, Y., COLE, K.A., DIAMOND, M., DISKIN, S.J., MOSSE, Y.P., WOOD, A.C., JI, L., SPOSTO, R., BADGETT, T., LONDON, W.B., MOYER, Y., GASTIER-FOSTER, J.M., SMITH, M.A., GUIDRY AUVIL, J.M., GERHARD, D.S., HOGARTY, M.D., JONES, S.J., LANDER, E.S., GABRIEL, S.B., GETZ, G., SEEGER, R.C., KHAN, J., MARRA, M.A., MEYERSON, M. and MARIS, J.M., 2013. The genetic landscape of high-risk neuroblastoma. *Nature genetics,* **45**(3), pp. 279-284.

QIU, Y. and KUNG, H.J., 2000. Signaling network of the Btk family kinases. *Oncogene,* **19**(49), pp. 5651-5661.

RABINOVICH, A., JIN, V.X., RABINOVICH, R., XU, X. and FARNHAM, P.J., 2008. E2F in vivo binding specificity: comparison of consensus versus nonconsensus binding sites. *Genome research,* **18**(11), pp. 1763-1777.

RAJKUMAR, P., MATHEW, B.S., DAS, S., ISAIAH, R., JOHN, S., PRABHA, R. and FLEMING, D.H., 2016. Cisplatin Concentrations in Long and Short Duration Infusion: Implications for the Optimal Time of Radiation Delivery. *Journal of clinical and diagnostic research : JCDR,* **10**(7), pp. XC01-XC04.

RAVI, R. and BEDI, A., 2002. Requirement of BAX for TRAIL/Apo2L-induced apoptosis of colorectal cancers: synergism with sulindac-mediated inhibition of Bcl-x(L). *Cancer research,* **62**(6), pp. 1583-1587.

REUSCH, H.P., ZIMMERMANN, S., SCHAEFER, M., PAUL, M. and MOELLING, K., 2001. Regulation of Raf by Akt controls growth and differentiation in vascular smooth muscle cells. *The Journal of biological chemistry,* **276**(36), pp. 33630-33637.

RINI, B.I. and ATKINS, M.B., 2009. Resistance to targeted therapy in renal-cell carcinoma. *The Lancet.Oncology,* **10**(10), pp. 992-1000.

ROBERTS, E.C., SHAPIRO, P.S., NAHREINI, T.S., PAGES, G., POUYSSEGUR, J. and AHN, N.G., 2002. Distinct cell cycle timing requirements for extracellular signal-regulated kinase and phosphoinositide 3-kinase signaling pathways in somatic cell mitosis. *Molecular and cellular biology,* **22**(20), pp. 7226-7241.

ROBERTSON, P.L., ZELTZER, P.M., BOYETT, J.M., RORKE, L.B., ALLEN, J.C., GEYER, J.R., STANLEY, P., LI, H., ALBRIGHT, A.L., MCGUIRE-CULLEN, P., FINLAY, J.L., STEVENS, K.R.,Jr, MILSTEIN, J.M., PACKER, R.J. and WISOFF, J., 1998. Survival and prognostic factors following radiation therapy and chemotherapy for ependymomas in children: a report of the Children's Cancer Group. *Journal of neurosurgery,* **88**(4), pp. 695-703.

ROBINSON, G., PARKER, M., KRANENBURG, T.A., LU, C., CHEN, X., DING, L., PHOENIX, T.N., HEDLUND, E., WEI, L., ZHU, X., CHALHOUB, N., BAKER, S.J., HUETHER, R., KRIWACKI, R., CURLEY, N., THIRUVENKATAM, R., WANG, J., WU, G., RUSCH, M., HONG, X., BECKSFORT, J., GUPTA, P., MA, J., EASTON, J., VADODARIA, B., ONAR-THOMAS, A., LIN, T., LI, S., POUNDS, S., PAUGH, S., ZHAO, D., KAWAUCHI, D., ROUSSEL, M.F., FINKELSTEIN, D., ELLISON, D.W., LAU, C.C., BOUFFET, E., HASSALL, T., GURURANGAN, S., COHN, R., FULTON, R.S., FULTON, L.L., DOOLING, D.J., OCHOA, K., GAJJAR, A., MARDIS, E.R., WILSON, R.K., DOWNING, J.R., ZHANG, J. and GILBERTSON, R.J., 2012. Novel mutations target distinct subgroups of medulloblastoma. *Nature,* **488**(7409), pp. 43-48.

RODRIGUEZ, E.F., SCHEITHAUER, B.W., GIANNINI, C., RYNEARSON, A., CEN, L., HOESLEY, B., GILMER-FLYNN, H., SARKARIA, J.N., JENKINS, S., LONG, J. and RODRIGUEZ, F.J., 2011. PI3K/AKT pathway alterations are associated with clinically aggressive and histologically anaplastic subsets of pilocytic astrocytoma. *Acta Neuropathologica,* **121**(3), pp. 407-420.

ROGERS, H.A., MAYNE, C., CHAPMAN, R.J., KILDAY, J.P., COYLE, B. and GRUNDY, R.G., 2013. PI3K pathway activation provides a novel therapeutic target for pediatric ependymoma and

is an independent marker of progression-free survival. *Clinical cancer research : an official journal of the American Association for Cancer Research,* **19**(23), pp. 6450-6460.

ROPER, J., RICHARDSON, M.P., WANG, W.V., RICHARD, L.G., CHEN, W., COFFEE, E.M., SINNAMON, M.J., LEE, L., CHEN, P.C., BRONSON, R.T., MARTIN, E.S. and HUNG, K.E., 2011. The dual PI3K/mTOR inhibitor NVP-BEZ235 induces tumor regression in a genetically engineered mouse model of PIK3CA wild-type colorectal cancer. *PloS one,* **6**(9), pp. e25132.

ROTH, J., ROACH, E.S., BARTELS, U., JOZWIAK, S., KOENIG, M.K., WEINER, H.L., FRANZ, D.N. and WANG, H.Z., 2013. Subependymal giant cell astrocytoma: diagnosis, screening, and treatment. Recommendations from the International Tuberous Sclerosis Complex Consensus Conference 2012. *Pediatric neurology,* **49**(6), pp. 439-444.

ROY, S.K., SRIVASTAVA, R.K. and SHANKAR, S., 2010. Inhibition of PI3K/AKT and MAPK/ERK pathways causes activation of FOXO transcription factor, leading to cell cycle arrest and apoptosis in pancreatic cancer. *Journal of molecular signaling,* **5**, pp. 10-2187-5-10.

ROYCE, M.E. and OSMAN, D., 2015. Everolimus in the Treatment of Metastatic Breast Cancer. *Breast cancer : basic and clinical research,* **9**, pp. 73-79.

SAKTHIVEL, K.M. and HARIHARAN, S., 2017. Regulatory players of DNA damage repair mechanisms: Role in Cancer Chemoresistance. *Biomedicine & pharmacotherapy = Biomedecine & pharmacotherapie,* **93**, pp. 1238-1245.

SARBASSOV, D.D., GUERTIN, D.A., ALI, S.M. and SABATINI, D.M., 2005. Phosphorylation and regulation of Akt/PKB by the rictor-mTOR complex. *Science (New York, N.Y.),* **307**(5712), pp. 1098-1101.

SARKER, D., ANG, J.E., BAIRD, R., KRISTELEIT, R., SHAH, K., MORENO, V., CLARKE, P.A., RAYNAUD, F.I., LEVY, G., WARE, J.A., MAZINA, K., LIN, R., WU, J., FREDRICKSON, J., SPOERKE, J.M., LACKNER, M.R., YAN, Y., FRIEDMAN, L.S., KAYE, S.B., DERYNCK, M.K., WORKMAN, P. and DE BONO, J.S., 2015. First-in-human phase I study of pictilisib (GDC-0941), a potent pan-class I phosphatidylinositol-3-kinase (PI3K) inhibitor, in patients with advanced solid tumors. *Clinical cancer research : an official journal of the American Association for Cancer Research,* **21**(1), pp. 77-86.

SASAKI, T., IRIE-SASAKI, J., JONES, R.G., OLIVEIRA-DOS-SANTOS, A.J., STANFORD, W.L., BOLON, B., WAKEHAM, A., ITIE, A., BOUCHARD, D., KOZIERADZKI, I., JOZA, N., MAK, T.W., OHASHI, P.S., SUZUKI, A. and PENNINGER, J.M., 2000. Function of PI3Kgamma in thymocyte development, T cell activation, and neutrophil migration. *Science (New York, N.Y.),* **287**(5455), pp. 1040-1046.

SAURA, C., RODA, D., ROSELLO, S., OLIVEIRA, M., MACARULLA, T., PEREZ-FIDALGO, J.A., MORALES-BARRERA, R., SANCHIS-GARCIA, J.M., MUSIB, L., BUDHA, N., ZHU, J., NANNINI, M., CHAN, W.Y., SANABRIA BOHORQUEZ, S.M., MENG, R.D., LIN, K., YAN, Y., PATEL, P., BASELGA, J., TABERNERO, J. and CERVANTES, A., 2017. A First-in-Human Phase I Study of the ATP-Competitive AKT Inhibitor Ipatasertib Demonstrates Robust and Safe Targeting of AKT in Patients with Solid Tumors. *Cancer discovery,* **7**(1), pp. 102-113.

SCHMIDT, M., FERNANDEZ DE MATTOS, S., VAN DER HORST, A., KLOMPMAKER, R., KOPS, G.J., LAM, E.W., BURGERING, B.M. and MEDEMA, R.H., 2002a. Cell cycle inhibition by FoxO

forkhead transcription factors involves downregulation of cyclin D. *Molecular and cellular biology,* **22**(22), pp. 7842-7852.

SCHMIDT, M., FERNANDEZ DE MATTOS, S., VAN DER HORST, A., KLOMPMAKER, R., KOPS, G.J., LAM, E.W., BURGERING, B.M. and MEDEMA, R.H., 2002b. Cell cycle inhibition by FoxO forkhead transcription factors involves downregulation of cyclin D. *Molecular and cellular biology,* **22**(22), pp. 7842-7852.

SCHROEDER, T.M., CHINTAGUMPALA, M., OKCU, M.F., CHIU, J.K., TEH, B.S., WOO, S.Y. and PAULINO, A.C., 2008. Intensity-modulated radiation therapy in childhood ependymoma. *International journal of radiation oncology, biology, physics,* **71**(4), pp. 987-993.

SCHWINDINGER, W.F. and ROBISHAW, J.D., 2001. Heterotrimeric G-protein betagamma-dimers in growth and differentiation. *Oncogene,* **20**(13), pp. 1653-1660.

SCOTTING, P.J., WALKER, D.A. and PERILONGO, G., 2005. Childhood solid tumours: a developmental disorder. *Nature reviews.Cancer,* **5**(6), pp. 481-488.

SEGERSTROM, L., BARYAWNO, N., SVEINBJORNSSON, B., WICKSTROM, M., ELFMAN, L., KOGNER, P. and JOHNSEN, J.I., 2011. Effects of small molecule inhibitors of PI3K/Akt/mTOR signaling on neuroblastoma growth in vitro and in vivo. *International journal of cancer,* **129**(12), pp. 2958-2965.

SEHGAL, S.N., 2003. Sirolimus: its discovery, biological properties, and mechanism of action. *Transplantation proceedings,* **35**(3 Suppl), pp. 7S-14S.

SEKIMOTO, T., FUKUMOTO, M. and YONEDA, Y., 2004. 14-3-3 suppresses the nuclear localization of threonine 157-phosphorylated p27(Kip1). *The EMBO journal,* **23**(9), pp. 1934-1942.

SEN, B., XIE, Z., CASE, N., THOMPSON, W.R., UZER, G., STYNER, M. and RUBIN, J., 2014. mTORC2 regulates mechanically induced cytoskeletal reorganization and lineage selection in marrow-derived mesenchymal stem cells. *Journal of bone and mineral research : the official journal of the American Society for Bone and Mineral Research,* **29**(1), pp. 78-89.

SEOANE, J., LE, H.V., SHEN, L., ANDERSON, S.A. and MASSAGUE, J., 2004. Integration of Smad and forkhead pathways in the control of neuroepithelial and glioblastoma cell proliferation. *Cell,* **117**(2), pp. 211-223.

SERRA, V., MARKMAN, B., SCALTRITI, M., EICHHORN, P.J., VALERO, V., GUZMAN, M., BOTERO, M.L., LLONCH, E., ATZORI, F., DI COSIMO, S., MAIRA, M., GARCIA-ECHEVERRIA, C., PARRA, J.L., ARRIBAS, J. and BASELGA, J., 2008a. NVP-BEZ235, a dual PI3K/mTOR inhibitor, prevents PI3K signaling and inhibits the growth of cancer cells with activating PI3K mutations. *Cancer research,* **68**(19), pp. 8022-8030.

SHARMA, P., ABRAMSON, V.G., O'DEA, A., PATHAK, H.B., PESSETTO, Z.Y., and WANG, Y.Y., 2018. Clinical and biomarker results from phase I/II study of PI3K inhibitor BYL 719 (alpelisib) plus nab-paclitaxel in HER2-negative metastatic breast cancer. *Journal of clinical oncology.* 36.15(Suppl.1018).

SHATS, I., GATZA, M.L., LIU, B., ANGUS, S.P., YOU, L. and NEVINS, J.R., 2013. FOXO transcription factors control E2F1 transcriptional specificity and apoptotic function. *Cancer research,* **73**(19), pp. 6056-6067.

SHEPHERD, C., BANERJEE, L., CHEUNG, C.W., MANSOUR, M.R., JENKINSON, S., GALE, R.E. and KHWAJA, A., 2013. PI3K/mTOR inhibition upregulates NOTCH-MYC signalling leading to an impaired cytotoxic response. *Leukemia,* **27**(3), pp. 650-660.

SHERR, C.J. and ROBERTS, J.M., 1999. CDK inhibitors: positive and negative regulators of G1-phase progression. *Genes & development,* **13**(12), pp. 1501-1512.

SHI, F., GUO, H., ZHANG, R., LIU, H., WU, L., WU, Q., LIU, J., LIU, T. and ZHANG, Q., 2017. The PI3K inhibitor GDC-0941 enhances radiosensitization and reduces chemoresistance to temozolomide in GBM cell lines. *Neuroscience,* **346**, pp. 298-308.

SHIM, K.W., KIM, D.S. and CHOI, J.U., 2009. The history of ependymoma management. *Child's nervous system : ChNS : official journal of the International Society for Pediatric Neurosurgery,* **25**(10), pp. 1167-1183.

SHTIVELMAN, E., SUSSMAN, J. and STOKOE, D., 2002. A role for PI 3-kinase and PKB activity in the G2/M phase of the cell cycle. *Current biology : CB,* **12**(11), pp. 919-924.

SHTUTMAN, M., ZHURINSKY, J., SIMCHA, I., ALBANESE, C., D'AMICO, M., PESTELL, R. and BEN-ZE'EV, A., 1999. The cyclin D1 gene is a target of the beta-catenin/LEF-1 pathway. *Proceedings of the National Academy of Sciences of the United States of America,* **96**(10), pp. 5522-5527.

SHYMANETS, A., PRAJWAL, BUCHER, K., BEER-HAMMER, S., HARTENECK, C. and NURNBERG, B., 2013. p87 and p101 subunits are distinct regulators determining class IB phosphoinositide 3-kinase (PI3K) specificity. *The Journal of biological chemistry,* **288**(43), pp. 31059-31068.

SIE, M., DEN DUNNEN, W.F., LOURENS, H.J., MEEUWSEN-DE BOER, T.G., SCHERPEN, F.J., ZOMERMAN, W.W., KAMPEN, K.R., HOVING, E.W. and DE BONT, E.S., 2015. Growth-Factor-Driven Rescue to Receptor Tyrosine Kinase (RTK) Inhibitors through Akt and Erk Phosphorylation in Pediatric Low Grade Astrocytoma and Ependymoma. *PloS one,* **10**(3), pp. e0122555.

SLANSKY, J.E. and FARNHAM, P.J., 1996. Introduction to the E2F family: protein structure and gene regulation. *Current topics in microbiology and immunology,* **208**, pp. 1-30.

SINNBERG, T., LASITHIOTAKIS, K., NIESSNER, H., SCHITTEK, B., FLAHERTY, K.T., KULMS, D., MACZEY, E., CAMPOS, M., GOGEL, J., GARBE, C. and MEIER, F., 2009. Inhibition of PI3K-AKT-mTOR signaling sensitizes melanoma cells to cisplatin and temozolomide. *The Journal of investigative dermatology,* **129**(6), pp. 1500-1515.

SONG, M.S., SALMENA, L. and PANDOLFI, P.P., 2012. The functions and regulation of the PTEN tumour suppressor. *Nature reviews.Molecular cell biology,* **13**(5), pp. 283-296.

SOULE, H.D., VAZGUEZ, J., LONG, A., ALBERT, S. and BRENNAN, M., 1973. A human cell line from a pleural effusion derived from a breast carcinoma. *Journal of the National Cancer Institute,* **51**(5), pp. 1409-1416.

SPANKUCH, B., KURUNCI-CSACSKO, E., KAUFMANN, M. and STREBHARDT, K., 2007. Rational combinations of siRNAs targeting Plk1 with breast cancer drugs. *Oncogene,* **26**(39), pp. 5793-5807.

SPERANZA, M.C., NOWICKI, M.O., BEHERA, P., CHO, C.F., CHIOCCA, E.A. and LAWLER, S.E., 2016. BKM-120 (Buparlisib): A Phosphatidyl-Inositol-3 Kinase Inhibitor with Anti-Invasive Properties in Glioblastoma. *Scientific reports,* **6**, pp. 20189.

SRIVASTAVA, V.K., YASRUEL, Z. and NALBANTOGLU, J., 2009. Impaired medulloblastoma cell survival following activation of the FOXO1 transcription factor. *International journal of oncology,* **35**(5), pp. 1045-1051.

STAMBOLIC, V., TSAO, M.S., MACPHERSON, D., SUZUKI, A., CHAPMAN, W.B. and MAK, T.W., 2000. High incidence of breast and endometrial neoplasia resembling human Cowden syndrome in pten+/- mice. *Cancer research,* **60**(13), pp. 3605-3611.

STUPP, R., HEGI, M.E., MASON, W.P., VAN DEN BENT, M.J., TAPHOORN, M.J., JANZER, R.C., LUDWIN, S.K., ALLGEIER, A., FISHER, B., BELANGER, K., HAU, P., BRANDES, A.A., GIJTENBEEK, J., MAROSI, C., VECHT, C.J., MOKHTARI, K., WESSELING, P., VILLA, S., EISENHAUER, E., GORLIA, T., WELLER, M., LACOMBE, D., CAIRNCROSS, J.G., MIRIMANOFF, R.O., EUROPEAN ORGANISATION FOR RESEARCH AND TREATMENT OF CANCER BRAIN TUMOUR AND RADIATION ONCOLOGY GROUPS and NATIONAL CANCER INSTITUTE OF CANADA CLINICAL TRIALS GROUP, 2009. Effects of radiotherapy with concomitant and adjuvant temozolomide versus radiotherapy alone on survival in glioblastoma in a randomised phase III study: 5-year analysis of the EORTC-NCIC trial. *The Lancet.Oncology,* **10**(5), pp. 459-466.

SUBRAMANIAM, P.S., WHYE, D.W., EFIMENKO, E., CHEN, J., TOSELLO, V., DE KEERSMAECKER, K., KASHISHIAN, A., THOMPSON, M.A., CASTILLO, M., CORDON-CARDO, C., DAVE, U.P., FERRANDO, A., LANNUTTI, B.J. and DIACOVO, T.G., 2012. Targeting nonclassical oncogenes for therapy in T-ALL. *Cancer cell,* **21**(4), pp. 459-472.

SUBRAMANIAN, A., TAMAYO, P., MOOTHA, V.K., MUKHERJEE, S., EBERT, B.L., GILLETTE, M.A., PAULOVICH, A., POMEROY, S.L., GOLUB, T.R., LANDER, E.S. and MESIROV, J.P., 2005. Gene set enrichment analysis: a knowledge-based approach for interpreting genome-wide expression profiles. *Proceedings of the National Academy of Sciences of the United States of America,* **102**(43), pp. 15545-15550.

SUBRAMANIAN, S., WEST, R.B., CORLESS, C.L., OU, W., RUBIN, B.P., CHU, K.M., LEUNG, S.Y., YUEN, S.T., ZHU, S., HERNANDEZ-BOUSSARD, T., MONTGOMERY, K., NIELSEN, T.O., PATEL, R.M., GOLDBLUM, J.R., HEINRICH, M.C., FLETCHER, J.A. and VAN DE RIJN, M., 2004. Gastrointestinal stromal tumors (GISTs) with KIT and PDGFRA mutations have distinct gene expression profiles. *Oncogene,* **23**(47), pp. 7780-7790.

SWANSON, E.L., AMDUR, R.J., MORRIS, C.G., GALLOWAY, T.J., MARCUS, R.B.,Jr, PINCUS, D.W. and SMITH, A., 2011. Intracranial ependymomas treated with radiotherapy: long-term results from a single institution. *Journal of neuro-oncology,* **102**(3), pp. 451-457.

TAI, D., WELLS, K., ARCAROLI, J., VANDERBILT, C., AISNER, D.L., MESSERSMITH, W.A. and LIEU, C.H., 2015. Targeting the WNT Signaling Pathway in Cancer Therapeutics. *The oncologist,* **20**(10), pp. 1189-1198.

TAKAHASHI, Y., RAYMAN, J.B. and DYNLACHT, B.D., 2000. Analysis of promoter binding by the E2F and pRB families in vivo: distinct E2F proteins mediate activation and repression. *Genes & development,* **14**(7), pp. 804-816.

TAN, M.H., MESTER, J., PETERSON, C., YANG, Y., CHEN, J.L., RYBICKI, L.A., MILAS, K., PEDERSON, H., REMZI, B., ORLOFF, M.S. and ENG, C., 2011. A clinical scoring system for selection of patients for PTEN mutation testing is proposed on the basis of a prospective study of 3042 probands. *American Journal of Human Genetics,* **88**(1), pp. 42-56.

TAN, P., GUAN, H., XIE, L., MI, B., FANG, Z., LI, J. and LI, F., 2015. FOXO1 inhibits osteoclastogenesis partially by antagnozing MYC. *Scientific reports,* **5**, pp. 16835.

TANG, G., LIU, D., XIAO, G., LIU, Q. and YUAN, J., 2016. Transcriptional repression of FOXO1 by KLF4 contributes to glioma progression. *Oncotarget,* **7**(49), pp. 81757-81767.

TANTAWY, M., ELZAYAT, M.G., YEHIA, D. and TAHA, H., 2018. Identification of microRNA signature in different pediatric brain tumors. *Genetics and molecular biology,* **41**(1), pp. 27-34.

TAYLOR, M.D., POPPLETON, H., FULLER, C., SU, X., LIU, Y., JENSEN, P., MAGDALENO, S., DALTON, J., CALABRESE, C., BOARD, J., MACDONALD, T., RUTKA, J., GUHA, A., GAJJAR, A., CURRAN, T. and GILBERTSON, R.J., 2005. Radial glia cells are candidate stem cells of ependymoma. *Cancer cell,* **8**(4), pp. 323-335.

TAZZARI, P.L., TABELLINI, G., RICCI, F., PAPA, V., BORTUL, R., CHIARINI, F., EVANGELISTI, C., MARTINELLI, G., BONTADINI, A., COCCO, L., MCCUBREY, J.A. and MARTELLI, A.M., 2008. Synergistic proapoptotic activity of recombinant TRAIL plus the Akt inhibitor Perifosine in acute myelogenous leukemia cells. *Cancer research,* **68**(22), pp. 9394-9403.

TENBAUM, S.P., ORDONEZ-MORAN, P., PUIG, I., CHICOTE, I., ARQUES, O., LANDOLFI, S., FERNANDEZ, Y., HERANCE, J.R., GISPERT, J.D., MENDIZABAL, L., AGUILAR, S., RAMON Y CAJAL, S., SCHWARTZ, S.,Jr, VIVANCOS, A., ESPIN, E., ROJAS, S., BASELGA, J., TABERNERO, J., MUNOZ, A. and PALMER, H.G., 2012. beta-catenin confers resistance to PI3K and AKT inhibitors and subverts FOXO3a to promote metastasis in colon cancer. *Nature medicine,* **18**(6), pp. 892-901.

THORPE, L.M., YUZUGULLU, H. and ZHAO, J.J., 2015. PI3K in cancer: divergent roles of isoforms, modes of activation and therapeutic targeting. *Nature reviews.Cancer,* **15**(1), pp. 7-24.

TIMMERMANN, B., KORTMANN, R.D., KUHL, J., MEISNER, C., SLAVC, I., PIETSCH, T. and BAMBERG, M., 2000. Combined postoperative irradiation and chemotherapy for anaplastic ependymomas in childhood: results of the German prospective trials HIT 88/89 and HIT 91. *International journal of radiation oncology, biology, physics,* **46**(2), pp. 287-295.

TODDE, V., VEENHUIS, M. and VAN DER KLEI, I.J., 2009. Autophagy: principles and significance in health and disease. *Biochimica et biophysica acta,* **1792**(1), pp. 3-13.

TSCHOPP, O., YANG, Z.Z., BRODBECK, D., DUMMLER, B.A., HEMMINGS-MIESZCZAK, M., WATANABE, T., MICHAELIS, T., FRAHM, J. and HEMMINGS, B.A., 2005. Essential role of protein kinase B gamma (PKB gamma/Akt3) in postnatal brain development but not in glucose homeostasis. *Development (Cambridge, England),* **132**(13), pp. 2943-2954.

TSURUTA, F., MASUYAMA, N. and GOTOH, Y., 2002. The phosphatidylinositol 3-kinase (PI3K)-Akt pathway suppresses Bax translocation to mitochondria. *The Journal of biological chemistry,* **277**(16), pp. 14040-14047.

TZIVION, G., DOBSON, M. and RAMAKRISHNAN, G., 2011. FoxO transcription factors; Regulation by AKT and 14-3-3 proteins. *Biochimica et biophysica acta,* **1813**(11), pp. 1938-1945.

VAHIDNEZHAD, H., YOUSSEFIAN, L. and UITTO, J., 2016. Molecular Genetics of the PI3K-AKT-mTOR Pathway in Genodermatoses: Diagnostic Implications and Treatment Opportunities. *The Journal of investigative dermatology,* **136**(1), pp. 15-23.

VAN DER HEIDE, L.P., HOEKMAN, M.F. and SMIDT, M.P., 2004. The ins and outs of FoxO shuttling: mechanisms of FoxO translocation and transcriptional regulation. *The Biochemical journal,* **380**(Pt 2), pp. 297-309.

VAN UMMERSEN, L., BINGER, K., VOLKMAN, J., MARNOCHA, R., TUTSCH, K., KOLESAR, J., ARZOOMANIAN, R., ALBERTI, D. and WILDING, G., 2004. A phase I trial of perifosine (NSC 639966) on a loading dose/maintenance dose schedule in patients with advanced cancer. *Clinical cancer research : an official journal of the American Association for Cancer Research,* **10**(22), pp. 7450-7456.

VANHAESEBROECK, B. and ALESSI, D.R., 2000. The PI3K-PDK1 connection: more than just a road to PKB. *The Biochemical journal,* **346 Pt 3**, pp. 561-576.

VANHAESEBROECK, B., LEEVERS, S.J., PANAYOTOU, G. and WATERFIELD, M.D., 1997. Phosphoinositide 3-kinases: a conserved family of signal transducers. *Trends in biochemical sciences,* **22**(7), pp. 267-272.

VANSTEENKISTE, J.F., CANON, J.L., DE BRAUD, F., GROSSI, F., DE PAS, T., GRAY, J.E., SU, W.C., FELIP, E., YOSHIOKA, H., GRIDELLI, C., DY, G.K., THONGPRASERT, S., RECK, M., AIMONE, P., VIDAM, G.A., ROUSSOU, P., WANG, Y.A., DI TOMASO, E. and SORIA, J.C., 2015. Safety and Efficacy of Buparlisib (BKM120) in Patients with PI3K Pathway-Activated Non-Small Cell Lung Cancer: Results from the Phase II BASALT-1 Study. *Journal of thoracic oncology : official publication of the International Association for the Study of Lung Cancer,* **10**(9), pp. 1319-1327.

VELMA, V., DASARI, S.R. and TCHOUNWOU, P.B., 2016. Low Doses of Cisplatin Induce Gene Alterations, Cell Cycle Arrest, and Apoptosis in Human Promyelocytic Leukemia Cells. *Biomarker insights,* **11**, pp. 113-121.

VENKATRAMANI, R., JI, L., LASKY, J., HALEY, K., JUDKINS, A., ZHOU, S., SPOSTO, R., OLSHEFSKI, R., GARVIN, J., TEKAUTZ, T., KENNEDY, G., RASSEKH, S.R., MOORE, T., GARDNER, S., ALLEN, J., SHORE, R., MOERTEL, C., ATLAS, M., DHALL, G. and FINLAY, J., 2013. Outcome of infants and young children with newly diagnosed ependymoma treated on the "Head Start" III prospective clinical trial. *Journal of neuro-oncology,* **113**(2), pp. 285-291.

VIJAYARAGHAVAN, S., KARAKAS, C., DOOSTAN, I., CHEN, X., BUI, T., YI, M., RAGHAVENDRA, A.S., ZHAO, Y., BASHOUR, S.I., IBRAHIM, N.K., KARUTURI, M., WANG, J., WINKLER, J.D., AMARAVADI, R.K., HUNT, K.K., TRIPATHY, D. and KEYOMARSI, K., 2017. CDK4/6 and autophagy inhibitors synergistically induce senescence in Rb positive cytoplasmic cyclin E negative cancers. *Nature communications,* **8**, pp. 15916.

VOLINIA, S., DHAND, R., VANHAESEBROECK, B., MACDOUGALL, L.K., STEIN, R., ZVELEBIL, M.J., DOMIN, J., PANARETOU, C. and WATERFIELD, M.D., 1995. A human phosphatidylinositol 3-kinase complex related to the yeast Vps34p-Vps15p protein sorting system. *The EMBO journal,* **14**(14), pp. 3339-3348.

VORA, S.R., JURIC, D., KIM, N., MINO-KENUDSON, M., HUYNH, T., COSTA, C., LOCKERMAN, E.L., POLLACK, S.F., LIU, M., LI, X., LEHAR, J., WIESMANN, M., WARTMANN, M., CHEN, Y., CAO, Z.A., PINZON-ORTIZ, M., KIM, S., SCHLEGEL, R., HUANG, A. and ENGELMAN, J.A., 2014. CDK 4/6 inhibitors sensitize PIK3CA mutant breast cancer to PI3K inhibitors. *Cancer cell,* **26**(1), pp. 136-149.

WALKER, O., DAWODU, A.H., ADEYOKUNNU, A.A., SALAKO, L.A. and ALVAN, G., 1983. Plasma chloroquine and desethylchloroquine concentrations in children during and after chloroquine treatment for malaria. *British journal of clinical pharmacology,* **16**(6), pp. 701-705.

WALLIN, J.J., EDGAR, K.A., GUAN, J., BERRY, M., PRIOR, W.W., LEE, L., LESNICK, J.D., LEWIS, C., NONOMIYA, J., PANG, J., SALPHATI, L., OLIVERO, A.G., SUTHERLIN, D.P., O'BRIEN, C., SPOERKE, J.M., PATEL, S., LENSUN, L., KASSEES, R., ROSS, L., LACKNER, M.R., SAMPATH, D., BELVIN, M. and FRIEDMAN, L.S., 2011. GDC-0980 is a novel class I PI3K/mTOR kinase inhibitor with robust activity in cancer models driven by the PI3K pathway. *Molecular cancer therapeutics,* **10**(12), pp. 2426-2436.

WALSH, J.G., CULLEN, S.P., SHERIDAN, C., LUTHI, A.U., GERNER, C. and MARTIN, S.J., 2008. Executioner caspase-3 and caspase-7 are functionally distinct proteases. *Proceedings of the National Academy of Sciences of the United States of America,* **105**(35), pp. 12815-12819.

WANG, H., IAKOVA, P., WILDE, M., WELM, A., GOODE, T., ROESLER, W.J. and TIMCHENKO, N.A., 2001. C/EBPalpha arrests cell proliferation through direct inhibition of Cdk2 and Cdk4. *Molecular cell,* **8**(4), pp. 817-828.

WANG, M., ZHANG, X., ZHAO, H., WANG, Q. and PAN, Y., 2009. FoxO gene family evolution in vertebrates. *BMC evolutionary biology,* **9**, pp. 222-2148-9-222.

WANG, Q., VON, T., BRONSON, R., RUAN, M., MU, W., HUANG, A., MAIRA, S.M. and ZHAO, J.J., 2013. Spatially distinct roles of class Ia PI3K isoforms in the development and maintenance of PTEN hamartoma tumor syndrome. *Genes & development,* **27**(14), pp. 1568-1580.

WANG, X., DING, J. and MENG, L.H., 2015. PI3K isoform-selective inhibitors: next-generation targeted cancer therapies. *Acta Pharmacologica Sinica,* **36**(10), pp. 1170-1176.

WANG, Y., PENNOCK, S.D., CHEN, X., KAZLAUSKAS, A. and WANG, Z., 2004. Platelet-derived growth factor receptor-mediated signal transduction from endosomes. *The Journal of biological chemistry,* **279**(9), pp. 8038-8046.

WANG, Y., WILTSHIRE, T., SENFT, J., WENGER, S.L., REED, E. and WANG, W., 2006. Fanconi anemia D2 protein confers chemoresistance in response to the anticancer agent, irofulven. *Molecular cancer therapeutics,* **5**(12), pp. 3153-3161.

WANI, K., ARMSTRONG, T.S., VERA-BOLANOS, E., RAGHUNATHAN, A., ELLISON, D., GILBERTSON, R., VAILLANT, B., GOLDMAN, S., PACKER, R.J., FOULADI, M., POLLACK, I., MIKKELSEN, T., PRADOS, M., OMURO, A., SOFFIETTI, R., LEDOUX, A., WILSON, C., LONG, L., GILBERT, M.R., ALDAPE, K. and COLLABORATIVE EPENDYMOMA RESEARCH NETWORK, 2012. A prognostic gene expression signature in infratentorial ependymoma. *Acta Neuropathologica,* **123**(5), pp. 727-738.

WARD, J., LOURDUSAMY, A., SPEED, D., GOULD, T., GRUNDY, R. and RAHMAN, R. 2014. HDACi sensitivity and gene expression analysis of two-dimensional and three-dimensional models of pediatric ependymoma. *Neuro-Oncology.* 16(Suppl 1): i17-i25.

WEN, P.Y., LEE, E.Q., REARDON, D.A., LIGON, K.L. and ALFRED YUNG, W.K., 2012. Current clinical development of PI3K pathway inhibitors in glioblastoma. *Neuro-oncology,* **14**(7), pp. 819-829.

WEST, K.A., CASTILLO, S.S. and DENNIS, P.A., 2002. Activation of the PI3K/Akt pathway and chemotherapeutic resistance. *Drug resistance updates : reviews and commentaries in antimicrobial and anticancer chemotherapy,* **5**(6), pp. 234-248.

WHITE, E., 2015. The role for autophagy in cancer. *The Journal of clinical investigation,* **125**(1), pp. 42-46.

WIEDEMANN, E., JELLINGHAUS, S., ENDE, G., AUGSTEIN, A., SCZECH, R., WIELOCKX, B., WEINERT, S., STRASSER, R.H. and POITZ, D.M., 2017. Regulation of endothelial migration and proliferation by ephrin-A1. *Cellular signalling,* **29**, pp. 84-95.

WITT, H., MACK, S.C., RYZHOVA, M., BENDER, S., SILL, M., ISSERLIN, R., BENNER, A., HIELSCHER, T., MILDE, T., REMKE, M., JONES, D.T., NORTHCOTT, P.A., GARZIA, L., BERTRAND, K.C., WITTMANN, A., YAO, Y., ROBERTS, S.S., MASSIMI, L., VAN METER, T., WEISS, W.A., GUPTA, N., GRAJKOWSKA, W., LACH, B., CHO, Y.J., VON DEIMLING, A., KULOZIK, A.E., WITT, O., BADER, G.D., HAWKINS, C.E., TABORI, U., GUHA, A., RUTKA, J.T., LICHTER, P., KORSHUNOV, A., TAYLOR, M.D. and PFISTER, S.M., 2011. Delineation of two clinically and molecularly distinct subgroups of posterior fossa ependymoma. *Cancer cell,* **20**(2), pp. 143-157.

WONG, C.H., MA, B.B., CHEONG, H.T., HUI, C.W., HUI, E.P. and CHAN, A.T., 2015. Preclinical evaluation of PI3K inhibitor BYL719 as a single agent and its synergism in combination with cisplatin or MEK inhibitor in nasopharyngeal carcinoma (NPC). *American journal of cancer research,* **5**(4), pp. 1496-1506.

WRIGHT, K.D., DARYANI, V.M., TURNER, D.C., ONAR-THOMAS, A., BOULOS, N., ORR, B.A., GILBERTSON, R.J., STEWART, C.F. and GAJJAR, A., 2015. Phase I study of 5-fluorouracil in children and young adults with recurrent ependymoma. *Neuro-oncology,* **17**(12), pp. 1620-1627.

WU, G., DIAZ, A.K., PAUGH, B.S., RANKIN, S.L., JU, B., LI, Y., ZHU, X., QU, C., CHEN, X., ZHANG, J., EASTON, J., EDMONSON, M., MA, X., LU, C., NAGAHAWATTE, P., HEDLUND, E.,

RUSCH, M., POUNDS, S., LIN, T., ONAR-THOMAS, A., HUETHER, R., KRIWACKI, R., PARKER, M., GUPTA, P., BECKSFORT, J., WEI, L., MULDER, H.L., BOGGS, K., VADODARIA, B., YERGEAU, D., RUSSELL, J.C., OCHOA, K., FULTON, R.S., FULTON, L.L., JONES, C., BOOP, F.A., BRONISCER, A., WETMORE, C., GAJJAR, A., DING, L., MARDIS, E.R., WILSON, R.K., TAYLOR, M.R., DOWNING, J.R., ELLISON, D.W., ZHANG, J. and BAKER, S.J., 2014. The genomic landscape of diffuse intrinsic pontine glioma and pediatric non-brainstem high-grade glioma. *Nature genetics,* **46**(5), pp. 444-450.

WU, J., ARMSTRONG, T.S. and GILBERT, M.R., 2016. Biology and management of ependymomas. *Neuro-oncology,* **18**(7), pp. 902-913.

WU, Y.L., ZHANG, L.I., TRANDAFIR, L., DONG, T., DUVAL, V., HAZELL, K. and XU, B., 2016. Phase I Study of the Pan-PI3K Inhibitor Buparlisib in Adult Chinese Patients with Advanced Solid Tumors. *Anticancer Research,* **36**(11), pp. 6185-6194.

WULLAERT, A., BONNET, M.C. and PASPARAKIS, M., 2011. NF-kappaB in the regulation of epithelial homeostasis and inflammation. *Cell research,* **21**(1), pp. 146-158.

WURZ, K., GARCIA, R.L., GOFF, B.A., MITCHELL, P.S., LEE, J.H., TEWARI, M. and SWISHER, E.M., 2010. MiR-221 and MiR-222 alterations in sporadic ovarian carcinoma: Relationship to CDKN1B, CDKNIC and overall survival. *Genes, chromosomes & cancer,* **49**(7), pp. 577-584.

XIA, Y., SHEN, S. and VERMA, I.M., 2014. NF-kappaB, an active player in human cancers. *Cancer immunology research,* **2**(9), pp. 823-830.

XING, X., ZHANG, L., WEN, X., WANG, X., CHENG, X., DU, H., HU, Y., LI, L., DONG, B., LI, Z. and JI, J., 2014. PP242 suppresses cell proliferation, metastasis, and angiogenesis of gastric cancer through inhibition of the PI3K/AKT/mTOR pathway. *Anti-Cancer Drugs,* **25**(10), pp. 1129-1140.

XU, C., LI, X., LI, T., WANG, X., YANG, Y., XIAO, L. and SHEN, H., 2011. Combination effects of paclitaxel with signaling inhibitors in endometrial cancer cells. *Asian Pacific journal of cancer prevention : APJCP,* **12**(11), pp. 2951-2957.

YAN, L., MIEULET, V. and LAMB, R.F., 2008. mTORC2 is the hydrophobic motif kinase for SGK1. *The Biochemical journal,* **416**(3), pp. e19-21.

YANG, J.Y., ZONG, C.S., XIA, W., YAMAGUCHI, H., DING, Q., XIE, X., LANG, J.Y., LAI, C.C., CHANG, C.J., HUANG, W.C., HUANG, H., KUO, H.P., LEE, D.F., LI, L.Y., LIEN, H.C., CHENG, X., CHANG, K.J., HSIAO, C.D., TSAI, F.J., TSAI, C.H., SAHIN, A.A., MULLER, W.J., MILLS, G.B., YU, D., HORTOBAGYI, G.N. and HUNG, M.C., 2008. ERK promotes tumorigenesis by inhibiting FOXO3a via MDM2-mediated degradation. *Nature cell biology,* **10**(2), pp. 138-148.

YANG, P., LING, L., SUN, W., YANG, J., ZHANG, L., CHANG, G., GUO, J., SUN, J., SUN, L. and LU, D., 2018. Ginsenoside Rg1 inhibits apoptosis by increasing autophagy via the AMPK/mTOR signaling in serum deprivation macrophages. *Acta biochimica et biophysica Sinica,* **50**(2), pp. 144-155.

YANG, S., LI, X., GUAN, W., QIAN, M., YAO, Z., YIN, X. and ZHAO, H., 2017. NVP-BKM120 inhibits colon cancer growth via FoxO3a-dependent PUMA induction. *Oncotarget,* **8**(47), pp. 83052-83062.

YANG, X.L., LIN, F.J., GUO, Y.J., SHAO, Z.M. and OU, Z.L., 2014. Gemcitabine resistance in breast cancer cells regulated by PI3K/AKT-mediated cellular proliferation exerts negative feedback via the MEK/MAPK and mTOR pathways. *OncoTargets and therapy,* **7**, pp. 1033-1042.

YAO, J.C., SHAH, M.H., ITO, T., BOHAS, C.L., WOLIN, E.M., VAN CUTSEM, E., HOBDAY, T.J., OKUSAKA, T., CAPDEVILA, J., DE VRIES, E.G., TOMASSETTI, P., PAVEL, M.E., HOOSEN, S., HAAS, T., LINCY, J., LEBWOHL, D., OBERG, K. and RAD001 IN ADVANCED NEUROENDOCRINE TUMORS, THIRD TRIAL (RADIANT-3) STUDY GROUP, 2011. Everolimus for advanced pancreatic neuroendocrine tumors. *The New England journal of medicine,* **364**(6), pp. 514-523.

YAO, Y., MACK, S.C. and TAYLOR, M.D., 2011. Molecular genetics of ependymoma. *Chinese journal of cancer,* **30**(10), pp. 669-681.

YEA, S.S. and FRUMAN, D.A., 2013. Achieving cancer cell death with PI3K/mTOR-targeted therapies. *Annals of the New York Academy of Sciences,* **1280**, pp. 15-18.

YEE, W.M. and WORLEY, P.F., 1997. Rheb interacts with Raf-1 kinase and may function to integrate growth factor- and protein kinase A-dependent signals. *Molecular and cellular biology,* **17**(2), pp. 921-933.

YIM, D.G., GHOSH, S., GUY, G.R. and VIRSHUP, D.M., 2015. Casein kinase 1 regulates Sprouty2 in FGF-ERK signaling. *Oncogene,* **34**(4), pp. 474-484.

YOSHIOKA, K., YOSHIDA, K., CUI, H., WAKAYAMA, T., TAKUWA, N., OKAMOTO, Y., DU, W., QI, X., ASANUMA, K., SUGIHARA, K., AKI, S., MIYAZAWA, H., BISWAS, K., NAGAKURA, C., UENO, M., ISEKI, S., SCHWARTZ, R.J., OKAMOTO, H., SASAKI, T., MATSUI, O., ASANO, M., ADAMS, R.H., TAKAKURA, N. and TAKUWA, Y., 2012. Endothelial PI3K-C2alpha, a class II PI3K, has an essential role in angiogenesis and vascular barrier function. *Nature medicine,* **18**(10), pp. 1560-1569.

YU, H.G., AI, Y.W., YU, L.L., ZHOU, X.D., LIU, J., LI, J.H., XU, X.M., LIU, S., CHEN, J., LIU, F., QI, Y.L., DENG, Q., CAO, J., LIU, S.Q., LUO, H.S. and YU, J.P., 2008. Phosphoinositide 3-kinase/Akt pathway plays an important role in chemoresistance of gastric cancer cells against etoposide and doxorubicin induced cell death. *International journal of cancer,* **122**(2), pp. 433-443.

YU, K., LUCAS, J., ZHU, T., ZASK, A., GAYDOS, C., TORAL-BARZA, L., GU, J., LI, F., CHAUDHARY, I., CAI, P., LOTVIN, J., PETERSEN, R., RUPPEN, M., FAWZI, M., AYRAL-KALOUSTIAN, S., SKOTNICKI, J., MANSOUR, T., FROST, P. and GIBBONS, J., 2005. PWT-458, a novel pegylated-17-hydroxywortmannin, inhibits phosphatidylinositol 3-kinase signaling and suppresses growth of solid tumors. *Cancer biology & therapy,* **4**(5), pp. 538-545.

YU, L., BAXTER, P.A., VOICU, H., GURUSIDDAPPA, S., ZHAO, Y., ADESINA, A., MAN, T.K., SHU, Q., ZHANG, Y.J., ZHAO, X.M., SU, J.M., PERLAKY, L., DAUSER, R., CHINTAGUMPALA, M., LAU, C.C., BLANEY, S.M., RAO, P.H., LEUNG, H.C. and LI, X.N., 2010. A clinically relevant orthotopic xenograft model of ependymoma that maintains the genomic signature of the primary tumor and preserves cancer stem cells in vivo. *Neuro-oncology,* **12**(6), pp. 580-594.

YU, Z., WANG, H., ZHANG, L., TANG, A., ZHAI, Q., WEN, J., YAO, L. and LI, P., 2009. Both p53-PUMA/NOXA-Bax-mitochondrion and p53-p21cip1 pathways are involved in the CDglyTK-mediated tumor cell suppression. *Biochemical and biophysical research communications,* **386**(4), pp. 607-611.

YUH, E.L., BARKOVICH, A.J. and GUPTA, N., 2009. Imaging of ependymomas: MRI and CT. *Child's nervous system : ChNS : official journal of the International Society for Pediatric Neurosurgery,* **25**(10), pp. 1203-1213.

YUN, J., 2010. Allosteric AKT inhibitors as a targeted cancer therapy. *Cancer biology & therapy,* **9**(7), pp. 504-506.

ZAKERI, Z., MELENDEZ, A. and LOCKSHIN, R.A., 2008. Detection of autophagy in cell death. *Methods in enzymology,* **442**, pp. 289-306.

ZAMECNIK, J., SNUDERL, M., ECKSCHLAGER, T., CHANOVA, M., HLADIKOVA, M., TICHY, M. and KODET, R., 2003. Pediatric intracranial ependymomas: prognostic relevance of histological, immunohistochemical, and flow cytometric factors. *Modern pathology : an official journal of the United States and Canadian Academy of Pathology, Inc,* **16**(10), pp. 980-991.

ZHA, J., HARADA, H., YANG, E., JOCKEL, J. and KORSMEYER, S.J., 1996. Serine phosphorylation of death agonist BAD in response to survival factor results in binding to 14-3-3 not BCL-X(L). *Cell,* **87**(4), pp. 619-628.

ZHANG, H.H., LIPOVSKY, A.I., DIBBLE, C.C., SAHIN, M. and MANNING, B.D., 2006. S6K1 regulates GSK3 under conditions of mTOR-dependent feedback inhibition of Akt. *Molecular cell,* **24**(2), pp. 185-197.

ZHANG, J., WU, G., MILLER, C.P., TATEVOSSIAN, R.G., DALTON, J.D., TANG, B., ORISME, W., PUNCHIHEWA, C., PARKER, M., QADDOUMI, I., BOOP, F.A., LU, C., KANDOTH, C., DING, L., LEE, R., HUETHER, R., CHEN, X., HEDLUND, E., NAGAHAWATTE, P., RUSCH, M., BOGGS, K., CHENG, J., BECKSFORT, J., MA, J., SONG, G., LI, Y., WEI, L., WANG, J., SHURTLEFF, S., EASTON, J., ZHAO, D., FULTON, R.S., FULTON, L.L., DOOLING, D.J., VADODARIA, B., MULDER, H.L., TANG, C., OCHOA, K., MULLIGHAN, C.G., GAJJAR, A., KRIWACKI, R., SHEER, D., GILBERTSON, R.J., MARDIS, E.R., WILSON, R.K., DOWNING, J.R., BAKER, S.J., ELLISON, D.W. and ST. JUDE CHILDREN'S RESEARCH HOSPITAL-WASHINGTON UNIVERSITY PEDIATRIC CANCER GENOME PROJECT, 2013. Whole-genome sequencing identifies genetic alterations in pediatric low-grade gliomas. *Nature genetics,* **45**(6), pp. 602-612.

ZHANG, W., MAO, J.H., ZHU, W., JAIN, A.K., LIU, K., BROWN, J.B. and KARPEN, G.H., 2016. Centromere and kinetochore gene misexpression predicts cancer patient survival and response to radiotherapy and chemotherapy. *Nature communications,* **7**, pp. 12619.

ZHANG, X., TANG, N., HADDEN, T.J. and RISHI, A.K., 2011. Akt, FoxO and regulation of apoptosis. *Biochimica et biophysica acta,* **1813**(11), pp. 1978-1986.

ZHANG, X.D., FRANCO, A., MYERS, K., GRAY, C., NGUYEN, T. and HERSEY, P., 1999. Relation of TNF-related apoptosis-inducing ligand (TRAIL) receptor and FLICE-inhibitory protein expression to TRAIL-induced apoptosis of melanoma. *Cancer research,* **59**(11), pp. 2747-2753.

ZHANG, Y., BAO, C., MU, Q., CHEN, J., WANG, J., MI, Y., SAYARI, A.J., CHEN, Y. and GUO, M., 2016. Reversal of cisplatin resistance by inhibiting PI3K/Akt signal pathway in human lung cancer cells. *Neoplasma,* **63**(3), pp. 362-370.

ZHANG, Z., ZHANG, G., KONG, C. and GONG, D., 2016. PP242 suppresses bladder cancer cell proliferation and migration through deactivating the mammalian target of rapamycin complex 2/AKT1 signaling pathway. *Molecular medicine reports,* **13**(1), pp. 333-338.

ZHAO, B., WEI, X., LI, W., UDAN, R.S., YANG, Q., KIM, J., XIE, J., IKENOUE, T., YU, J., LI, L., ZHENG, P., YE, K., CHINNAIYAN, A., HALDER, G., LAI, Z.C. and GUAN, K.L., 2007. Inactivation of YAP oncoprotein by the Hippo pathway is involved in cell contact inhibition and tissue growth control. *Genes & development,* **21**(21), pp. 2747-2761.

ZHAO, H.F., WANG, J., SHAO, W., WU, C.P., CHEN, Z.P., TO, S.T. and LI, W.P., 2017. Recent advances in the use of PI3K inhibitors for glioblastoma multiforme: current preclinical and clinical development. *Molecular cancer,* **16**(1), pp. 100-017-0670-3.

ZHAO, P., HALL, J., DURSTON, M., VOYDANOFF, A., VANSICKLE, E., KELLY, S., NAGULAPALLY, A.B., BOND, J. and SAULNIER SHOLLER, G., 2017. BKM120 induces apoptosis and inhibits tumor growth in medulloblastoma. *PloS one,* **12**(6), pp. e0179948.

ZHOU, J., TAN, S.H., NICOLAS, V., BAUVY, C., YANG, N.D., ZHANG, J., XUE, Y., CODOGNO, P. and SHEN, H.M., 2013. Activation of lysosomal function in the course of autophagy via mTORC1 suppression and autophagosome-lysosome fusion. *Cell research,* **23**(4), pp. 508-523.

ZHOU, Y., SUN, K., MA, Y., YANG, H., ZHANG, Y., KONG, X. and WEI, L., 2014. Autophagy inhibits chemotherapy-induced apoptosis through downregulating Bad and Bim in hepatocellular carcinoma cells. *Scientific reports,* **4**, pp. 5382.

ZIMMERMANN, S. and MOELLING, K., 1999. Phosphorylation and regulation of Raf by Akt (protein kinase B). *Science (New York, N.Y.),* **286**(5445), pp. 1741-1744.

ZOU, P., LIU, L., ZHENG, L., LIU, L., STONEMAN, R.E., CHO, A., EMERY, A., GILBERT, E.R. and CHENG, Z., 2014. Targeting FoxO1 with AS1842856 suppresses adipogenesis. *Cell cycle (Georgetown, Tex.),* **13**(23), pp. 3759-3767.

APPENDIX

Appendix 1: RCAS GFP plasmid details (Chen, C.M., Smith et al. 1999)

BACKBONE	
Vector backbone	RCAS (A)
Backbone size	11,600 bp
Vector type	Retroviral; avian expression
GROWTH IN BACTERIA	
Antibiotic resistance	Ampicillin
Growth temperature	37^{o}C
Bacterial strain	DH5α
Copy number	High copy
CLONING INFORMATION	
Cloning method	Restriction enzyme
5' cloning site	*ClaI* (not destroyed)
3' cloning site	*ClaI* (destroyed during cloning)
5' sequencing primer	RCAS-F

Appendix 2: LB agar

- 5 g tryptone
- 2.5 g yeast extract
- 5 g NaCl
- 7.5 g agar
- Dissolve in 500 ml of water prior to autoclaving

Appendix 3: LB media

- 5 g tryptone
- 2.5 g yeast extract
- 5 g NaCl
- Dissolve in 500 ml of water prior to autoclaving

Appendix 4: Protease cocktail buffer

- 5 ml of 3 M NaCl solution
- 2.5 ml of 2 M Tris solution
- 1 ml of 10% SDS solution
- 1 ml of Triton X-100

- Bring up to a final volume of 100 ml

Appendix 5: Gel buffers and recipes

Gel	Composition	
	Chemicals	**Amount**
Lower gel buffer (250 ml)	Tris	45.41 g
	10% SDS solution	10 ml
	Adjust pH to 8.8 then filter through 0.45 µm filter	
Upper gel buffer (100 ml)	Tris	6.06 g
	10% SDS solution	4 ml
	Adjust pH to 6.7 then filter through 0.45 µm filter	

Lower (resolving) gel					
Chemicals	**Percentage of lower gel for 0.75 µm gel (double these for 1.5 µm gel)**				
	5%	**7%**	**10%**	**13%**	**15%**
Lower gel buffer	1 ml	1 ml	1 ml	1 ml	1 ml
Acrylamide	0.67 ml	0.93 ml	1.33 ml	1.73 ml	2 ml
dH_2O	2.33 ml	2.07 ml	1.67 ml	1.27 ml	1 ml
10% APS	25 µl	25 µl	25 µl	25 µl	25 µl
Temed	3.3 µl	3.3 µl	3.3 µl	3.3 µl	3.3 µl

Upper (stacking) gel				
Chemicals	**Amounts correspond to the number of 0.75 µm gel (double these for 1.5 µm gel)**			
	x1	**x2**	**x3**	**x4**
Lower gel buffer	625 µl	1250 µl	1875 µl	2500 µl
Acrylamide	312 µl	624 µl	936 µl	1248 µl

dH_2O	1500 µl	3000 µl	4500 µl	6000 µl
10% APS	12.5 µl	25 µl	37.5 µl	50 µl
Temed	2.5 µl	5 µl	7.5 µl	10 µl

Appendix 6: Western blot buffers

Buffer	**Chemicals**	**Required Volume**		
		1 Litre	**3 Litres**	**5 Litres**
Electrode buffer	Tris	3.03 g	9.09 g	15.15g
	Glycine	14.4 g	43.2 g	72.05 g
	10% SDS	10 ml	30 ml	50 ml
Transfer buffer	Tris	3.03 g	9.09 g	15.15g
	Glycine	14.4 g	43.2 g	72.05 g
	Methanol	200 ml	600 ml	1000 ml
	10% SDS	10 ml	30 ml	50 ml
TBS (10x)	Tris	24.2 g	---	---
	NaCl	80 g	---	---
	Dissolve in 800 ml of dH_2O then adjust pH to 7.6 before making it up to a final volume of 1 Litre.			
TBS-T (1x)	TBS	1 Litre		
	Tween	1 ml		
	Mix thoroughly.			
Blocking solution	TBS-T	500 ml		
	Milk powder	25 g		
	Mix thoroughly.			
Stripping buffer (mild)	Glycine	15 g		
	SDS	1 g		
	Tween	10 ml		
	• Adjust pH to 2.2.			

	• Amounts usually adjusted so a final volume of 200 ml was made.

Appendix 7: Significant DEGs identified in the transcriptomic work for the BXD-1425EPN dataset

Column ID	Gene	p value	Fold Change
17045938	*ABCA13*	0.0496086	2.0114
16945137	*ABTB1*	0.00378455	2.17549
17013773	*AKAP12*	0.0423462	2.32404
16798919	*ARHGAP11A*	0.00248109	-2.52232
16869588	*ASF1B*	0.00243833	-2.0554
16697544	*ASPM*	0.028889	-2.19332
16840902	*AURKB*	0.00212925	-2.77462
16838359	*BIRC5*	0.00634555	-2.72889
16775324	*BORA*	0.00578241	-2.29072
16901755	*BUB1*	0.0154433	-2.5653
16730967	*C11orf87*	0.000639054	-2.90468
16815108	*C16orf59*	0.000487911	-2.04363
16842484	*C17orf51*	0.000186942	-2.00913
16980998	*C4orf46*	0.000197486	-2.14112
16995938	*C5orf34*	0.00483652	-2.46263
16765404	*CALCOCO1*	0.000102837	2.50045
16799598	*CASC5*	0.0041156	-2.66993
16884162	*CCDC138*	0.000303733	-2.00156
16979515	*CCNA2*	0.00539157	-2.38847
16985599	*CCNB1*	0.00882206	-3.09777
16801557	*CCNB2*	0.0119724	-2.48558
16815090	*CCNF*	0.000266347	-3.30258

16676764	*CD55*	5.38E-06	2.17229
16663514	*CDC20*	0.00707156	-3.01804
16927052	*CDC45*	0.0266193	-2.01829
16667037	*CDC7*	0.0151384	-2.05466
17067102	*CDCA2*	0.0047444	-3.0019
16760621	*CDCA3*	0.00417962	-2.76852
16662648	*CDCA8*	0.00130611	-3.34153
16994779	*CDH10*	0.0284988	-2.21321
16705159	*CDK1*	0.00636669	-2.49593
16784299	*CDKN3*	0.00371252	-2.00627
16877956	*CENPA*	0.00891586	-2.12359
16978568	*CENPE*	0.0104356	-2.55827
16677425	*CENPF*	0.032952	-2.03519
17105401	*CENPI*	0.00259488	-2.28695
16696490	*CENPL*	0.000159715	-2.13351
16935517	*CENPM*	0.00790293	-2.4332
17086784	*CENPP*	0.000900931	-2.23042
17012379	*CENPW*	0.000106805	-2.20541
16707551	*CEP55*	0.00269072	-2.53872
17086167	*CEP78*	0.00247838	-2.16425
16675398	*CFH*	0.00281574	2.22001
16799739	*CHAC1*	0.0127315	-3.12684
16922584	*CHAF1B*	0.00671322	-2.00358
16803562	*CHRNA5*	0.00572594	-2.02011
16901957	*CKAP2L*	0.0130425	-2.36265
17086634	*CKS2*	0.022741	-2.09129
16685165	*CLSPN*	0.0327589	-2.02987

16909828	*COL6A3*	0.030658	2.01278
16992467	*CREBRF*	0.000167935	2.64193
16811858	*CSPG4*	0.0264734	-2.21329
17071640	*CTHRC1*	0.0189626	2.03607
16980918	*CTSO*	0.0311612	2.16469
17047965	*DBF4*	0.00061544	-2.00299
16834812	*DBF4B*	0.00229749	-2.08671
16971382	*DCLK2*	0.0182833	-2.01843
16688386	*DEPDC1*	0.0150746	-2.90993
16996545	*DEPDC1B*	0.00384464	-2.66498
16779546	*DIAPH3*	0.00512595	-2.15677
17118260	*DKFZP434F142*	0.0169935	2.03763
16793225	*DLGAP5*	0.0175958	-2.8042
16868862	*DOCK6*	0.00479621	2.09105
16800933	*DTWD1*	0.016678	2.46023
16768297	*DUSP6*	0.00942287	2.43001
17000644	*ECSCR*	0.00391481	-2.14458
16835797	*EME1*	0.0157766	-2.40567
16996146	*ESM1*	0.00702773	7.15291
16751709	*ESPL1*	0.0219297	-2.20089
16683920	*FAM46B*	0.00024371	-2.88901
16830173	*FAM64A*	0.00962775	-2.50976
16913681	*FAM83D*	0.00818793	-4.14944
16734299	*FAM99B*	0.0161959	2.00877
17109211	*FANCB*	0.0062321	-2.22549
16937505	*FANCD2*	0.0156554	-2.1824
16844137	*FBXL20*	0.00397064	2.18092

17080788	*FBXO32*	0.00168214	3.02143
16723058	*FIBIN*	0.000270912	2.43407
17084025	*FLJ35282*	0.0487798	2.24651
16760048	*FOXM1*	0.00138715	-2.79969
16755692	*GAS2L3*	0.00989371	-2.41244
16689752	*GCLM*	0.00433592	-2.0825
16912192	*GINS1*	0.000538833	-2.37793
17068385	*GINS4*	0.00673054	-2.00035
17005396	*GMNN*	0.0032669	-2.43457
16829764	*GSG2*	0.00119303	-2.18343
17058672	*GTF2IRD2*	0.00305871	2.08713
16931384	*GTSE1*	0.0040709	-2.51858
16745236	*H2AFX*	0.0030149	-2.30433
16845537	*HDAC5*	0.00544163	2.11669
17016499	*HIST1H1B*	0.0220179	-2.30084
17005569	*HIST1H1E*	0.000934519	-2.15482
17005858	*HIST1H2AI*	0.0185692	-2.27881
17005603	*HIST1H2BC*	0.000490292	-2.90889
17016379	*HIST1H2BC*	0.00382221	2.2804
17005865	*HIST1H2BM*	0.00605018	-2.18022
17016363	*HIST1H3B*	0.0223391	-2.00534
17016400	*HIST1H3F*	0.0421956	-2.49272
17016403	*HIST1H3G*	0.0156958	-2.45406
17016503	*HIST1H3I*	0.00218614	-2.02118
17016360	*HIST1H4B*	0.00635529	-2.81829
17016383	*HIST1H4D*	0.00144966	-2.37025
16670387	*HIST2H3D*	0.0120533	-2.29826

16692616	*HIST2H3D*	0.0120533	-2.29826
16909700	*HJURP*	0.0314485	-2.24886
16675045	*HMCN1*	0.011514	2.49141
16901986	*IL1B*	0.0280693	2.46483
16967771	*IL8*	0.0010915	5.61359
16725806	*INCENP*	0.000566123	-2.40288
16881708	*INO80B*	0.00552233	2.01719
16780917	*IRS2*	0.00136869	2.17809
16984689	*ITGA2*	0.0020377	3.88888
16986583	*JMY*	5.03E-05	2.17382
16844872	*JUP*	0.00938631	3.44065
16837391	*KCNJ2*	0.0181529	2.47598
16957170	*KIAA1524*	0.00325455	-2.23383
16707468	*KIF11*	0.0158211	-2.25123
16697695	*KIF14*	0.024816	-2.48098
16939960	*KIF15*	0.0382981	-2.04037
16845794	*KIF18B*	0.0117567	-3.09522
16989636	*KIF20A*	0.0165701	-3.00198
16707221	*KIF20B*	0.0157253	-2.41192
16802519	*KIF23*	0.0177201	-2.38964
17093397	*KIF24*	0.00478876	-2.14753
16663958	*KIF2C*	0.00780664	-2.12603
17104484	*KIF4A*	0.0125035	-2.55087
17007459	*KIFC1*	0.00649455	-2.48874
17041352	*KIFC1*	0.00649455	-2.48874
17038792	*KIFC1*	0.00679384	-2.44007
16948572	*KLHL24*	0.000278137	3.84283

16799517	*KNSTRN*	0.00554696	-2.31924
16837270	*KPNA2*	0.00274394	-2.13553
17022754	*LAMA4*	0.015398	2.03017
16866951	*LMNB2*	0.000605862	-2.11504
17085500	*LOC100132352*	0.00613339	2.52559
16798812	*LOC100288637*	0.0219041	-2.11602
16979389	*MAD2L1*	0.0248047	-2.33656
16980031	*MAML3*	0.00731516	2.09153
16911212	*MCM8*	0.0262788	-2.01773
17084904	*MELK*	0.000961052	-2.47075
16745509	*MIR100*	0.0440949	2.26204
16849744	*MIR1250*	0.00322085	2.1292
16836624	*MIR21*	0.0198514	2.64349
17110365	*MIR221*	0.0113575	2.02823
17110367	*MIR222*	0.0115479	2.44069
17062941	*MIR29A*	0.0161902	2.38286
16989241	*MIR3661*	0.00824835	-2.12463
16830912	*MIR3676*	0.0396899	-2.97501
16994952	*MIR4279*	0.0031929	2.81244
16848095	*MIR635*	0.0134862	2.15174
17114774	*MIR891A*	0.0374005	-2.04494
16719515	*MKI67*	0.0186226	-2.3931
16743721	*MMP1*	0.000253948	2.38218
16743735	*MMP3*	0.0116166	2.74675
16809748	*MNS1*	0.0110281	-2.44602
16973708	*MXD4*	0.000158309	2.11395
16913957	*MYBL2*	2.98E-05	-3.43392

16965346	*NCAPG*	0.0147133	-2.36332
17064939	*NCAPG2*	0.00246093	-2.04203
16882975	*NCAPH*	0.0126914	-2.82909
16687418	*NDC1*	0.00666413	-2.15667
16850517	*NDC80*	0.0333744	-2.34388
17081401	*NDRG1*	3.15E-05	2.21515
16972616	*NEIL3*	0.00933458	-2.34272
16951696	*NEK10*	0.000462696	3.6383
16698984	*NEK2*	0.0273571	-2.3573
16743148	*NOX4*	0.0325216	3.37769
16732891	*NRGN*	5.99E-05	-2.23888
17010760	*NT5E*	4.80E-05	2.16994
16673154	*NUF2*	0.0225641	-2.55938
16799793	*NUSAP1*	0.0421257	-2.19848
16839277	*NXN*	0.0425307	-2.22331
16807605	*OIP5*	0.00251	-2.73597
16687188	*ORC1*	0.0189568	-2.00329
16818600	*ORC6*	0.000798431	-2.1908
16888106	*OSBPL6*	0.00137297	-2.08095
16773240	*OTTHUMG00000016583*	0.0140559	2.03753
16699560	*OTTHUMG00000037425*	0.0249016	2.97156
16753630	*OTTHUMG00000168899*	0.00022047	2.07481
16737344	*PAMR1*	0.000187573	3.67109
16755928	*PARPBP*	0.00150733	-2.21439
17075776	*PBK*	0.0049139	-3.19618
16990294	*PCDHB9*	0.00434446	2.18599
16916261	*PCMTD2*	0.000515526	2.35097

16966809	*PDGFRA*	0.00210782	2.5542
17048563	*PEG10*	0.0139234	-2.39223
16669389	*PHGDH*	0.000305241	-2.68383
17076726	*PLAT*	0.00286771	2.93337
16707631	*PLCE1*	0.00416221	-2.52615
16817017	*PLK1*	0.00585842	-3.07487
16970563	*PLK4*	0.0279201	-2.29587
17010929	*PNRC1*	0.00761447	2.50143
16957951	*POLQ*	0.00169475	-3.09915
16813342	*PRC1*	0.00974727	-2.21768
16836492	*PRR11*	0.0162334	-2.31488
17086193	*PSAT1*	0.0167923	-3.94105
16690535	*PSRC1*	0.000416362	-2.52501
16664243	*RAD54L*	0.0115546	-2.00928
16911835	*RIN2*	0.00158542	2.40199
16858714	*RNASEH2A*	0.0132862	-2.04768
16802102	*RNU5B-1*	0.0222344	2.71077
17104519	*RNY4P23*	0.00841157	-3.6668
16665588	*ROR1*	0.00986906	-2.39113
16714747	*RTKN2*	0.00214003	-2.52311
17102129	*SAT1*	6.98E-05	2.74095
17007738	*SCUBE3*	0.0131043	3.21466
16951485	*SGOL1*	0.0435368	-2.17812
16889251	*SGOL2*	0.00336018	-2.072
16990572	*SH3RF2*	0.017113	-2.25061
16826160	*SHCBP1*	0.00076121	-2.78904
16852312	*SKA1*	0.00249054	-3.20155

16777278	*SKA3*	0.00663632	-2.27386
16806870	*SLC12A6*	0.000354148	2.19167
16852179	*SLC14A1*	0.0221344	3.0216
16848070	*SLC16A6*	0.00241123	3.47068
16838887	*SLC25A10*	0.00453961	-2.26212
16680435	*SLC35E2*	4.57E-05	2.3292
16832104	*SLC47A1*	0.0023449	-2.69018
16951756	*SLC4A7*	0.00219481	2.01338
16686201	*SLC6A9*	0.0311588	-2.35284
16893349	*SNED1*	0.0237135	2.19142
16798146	*SNORD116-5*	0.0364146	2.13814
16798150	*SNORD116-5*	0.0364146	2.13814
17098171	*SNORD90*	0.0459707	2.01604
16842673	*SPAG5*	0.00925866	-2.98561
16868838	*SPC24*	0.00444197	-2.52852
16904780	*SPC25*	0.0168846	-2.20429
16780069	*SPRY2*	0.00635531	2.98047
17103413	*SUV39H1*	0.000504861	-2.23924
16712879	*SVIL*	0.00195252	2.04136
16964000	*TACC3*	0.00242574	-2.52742
17027710	*TCF19*	0.00412222	-2.04727
17030560	*TCF19*	0.00412222	-2.04727
17033265	*TCF19*	0.00412222	-2.04727
17035356	*TCF19*	0.00412222	-2.04727
17038044	*TCF19*	0.00412222	-2.04727
17040632	*TCF19*	0.00412222	-2.04727
16756310	*TCP11L2*	0.00171849	2.58589

16856812	*THOP1*	0.000146429	-2.28578
16804631	*TICRR*	0.0186447	-2.21314
16766137	*TIMELESS*	0.0160357	-2.03601
17112729	*TIMM8A*	0.00342066	-2.01853
16849379	*TK1*	0.000840632	-2.42568
16752233	*TMEM198B*	0.000158854	2.65038
16721759	*TMEM9B-AS1*	0.000575511	2.43592
16755498	*TMPO*	0.0120446	-2.17526
16768936	*TMPO-AS1*	0.010628	-2.09851
17077502	*TOX*	0.003771	-2.38701
16757427	*TPCN1*	0.0296603	2.18474
16912379	*TPX2*	0.0296172	-2.25673
16954251	*TRAIP*	0.0136702	-2.14451
17019218	*TRERF1*	0.00902341	-2.35028
17115160	*TREX2*	0.0202315	-2.28884
16982635	*TRIP13*	0.00350176	-2.31201
17005836	*TRNAI6*	0.0356669	-2.15794
16750761	*TROAP*	0.00889412	-2.82668
17010552	*TTK*	0.0292019	-2.58985
16850477	*TYMS*	0.0120809	-2.10458
16914315	*UBE2C*	0.00555239	-3.50796
16875763	*UBE2S*	0.00496995	-2.15764
16698023	*UBE2T*	0.0129731	-2.13144
16683788	*UBXN11*	0.0102253	-2.20283
16870221	*UNC13A*	0.00169136	2.79308
16861318	*WDR62*	0.00127505	-2.2228
16797025	*XRCC3*	0.000535505	-2.06474

16825638	*YPEL3*	0.00108817	2.43973
17112835	*ZMAT1*	0.00685897	2.09455
16860103	*ZNF93*	0.00682546	-2.20916
16714504	*ZWINT*	0.0168798	-2.04769
16694686	…	9.79E-05	2.33903
16653961	…	0.00012816	2.15412
16717676	…	0.000132604	-2.29414
16664044	…	0.000162568	2.42855
16876590	…	0.000212681	2.03581
16654645	…	0.000360053	2.01179
16898487	…	0.000538154	4.30048
16652445	…	0.000946447	-2.00756
16771547	…	0.00121048	-3.84662
16900491	…	0.00137287	-6.40884
16654639	…	0.00156708	2.07992
16692433	…	0.00284202	-2.40453
17123262	…	0.00344397	2.37425
16769756	…	0.00390106	-2.1783
17126034	…	0.00401466	2.23773
17126144	…	0.00401466	2.23773
16656845	…	0.00422722	2.87595
17079431	…	0.00459994	-3.21385
16698947	…	0.00507308	-3.57586
16802939	…	0.00507472	2.01568
16744706	…	0.00510612	-3.00059
16943040	…	0.00515324	2.50354
16656335	…	0.00517724	-2.48796

16657121	…	0.00543416	-2.09678
17064088	…	0.00556006	2.62566
17119680	…	0.00556006	2.62566
16653793	…	0.00572775	4.17217
16735813	…	0.00623384	2.58187
16654095	…	0.00724964	2.32458
17125742	…	0.0088084	3.65063
16988435	…	0.00913498	2.34124
17120582	…	0.0101788	4.42357
16651473	…	0.010316	-3.73731
16769744	…	0.0111026	-2.4499
16735146	…	0.0115018	-2.0216
16876665	…	0.0119053	-2.52016
16722386	…	0.012161	2.24748
16653007	…	0.0121705	-2.28386
17120584	…	0.0122918	4.49692
17120506	…	0.0127021	-2.27415
16992314	…	0.0134362	2.00153
16655123	…	0.0135199	3.15121
16653011	…	0.0138083	-2.3448
17120580	…	0.0147164	3.96948
16855178	…	0.0148991	-2.30459
17068626	…	0.0150822	2.71761
16653493	…	0.0157946	-2.38328
16656707	…	0.0160197	2.51094
16745158	…	0.0161026	-3.27103
16653767	…	0.016348	2.06785

17119708	…	0.0165083	-3.5216
16823195	…	0.0167199	-2.1413
17123164	…	0.0172277	-2.03972
16654111	…	0.0175728	2.28853
16657045	…	0.018517	2.08385
16650623	…	0.0191885	-2.41199
17125282	…	0.0194019	2.3339
16880237	…	0.0194637	2.33841
16711457	…	0.0194643	2.623
16653597	…	0.0194707	2.01529
16653651	…	0.0204204	-2.83602
16652435	…	0.0205564	2.14033
16654327	…	0.0212041	-2.57594
17084034	…	0.0212591	2.9487
16653485	…	0.0213002	-2.18912
16900018	…	0.0219452	-2.66776
16653537	…	0.0222413	-2.05795
16656687	…	0.0224141	-3.27951
16653503	…	0.0235125	-2.83561
16977342	…	0.0243066	2.10299
16850406	…	0.0252464	2.14045
16798810	…	0.0260554	-2.3342
16823108	…	0.0265411	-2.17134
16652409	…	0.0268552	4.23952
16657007	…	0.0280162	-2.2456
17113488	…	0.0287824	2.17593
17017216	…	0.0288854	-2.08406

16876431	…	0.029287	-2.59771
16880232	…	0.0293308	2.00884
16837324	…	0.0293777	2.08647
16669630	…	0.0302234	-2.11087
17120106	…	0.0314019	-3.23443
16706413	…	0.0328491	-2.34192
16854406	…	0.0332411	2.17453
17124802	…	0.0333062	-2.07078
17120586	…	0.034681	3.46905
16764096	…	0.0348821	-2.41176
16656787	…	0.037049	-4.2899
17124574	…	0.0373636	2.00487
16769552	…	0.0380322	-2.17471
16939501	…	0.0393032	-2.41764
16653811	…	0.0400341	2.72119
16761776	…	0.0400817	2.44032
16829420	…	0.0422546	-2.64813
16657049	…	0.0457199	2.27134
16764072	…	0.0479556	2.05613
17007838	…	0.0487983	-2.16564

Appendix 8: Significant DEGs identified in the transcriptomic work for the EPN1 dataset

Column ID	Gene	p value	Fold Change
17096728	*ABCA1*	0.0133742	3.48343
16708192	*ABCC2*	0.00651988	-3.35041
16803743	*ABHD17C*	0.000306985	2.06957

16854202	*ABHD3*	9.37E-08	-2.40319
16719417	*ADAM12*	0.000133977	-2.00607
17065313	*AGPAT5*	3.89E-05	-3.12498
17013773	*AKAP12*	0.0351509	2.42314
16749875	*ALG10*	0.000462506	-2.39836
16849982	*ALYREF*	0.000886787	-2.43353
16969911	*ANK2*	1.32E-05	-2.08083
17045198	*ANLN*	0.000974018	-5.63966
16692724	*ANP32E*	0.00071807	-2.38239
16798919	*ARHGAP11A*	0.000112429	-4.45
16798801	*ARHGAP11B*	0.00165507	-4.71049
17093724	*ARHGEF39*	0.000248201	-3.73919
16824470	*ARL6IP1*	0.00420656	-2.11896
16749423	*ARNTL2*	0.000185053	-3.58621
16837308	*ARSG*	0.00313525	2.53081
16869588	*ASF1B*	8.25E-06	-5.26831
16697544	*ASPM*	0.000737066	-4.77372
17080749	*ATAD2*	0.000213266	-3.31545
16832852	*ATAD5*	0.000147724	-3.25766
16682348	*ATP13A2*	0.0120476	-2.41404
16920548	*AURKA*	0.000119038	-4.36644
16840902	*AURKB*	1.89E-05	-7.82309
16766627	*B4GALNT1*	0.00374326	-2.18164
16907960	*BARD1*	0.00254094	-2.68777
16836697	*BCAS3*	0.00127767	2.11997
16864234	*BCL2L12*	3.79E-05	-2.67475
16796727	*BEGAIN*	5.72E-05	2.48633

16838359	*BIRC5*	0.00010349	-6.96009
16804902	*BLM*	6.29E-05	-3.59588
17004657	*BMP6*	0.00488582	2.47926
16899086	*BOLA3*	0.000642673	-2.2366
16775324	*BORA*	0.000103764	-4.82396
16845349	*BRCA1*	0.000232305	-4.73492
16773840	*BRCA2*	0.000520646	-4.44204
16847432	*BRIP1*	0.000731378	-7.95953
16664028	*BTBD19*	6.71E-05	2.01263
16901755	*BUB1*	0.000229263	-6.95999
16799426	*BUB1B*	6.93E-05	-3.11437
16729557	*C11orf82*	0.00533487	-2.19087
16730967	*C11orf87*	0.00651875	-2.05245
16834711	*C17orf53*	0.00743642	-2.14845
16852445	*C18orf54*	0.00104968	-2.38958
16673557	*C1orf112*	7.79E-05	-2.99166
16979060	*C4orf21*	0.00217212	-2.34475
16980998	*C4orf46*	3.91E-05	-2.60722
16995938	*C5orf34*	0.000801439	-3.38825
16851427	*CABLES1*	0.00109528	2.89482
16921036	*CABLES2*	5.50E-06	-2.61693
16851586	*CABYR*	1.95E-05	-2.18023
16989325	*CAMLG*	1.42E-05	2.00433
16800061	*CAPN3*	0.00021244	2.30466
16799598	*CASC5*	6.10E-05	-6.60816
16956983	*CBLB*	0.0347	2.0626
16791393	*CBLN3*	0.000539607	2.46298

16765513	*CBX5*	9.40E-05	-2.02656
16930758	*CCDC134*	0.00659399	-2.44836
16732960	*CCDC15*	9.35E-06	-3.4819
17018733	*CCDC167*	0.00659482	-2.15209
16667206	*CCDC18*	0.00131818	-3.05532
16736807	*CCDC34*	0.000470313	-2.72909
16746524	*CCDC77*	0.000634333	-2.10036
16979515	*CCNA2*	7.13E-05	-5.58806
16985599	*CCNB1*	0.00114601	-5.05886
16801557	*CCNB2*	0.000679626	-4.51798
16860418	*CCNE1*	0.0225338	-2.28775
17079293	*CCNE2*	0.000592793	-3.11384
16815090	*CCNF*	1.10E-05	-6.48159
16816479	*CCP110*	0.00870407	-2.2913
16858970	*CD97*	0.00452192	-2.17374
16663514	*CDC20*	0.000453362	-5.77663
16953279	*CDC25A*	3.32E-05	-3.12616
17000439	*CDC25C*	0.00266312	-4.56173
16927052	*CDC45*	0.000739576	-3.934
16834056	*CDC6*	8.98E-05	-6.15816
16667037	*CDC7*	6.69E-05	-5.82876
17067102	*CDCA2*	0.000757028	-4.46623
16760621	*CDCA3*	0.000120721	-5.94444
16797213	*CDCA4*	0.000247325	-2.14298
16740282	*CDCA5*	0.000693328	-2.86847
16662648	*CDCA8*	4.83E-05	-7.17468
16952769	*CDCP1*	0.000873994	-2.99715

16705159	*CDK1*	5.38E-05	-6.95866
16752305	*CDK2*	0.000498763	-2.82565
16741075	*CDK2AP2*	0.00918452	-2.01946
16664569	*CDKN2C*	0.000298074	-2.85122
16868793	*CDKN2D*	0.000417607	-3.00168
16784299	*CDKN3*	5.40E-05	-3.80758
16821869	*CDT1*	0.000416921	-2.3342
16877956	*CENPA*	0.000330688	-3.71311
16978568	*CENPE*	0.00120916	-3.97773
16677425	*CENPF*	0.000989667	-4.03235
16985614	*CENPH*	4.72E-05	-2.96095
17105401	*CENPI*	6.73E-06	-7.25533
16777502	*CENPJ*	0.0012177	-2.2265
16996722	*CENPK*	5.56E-05	-6.47197
16696490	*CENPL*	4.28E-06	-3.4804
16935517	*CENPM*	0.00345846	-2.81815
16821239	*CENPN*	0.000383392	-3.0718
16877762	*CENPO*	1.92E-05	-3.05094
17086784	*CENPP*	3.45E-05	-3.64538
17009482	*CENPQ*	0.00155971	-3.18834
17012379	*CENPW*	5.04E-07	-5.07714
16795304	*CEP128*	0.000212984	-3.19579
16808876	*CEP152*	0.00756016	-2.48518
16707551	*CEP55*	4.37E-05	-5.70506
16854046	*CEP76*	0.000362742	-2.04508
17086167	*CEP78*	0.000658162	-2.60614
16661117	*CEP85*	5.03E-06	-2.92799

16943435	*CEP97*	0.00034153	-2.69302
17006949	*CFB*	0.0394247	2.13991
16857192	*CHAF1A*	0.000142031	-3.71717
16922584	*CHAF1B*	0.000819694	-2.70963
16851022	*CHMP1B*	0.00599304	2.00926
16803562	*CHRNA5*	0.000143539	-3.5674
16775014	*CKAP2*	0.000463817	-3.90529
16901957	*CKAP2L*	0.00027563	-5.27259
16796998	*CKB*	0.0408967	-3.13936
16671503	*CKS1B*	0.00124209	-2.16578
17086634	*CKS2*	0.000470963	-4.42329
16811073	*CLN6*	0.00031505	-2.72837
16685165	*CLSPN*	2.22E-05	-11.1608
16828622	*CMC2*	0.00184231	-2.16126
16727363	*CNIH2*	0.00738793	-3.47172
16977520	*COQ2*	0.000590507	-2.33627
16817824	*CORO1A*	0.00970586	-2.34052
16992467	*CREBRF*	0.000246454	2.50536
16914671	*CSE1L*	8.72E-05	-2.23671
17071640	*CTHRC1*	0.0192256	2.03163
16740828	*CTSF*	0.00161259	2.23636
17047965	*DBF4*	3.42E-05	-2.87631
16834812	*DBF4B*	0.000245417	-2.84593
16733278	*DCPS*	7.39E-05	-2.03473
16869624	*DDX39A*	5.69E-05	-2.72384
16688386	*DEPDC1*	0.000475281	-7.11394
16996545	*DEPDC1B*	0.000196295	-4.83226

16681827	*DHRS3*	0.000152147	2.65167
16779546	*DIAPH3*	4.56E-05	-4.96427
16793225	*DLGAP5*	0.000446857	-7.22229
16714998	*DNA2*	6.35E-05	-3.4989
16868576	*DNMT1*	5.40E-05	-3.22845
17089982	*DOLPP1*	0.000731149	-2.15274
16925239	*DONSON*	1.36E-05	-2.06115
16727427	*DPP3*	6.60E-05	-2.29295
17080595	*DSCC1*	0.000583956	-2.32784
16918976	*DSN1*	0.000333369	-2.21255
16677201	*DTL*	7.01E-05	-7.9253
16800933	*DTWD1*	0.0184549	2.41197
16910501	*DTYMK*	0.000127654	-2.56514
16918445	*E2F1*	8.95E-06	-3.69035
16736638	*E2F8*	0.000231319	-4.09606
16948021	*ECT2*	0.000307227	-3.63023
16779958	*EDNRB*	0.0472104	2.16915
16807763	*EHD4*	0.0263594	-2.07424
16835797	*EME1*	0.000944535	-4.32023
16823825	*EMP2*	0.0029363	-2.55182
17089863	*ENDOG*	0.00483153	-2.02417
16987986	*EPB41L4A-AS1*	0.00992884	2.06775
17111998	*ERCC6L*	0.0016225	-2.55365
16717452	*ERLIN1*	0.00147955	-2.01003
17067332	*ESCO2*	2.67E-05	-7.00737
16751709	*ESPL1*	0.0011942	-3.90659
16679411	*EXO1*	0.000203045	-6.71092

16774082	*EXOSC8*	0.000828361	-2.08085
17064105	*EZH2*	0.000118353	-4.71318
17025191	*EZR*	0.000428936	-2.56401
16725049	*FAM111A*	0.048731	-2.01882
16725041	*FAM111B*	0.000255955	-5.99835
17114348	*FAM122B*	0.000166501	-2.38335
16683920	*FAM46B*	0.000783455	-2.43116
16830173	*FAM64A*	0.000874135	-4.06213
16676526	*FAM72A*	0.00874483	-2.37423
16692583	*FAM72C*	0.00315202	-3.4799
16691883	*FAM72D*	0.0115074	-3.31369
16913681	*FAM83D*	0.00132055	-7.13462
16829369	*FANCA*	7.78E-06	-5.77125
17109211	*FANCB*	0.000642089	-3.23961
17096054	*FANCC*	3.15E-05	-2.17816
16937505	*FANCD2*	0.00021039	-5.11648
17093595	*FANCG*	0.000301511	-2.23409
16804559	*FANCI*	7.33E-05	-6.89411
16783836	*FANCM*	0.00126864	-2.0739
16970465	*FAT4*	0.041511	2.08919
17002052	*FAXDC2*	0.0203218	2.34463
17080788	*FBXO32*	0.000623302	3.65481
17024980	*FBXO5*	5.12E-06	-4.56974
16725735	*FEN1*	0.00010404	-3.70103
16800921	*FGF7*	0.0447794	3.91324
17057718	*FIGNL1*	6.83E-06	-3.43978
17056310	*FKBP14*	0.00233876	-2.08458

16979330	*FLJ14186*	0.0179229	2.24223
17062955	*FLJ43663*	0.0496	2.03682
16839106	*FN3KRP*	0.00359939	-2.00738
16760048	*FOXM1*	4.42E-05	-5.58169
16748304	*GABARAPL1*	0.0015638	3.23168
17016697	*GABBR1*	0.00513812	2.03233
17114970	*GABRE*	0.0359562	2.60558
17095499	*GAS1*	0.0227525	2.45489
16755692	*GAS2L3*	0.00232939	-3.15413
16689332	*GBP1*	0.0379296	-2.28075
16793176	*GCH1*	0.00506382	2.58472
16877473	*GEN1*	0.00045433	-3.39314
16912192	*GINS1*	1.50E-05	-4.24124
16828886	*GINS2*	0.00195643	-4.17924
16819678	*GINS3*	0.000241445	-2.76997
17068385	*GINS4*	0.000152341	-3.60306
16863667	*GLTSCR2*	0.000440051	2.12554
17005396	*GMNN*	0.000480736	-3.37181
16780592	*GPR183*	0.000656531	2.74775
16661429	*GPR3*	0.00013573	-2.19941
16668079	*GPSM2*	0.000140014	-2.67351
16701037	*GREM2*	0.0202453	2.23483
16829764	*GSG2*	3.03E-05	-3.82335
16918589	*GSS*	2.53E-05	-2.01108
16969473	*GSTCD*	0.000115587	-2.41892
17058413	*GTF2IRD2P1*	0.0285354	2.42248
16931384	*GTSE1*	0.000166865	-4.64468

17020480	*GUSBP4*	0.0268685	2.05731
16745236	*H2AFX*	5.65E-05	-4.64386
16978334	*H2AFZ*	2.70E-05	-2.68204
16861068	*HAUS5*	0.00031676	-2.21586
17092688	*HAUS6*	4.55E-05	-2.1805
16870131	*HAUS8*	0.000261861	-3.00645
16845537	*HDAC5*	0.000834741	2.8039
16707695	*HELLS*	5.37E-05	-5.15164
17016499	*HIST1H1B*	4.52E-05	-10.3914
17016372	*HIST1H1C*	0.0180222	-2.31559
17016393	*HIST1H1D*	0.00451344	-2.01908
17005569	*HIST1H1E*	0.000304512	-2.48945
17016366	*HIST1H2AB*	0.000406992	-7.06873
17016386	*HIST1H2AD*	0.0128348	-2.23029
17005589	*HIST1H2AE*	4.03E-06	-4.4927
17005858	*HIST1H2AI*	1.46E-05	-13.4668
17016490	*HIST1H2AJ*	0.000894256	-3.3821
17016496	*HIST1H2AK*	0.000286317	-4.98436
17016512	*HIST1H2AM*	0.000393368	-3.84297
17016369	*HIST1H2BB*	0.00037144	-4.18174
17005603	*HIST1H2BC*	0.000410984	-2.9946
17005578	*HIST1H2BC*	0.0275735	-2.49106
17016486	*HIST1H2BL*	0.000591197	-3.48544
17005865	*HIST1H2BM*	6.86E-06	-8.74
17005532	*HIST1H3A*	0.0116604	-2.57712
17016363	*HIST1H3B*	0.000394978	-4.1969
17005593	*HIST1H3E*	3.10E-05	-3.70873

17016400	*HIST1H3F*	0.00115174	-6.45064
17016403	*HIST1H3G*	1.72E-05	-14.449
17016503	*HIST1H3I*	6.38E-05	-3.33379
17016509	*HIST1H3J*	4.90E-06	-8.36808
17005535	*HIST1H4A*	0.00291308	-2.94493
17016360	*HIST1H4B*	0.0158712	-2.36713
17016383	*HIST1H4D*	9.35E-05	-3.69353
16692636	*HIST2H2AB*	9.32E-05	-4.3201
16669437	*HIST2H2BA*	0.00191209	-2.5689
16670387	*HIST2H3D*	9.19E-05	-6.40076
16692616	*HIST2H3D*	9.19E-05	-6.40076
17005560	*HIST2H4B*	5.18E-05	-3.0247
16909700	*HJURP*	0.000657086	-5.34692
16981506	*HMGB2*	0.00246732	-3.31851
17107753	*HMGB3*	6.81E-05	-2.4311
16991859	*HMMR*	0.00780993	-4.54153
16848739	*HN1*	1.38E-05	-3.07151
16814779	*HN1L*	0.00773157	-2.10728
16993268	*HNRNPAB*	0.000976321	-2.11785
16857913	*HNRNPM*	8.31E-08	-2.11141
16673104	*HSD17B7*	0.00944913	2.04509
16745186	*HYOU1*	0.00437933	-2.01885
16813270	*IDH2*	5.68E-05	-3.15178
16725806	*INCENP*	9.58E-06	-4.78326
16881708	*INO80B*	0.00363393	2.13212
16699021	*INTS7*	0.0073582	-2.07603
16694617	*IQGAP3*	0.00122898	-4.69849

16780917	*IRS2*	0.000101662	3.17023
16887702	*ITGA6*	0.00799591	-2.27256
16688123	*ITGB3BP*	0.0012183	-2.19423
16986583	*JMY*	4.75E-06	2.91448
16784710	*KIAA0586*	0.000193941	-2.29944
16803754	*KIAA1199*	0.0104636	5.49006
16957170	*KIAA1524*	4.41E-05	-4.71751
16707468	*KIF11*	0.000285159	-5.08646
16697695	*KIF14*	0.000735464	-5.7235
16939960	*KIF15*	0.00017484	-6.62938
16736891	*KIF18A*	0.00797164	-2.57282
16845794	*KIF18B*	0.000402354	-7.54176
16989636	*KIF20A*	0.00147446	-5.6045
16707221	*KIF20B*	0.000738911	-4.59281
16817647	*KIF22*	0.000391307	-3.71959
16802519	*KIF23*	0.000320659	-5.80565
17093397	*KIF24*	5.67E-05	-4.60051
16663958	*KIF2C*	0.000140733	-4.26863
17104484	*KIF4A*	0.000296614	-5.90274
16991460	*KIF4B*	0.0344107	-2.08643
17038792	*KIFC1*	0.00022465	-4.7639
17007459	*KIFC1*	0.000236449	-4.80734
17041352	*KIFC1*	0.000236449	-4.80734
16859314	*KLF2*	0.0153283	-3.28108
17094761	*KLF9*	0.0339898	2.44536
16783927	*KLHDC1*	0.00174955	3.06799
16948572	*KLHL24*	0.00129997	2.88706

16799517	*KNSTRN*	0.00066642	-3.32826
16758336	*KNTC1*	2.54E-05	-3.72371
16837270	*KPNA2*	4.24E-05	-4.17479
16844663	*KRT34*	0.0476429	-2.77594
16940065	*LARS2*	0.00324901	-2.08802
16699877	*LBR*	0.00196272	-2.18622
16873848	*LIG1*	0.000472932	-2.59985
16700034	*LIN9*	9.21E-05	-2.65002
16988703	*LMNB1*	1.81E-05	-7.22795
16866951	*LMNB2*	3.57E-06	-4.66948
16944736	*LOC100129550*	0.000808513	2.43585
16689678	*LOC100131564*	0.000834115	3.00085
16982607	*LOC100288152*	0.00731729	2.00566
16886041	*LOC100507600*	0.00211832	-3.01571
16872399	*LOC100507646*	0.000905933	2.02492
17113053	*LOC286437*	0.000124478	2.11667
16973180	*LOC401164*	0.00290878	-2.03461
17118262	*LOC644794*	0.0142312	2.22698
16840318	*LOC728392*	0.0469339	4.16754
16816627	*LOC81691*	0.000514594	-3.3832
16687352	*LRP8*	9.93E-06	-2.08001
16783905	*LRR1*	0.000116992	-2.08468
16846675	*LRRC59*	0.00173133	-2.19851
16944262	*LSAMP-AS1*	0.0467308	2.36716
16979389	*MAD2L1*	0.000583187	-5.41426
16912625	*MAPRE1*	4.65E-05	-2.22315
16703478	*MASTL*	0.000247809	-2.50933

16702571	*MCM10*	3.72E-05	-9.21838
16945101	*MCM2*	4.29E-05	-2.94169
17020019	*MCM3*	0.00115879	-2.72897
16929573	*MCM5*	0.000530838	-2.73242
16903090	*MCM6*	0.000143234	-2.30451
17060412	*MCM7*	0.000261951	-2.30205
16911212	*MCM8*	0.000329407	-4.68624
16773681	*MEDAG*	0.0100138	2.82096
16788488	*MEG3*	0.00499856	2.04079
17084904	*MELK*	4.21E-06	-7.08072
16752185	*METTL7B*	0.0164956	-3.3608
16694446	*MEX3A*	0.00197793	-2.05678
16911675	*MGME1*	0.00403713	-2.60082
16745470	*MIR100HG*	9.15E-05	2.33032
16788772	*MIR134*	0.00247768	2.10571
16788780	*MIR154*	0.000115585	4.19055
16836624	*MIR21*	0.00874796	3.17259
17110365	*MIR221*	0.00342872	2.42806
17110367	*MIR222*	0.0257769	2.1127
17087109	*MIR27B*	0.00112877	3.16758
16788778	*MIR323B*	0.00259233	3.56846
16788725	*MIR329-1*	0.0266562	2.16784
16788739	*MIR376A2*	0.00144285	2.66565
16788743	*MIR376B*	0.0269068	3.19338
16788784	*MIR377*	0.0148351	2.68245
16788717	*MIR380*	0.0212082	2.24077
16788770	*MIR382*	0.00750541	2.46444

16788788	*MIR409*	0.00811329	2.10959
16788764	*MIR544A*	0.00974492	2.86662
16848095	*MIR635*	0.00849574	2.32012
16788741	*MIR654*	0.000193956	2.89699
16788762	*MIR889*	0.0163931	2.51154
17114774	*MIR891A*	0.00153799	-3.85614
16924966	*MIS18A*	0.000391867	-2.80794
16792381	*MIS18BP1*	0.00365098	-2.44436
16719515	*MKI67*	0.000162321	-7.16348
16982024	*MLF1IP*	0.000303165	-3.69811
16670739	*MLLT11*	0.00368737	-2.34278
17021845	*MMS22L*	0.00151121	-2.46398
16971573	*MND1*	0.00387684	-3.33988
17018292	*MNF1*	5.23E-06	-2.31331
16809748	*MNS1*	0.000284594	-5.27408
16771894	*MPHOSPH9*	0.000516889	-2.02568
17072225	*MTBP*	0.00692372	-2.6589
17024002	*MTFR2*	0.000198212	-2.442
16785316	*MTHFD1*	1.76E-06	-2.56848
17003193	*MXD3*	0.0104514	-2.00134
16709108	*MXI1*	0.00209745	2.08286
17077826	*MYBL1*	0.00204302	-3.41908
16913957	*MYBL2*	1.43E-06	-6.36569
16777944	*N4BP2L1*	0.00269763	2.37452
16664118	*NASP*	0.00262634	-2.10983
16747287	*NCAPD2*	0.000100691	-2.97092
16746379	*NCAPD3*	2.69E-05	-2.77672

16965346	*NCAPG*	0.000372397	-5.10845
17064939	*NCAPG2*	1.30E-05	-4.71789
16882975	*NCAPH*	0.000196106	-8.18516
16961637	*NCEH1*	0.00147521	-2.09465
16856910	*NCLN*	2.47E-05	-2.39418
16687418	*NDC1*	0.000114141	-4.38587
16850517	*NDC80*	0.000121192	-9.97577
16816200	*NDE1*	0.00014892	-2.07912
16972616	*NEIL3*	4.91E-05	-7.16887
16951696	*NEK10*	0.0132414	2.05385
16698984	*NEK2*	0.00290068	-3.83752
16826230	*NETO2*	0.0234765	-2.5694
16842517	*NOS2*	0.00545511	-2.37265
16903897	*NR4A2*	0.0322787	4.16281
17087517	*NR4A3*	0.000241894	2.77217
16735545	*NRIP3*	0.000762166	-2.15909
17016956	*NRM*	0.00513789	-2.56503
17042936	*NUDT1*	0.000115745	-2.29373
16774669	*NUDT15*	0.000500994	-2.0936
16673154	*NUF2*	0.00069527	-5.93209
16753800	*NUP107*	4.96E-05	-2.60265
16995409	*NUP155*	3.01E-06	-2.26011
17089898	*NUP188*	1.91E-06	-2.43509
17051965	*NUP205*	1.46E-06	-2.71437
16819269	*NUP93*	1.73E-06	-2.40522
16799793	*NUSAP1*	0.00039355	-6.68358
16752825	*NXPH4*	0.00178752	-2.04063

16807605	*OIP5*	0.000165808	-4.6585
16687188	*ORC1*	0.00139917	-3.10125
16818600	*ORC6*	4.64E-06	-5.08932
16688214	*OTTHUMG00000009304*	0.00895483	2.22184
17085859	*OTTHUMG00000020009*	6.41E-05	2.21727
16701041	*OTTHUMG00000040729*	0.0453972	2.55712
17117588	*OTTHUMG00000169968*	2.25E-05	-2.24826
16703242	*OTUD1*	0.00141693	2.39827
16872767	*PAFAH1B3*	4.84E-05	-2.12475
17088462	*PAPPA*	0.0384056	2.80751
16699739	*PARP1*	0.000198015	-2.00256
16781482	*PARP2*	1.95E-05	-2.24686
16755928	*PARPBP*	0.000617919	-2.50006
17075776	*PBK*	0.000236195	-6.68523
16673191	*PBX1*	0.0193654	2.0336
16916958	*PCNA*	0.000103425	-2.67006
16966809	*PDGFRA*	0.00552797	2.20514
16830914	*PFAS*	0.00102335	-2.24737
16823083	*PGP*	2.99E-05	-2.0031
17097914	*PHF19*	0.000369807	-3.16771
16669389	*PHGDH*	6.19E-05	-3.46599
16965527	*PI4K2B*	0.000258413	-2.00726
16831429	*PIGL*	0.0333566	2.11158
17070221	*PKIA*	0.00383466	-2.0702
17077331	*PLAG1*	0.0110994	2.0805
16817017	*PLK1*	0.000452574	-5.59268
16911923	*PLK1S1*	0.00230317	2.07386

16970563	*PLK4*	0.000972914	-4.80746
16852683	*PMAIP1*	1.80E-05	-3.34266
16781536	*PNP*	0.0371238	-2.24227
16954707	*POC1A*	0.000502198	-3.63803
17062985	*PODXL*	0.0462124	-2.48295
17102230	*POLA1*	3.02E-05	-3.09564
16726790	*POLA2*	5.40E-06	-2.50791
16864490	*POLD1*	0.00113994	-2.41006
16772625	*POLE*	0.00284421	-2.00522
16792519	*POLE2*	0.000381908	-2.64081
16957951	*POLQ*	2.66E-05	-8.11619
17071265	*POP1*	0.00019079	-2.15098
16764706	*POU6F1*	0.000429517	2.00316
17018685	*PPIL1*	0.000480638	-3.36173
16659395	*PRAMEF22*	0.0106834	-3.28462
16681891	*PRAMEF3*	0.0217302	-2.31372
16813342	*PRC1*	0.000422627	-3.89996
16766318	*PRIM1*	0.000200794	-4.64044
17009862	*PRIM2*	0.000969803	-2.13738
17088185	*PRPF4*	0.000265219	-2.28444
16836492	*PRR11*	0.000870027	-4.16325
17086193	*PSAT1*	0.00158836	-8.41759
16738023	*PSMC3*	0.00161508	-2.01594
16845172	*PSMC3IP*	0.000756368	-4.11499
16886919	*PSMD14*	5.25E-06	-2.06852
16690535	*PSRC1*	0.000309017	-2.63453
16920156	*PTGIS*	0.00770382	2.04782

16697370	*PTGS2*	0.0281816	4.9551
16991741	*PTTG1*	0.000479447	-2.54345
16764500	*RACGAP1*	1.95E-05	-2.37588
16799637	*RAD51*	0.00260316	-3.35373
16747014	*RAD51AP1*	9.94E-05	-4.82847
17079220	*RAD54B*	0.000654798	-2.69852
16664243	*RAD54L*	0.000766225	-3.08334
16851397	*RBBP8*	1.67E-07	-2.90063
16919044	*RBL1*	0.00020919	-4.54874
17082782	*RECQL4*	0.000359105	-2.13054
17058617	*RFC2*	1.02E-05	-2.89478
16773946	*RFC3*	0.000199968	-3.78294
16962493	*RFC4*	0.000351997	-2.83918
16757687	*RFC5*	5.93E-05	-2.95901
16828327	*RFWD3*	0.00117139	-2.8414
16931225	*RIBC2*	0.000200808	-2.34336
17086353	*RMI1*	0.000559919	-2.41577
16858714	*RNASEH2A*	0.000139	-4.65418
16732315	*RNF26*	0.00111515	-2.13592
17104519	*RNY4P23*	0.0181832	-3.02542
16995715	*RPL37*	4.06E-06	2.27264
16721126	*RRM1*	0.000460307	-2.31326
16877019	*RRM2*	0.000131324	-5.42894
16714747	*RTKN2*	1.32E-05	-7.09229
16863946	*RUVBL2*	0.000705551	-2.16642
16690067	*SASS6*	0.00017155	-2.98548
17102129	*SAT1*	0.000110075	2.57333

17067314	*SCARA3*	6.28E-05	-3.27397
16927633	*SDF2L1*	0.00139736	-2.32156
16906615	*SDPR*	0.000843247	-3.87479
16980762	*SFRP2*	0.00387286	2.25134
16951485	*SGOL1*	0.000371929	-6.75291
16889251	*SGOL2*	0.000348403	-2.85778
16826160	*SHCBP1*	3.55E-06	-8.92218
16852312	*SKA1*	3.29E-05	-9.32186
16777278	*SKA3*	3.25E-05	-6.57788
16984032	*SKP2*	0.00123884	-2.41693
16848070	*SLC16A6*	0.000953516	4.26141
16838887	*SLC25A10*	0.000114444	-4.31257
16848793	*SLC25A19*	0.000720756	-2.0137
17009193	*SLC29A1*	2.96E-06	-3.90757
16680435	*SLC35E2*	0.000137211	2.06225
16832104	*SLC47A1*	0.000552743	-3.48846
16951756	*SLC4A7*	0.00200429	2.03525
17111219	*SMC1A*	1.70E-05	-2.55486
17087716	*SMC2*	0.000950026	-2.97455
16947556	*SMC4*	0.000765519	-2.93755
16874508	*SNAR-B1*	0.0363668	-3.62895
16874510	*SNAR-B1*	0.0363668	-3.62895
16863705	*SNAR-C1*	0.0357065	-2.26279
16863711	*SNAR-C1*	0.0357065	-2.26279
16863721	*SNAR-C1*	0.0357065	-2.26279
16873645	*SNAR-E*	0.0310007	-5.67506
16970068	*SNHG8*	0.0005787	2.03731

17047459	*SNORA14A*	0.0260707	2.04218
16788610	*SNORD113-7*	0.00314403	2.4747
16798132	*SNORD116-1*	0.0142152	3.05744
16798206	*SNORD116-20*	0.0378141	2.18988
16798144	*SNORD116-3*	0.0175306	2.10048
16798154	*SNORD116-3*	0.0175306	2.10048
16798242	*SNORD116-30*	0.00042301	2.82062
16798146	*SNORD116-5*	0.036094	2.14182
16798150	*SNORD116-5*	0.036094	2.14182
16798148	*SNORD116-6*	0.0104945	2.07895
16798152	*SNORD116-8*	0.0180856	2.1302
16790360	*SNORD9*	0.0191093	2.10081
17098171	*SNORD90*	0.0260067	2.24775
16851344	*SNRPD1*	1.35E-05	-2.89289
16732880	*SPA17*	0.00208454	-2.0817
16842673	*SPAG5*	0.0001806	-8.15787
16970409	*SPATA5*	0.00191479	-2.0032
16868838	*SPC24*	1.24E-05	-9.50661
16904780	*SPC25*	3.40E-05	-8.82046
17111594	*SPIN4*	0.000367244	-2.42627
16861630	*SPINT2*	0.00913817	2.05685
16780069	*SPRY2*	0.0200439	2.36944
16686796	*STIL*	0.000644409	-4.02735
16683723	*STMN1*	0.00112524	-2.08102
17070249	*STMN2*	0.0280615	2.24771
16850063	*STRA13*	0.000883989	-2.73384
17051441	*STRIP2*	0.00941106	-2.32545

17103413	*SUV39H1*	1.71E-05	-3.69791
16702685	*SUV39H2*	1.18E-05	-2.45069
17097072	*SVEP1*	0.0122964	2.26389
16785155	*SYNE2*	2.09E-07	-4.5644
16964000	*TACC3*	2.11E-05	-6.56745
16901161	*TBC1D8*	0.0301492	2.25141
17027710	*TCF19*	9.80E-06	-5.87466
17030560	*TCF19*	9.80E-06	-5.87466
17033265	*TCF19*	9.80E-06	-5.87466
17035356	*TCF19*	9.80E-06	-5.87466
17038044	*TCF19*	9.80E-06	-5.87466
17040632	*TCF19*	9.80E-06	-5.87466
17006568	*TCF19*	0.0204089	-2.03237
16756310	*TCP11L2*	0.00660509	2.11445
17084130	*TEK*	0.000364969	-2.68203
16780793	*TEX30*	0.000578657	-2.36056
16776905	*TFDP1*	0.000988761	-2.04189
16963241	*TFRC*	0.00653069	-3.24388
16734397	*TH*	0.0239784	-3.4337
16811299	*THAP10*	0.0168395	-2.45329
16856812	*THOP1*	4.02E-05	-2.69798
16804631	*TICRR*	0.000296435	-5.16125
16766137	*TIMELESS*	7.69E-05	-5.6277
16849379	*TK1*	3.45E-06	-6.87122
16750488	*TMEM106C*	0.00713441	-2.52516
16754177	*TMEM19*	0.00309516	-2.02837
16766403	*TMEM194A*	0.000758414	-2.38229

16752233	*TMEM198B*	0.000534854	2.25568
16755498	*TMPO*	0.000144873	-5.07345
16768936	*TMPO-AS1*	0.000636487	-3.35493
16857237	*TNFAIP8L1*	0.000278203	-2.11385
16863104	*TOMM40*	0.000339656	-2.38812
16844312	*TOP2A*	0.00336894	-4.46234
16658192	*TP73*	0.00269622	-3.36317
16801789	*TPM1*	0.0108091	2.00293
17015975	*TPMT*	0.00697382	-2.28196
16827344	*TPPP3*	0.0281828	-2.49709
16774515	*TPT1-AS1*	0.00229282	2.13089
16912379	*TPX2*	0.000727265	-5.11972
16982635	*TRIP13*	2.51E-05	-5.87567
16750761	*TROAP*	0.00265304	-3.66104
17103951	*TSPYL2*	1.28E-05	2.56109
16669212	*TTF2*	0.00255041	-2.5355
17010552	*TTK*	0.00124069	-5.74221
17117565	*TUBA1A*	0.00307078	-2.19773
17117560	*TUBA1B*	0.025439	-2.03802
17015143	*TUBB2A*	0.0411908	-2.17292
17091695	*TUBB4B*	2.23E-05	-2.78608
16851081	*TUBB6*	0.00341233	-2.06398
16834381	*TUBG1*	0.000250424	-2.95706
16850477	*TYMS*	4.52E-05	-6.2653
16914315	*UBE2C*	0.000527087	-6.42646
16875763	*UBE2S*	0.00387727	-2.23535
16698023	*UBE2T*	2.48E-05	-7.83026

16803008	*UBL7-AS1*	0.01833	-2.03431
16787679	*UBR7*	4.09E-05	-2.60487
16857258	*UHRF1*	0.000176194	-3.58297
16669067	*VANGL1*	0.000676004	-2.31635
16667702	*VCAM1*	0.000226983	4.42693
16788142	*VRK1*	0.00114644	-2.43106
16793190	*WDHD1*	7.73E-05	-5.18974
16861318	*WDR62*	1.64E-05	-4.51547
17072313	*WDR67*	0.00313619	-2.0326
16800355	*WDR76*	0.00135497	-3.63376
16964050	*WHSC1*	3.68E-05	-2.65605
17064679	*XRCC2*	4.90E-06	-2.79806
16836528	*YPEL2*	0.00573054	2.59451
17096205	*ZNF367*	0.00479245	-3.19718
16865726	*ZNF581*	9.56E-05	2.76187
16864829	*ZNF610*	0.00168012	2.39411
16870925	*ZNF724P*	0.00535433	-4.98813
17053100	*ZNF783*	0.00497124	2.29489
16980364	*ZNF827*	0.000542604	2.07276
16875114	*ZNF888*	0.000317481	-2.37159
16860103	*ZNF93*	0.000520254	-3.40066
16802204	*ZWILCH*	2.02E-06	-3.82231
16714504	*ZWINT*	0.000359633	-4.08488
16995716	…	4.06E-06	2.27264
16664044	…	1.66E-05	3.39175
16857933	…	2.44E-05	-2.0125
17100614	…	2.62E-05	-2.39283

16963646	…	2.96E-05	-2.14632
16857928	…	2.99E-05	-2.25058
16857926	…	5.76E-05	-3.97713
16698947	…	7.62E-05	-11.7839
16798893	…	9.14E-05	2.44787
16693521	…	0.000114618	-2.45102
16857929	…	0.000115161	-2.03448
16796749	…	0.000142203	2.43311
17121296	…	0.000200066	-2.24504
16857915	…	0.000202034	-2.53083
16701689	…	0.000246267	-2.52578
17123142	…	0.000256442	-4.12287
17120690	…	0.000359283	2.02297
17119822	…	0.000381584	3.04863
16737102	…	0.000419131	2.41093
17121990	…	0.000471011	-2.92231
17125150	…	0.000475999	2.09607
16824022	…	0.000486195	2.21153
16857922	…	0.000617513	-2.14564
16679981	…	0.000627345	-2.0342
17120506	…	0.000653958	-3.99834
16850426	…	0.00079164	-2.29853
17121236	…	0.000903343	2.07563
16692580	…	0.000936843	-2.63558
17125084	…	0.000952352	-2.15432
16655581	…	0.000971843	-2.05834
17126212	…	0.000975363	-3.89439

16678343	…	0.000996666	-3.03778
17126208	…	0.00101837	-2.78775
16706426	…	0.00104898	2.91026
17121832	…	0.00119681	2.31725
17125684	…	0.00123482	2.12686
17124130	…	0.00132839	-2.26201
17125788	…	0.00134904	-2.80352
16651439	…	0.00145188	-2.05552
17099165	…	0.00150883	2.23617
17068626	…	0.00156469	4.57724
17050249	…	0.00195423	-2.41662
16835626	…	0.00211011	-3.6221
16805623	…	0.00224217	2.25118
16857925	…	0.00224649	-2.59137
16846042	…	0.00248662	2.18315
16800091	…	0.00266665	2.05062
16857932	…	0.00276006	-2.09796
16771315	…	0.00309706	-2.39843
16764325	…	0.00311212	-3.46651
16651571	…	0.0032774	2.02662
16686273	…	0.00355995	-4.35594
16658582	…	0.00389843	-3.02262
16857917	…	0.00447951	-2.22149
16857931	…	0.00449721	-2.18245
16652941	…	0.00456258	2.06112
16692433	…	0.0045719	-2.23971
16857916	…	0.00465697	-2.36146

17026696	…	0.00513789	-2.56503
17028847	…	0.00513789	-2.56503
17031625	…	0.00513789	-2.56503
17034080	…	0.00513789	-2.56503
17036347	…	0.00513789	-2.56503
17039123	…	0.00513789	-2.56503
17036121	…	0.00532951	2.06776
17038872	…	0.00532951	2.06776
16686271	…	0.00547665	-3.2979
17028593	…	0.00547675	2.08135
16853994	…	0.00595397	-2.71862
16880233	…	0.00605149	-4.24249
16771524	…	0.00616189	-5.81084
16655401	…	0.0061632	2.1583
16652905	…	0.00635475	2.15227
16794258	…	0.00652851	-2.03445
17017212	…	0.00658305	2.89317
17017207	…	0.00661423	4.94173
16706413	…	0.00666728	-3.32022
16880231	…	0.00706024	-2.26759
17031378	…	0.00709524	2.08659
16771483	…	0.00711225	-4.3473
16745155	…	0.00721102	2.76802
17026529	…	0.008023	2.01835
16823103	…	0.00829282	-2.65498
16900018	…	0.0087736	-3.29216
17118037	…	0.00879186	2.09504

17004335	…	0.00906722	-2.4449
16771499	…	0.00966753	2.21384
16650617	…	0.00973981	3.75959
17120106	…	0.00991917	-4.5485
16880232	…	0.0102655	-2.40883
16778489	…	0.0116101	-2.17865
16977350	…	0.0118885	-3.13394
16693518	…	0.0119249	-2.15894
17121132	…	0.0120683	2.09138
17123164	…	0.0121017	-2.15632
16655249	…	0.0127238	-3.0465
16976219	…	0.0127638	2.1045
16857921	…	0.0131483	-3.6714
16656917	…	0.0135313	2.04606
16900533	…	0.0140731	-2.64537
16652561	…	0.0142224	2.03143
17121716	…	0.014818	2.52793
16770448	…	0.0148518	2.80349
16977342	…	0.015329	2.27998
16855178	…	0.0156404	-2.28474
17006292	…	0.0157061	-2.22369
16835638	…	0.0159304	-2.24194
17117443	…	0.0160411	2.37678
17126086	…	0.0161489	2.12895
17126122	…	0.0161489	2.12895
17123952	…	0.0162821	-2.05489
17124564	…	0.0166415	2.07912

17117752	…	0.0170447	2.80608
16657061	…	0.0186566	2.10038
16948561	…	0.019029	2.19769
16655757	…	0.0193943	-2.70955
17017184	…	0.0194982	2.17362
16692557	…	0.0196567	-2.19236
16653767	…	0.0198119	2.00637
16652903	…	0.0203654	2.14194
16652427	…	0.0212211	-2.23438
16651077	…	0.0220564	-2.97218
16758621	…	0.0228575	3.21864
17113488	…	0.0234341	2.2621
17104672	…	0.0236455	-3.9052
16716237	…	0.024696	2.33037
16794261	…	0.0248707	-2.03638
16650685	…	0.0263948	2.17123
16653157	…	0.0267142	2.08556
16650163	…	0.0271081	2.21711
16756132	…	0.0272896	2.08701
17124574	…	0.027478	2.11859
16692555	…	0.0284538	-2.28747
16798810	…	0.0288669	-2.28666
16885976	…	0.0295668	2.01819
17120100	…	0.0306959	2.27828
16685153	…	0.0308699	-2.36755
17119138	…	0.0310007	-5.67506
17119142	…	0.0310007	-5.67506

16752031	…	0.0316599	2.91043
16798080	…	0.0325544	2.35231
16744687	…	0.0329382	-3.09384
17126140	…	0.0331889	3.2342
16656003	…	0.0336743	-2.19288
16656945	…	0.034324	-2.49755
16841481	…	0.0343812	-2.05307
17006301	…	0.0354494	-2.09896
16764072	…	0.0360971	-2.17515
16893453	…	0.0377248	2.16873
16651455	…	0.0378987	2.52044
16651611	…	0.0380218	-2.88074
16652957	…	0.0380475	2.1265
17098326	…	0.039285	-2.33983
17006314	…	0.0402927	-2.90534
16718666	…	0.0403097	2.17594
16652399	…	0.0415396	2.10298
16653835	…	0.0416653	2.0676
16653845	…	0.042013	2.11352
16655095	…	0.0421538	2.68422
16771558	…	0.0435978	-3.30775
16678326	…	0.0437674	-2.29543
16722394	…	0.0438588	2.36216
17079423	…	0.0444397	2.83447
16656941	…	0.044568	-2.00868
16653143	…	0.0452117	2.30201
17098331	…	0.0468909	-3.21576

16653115	…	0.047632	2.06226
16975773	…	0.0483854	2.03399
17125110	…	0.0490871	2.6509
16685279	…	0.049225	2.77274

Appendix 9: Overlapping ependymoma DEGs identified in the transcriptomic work

Column ID	Gene	p value	Fold Change
17013773	*AKAP12*	0.0423462	2.32404
16798919	*ARHGAP11A*	0.00248109	-2.52232
16869588	*ASF1B*	0.00243833	-2.0554
16697544	*ASPM*	0.028889	-2.19332
16840902	*AURKB*	0.00212925	-2.77462
16838359	*BIRC5*	0.00634555	-2.72889
16775324	*BORA*	0.00578241	-2.29072
16901755	*BUB1*	0.0154433	-2.5653
16730967	*C11orf87*	0.000639054	-2.90468
16980998	*C4orf46*	0.000197486	-2.14112
16995938	*C5orf34*	0.00483652	-2.46263
16799598	*CASC5*	0.0041156	-2.66993
16979515	*CCNA2*	0.00539157	-2.38847
16985599	*CCNB1*	0.00882206	-3.09777
16801557	*CCNB2*	0.0119724	-2.48558
16815090	*CCNF*	0.000266347	-3.30258
16663514	*CDC20*	0.00707156	-3.01804
16927052	*CDC45*	0.0266193	-2.01829
16667037	*CDC7*	0.0151384	-2.05466

17067102	*CDCA2*	0.0047444	-3.0019
16760621	*CDCA3*	0.00417962	-2.76852
16662648	*CDCA8*	0.00130611	-3.34153
16705159	*CDK1*	0.00636669	-2.49593
16784299	*CDKN3*	0.00371252	-2.00627
16877956	*CENPA*	0.00891586	-2.12359
16978568	*CENPE*	0.0104356	-2.55827
16677425	*CENPF*	0.032952	-2.03519
17105401	*CENPI*	0.00259488	-2.28695
16696490	*CENPL*	0.000159715	-2.13351
16935517	*CENPM*	0.00790293	-2.4332
17086784	*CENPP*	0.000900931	-2.23042
17012379	*CENPW*	0.000106805	-2.20541
16707551	*CEP55*	0.00269072	-2.53872
17086167	*CEP78*	0.00247838	-2.16425
16922584	*CHAF1B*	0.00671322	-2.00358
16803562	*CHRNA5*	0.00572594	-2.02011
16901957	*CKAP2L*	0.0130425	-2.36265
17086634	*CKS2*	0.022741	-2.09129
16685165	*CLSPN*	0.0327589	-2.02987
16992467	*CREBRF*	0.000167935	2.64193
17071640	*CTHRC1*	0.0189626	2.03607
17047965	*DBF4*	0.00061544	-2.00299
16834812	*DBF4B*	0.00229749	-2.08671
16688386	*DEPDC1*	0.0150746	-2.90993
16996545	*DEPDC1B*	0.00384464	-2.66498
16779546	*DIAPH3*	0.00512595	-2.15677

16793225	*DLGAP5*	0.0175958	-2.8042
16800933	*DTWD1*	0.016678	2.46023
16835797	*EME1*	0.0157766	-2.40567
16751709	*ESPL1*	0.0219297	-2.20089
16683920	*FAM46B*	0.00024371	-2.88901
16830173	*FAM64A*	0.00962775	-2.50976
16913681	*FAM83D*	0.00818793	-4.14944
17109211	*FANCB*	0.0062321	-2.22549
16937505	*FANCD2*	0.0156554	-2.1824
17080788	*FBXO32*	0.00168214	3.02143
16760048	*FOXM1*	0.00138715	-2.79969
16755692	*GAS2L3*	0.00989371	-2.41244
16912192	*GINS1*	0.000538833	-2.37793
17068385	*GINS4*	0.00673054	-2.00035
17005396	*GMNN*	0.0032669	-2.43457
16829764	*GSG2*	0.00119303	-2.18343
16931384	*GTSE1*	0.0040709	-2.51858
16745236	*H2AFX*	0.0030149	-2.30433
16845537	*HDAC5*	0.00544163	2.11669
17016499	*HIST1H1B*	0.0220179	-2.30084
17005569	*HIST1H1E*	0.000934519	-2.15482
17005858	*HIST1H2AI*	0.0185692	-2.27881
17005603	*HIST1H2BC*	0.000490292	-2.90889
17005865	*HIST1H2BM*	0.00605018	-2.18022
17016363	*HIST1H3B*	0.0223391	-2.00534
17016400	*HIST1H3F*	0.0421956	-2.49272
17016403	*HIST1H3G*	0.0156958	-2.45406

17016503	*HIST1H3I*	0.00218614	-2.02118
17016360	*HIST1H4B*	0.00635529	-2.81829
17016383	*HIST1H4D*	0.00144966	-2.37025
16670387	*HIST2H3D*	0.0120533	-2.29826
16692616	*HIST2H3D*	0.0120533	-2.29826
16909700	*HJURP*	0.0314485	-2.24886
16725806	*INCENP*	0.000566123	-2.40288
16881708	*INO80B*	0.00552233	2.01719
16780917	*IRS2*	0.00136869	2.17809
16986583	*JMY*	5.03E-05	2.17382
16957170	*KIAA1524*	0.00325455	-2.23383
16707468	*KIF11*	0.0158211	-2.25123
16697695	*KIF14*	0.024816	-2.48098
16939960	*KIF15*	0.0382981	-2.04037
16845794	*KIF18B*	0.0117567	-3.09522
16989636	*KIF20A*	0.0165701	-3.00198
16707221	*KIF20B*	0.0157253	-2.41192
16802519	*KIF23*	0.0177201	-2.38964
17093397	*KIF24*	0.00478876	-2.14753
16663958	*KIF2C*	0.00780664	-2.12603
17104484	*KIF4A*	0.0125035	-2.55087
17007459	*KIFC1*	0.00649455	-2.48874
17038792	*KIFC1*	0.00679384	-2.44007
17041352	*KIFC1*	0.00649455	-2.48874
16948572	*KLHL24*	0.000278137	3.84283
16799517	*KNSTRN*	0.00554696	-2.31924
16837270	*KPNA2*	0.00274394	-2.13553

16866951	*LMNB2*	0.000605862	-2.11504
16979389	*MAD2L1*	0.0248047	-2.33656
16911212	*MCM8*	0.0262788	-2.01773
17084904	*MELK*	0.000961052	-2.47075
16836624	*MIR21*	0.0198514	2.64349
17110365	*MIR221*	0.0113575	2.02823
17110367	*MIR222*	0.0115479	2.44069
16848095	*MIR635*	0.0134862	2.15174
17114774	*MIR891A*	0.0374005	-2.04494
16719515	*MKI67*	0.0186226	-2.3931
16809748	*MNS1*	0.0110281	-2.44602
16913957	*MYBL2*	2.98E-05	-3.43392
16965346	*NCAPG*	0.0147133	-2.36332
17064939	*NCAPG2*	0.00246093	-2.04203
16882975	*NCAPH*	0.0126914	-2.82909
16687418	*NDC1*	0.00666413	-2.15667
16850517	*NDC80*	0.0333744	-2.34388
16972616	*NEIL3*	0.00933458	-2.34272
16951696	*NEK10*	0.000462696	3.6383
16698984	*NEK2*	0.0273571	-2.3573
16673154	*NUF2*	0.0225641	-2.55938
16799793	*NUSAP1*	0.0421257	-2.19848
16807605	*OIP5*	0.00251	-2.73597
16687188	*ORC1*	0.0189568	-2.00329
16818600	*ORC6*	0.000798431	-2.1908
16755928	*PARPBP*	0.00150733	-2.21439
17075776	*PBK*	0.0049139	-3.19618

16966809	*PDGFRA*	0.00210782	2.5542
16669389	*PHGDH*	0.000305241	-2.68383
16817017	*PLK1*	0.00585842	-3.07487
16970563	*PLK4*	0.0279201	-2.29587
16957951	*POLQ*	0.00169475	-3.09915
16813342	*PRC1*	0.00974727	-2.21768
16836492	*PRR11*	0.0162334	-2.31488
17086193	*PSAT1*	0.0167923	-3.94105
16690535	*PSRC1*	0.000416362	-2.52501
16664243	*RAD54L*	0.0115546	-2.00928
16858714	*RNASEH2A*	0.0132862	-2.04768
17104519	*RNY4P23*	0.00841157	-3.6668
16714747	*RTKN2*	0.00214003	-2.52311
17102129	*SAT1*	6.98E-05	2.74095
16951485	*SGOL1*	0.0435368	-2.17812
16889251	*SGOL2*	0.00336018	-2.072
16826160	*SHCBP1*	0.00076121	-2.78904
16852312	*SKA1*	0.00249054	-3.20155
16777278	*SKA3*	0.00663632	-2.27386
16848070	*SLC16A6*	0.00241123	3.47068
16838887	*SLC25A10*	0.00453961	-2.26212
16680435	*SLC35E2*	4.57E-05	2.3292
16832104	*SLC47A1*	0.0023449	-2.69018
16951756	*SLC4A7*	0.00219481	2.01338
16798146	*SNORD116-5*	0.0364146	2.13814
16798150	*SNORD116-5*	0.0364146	2.13814

17098171	*SNORD90*	0.0459707	2.01604
16842673	*SPAG5*	0.00925866	-2.98561
16868838	*SPC24*	0.00444197	-2.52852
16904780	*SPC25*	0.0168846	-2.20429
16780069	*SPRY2*	0.00635531	2.98047
17103413	*SUV39H1*	0.000504861	-2.23924
16964000	*TACC3*	0.00242574	-2.52742
17027710	*TCF19*	0.00412222	-2.04727
17030560	*TCF19*	0.00412222	-2.04727
17033265	*TCF19*	0.00412222	-2.04727
17035356	*TCF19*	0.00412222	-2.04727
17038044	*TCF19*	0.00412222	-2.04727
17040632	*TCF19*	0.00412222	-2.04727
16756310	*TCP11L2*	0.00171849	2.58589
16856812	*THOP1*	0.000146429	-2.28578
16804631	*TICRR*	0.0186447	-2.21314
16766137	*TIMELESS*	0.0160357	-2.03601
16849379	*TK1*	0.000840632	-2.42568
16752233	*TMEM198B*	0.000158854	2.65038
16755498	*TMPO*	0.0120446	-2.17526
16768936	*TMPO-AS1*	0.010628	-2.09851
16912379	*TPX2*	0.0296172	-2.25673
16982635	*TRIP13*	0.00350176	-2.31201
16750761	*TROAP*	0.00889412	-2.82668
17010552	*TTK*	0.0292019	-2.58985
16850477	*TYMS*	0.0120809	-2.10458
16914315	*UBE2C*	0.00555239	-3.50796

16875763	*UBE2S*	0.00496995	-2.15764
16698023	*UBE2T*	0.0129731	-2.13144
16861318	*WDR62*	0.00127505	-2.2228
16860103	*ZNF93*	0.00682546	-2.20916
16714504	*ZWINT*	0.0168798	-2.04769
16653767	…	0.016348	2.06785
16664044	…	0.000162568	2.42855
16692433	…	0.00284202	-2.40453
16698947	…	0.00507308	-3.57586
16706413	…	0.0328491	-2.34192
16764072	…	0.0479556	2.05613
16798810	…	0.0260554	-2.3342
16855178	…	0.0148991	-2.30459
16880232	…	0.0293308	2.00884
16900018	…	0.0219452	-2.66776
16977342	…	0.0243066	2.10299
17068626	…	0.0150822	2.71761
17113488	…	0.0287824	2.17593
17120106	…	0.0314019	-3.23443
17120506	…	0.0127021	-2.27415
17123164	…	0.0172277	-2.03972
17124574	…	0.0373636	2.00487

Appendix 10: Genes associated with GO enrichment identified with DAVID analysis

GO Term	Related genes
Cell division	*BUB1, CKS2, MAD2L1, NDC80, NEK2, NUF2, OIP5, SPC24, SPC25, TPX2, ZWINT, BIRC5, BORA, CDC20, CDC7, CDCA2, CDCA3, CDCA8, CENPE,*

	CENPF, CENPW, CCNA2, CCNB1, CCNB2, CCNF, CDK1, FAM64A, FAM83D, KIF11, KIF14, KIF18B, KIF20B, KIF2C, KIFC1, KNSTRN, NCAPG, NCAPH, NCAPG2, PSRC1, SPAG5, SKA1, SKA3, TIMELESS, TACC3, UBE2C, UBE2S
Sister chromatid cohesion	*BUB1, MAD2L1, NDC80, NUF2, SPC24, SPC25, ZWINT, AURKB, BIRC5, CDC20, CDCA8, CENPA, CENPE, CENPF, CENPI, CENPL, CENPM, CENPP, INCENP, KIF2C, PLK1, SKA1,*
Chromosome segregation	*HJURP, NDC80, NEK10, NEK2, NUF2, OIP5, SPC25, CDCA2, CENPE, CENPF, CENPW, INCENP, KIF11, KNSTRN, SPAG5, SKA1, SKA3*
Microtubule based movement	*CENPE, KIF11, KIF14, KIF15, KIF18B, KIF20A, KIF20B, KIF23, KIF24, KIF2C, KIF4A, KIFC1*
DNA replication	*DBF4, GINS4, TICRR, CDC45, CDC7, CHAF1B, CLSPN, CDK1, MCM8, ORC1, ORC6, RNASEH2A, TIMELESS*
G2/M transition of mitotic cell cycle	*NEK2, TPX2, BIRC5, BORA, CEP78, CCNB1, CCNB2, CDK1, FOXM1, MELK, PLK1, PLK4*
Cell proliferation	*BUB1, CKS2, DLGAP5, TPX2, AURKB, CENPF, CDK1, FAM83D, IRS2, KIF15, KIF2C, MKI67, MELK, PLK1, TYMS, TCF19, TACC3*
Spindle organisation	*TTK, ASPM, AURKB, KIF11, KNSTRN, SPAG5*
DNA repair	*POLQ, FANCD2, INO80B, PARPBP, RAD54L, TICRR, CHAF1B, CLSPN, CDK1, EME1, FOXM1, JMY, UBE2T*
G1/S transition of mitotic cell cycle	*DBF4, CDC45, CDC7, CDK1, CDKN3, MCM8, ORC1, ORC6, TYMS*
Cytokinesis	*BIRC5, ESPL1, INCENP, KIF20A, KIF23, PLK1, PRC1*
DNA replication initiation	*GINS4, CDC45, CDC7, ORC1, ORC6*
Double-strand break repair via break-induced replication	*GINS4, CDC45, CDC7*
Cerebral cortex development	*H2AFX, WDR62, ASPM, KIF14, TACC3*

DNA biosynthetic process	*POLQ, CENPF, TK1, TYMS*
Protein localisation to kinetochore	*TTK, AURKB, CDK1*

Appendix 11: Publications

Published abstracts

- ESTRANERO, J., ASCOUGH, A., DUANE, H., CHAPMAN, R., ROGERS, H. AND GRUNDY, R., 2015. PO38 Investigating the role the PI3K pathway plays in ependymoma pathogenesis. *Neuro-Oncology*, 17(Suppl 8): viii7.
- ESTRANERO, J., ASCOUGH, A., DUANE, H., CHAPMAN, R., ROGERS, H. AND GRUNDY, R., 2016. EPN-19 Activation of the PI3K pathway is a key molecular event that contributes towards the tumourigenicity and survival of paediatric ependymomas. *Neuro-Oncology*, 18(Suppl 3): iii34.
- ESTRANERO, J., ASCOUGH, A., DUANE, H., CHAPMAN, R., ROGERS, H. AND GRUNDY, R., 2017. EPND-04 Investigating the biological consequences of PI3K pathway inhibition on paediatric ependymoma tumours. *Neuro-Oncology*, 19(Suppl 4): iv15–iv16.

Published review articles

- ROGERS, H.A., ESTRANERO, J., GUDKA, K. and GRUNDY, R.G., 2017. The therapeutic potential of targeting the PI3K pathway in pediatric brain tumors. *Oncotarget,* 8(2).

Articles submitted for peer review

- SERVANTE, J., ESTRANERO, J. MEIJER, L. LAYFIELD, R. and GRUNDY, R.G., 2018. Chemical moedulation of autophagy as an adjunct chemotherapy in childhood and adolescent brain tumors. *Oncotarget.*